A QED framework for nonlinear and singular optics

A thesis submitted by:

Matt M. Coles

as part of the requirements for the degree of PhD in the

School of Chemistry
University of East Anglia
Norwich NR4 7TJ

The research in this thesis has not been submitted previously for a degree at this or any other university. Except where explicitly mentioned, the work is of my own.

M. M. Coles

January 2014

Abstract

The theory of quantum electrodynamics is employed in the description of linear and nonlinear optical effects. We study the effects of using a two energy level approximation in simplifying expressions obtained from perturbation theory, equivalent to truncating the completeness relation. However, applying a two-level model with a lack of regard for its domain of validity may deliver misleading results. A new theorem on the expectation values of analytical operator functions imposes additional constraints on any atom or molecule modelled as a two-level system. We introduce measures designed to indicate occasions when the two-level approximation may be valid.

Analysis of the optical angular momentum operator delivers a division into spin and orbital parts satisfying electric-magnetic democracy, and determine a new compartmentalisation of the optical angular momentum. An analysis is performed on the recently rediscovered optical chirality, and its corresponding flux, delivering results proportional to the helicity and spin angular momentum in monochromatic beams. A new polarisation basis is introduced to determine the maximum values that an infinite family of optical helicity- and spin- type measures may take, and disproves recent claims of 'superchiral light'. A theoretical description of recent experiments relate helicity- and spin- type measures to the circular differential response of molecules, and show that nodal enhancements to circular dichroism relate only to photon number-phase uncertainty relation and do not signify 'superchiral' regions. The six-wave mixing of optical vortex input, in nonlinear media, demonstrates the quantum entanglement of pairs of optical vortex modes. The probability for each possible output pair displays a combinatorial weighting, associated with Pascal's triangle.

A quantum electrodynamic analysis of the effect of a second body on absorption can be extended by integrating over all possible positions of the mediator molecules, modelling a continuous medium. This provides links with both the molecular and bulk properties of materials.

To my family and friends.

Contents

202 Pages

Publications

"We have a habit in writing articles published in scientific journals to make the work as finished as possible, to cover up all the tracks, to not worry about the blind alleys or describe how you had the wrong idea first, and so on. So there isn't any place to publish, in a dignified manner, what you actually did in order to get to do the work."

– Richard P. Feynman[†]

[†]Feynman, Richard P., Nobel Lecture (1965).

The following are published papers resulting from research undertaken for this thesis;

1. David L. Andrews, Luciana C. Dávila Romero, Jamie M. Leeder and **Matt M. Coles**, Optomechanical control of molecular motors, *Proceedings of SPIE* **7762**, Optical Trapping and Optical Micromanipulation VII, 776202 (2010).

2. David L. Andrews, David S. Bradshaw and **Matt M. Coles**, Perturbation theory and the two-level approximation: A corollary and critique, *Chemical Physics Letters* **503**, pp. 153-156 (2011).

3. David L. Andrews, David S. Bradshaw and **Matt M. Coles**, Limitations and improvements upon the two-level approximation for molecular nonlinear optics, *Proceedings of SPIE* **7917**, Nonlinear Frequency Generation and Conversion: Materials, Devices, and Applications X, 79171K (2011).

4. **Matt M. Coles**, Jamie N. Peck, Vasily S. Oganesyan and David L. Andrews, Assessing limitations to the two-level approximation in nonlinear optics for organic chromophores by ab initio methods, *Proceedings of SPIE* **8113**, Linear and Nonlinear Optics of Organic Materials XI, 81130K (2011);

5. Scott N. A. Smith, **Matt M. Coles** and David L. Andrews, Optical binding with anisotropic particles: resolving the forces and torques, *Proceedings of SPIE* **8097**, Optical Trapping and Optical Micromanipulation VIII, 80971E (2011).

6. David L. Andrews and **Matt M. Coles**, Optical superchirality and electromagnetic angular momentum, *Proceedings of SPIE* **8274**, Complex Light and Optical Forces VI, 827405 (2012).;

7. **Matt M. Coles**, Jamie N. Peck, Vasily S. Oganesyan and David L. Andrews, Failure of the two-level and sum over states methods in nonlinear optics, demonstrated by ab initio methods, *Proceedings of SPIE* **8434**, Nonlinear Optics and Applications VI, 84340K (2012).

8. David L. Andrews and **Matt M. Coles**, Measures of chirality and angular momentum in the electromagnetic field, *Optics Letters* **37**, 3009-3011 (2012).

9. **Matt M. Coles** and David L. Andrews, Chirality and angular momentum in optical radiation, *Physical Review A* **85**, 063810 (2012).

10. **Matt M. Coles** and David L. Andrews, Directions in optical angular momentum, *Proceedings of SPIE* **8637**, Complex Light and Optical Forces VII, 863707 (2013).

11. **Matt M. Coles** and David L. Andrews, Photonic measures of helicity: optical vortices and circularly polarized reflection, *Optics Letters* **38**, 869-871 (2013).

12. **Matt M. Coles**, Mathew D. Williams and David L. Andrews, Second harmonic generation in isotropic media: six-wave mixing of optical vortices, *Optics Express* **21**, 12783 (2013).

13. **Matt M. Coles** and David L. Andrews, Expanded horizons for generating and exploring optical angular momentum in vortex structures, *Proceedings of SPIE* **8813**, Spintronics VI, 881333 (2013).

14. Mathew D. Williams, **Matt M. Coles**, Kamel Saadi, David S. Bradshaw and David L. Andrews, Optical vortex generation from molecular chromophore arrays, *Physical Review Letters* **111**, 153603 (2013)

15. **Matt Coles**, Mathew Williams, Kamel Saadi, David Bradshaw and David Andrews, Chiral nanoemitter array: a launchpad for optical vortices, *Laser & Photonics Reviews* **7**, 1088-1092 (2013).

Preface

Quantum electrodynamics emerges from the application of quantum field theory to problems of electromagnetic origin, and describes, with unparalleled accuracy, phenomena involving light and matter. In this thesis, quantum electrodynamics is applied to molecular systems, using the formulation developed by D. P. Craig, E. A. Power and T. Thirunamachandran. Moreover, quantum optical techniques are employed in the description of various conserved electromagnetic quantities of interest, notably optical angular momentum.

Chapter One is intended as an introduction to (and derivation of) the methods used in this thesis to describe light, matter and their interaction, and loosely follows the structure of the first chapters of *Molecular Quantum Electrodynamics* by Craig and Thirunamachandran. It develops a fully quantised framework by which we may analyse problems in quantum and nonlinear optics. Formally, the QED Lagrangian is shown to lead to the correct equations of motion for a system comprising the electromagnetic field and a system of electrons, bound by atomic and molecular potentials. A gauge transformation is applied so that the emerging Hamiltonian models the system of particles as electric and magnetic multipoles. This formulation lends itself to perturbation theory, where the light-matter interaction is weak compared with the Coulomb binding between the electrons and the nuclei. Thus, the atomic, molecular and optical problems discussed in this thesis are given a theoretical basis on which they can be analysed.

Chapter Two presents a theoretical study of the validity of the two-level approximation, generally and in the context of nonlinear optics. In both analytical and computational settings, it is determined that the use of a two-state model without full cognisance of its limitations delivers potentially misleading results. A new analytical theorem on the expectation values of quantum operators shows the invalidity of the two-level approximation in even simple systems. Furthermore, the two-level approximation when applied to the optical susceptibility tensors of nonlinear optical processes is discussed, and the commonly held idea that ‘push-pull’ chromophores are associated with enhanced second harmonic response is disproved. It is shown that *ab*

initio calculations (performed by collaborators Peck and Oganesyan), combined with introduction of an error-gauging parameter, indicates that for two specified molecules the two-level approximation is valid in the case of Rayleigh scattering and invalid in the case of second harmonic generation. Finally, it is proved that the number of terms in the p^{th}-order optical susceptibility is a polynomial of order $n^{(p-1)}$, where n is the number of energy levels included in the sum-over-states computation, which puts these calculations in the class of problems quickly solvable by a computer.

Chapter Three departs from the nonlinear optics of Chapter Two, to discuss the electromagnetic field in free-space. This chapter develops a precise quantum optical framework for the study of optical angular momentum. The new results from such an analysis emerge in terms of number operators and expectation values, delivering both qualitative and quantitative insight, and also perfectly mirror the results of other researchers (Bliokh and Nori), who use a purely classical framework. It is shown that a new analysis of the optical angular momentum allows division into parts that satisfy duplex symmetry. Introduction of a general Poincaré sphere representation of polarisation determines the orbital and spin parts of the angular momentum as dependant on the sum and difference of number operators for modes of opposing helicity, respectively. These results are extended to the case of beams with orbital angular momentum. A similar analysis of the optical chirality density and corresponding flux shows that they are proportional only to differences of number operators for modes of opposing helicity. Introduction of a Laguerre-Gaussian basis reveals that beams with nonzero values of the optical chirality also do not possess orbital angular momentum characteristics. The infinite hierarchy of helicity- and spin- type measures, introduced by Cameron, Barnett and Yao, all emerge with similar quantum operator form: identical to the helicity and spin operators, except with an additional k^2 inside the mode summation for each successive pair of operators. Such analysis disproves the recent claim that light with nonzero values of optical chirality can differentiate between left- and right- handed molecules many times better than pure circularly polarised light. This novel quantum optical analysis proves that the maximum (or minimum) value any helicity- or spin- type measure can take is that of pure left- or right- handed light.

Chapter Four combines the nonlinear optical techniques developed in Chapter

Two and the quantum optical techniques developed in Chapter Three. It is shown that, when taking expectation values, measureable electromagnetic quantities must contain equal numbers of annihilation and creation operators. This avoids the introduction of a rapidly oscillating phase factor, the real part of which averages to zero in any realistic measurement. The first quantum electrodynamic treatment of recent experiments is presented, calculating the rates of circular differential processes and their relation to measures of helicity, spin and recently rediscovered measures of chirality. The increase in circular dichroism at regular intervals from the mirror corresponds to Tang and Cohen's claim of nodal enhancements and is proven to be associated only with the known behaviour of the electromagnetic field vectors. Furthermore, any increase or decrease in differential response at these locations is shown to be limited by the phase-photon number uncertainty principle and displays features associated with the reported shot-noise, deriving from the quantum nature of light. A section on the new theoretical analysis of six-wave mixing of optical vortices demonstrates the quantum entanglement of pairs of optical vortex modes, where the probability for each output displays a neat combinatorial weighting, associated with Pascal's triangle.

In **Chapter Five**, a new nonlinear optical technique is detailed, which extends a quantum electrodynamic framework for the effect of a third body on absorption by integrating over all possible positions of the mediator molecules. Developing such a theory provides links with both the molecular and bulk properties of materials. Moreover, it is determined which properties need to be optimised in order to tailor the medium modified effect.

In **Chapter Six**, the new work done in this thesis is summarised and possible avenues of further investigation are identified.

Acknowledgments

Firstly, I would like to wholeheartedly thank my parents; without their support this work (and much more beside) would not have been possible. I also thank the rest of my family and friends for their continuous moral support and guidance; a special mention to my girlfriend, Lucy, for, what must have felt like, never-ending journeys to and from Norwich.

I would also like to thank my two examiners, Dr. Sonja Franke-Arnold and Dr. Garth Jones, for their insightful comments and corrections.

For various discussions within the QED group, I thank Jack Ford, Mathew Williams, Dr. Jamie Leeder, Scott Smith, Dr. Luciana Dávila-Romero, and especially Dr. David Bradshaw, for his extensive help and proof-reading. Last but certainly not least, I wish to thank Prof. David Andrews: expert, teacher and friend.

Chapter 1

Introduction

"On account of its extreme complexity, most physicists will be very glad to see the end of [QED]" – Paul A. M. Dirac[†]

"It is my task to convince you not to turn away because you don't understand it. You see my physics students don't understand it... That is because I don't understand it. Nobody does." – Richard P. Feynman[‡]

[†]Kragh, Helge S., *Dirac: A scientific biography* (Cambridge University Press, 1990).
[‡]Feynman, Richard P., *QED: The Strange Theory of Light and Matter* (Princeton University Press, 1988).

1.1 Background

Quantum electrodynamics (QED) is the analytical tool of choice for the description of the electromagnetic field, the charge distributions in systems of matter, and the interaction between the two. Precisely, QED is a relativistic quantum field theory of electrodynamics. In simple terms, this means that both the matter and radiation are quantised and treated relativistically; it is this full treatment that gives rise to the remarkable precision tests of this theory [1–4]. It has unparalleled success in describing the physical world. For example, the QED prediction and the experimental value of the anomalous magnetic moment of the electron agree to more than ten significant figures [5]: this is the most accurately verified prediction in the history of physics.

In its region of applicability, QED gives qualitative and quantitative insight unmatched by either classical electrodynamics, or semi-classical theory (in which the matter is treated quantum mechanically and the radiation is described classically). In QED formulations, the radiation is described quantum mechanically and, as a consequence of being modelled as a set of harmonic oscillators, its ground state has a non-zero energy expectation value. Therefore, there exists *zero-point* energy that influences matter, and explains deviations from classical and semi-classical theory. For example, both QED and semi-classical theory deliver the same result for stimulated emission, but only the former acknowledges vacuum fluctuations that drive the perturbations responsible for 'spontaneous' emission [6]. Furthermore, it is only by considering the quantum nature of the optical field that, for example, the difference in energies between the $^2S_{1/2}$ and the $^2P_{1/2}$ orbitals of the hydrogen atom (Lamb shift

[7]) or the force between two uncharged metal plates in a vacuum (Casmir effect [8,9]), and the related Casimir-Polder interaction [10], can be accounted for.

In 1927, Paul Dirac published a formulation of quantum theory, which, for the first time, incorporated special relativity, and correctly computed the Einstein A-coefficient for spontaneous radiative emission of an atom [11]. He went on to derive, what later came to be known as, the Dirac equation: a relativistic generalisation of the Schrödinger wave equation that predicted the existence of anti-matter [12] and led to his awarding of the Nobel Prize for Physics in 1933. The early contributions of, among others, Fermi, Heisenberg and Pauli [13] indicated that any processes involving the interaction of light and matter would be computable. However, it was quickly discovered by Oppenheimer [14] and others [15,16] that only the first-order perturbative contributions to the theory could be guaranteed to be finite. Higher order terms involved infinities, which were believed to indicate an insurmountable inconsistency between quantum theory and special relativity.

The concept of renormalisation was first incorporated into QED by Hans Bethe in the late 1940s [17] with his calculation of the Lamb shift. Generalisation of this work delivered a Lorentz covariant formulation of QED with a perturbation series that was finite to *any* order, and earned its discoverers: Richard Feynman [18–20], Julian Schwinger [21,22] and Sin-Itiro Tomonaga [23], the Nobel prize for physics in 1967. Initially, the formulations of Feynman, Schwinger and Tomonaga seemed quite different; the former relying heavily on Feynman diagrams and the latter centred on operators in quantum field theory. However, in 1949 Freeman Dyson showed that the superficially different approaches were, in fact, equivalent [24]. Feynman (or time-

ordered) diagrams were introduced as a way to visualise the terms in the equations of QED. For example, in a simple scattering process an atom (or molecule) absorbs a photon of light and then re-emits it; less obviously, calculation of the probability amplitude requires an additional term that corresponds to the photon being emitted *before* it is absorbed. Although counterintuitive, without this term the predictions of the theory are inexact. For situations where large numbers of light-matter interactions take place (for example, in harmonic generation and *n*-wave mixing), the number of Feynman diagrams is also large and a *state-sequence* diagrammatic method becomes more useful.

The Lorentz covariant or *relativistic* formulation of QED is necessary when dealing with charged (or uncharged) particles moving at, as the name suggests, relativistic speeds. For the systems discussed in this thesis, it is appropriate to consider atomic or molecular states – or, more precisely, electron fields that are bound in an electromagnetic potential generated by nuclei. Non-relativistic or molecular QED was first formulated by Edwin Power and Sigurd Zienau in 1959 [25] and the Power-Zienau-Woolley representation [26,27] is the most convenient way of modelling the interaction of bound charges with the electromagnetic field.

The non-relativistic formulation of QED was later clarified in a series of works by Edwin Power and Thuraiappah Thirunamachandran [28–32], in which, along with a new perspective on fundamental theory, they tackled intermolecular interactions such as electronic energy transfer (EET). Later, molecular QED had many of its own successes, distinct from the successes of the QED associated with particle physics, such as further unifying studies on EET [33,34], and the related laser assisted resonant

energy transfer (LARET) [35]. Furthermore, molecular QED laid the foundation of Rayleigh and Raman optical activity [36], second harmonic generation in randomly oriented media [37], four-wave mixing [38] and multiphoton absorption spectroscopy [39].

1.2. The macroscopic electromagnetic field

Classical electrodynamics is an excellent description of the electromagnetic field when quantum effects are negligible and, when this is true, is compatible with Maxwell's equations. The most well-known version of the macroscopic version of these equations is [6]:

$$\nabla \cdot \mathbf{D} = \rho^{true}; \tag{1.2.1}$$

$$\nabla \cdot \mathbf{B} = 0; \tag{1.2.2}$$

$$\nabla \times \mathbf{E} = -\frac{\partial \mathbf{B}}{\partial t}; \tag{1.2.3}$$

$$\nabla \times \mathbf{H} = \frac{\partial \mathbf{D}}{\partial t} + \mathbf{J}^{true}. \tag{1.2.4}$$

These equations give the relationship between the charges - represented by the charge density ρ^{true} and the related charge current $\mathbf{J}^{true}$ - and the four field vectors $\mathbf{E}(\mathbf{r},t), \mathbf{B}(\mathbf{r},t), \mathbf{D}(\mathbf{r},t)$ and $\mathbf{H}(\mathbf{r},t)$. The vectors $\mathbf{E}$ and $\mathbf{B}$ represent the electric and magnetic fields, and may exist even in regions where there are no charges, i.e. in *source-free* space. The vectors $\mathbf{D}$ and $\mathbf{H}$ are the *auxiliary* fields and are basically the

electric and magnetic fields, respectively, when modified by matter in that region. Precisely, they are given by [40]:

$$\mathbf{D} = \varepsilon_0 \mathbf{E} + \mathbf{P}; \tag{1.2.5}$$

$$\mathbf{H} = \frac{1}{\mu_0}\mathbf{B} - \mathbf{M}, \tag{1.2.6}$$

where ε_0 and μ_0 are the electric permittivity and magnetic permeability, respectively, of free space. Here $\mathbf{P}(\mathbf{r},t)$ is the *polarisation* field and $\mathbf{M}(\mathbf{r},t)$ is the *magnetisation* field, which, as mentioned above, represent the charges not included in the true charge density and current. Therefore, given a certain $\{\rho^{true}, \mathbf{J}^{true}, \mathbf{P}, \mathbf{M}\}$ and it is possible to calculate (not necessarily analytically) the $\mathbf{E}$ and $\mathbf{B}$ fields at every point subject to some specified boundary conditions. Furthermore, adding the *Lorentz force*:

$$\mathbf{F} = e(\mathbf{E} + \mathbf{v} \times \mathbf{B}), \tag{1.2.7}$$

to our system of equation allows, with the help of the classical equations of motion, the calculation of the trajectory of a point particle with charge e and velocity $\mathbf{v}$.

1.3. The microscopic electromagnetic field

The polarisation and magnetisation fields are *bulk* quantities and are suitable for macroscopic problems. In the microscopic formulation of electromagnetism,

however, the bulk fields are removed, in favour of the constituent charges and currents,

$$\rho^{bulk} = -\nabla \cdot \mathbf{P}; \tag{1.3.1}$$

$$\mathbf{J}^{bulk} = \nabla \times \mathbf{M} + \frac{\partial \mathbf{P}}{\partial t}. \tag{1.3.2}$$

It is then straightforward to define the total charge and current as:

$$\rho = \rho^{true} + \rho^{bulk}; \tag{1.3.3}$$

$$\mathbf{J} = \mathbf{J}^{true} + \mathbf{J}^{bulk}. \tag{1.3.4}$$

Using these relations, we obtain the microscopic version of Maxwell's equations, which are written in terms of lower case variables to make clear the distinction with the macroscopic field:

$$\nabla \cdot \mathbf{e} = \frac{\rho}{\varepsilon_0}; \tag{1.3.5}$$

$$\nabla \cdot \mathbf{b} = 0; \tag{1.3.6}$$

$$\nabla \times \mathbf{e} = -\frac{\partial \mathbf{b}}{\partial t}; \tag{1.3.7}$$

$$\nabla \times \mathbf{b} = \frac{1}{c^2}\frac{\partial \mathbf{e}}{\partial t} + \mu_0 \mathbf{j}, \tag{1.3.8}$$

where $c^2 \varepsilon_0 \mu_0 = 1$ can be used to eliminate one of the free space constants. Furthermore, the charge and current are not considered here in terms of some

continuous charge distribution, but are more accurately portrayed as particles indexed by α, with charge e_α and position vector $\mathbf{q}_\alpha$. The charge density and current are then given by,

$$\rho(\mathbf{r}) = \sum_\alpha e_\alpha \, \delta(\mathbf{r} - \mathbf{q}_\alpha); \tag{1.3.9}$$

$$\mathbf{j}(\mathbf{r}) = \sum_\alpha e_\alpha \frac{\partial \mathbf{q}_\alpha}{\partial t} \delta(\mathbf{r} - \mathbf{q}_\alpha), \tag{1.3.10}$$

where $\delta(\mathbf{r} - \mathbf{q}_\alpha)$ is the Dirac delta function, characterised by its two properties [41]:

$$\delta(\mathbf{r} - \mathbf{q}_\alpha) = \begin{cases} 0, & \mathbf{r} \neq \mathbf{q}_\alpha \\ +\infty, & \mathbf{r} = \mathbf{q}_\alpha \end{cases}; \tag{1.3.11}$$

$$\int_V dV \, \delta(\mathbf{r} - \mathbf{q}_\alpha) = 1. \tag{1.3.12}$$

1.4. Gauge transformations

It is a standard result of mathematics that if the divergence of a vector field vanishes, then the field can be expressed as the curl of an underlying field [42]. As the magnetic field, Eq.(1.3.6), satisfies this condition we introduce the *vector potential*:

$$\mathbf{b} = \nabla \times \mathbf{a}. \tag{1.3.13}$$

Substituting this expression into Faraday's law, Eq. (1.3.7), delivers

$$\nabla\times\left(\mathbf{e}+\frac{\partial\mathbf{a}}{\partial t}\right)=0. \tag{1.3.14}$$

The term inside the brackets satisfies the condition for a curl free field, which means that it can be expressed as the gradient of a scalar field [41]:

$$\mathbf{e}+\frac{\partial\mathbf{a}}{\partial t}=-\nabla\phi, \tag{1.3.15}$$

where ϕ is called the *scalar potential*. We choose the right hand side of Eq. (1.3.15) to have a negative sign with the foresight that it will be convenient later.

As above, the curl of the gradient of a scalar field is necessarily zero. Thus, making the substitutions:

$$\mathbf{a}\rightarrow\mathbf{a}+\nabla\chi; \tag{1.3.16}$$

$$\phi\rightarrow\phi-\frac{\partial\chi}{\partial t}, \tag{1.3.17}$$

leaves Eq. (1.3.13) and (1.3.15) unchanged; this is known as a *gauge transformation*. This means that any choice of scalar field, χ, will give a set of potentials $(\mathbf{a},\phi)$ that all deliver the same pair of $\mathbf{e}$ and $\mathbf{b}$ fields.

It is curious to note that the electric and magnetic fields do not seem to be on equal footing in this formulation; the former is delivered as the time derivative of the underlying vector potential, whereas the latter is the curl. The central theme of electromagnetic theory is that electricity and magnetism are different manifestations of the same phenomena; a suitable Lorentz transformation replaces the electric force with the magnetic force (or *vice versa*) in any given system. This is often called the *electric-magnetic democracy* [43,44]. The key point here is that in source-free space the charge density is zero and the electric field is also divergence-free; the electric field can then also be represented as the curl of some underlying potential (normally, denoted $\mathbf{c}$). Thus, it is the presence of matter that breaks the electric-magnetic symmetry.

Up to this point we have only used two, Eq. (1.3.6) and (1.3.7), of Maxwell's equations; we may use the remaining two to establish the connection between the potentials, Eq. (1.3.13) and (1.3.15), and the charge distribution. Combining the expression for the scalar potential, Eq. (1.3.15), and Gauss' law, Eq. (1.3.5), reveals:

$$\nabla^2\phi + \frac{\partial}{\partial t}\nabla\cdot\mathbf{a} = -\frac{\rho}{\varepsilon_0}. \tag{1.3.18}$$

Use of expressions for both the scalar and vector potentials, Eq. (1.3.13) and (1.3.15), along with the modified Ampère's law, Eq. (1.3.8), gives

$$\nabla^2\mathbf{a} - \frac{1}{c^2}\frac{\partial^2\mathbf{a}}{\partial t^2} - \nabla(\nabla\cdot\mathbf{a}) - \frac{1}{c^2}\nabla\left(\frac{\partial\phi}{\partial t}\right) = -\mu_0\mathbf{j}. \tag{1.3.19}$$

Now the sources have been related to the potentials, we can choose a particular gauge that can simplify Eq. (1.3.18) and (1.3.19); this is a process known as *gauge fixing*.

1.4. Gauge fixing

The most commonly used gauges in the study of electromagnetism are the *Lorenz* [45] and *Coulomb gauges,* although, depending on the situation, others (Landau, Feynman-'t Hooft, Yennie etc. [46]) may make calculations easier. In the Lorenz gauge, the choice of vector potential is partially fixed by the condition:

$$\nabla \cdot \mathbf{a} = -\varepsilon_0 \mu_0 \frac{\partial \phi}{\partial t}. \tag{1.4.1}$$

For problems involving particles moving at relativistic speeds, the Lorenz gauge is the most appropriate choice to deliver a manifestly Lorentz invariant formulation of quantum electrodynamics. In this framework, the scalar potential is driven by the charge density and the vector potential by the currents.

To address the interaction of light with non-relativistic molecular states, we develop a non-covariant QED framework; to this end the Coulomb gauge,

$$\nabla \cdot \mathbf{a} = 0, \tag{1.4.2}$$

is most convenient. Proof that it is always possible to choose a vector potential that satisfies this condition is presented in Appendix A. Substitution of the Coulomb

gauge condition, Eq. (1.4.2), into Eq. (1.3.18) and (1.3.19) produces:

$$\nabla^2\phi = \frac{\rho}{\varepsilon_0}; \tag{1.4.3}$$

$$\left(\nabla^2 - \frac{1}{c^2}\frac{\partial^2}{\partial t^2}\right)\mathbf{a} = \frac{1}{c^2}\nabla\left(\frac{\partial\phi}{\partial t}\right) - \mu_0\mathbf{j}. \tag{1.4.4}$$

Considering the vector potential is never measured or observed, it will be instructive to relate Eq. (1.4.3) and (1.4.4) to the electric and magnetic fields. First, we decompose the electric and magnetic fields into the transverse and longitudinal parts,

$$\mathbf{e} = \mathbf{e}^{\perp} + \mathbf{e}^{\parallel}; \tag{1.4.5}$$

$$\mathbf{b} = \mathbf{b}^{\perp} + \mathbf{b}^{\parallel}, \tag{1.4.6}$$

respectively. Since, at least in currently observed situations, there are no magnetic monopoles, Eq. (1.3.6), the magnetic field is purely transverse: $\mathbf{b} = \mathbf{b}^{\perp}$. In free space, this is also true for the electric field. However, in the presence of charges the $\mathbf{e}$ field has both transverse *and* longitudinal parts,

$$\nabla\times\mathbf{e} = \nabla\times\mathbf{e}^{\perp} = -\frac{\partial\mathbf{b}}{\partial t}; \tag{1.4.7}$$

$$\nabla\cdot\mathbf{e} = \nabla\cdot\mathbf{e}^{\parallel} = \frac{\rho}{\varepsilon_0}, \tag{1.4.8}$$

respectively. Taking the remaining Maxwell equation, Eq. (1.3.8) and substituting the

above transverse/longitudinal split delivers:

$$\frac{1}{c^2}\frac{\partial \mathbf{e}^{\|}}{\partial t} = -\mu_0 \mathbf{j}^{\|}, \tag{1.4.9}$$

where $\mathbf{j} = \mathbf{j}^{\perp} + \mathbf{j}^{\|}$ are the transverse and longitudinal components of the current. Clearly, Eq. (1.4.9) along with Eq. (1.4.8), represents the equation of local conservation for charge and current. Furthermore, the transverse component of the current can be obtained as:

$$\nabla \times \mathbf{b} = \frac{1}{c^2}\frac{\partial \mathbf{e}^{\perp}}{\partial t} + \mu_0 \mathbf{j}^{\perp}. \tag{1.4.10}$$

In the Coulomb gauge, there is no longitudinal component of the vector potential and no transverse component of the scalar potential, which allows complete characterisation of the electric and magnetic fields in terms of the underlying potentials:

$$\mathbf{e}^{\|} = -\nabla \phi; \tag{1.4.11}$$

$$\mathbf{e}^{\perp} = -\frac{\partial \mathbf{a}}{\partial t}; \tag{1.4.12}$$

$$\mathbf{b}^{\|} = 0; \tag{1.4.13}$$

$$\mathbf{b}^{\perp} = \nabla \times \mathbf{a}. \tag{1.4.14}$$

Thus, using Eq. (1.4.2), allows decoupling of the vector potential and the transverse current from the scalar potential and the longitudinal current. Eq. (1.4.4) and (1.4.3)

become:

$$\left(\nabla^2 - \frac{1}{c^2}\frac{\partial^2}{\partial t^2}\right)\mathbf{a} = -\mu_0 \mathbf{j}^{\perp}; \tag{1.4.15}$$

$$\nabla^2 \phi = \frac{1}{\varepsilon_0}\int \nabla \cdot \mathbf{j}^{\parallel} dt, \tag{1.4.16}$$

where the integral is over the time period considered. Thus, the scalar potential, ϕ, is the electrostatic potential energy and, for example, relates to the force between bound electrons and the charges in the nuclei of atoms and molecules; whereas the vector potential, $\mathbf{a}$, describes the radiation field, as ϕ disappears beyond a set of charges that is overall electrically neutral. This separation is unique in the Coulomb gauge and will prove to be useful in considering physical situations in which the radiation is coupled to slow-moving optical centres – atoms and molecules. It will be shown that the QED Hamiltonian in the Coulomb gauge lends itself to a perturbation theory based on small modifications to the Schrödinger wave equation relating to the motion of the atoms and molecules.

1.5. Lagrangian Formulation

There are no extra assumptions in quantum field theory, compared to quantum mechanics: The prescription is simply to take a classical field and apply the principles of quantum mechanics to it. In the case of electrodynamics, the classical field equations are Maxwell's equations, Eq. (1.2.1) - (1.2.4) and we can pick a Lagrangian density that leads, via the Euler-Lagrange equations of motion

$$\frac{\partial}{\partial t}\left(\frac{\partial \mathcal{L}}{\partial \dot{a}_i}\right)+\sum_j \frac{\partial}{\partial x_j}\frac{\partial \mathcal{L}}{\partial\left(\partial a_i/\partial x_j\right)}-\frac{\partial \mathcal{L}}{\partial a_i}=0, \tag{1.5.1}$$

to the correct classical description of the fields. Here, $\mathcal{L}$ is the *Lagrangian density*, which is integrated over space-time to obtain the action, whose minimum value signifies the classical path. Precisely, the action is a *functional*, i.e. a map from a vector space (set of functions) to its underlying scalar field [47]. This becomes particularly important when considering the *path integral formulation* of quantum fields, which can be done for quantum electrodynamics [48,49]. The Lagrangian density is related to the Lagrangian by:

$$\mathrm{L}=\int \mathcal{L}\,\partial \mathrm{t}, \tag{1.5.2}$$

and is often used in relativistic theories instead of the Lagrangian because of the manifest Lorentz invariance. Precisely, Eq. (1.5.1) arises from the principle of stationary action (Hamilton's principle):

$$\delta S=\delta\int_{t_1}^{t_2}\int_{\mathbf{r}_1}^{\mathbf{r}_2}\mathcal{L}\,\mathrm{d}^3\mathbf{r}\mathrm{d}t=0. \tag{1.5.3}$$

At this juncture it is worthwhile to consider the parameters of the Lagrangian density; of course, in classical mechanics Hamilton's principle is equivalent to saying that a particle calculates the action for all possible paths and takes the path for which it is least. Therefore, one would expect the Lagrangian to be dependant on the current space-time coordinates and the future space-time coordinates. In the former case, this

is true; the generalised coordinates for the electromagnetic field will be shown to be $\mathbf{a}$, the vector potential. However, one can connect the current coordinates with the future ones by use of infinitesimal changes in these coordinates: precisely, the derivatives with respect to each space interval and the one time interval. The Lagrangian density is therefore expressed as:

$$\mathcal{L} = \left(\mathbf{a}, \nabla\mathbf{a}, \partial\mathbf{a}/\partial t\right). \tag{1.5.4}$$

In a fully covariant formalism, the space and time derivatives can be compactly written as:

$$\partial^{\mu}\partial_{\mu}\mathbf{a}, \tag{1.5.5}$$

where the Greek index indicates summing over the four components of a space-time, and the upper and lower indices are related by the Minkowski metric [50].

It emerges that the Lagrangian density for quantum electrodynamics is expressed as:

$$\mathcal{L} = \underbrace{\sum_{n} m_n \dot{\mathbf{q}}_n}_{\text{particles}} + \underbrace{\mathbf{a}\cdot\mathbf{j} - \phi\rho}_{\text{interaction}} + \underbrace{\frac{\varepsilon_0}{2}\left\{\left(\frac{\partial\mathbf{a}}{\partial t} + \nabla\phi\right)^2 - c^2\left(\nabla\times\mathbf{a}\right)^2\right\}}_{\text{radiation}}, \tag{1.5.6}$$

where $m_n\mathbf{q}_n$ is the generalised momentum of particle n. The Lagrangian density can be written as the sum of three independent terms for the particles, radiation and their interaction,

$$\mathcal{L} = \mathcal{L}_{\text{part}} + \mathcal{L}_{\text{rad}} + \mathcal{L}_{\text{int}}. \tag{1.5.7}$$

In free space the Lagrangian density, Eq. (1.5.6), reduces to:

$$\mathcal{L} = \frac{\varepsilon_0}{2}\left(\frac{\partial \mathbf{a}}{\partial t}\right)^2 - \frac{1}{2\mu_0}\left(\nabla \times \mathbf{a}\right)^2, \tag{1.5.8}$$

which, from Eq. (1.4.11) – (1.4.14), is equivalent to:

$$\mathcal{L} = \frac{\varepsilon_0}{2}\left(\mathbf{e}^{\perp}\right)^2 - \frac{1}{2\mu_0}\left(\mathbf{b}^{\parallel}\right)^2. \tag{1.5.9}$$

It is readily verified that these Lagrangian densities lead, through use of Eq. (1.5.1), to the wave equation governing **a**, Eq. (1.4.15), in a free field and Maxwell's equations. This confirms, at least for a charge-free region, our choice of Lagrangian density. Furthermore, if we apply the Euler-Lagrange equation for a system of particles, instead of that for a field, the equation for the Lorentz force emerges.

There are various methods for quantising the Lagrangian of a physical system; however, except for the simplest systems [51–53], exact solutions are generally intractable. The next section is concerned with the conversion of the Lagrangian formalism to one focussing on a Hamiltonian, which lends itself more easily to perturbative solutions for complex systems.

1.6. The Minimal Coupling Hamiltonian

In the particle picture, the generalised coordinates are labelled $\mathbf{q}_n$, with the canonically conjugate momentum density given by:

$$\mathcal{p}_n = \frac{\partial \mathcal{L}}{\partial \dot{\mathbf{q}}_n}, \tag{1.6.1}$$

where we have used $\mathcal{p}$ to denote the momentum density. Note, that this is a density because we use the Lagrangian density in the definition; indeed, if we use the Lagrangian, then we would obtain the particle's momentum. Analogously, in the field picture the momentum density is obtained by the definition:

$$\mathbf{\Pi}(\mathbf{r}) = \frac{\partial \mathcal{L}}{\partial \dot{\mathbf{a}}}. \tag{1.6.2}$$

It is preferable to use densities in quantum field theory to avoid unnecessary infinities: commonly, the infrared and ultraviolet divergences [54]. To obtain the explicit forms of the canonically conjugate momentum densities, we proceed by substituting Eq. (1.5.6) into Eq. (1.6.1) and (1.6.2) revealing

$$\mathcal{p}_n = m_n \dot{\mathbf{q}}_n + e_n \mathbf{a}(\mathbf{q}_n), \tag{1.6.3}$$

and

$$\mathbf{\Pi} = \varepsilon_0 \frac{\partial \mathbf{a}}{\partial t} + \nabla \phi, \tag{1.6.4}$$

respectively. Here, the field $\mathbf{a}(\mathbf{q}_n)$ is explicitly evaluated at position $\mathbf{q}_n$. The Hamiltonian density is now obtained from the Lagrangian density by [6]:

$$\mathscr{H} = \sum_n \boldsymbol{p}_n \cdot \dot{\mathbf{q}}_n + \mathbf{\Pi} \cdot \frac{\partial \mathbf{a}}{\partial t} - \mathscr{L}. \tag{1.6.5}$$

We proceed by substituting into Eq. (1.6.5) the expressions for the momentum densities, Eq. (1.6.3) and (1.6.4), and the Lagrangian density, Eq. (1.5.6):

$$\begin{aligned} \mathscr{H} = & \sum_n \frac{\boldsymbol{p}_n}{m_n} \cdot \left\{ \boldsymbol{p}_n - e_n \mathbf{a}(\mathbf{q}_n) \right\} - \sum_n \frac{1}{2m_n} \left\{ \boldsymbol{p}_n - e_n \mathbf{a}(\mathbf{q}_n) \right\}^2 \\ & - \sum_n \frac{e_n}{m_n} \mathbf{a}(\mathbf{q}_n) \cdot \left\{ \boldsymbol{p}_n - e_n \mathbf{a}(\mathbf{q}_n) \right\} + \phi \rho \\ & + \frac{1}{\varepsilon_0} \mathbf{\Pi} \left\{ \mathbf{\Pi} - \varepsilon_0 \nabla \phi \right\} - \frac{1}{2\varepsilon_0} \left\{ \mathbf{\Pi}^2 - \varepsilon_0^2 c^2 (\nabla \times \mathbf{a})^2 \right\}. \end{aligned} \tag{1.6.6}$$

Under the assumption that the fields tend to zero at infinity we can integrate Eq. (1.6.6) over all space to obtain the Hamiltonian:

$$\begin{aligned} H &= \int \mathscr{H} \partial^3 \mathbf{r} \\ &= \frac{1}{2} \sum_n \frac{1}{m_n} \left(\mathbf{p}_n - e_n \mathbf{a}(\mathbf{q}_n) \right)^2 + \frac{1}{2\varepsilon_0} \int \left\{ \mathbf{\Pi}^2 + \varepsilon_0^2 c^2 (\nabla \times \mathbf{a})^2 \right\} \mathrm{d}^3 \mathbf{r} + V(\mathbf{q}), \end{aligned} \tag{1.6.7}$$

where $\mathbf{p}_n$ is the momentum of particle n, and $\mathbf{\Pi}$ now represents the field momentum.

A term, $V(\mathbf{q})$ has been added to take account of the total electrostatic potential, and can be divided into:

$$V(\mathbf{q}) = \sum_{\zeta<\zeta'} \{V(\zeta) + V(\zeta;\zeta')\}, \tag{1.6.8}$$

where ζ labels the *optical centre* and the sum is over the range $\zeta < \xi'$ to ensure that there is no double counting. In this context, optical centre refers to an electrically neutral system, such as an atom, molecule or chromophore. Furthermore, $V(\zeta)$ refers to the intramolecular Coulomb binding and $V(\zeta;\zeta')$ refers to the intermolecular energy between particles with labels ζ and ζ'. For the systems considered here – namely atoms and molecules – we can assume that the nuclear motion is negligible. The Hamiltonian, Eq. (1.6.7), is recast with the molecular label, ζ, defining the position of the electron labelled by *n*:

$$\begin{aligned} H_{\min} = \sum_n \sum_{\xi<\xi'} \left\{ \frac{1}{2m_n} \left\{ \mathbf{p}_n(\xi) - e_n \mathbf{a}\left(\mathbf{q}_n(\xi)\right) \right\}^2 + V(\xi) + V(\xi,\xi') \right\} \\ + \frac{1}{2\varepsilon_0} \int \left\{ \mathbf{\Pi}(\mathbf{r})^2 + \varepsilon_0^2 c^2 \left(\nabla \times \mathbf{a}(\mathbf{r}) \right)^2 \right\} \mathrm{d}^3\mathbf{r}. \end{aligned} \tag{1.6.9}$$

The subscript 'min' draws attention to the fact that this is the *minimal coupling* Hamiltonian and corresponds to the transformation:

$$\mathbf{p}_n \to \mathbf{p}_n - e_n \mathbf{a}_n, \tag{1.6.10}$$

which is called the *Principle of Minimal Coupling*. By applying a canonical

transformation to the minimal coupling Hamiltonian, Eq. (1.6.9) the *multipolar* Hamiltonian can be obtained.

1.7. The Multipolar Hamiltonian

There are various, equivalent, ways to transition from classical theory to a quantum representation: one is by promoting Moyal brackets to commutators [55]. In the following a canonical transformation is applied to the minimal coupling Hamiltonian to obtain the multipolar Hamiltonian and the commutator formalism is used, however a classical version of the derivation can be carried out by the above correspondence. It should be stressed that the two different Hamiltonians are equivalent, in that they will give the same results for describing a physical system. In fact, it has been shown that the two Hamiltonians describe the same electrodynamics, but with different gauge transformations applied [56].

In the quantum formalism, all variables and fields are promoted to operators. In the following the traditional caret placed above variables to denote operators will be omitted, except to eliminate ambiguity. For a general variable in the minimal coupling formalism, $\mathbf{v}_{\min}$, the generalised approach, based on that of Power, Zienau and Wooley, involves the application of a unitary transformation:

$$\mathbf{v}_{multi} = e^{iS}\mathbf{v}_{\min}e^{-iS}, \tag{1.6.11}$$

where the generator, S, is given by:

$$S = \frac{1}{\hbar}\int \mathbf{p}^{\perp}(\mathbf{r})\cdot\mathbf{a}(\mathbf{r})\,d^3\mathbf{r}, \tag{1.6.12}$$

where $\mathbf{p}^{\perp}$ is the transverse component of the polarisation field [25,26,57]. By converting the exponential factors in Eq. (1.6.11) to power series, the multipolar form of the polarisation field can be obtained:

$$\begin{aligned}\mathbf{p}_{n;\text{multi}} &= e^{iS}\mathbf{p}_{n;\text{min}}e^{-iS} \\ &= \mathbf{p}_{n;\text{min}} + i\left[S,\mathbf{p}_{n;\text{min}}\right] - \frac{1}{2}\left[S,\left[S,\mathbf{p}_{n;\text{min}}\right]\right] + \ldots\end{aligned} \tag{1.6.13}$$

The commutator, $\left[S,\mathbf{p}_{n;\text{min}}\right]$, commutes with S, thus the remaining expression is:

$$\mathbf{p}_{n;\text{multi}} = \mathbf{p}_{n;\text{min}} + i\left[S,\mathbf{p}_{n;\text{min}}\right]. \tag{1.6.14}$$

We proceed by using the expression:

$$\mathbf{p}(\mathbf{r}) = -e\sum_{n}(\mathbf{q}_n - \mathbf{R})\int_0^1 \delta\left(\mathbf{r} - \mathbf{R} - \lambda(\mathbf{q}_n - \mathbf{R})\right)\mathrm{d}\lambda, \tag{1.6.15}$$

where $\delta(\mathbf{r})$ is the Dirac delta function [57]. This allows Eq. (1.6.14) to be rewritten as:

$$\mathbf{p}_{n;\text{multi}} = \mathbf{p}_{n;\text{min}} - \frac{ie}{\hbar}\left[\int\left\{\sum_n(\mathbf{q}_n-\mathbf{R})\int_0^1\delta\big(\mathbf{r}-\mathbf{R}-\lambda(\mathbf{q}_n-\mathbf{R})\big)\mathrm{d}\lambda\cdot\mathbf{a}(\mathbf{r})\right\}d^3\mathbf{r},\mathbf{p}_{n;\text{min}}\right]. \quad (1.6.16)$$

We proceed by explicitly referring to the components of the vectors,

$$\begin{aligned} p_{n;\text{multi};i} = p_{n;\text{min};i} &+ e\int_0^1 a_i(\mathbf{r})\left(1+\lambda\frac{\mathrm{d}}{\mathrm{d}\lambda}\right)\delta\big(\mathbf{r}-\mathbf{R}-\lambda(\mathbf{q}-\mathbf{R})\big) \\ &+ e\big(\nabla_i a_j(\mathbf{r})-\nabla_j a_i(\mathbf{r})\big)(\mathbf{q}-\mathbf{R})_j\,\lambda\delta\big(\mathbf{r}-\mathbf{R}-\lambda(\mathbf{q}-\mathbf{R})\big)\mathrm{d}\lambda\mathrm{d}^3\mathbf{r}, \end{aligned} \quad (1.6.18)$$

where we have used the identities for any function, f [48]:

$$\left.\begin{aligned} \big[f(q_i),p_i\big] &= \mathrm{i}\hbar\frac{\partial f(q_i)}{\partial q_i} \\ \frac{\partial}{\partial a_i}f(\mathbf{r}-\lambda\mathbf{a}) &= -\lambda\big\{\nabla f(\mathbf{r}-\lambda\mathbf{a})\big\}_i \\ a_i\frac{\partial}{\partial a_i}f(\mathbf{r}-\lambda\mathbf{a}) &= \lambda\frac{\mathrm{d}}{\mathrm{d}\lambda}f(\mathbf{r}-\lambda\mathbf{a}) \end{aligned}\right\} \quad (1.6.19)$$

Solving Eq. (1.6.18) and restoring the bold vector notation gives:

$$\begin{aligned} \mathbf{p}_{n;\text{multi}} &= \mathbf{p}_{n;\text{min}} + e\mathbf{a}(\mathbf{q}) \\ &- \int\left\{-e(\mathbf{q}-\mathbf{R})\int_0^1\lambda\delta\big(\mathbf{r}-\mathbf{R}-\lambda(\mathbf{q}-\mathbf{R})\big)\mathrm{d}\lambda\right\}\times\big\{\nabla\times\mathbf{a}(\mathbf{r})\big\}d^3\mathbf{r}, \end{aligned} \quad (1.6.20)$$

With the goal of constructing the multipolar Hamiltonian, we calculate the expression for the multipolar field momentum:

$$\begin{aligned}\boldsymbol{\Pi}_{\text{multi}} &= e^{is}\boldsymbol{\Pi}_{\text{min}}e^{-iS} \\ &= \boldsymbol{\Pi}_{\text{multi}} + \frac{\mathrm{i}}{\hbar}\left[\int \mathbf{p}^{\perp}(\mathbf{r}')\cdot\mathbf{a}(\mathbf{r}')\,\mathrm{d}^3\mathbf{r}', \boldsymbol{\Pi}_{\text{min}}(\mathbf{r})\right] \\ &= \boldsymbol{\Pi}_{\text{min}}(\mathbf{r}) - \mathbf{p}^{\perp}(\mathbf{r}),\end{aligned} \tag{1.6.21}$$

where we have used the same reasoning for discarding the higher-order commutator brackets as in Eq. (1.6.13), and deployed the quantum commutation relation for conjugate pairs:

$$\left[\mathbf{a}(\mathbf{r}), \boldsymbol{\Pi}(\mathbf{r}')\right] = i\hbar\delta(\mathbf{r}-\mathbf{r}'). \tag{1.6.22}$$

Thus, we may now construct the multipolar Hamiltonian, from Eq. (1.6.9), (1.6.20) and (1.6.21):

$$\begin{aligned}&H_{\text{multi}} = \\ &\sum_{\substack{n \\ \zeta<\zeta'}}\left\{\frac{1}{2m_n}\left(\mathbf{p}_n(\zeta) - \int\left(\nabla\times\mathbf{a}(\mathbf{r})\right)\times e(\mathbf{q}-\mathbf{R})\int_0^1 \lambda\delta\left(\mathbf{r}-\mathbf{R}-\lambda(\mathbf{q}-\mathbf{R})\right)\mathrm{d}\lambda d^3\mathbf{r}\right)^2\right. \\ &\left.+V(\zeta)+V(\zeta;\zeta')\right\} + \frac{1}{2\varepsilon_0}\int\left\{\left(\boldsymbol{\Pi}(\mathbf{r})+\mathbf{p}^{\perp}(\mathbf{r})\right)^2 + \varepsilon_0^2c^2\left(\nabla\times\mathbf{a}(\mathbf{r})\right)^2\right\}d^3\mathbf{r}.\end{aligned} \tag{1.6.23}$$

To put Eq. (1.6.23) into a form with explicit dependence on multipoles, we expand the brackets and correspondingly identify the importance of each term. However, for the sake of clarity, we compartmentalise the Hamiltonian into terms representing the particles, interaction, radiation and self energy, respectively:

$$H_{\text{part}} = \sum_{\substack{n \\ \zeta<\zeta'}}\left\{\frac{1}{2m_n}\left(\mathbf{p}_n(\zeta)\right)^2 + V(\zeta) + V(\zeta;\zeta')\right\}; \tag{1.6.24}$$

$$H_{\text{self}} = \frac{1}{2\varepsilon_0}\int \left(\mathbf{p}^{\perp}(\mathbf{r})\right)^2 d^3\mathbf{r}. \tag{1.6.25}$$

$$\begin{aligned} H_{\text{int}} = {} & \frac{1}{\varepsilon_0}\int \boldsymbol{\Pi}(\mathbf{r})\cdot\mathbf{p}^{\perp}(\mathbf{r})\,d^3\mathbf{r} + \\ & \int \sum_{\substack{n \\ \zeta<\zeta'}} \left\{ \frac{1}{2m_n}\left(\left(\nabla\times\mathbf{a}(\mathbf{r})\right)\times e(\mathbf{q}-\mathbf{R}) \int_0^1 \lambda\delta\left(\mathbf{r}-\mathbf{R}-\lambda(\mathbf{q}-\mathbf{R})\right) \right)^2 \mathrm{d}\lambda d^3\mathbf{r} - \right. \\ & \int \sum_{n,\xi} \left\{ \frac{1}{2m_n}\mathbf{p}_n(\xi)\cdot\left(\left(\nabla\times\mathbf{a}(\mathbf{r})\right)\times e(\mathbf{q}-\mathbf{R}) \int_0^1 \lambda\delta\left(\mathbf{r}-\mathbf{R}-\lambda(\mathbf{q}-\mathbf{R})\right)\mathrm{d}\lambda \right) \right\} \mathrm{d}^3\mathbf{r} - \\ & \left. \int \sum_{n,\xi} \left\{ \frac{1}{2m_n}\left(\left(\nabla\times\mathbf{a}(\mathbf{r})\right)\times e(\mathbf{q}-\mathbf{R}) \int_0^1 \lambda\delta\left(\mathbf{r}-\mathbf{R}-\lambda(\mathbf{q}-\mathbf{R})\right)\mathrm{d}\lambda \right)\cdot\mathbf{p}_n(\xi) \right\} \mathrm{d}^3\mathbf{r}; \end{aligned} \tag{1.6.26}$$

$$H_{\text{rad}} = \frac{1}{2\varepsilon_0}\int \left\{ \left(\boldsymbol{\Pi}(\mathbf{r})\right)^2 + \varepsilon_0^2 c^2 \left(\nabla\times\mathbf{a}(\mathbf{r})\right)^2 \right\} d^3\mathbf{r}; \tag{1.6.27}$$

Assuming that the electron fields are bound by the molecules, and that there are no free charges, allows separation of $\mathbf{p}^{\perp}$ into parts, $\mathbf{p}_{\zeta}^{\perp}$, belonging to each optical centre. Thus the intermolecular part of the self energy corresponds to the overlap of the $\mathbf{p}_{\zeta}^{\perp}$ of each source:

$$\begin{aligned} H_{\text{self}}^{\text{inter}} &= \left[\frac{1}{2\varepsilon_0}\int \left(\mathbf{p}^{\perp}(\mathbf{r})\right)^2 d^3\mathbf{r} \right]^{\text{inter}} = \sum_{\zeta,\zeta'} \frac{1}{2\varepsilon_0}\int \mathbf{p}_{\zeta}^{\perp}(\mathbf{r})\cdot\mathbf{p}_{\zeta'}^{\perp}(\mathbf{r})\,d^3\mathbf{r} \\ &= \sum_{\zeta<\zeta'} \frac{1}{\varepsilon_0}\int \mathbf{p}_{\zeta}^{\perp}(\mathbf{r})\cdot\mathbf{p}_{\zeta'}^{\perp}(\mathbf{r})\,d^3\mathbf{r} \\ &= -\sum_{\zeta<\zeta'} V(\zeta;\zeta'), \end{aligned} \tag{1.6.28}$$

and exactly cancels the electrostatic intermolecular interaction [6]. Therefore, the potential energy between optical centres is not conveyed instantaneously but through

the retarded mediation of the radiation field. The remaining part of the self-energy Hamiltonian of the system, Eq. (1.6.25), is negligible in radiative processes, and is henceforth ignored. It does, however, play an important role in self-energy calculations [58,59]. Introducing the definition of the auxiliary displacement field:

$$\mathbf{d}(\mathbf{r}) = \varepsilon_0 \mathbf{e}(\mathbf{r}) + \mathbf{p}(\mathbf{r}), \tag{1.6.29}$$

allows comparison with:

$$\mathbf{\Pi}(\mathbf{r}) = -\varepsilon_0 \mathbf{e}^{\perp}(\mathbf{r}) - \mathbf{p}^{\perp}(\mathbf{r}), \tag{1.6.30}$$

to deliver:

$$\mathbf{\Pi}(\mathbf{r}) = -\mathbf{d}^{\perp}(\mathbf{r}), \tag{1.6.31}$$

which can be substituted into Eq. (1.6.26) along with the explicit (component indexed) multipole expansion of $\mathbf{p}^{\perp}(\mathbf{r})$,

$$p_i^{\perp}(\mathbf{r}) = \sum_{\xi} \left\{ \delta_{ij}^{\perp}(\mathbf{r} - \mathbf{R}_{\xi}) \mu_j(\xi) - \delta_{ij}^{\perp}(\mathbf{r} - \mathbf{R}_{\xi}) Q_{jk}^{\text{elec}}(\xi) \nabla_k + \ldots \right\}, \tag{1.6.32}$$

where μ_i, Q_{ij} represent the electric dipole and quadrupole moments and the magnetisation field:

$$\begin{aligned}\mathbf{m}(\mathbf{r}) &= \sum_{n,\xi}\frac{1}{2m_n}\left\{\mathbf{p}_n(\xi)\times e(\mathbf{q}-\mathbf{R})\int_0^1 \lambda\delta\big(\mathbf{r}-\mathbf{R}-\lambda(\mathbf{q}-\mathbf{R})\big)\mathrm{d}\lambda\right.\\ &\left.\quad -e(\mathbf{q}-\mathbf{R})\int_0^1 \lambda\delta\big(\mathbf{r}-\mathbf{R}-\lambda(\mathbf{q}-\mathbf{R})\big)\mathrm{d}\lambda\times\mathbf{p}_n(\xi)\right\}\\ &= -\sum_{n,\xi}\frac{1}{m_n}e(\mathbf{q}-\mathbf{R})\int_0^1 \lambda\delta\big(\mathbf{r}-\mathbf{R}-\lambda(\mathbf{q}-\mathbf{R})\big)\mathrm{d}\lambda\times\mathbf{p}_n(\xi)\\ &= -\sum_{n,\xi}e(\mathbf{q}-\mathbf{R})\int_0^1 \lambda\delta\big(\mathbf{r}-\mathbf{R}-\lambda(\mathbf{q}-\mathbf{R})\big)\mathrm{d}\lambda\times\frac{\partial\mathbf{q}_n(\xi)}{\partial t}.\end{aligned} \tag{1.6.33}$$

This can now be written in terms of magnetic multipole moments,

$$m_i(\mathbf{r}) = \sum_\zeta m_i\delta\big(\mathbf{r}-\mathbf{R}_\zeta\big) - \sum_\zeta Q_{ij}^{\mathrm{mag}}\nabla_j\delta\big(\mathbf{r}-\mathbf{R}_\zeta\big)+\ldots \tag{1.6.34}$$

We are now in a position to write Eqs. (1.6.24)-(1.6.27) in a more identifiable form:

$$H_{\mathrm{part}} = \sum_{n;\zeta}\left\{\frac{1}{2m_n}\big(\mathbf{p}_n(\zeta)\big)^2 + V(\zeta)\right\}; \tag{1.6.35}$$

$$H_{\mathrm{int}} = -\frac{1}{\varepsilon_0}\sum_\xi\left\{\mu_i(\xi)d_i^\perp\big(\mathbf{R}_\xi\big) - Q_{ij}(\xi)\nabla_i d_j^\perp\big(\mathbf{R}_\xi\big) - m_i(\xi)b_i\big(\mathbf{R}_\xi\big)+\ldots\right\}; \tag{1.6.36}$$

$$H_{\mathrm{rad}} = \frac{1}{2\varepsilon_0}\int\left\{\mathbf{d}^\perp(\mathbf{r})^2 + \varepsilon_0^2c^2\mathbf{b}(\mathbf{r})^2\right\}\mathrm{d}^3\mathbf{r}; \tag{1.6.37}$$

$$H_{\mathrm{self}} \approx 0. \tag{1.6.38}$$

It is worth noting that couplings involving magnetic dipole and electric quadrupole moments, when they are both allowed, are of similar magnitude and much less significant than electric dipole interactions [60].

1.8.Quantisation

"Physics is that subset of human experience which can be reduced to coupled harmonic oscillators" - Michael Peskin[†]

As mentioned above, the transition from classical mechanics to quantum mechanics can be enacted by promoting the field vectors to operators; and the transition in field theory is no different. By the promotion,

$$\mathbf{p}_n \to -i\hbar \frac{\partial}{\partial \mathbf{q}_n}, \tag{1.8.1}$$

the matter Hamiltonian, Eq. (1.6.35), acts on the quantum state of a physical system to deliver:

$$H_{\text{part}} |\psi\rangle = \sum_{n;\zeta} \left(\frac{\hbar^2}{2m_n} \nabla_n^2 + V(\zeta) \right) |\psi\rangle = E|\psi\rangle, \tag{1.8.2}$$

which is the Schrödinger wave-equation for a many-particle system [61]. This is identical to a semi-classical treatment of electrodynamics. Thus, the radiation Hamiltonian, Eq. (1.6.37), is neglected in semi-classical theory, and the interaction Hamiltonian is introduced as a perturbation on the stationary atomic and molecular states.

[†]Tong, David, *Classical Dynamics* (Cambridge University Part II Mathematical Tripos 2004).

In the Coulomb gauge, the vector potential, **a**, satisfies a free-field wave equation, Eq. (1.4.15), which allows the solutions to be written as a complete set of plane waves, through a discrete Fourier decomposition:

$$\mathbf{a}(\mathbf{r},t)=\sum_{\mathbf{k},\lambda}\left\{\mathbf{e}^{(\lambda)}(\mathbf{k})\,a^{(\lambda)}(\mathbf{k},t)\,\mathrm{e}^{\mathrm{i}\mathbf{k}\cdot\mathbf{r}}+\overline{\mathbf{e}}^{(\lambda)}(\mathbf{k})\,\overline{a}^{(\lambda)}(\mathbf{k},t)\,\mathrm{e}^{-\mathrm{i}\mathbf{k}\cdot\mathbf{r}}\right\}, \tag{1.8.3}$$

where $\mathbf{e}^{(\lambda)}(\mathbf{k})$ is the (electric) unit polarisation vector, and $a^{(\lambda)}(\mathbf{k},t)=e^{-ic|\mathbf{k}|t}$ is the time dependent amplitude; here overbar denotes the complex conjugate [6]. Furthermore, $\mathbf{k}$ and λ are labels representing the wavevector and the polarisation respectively, characterising plane wave modes unambiguously. The expressions for the corresponding electric and magnetic field vectors can be determined from Eqs.(1.4.14) and (1.4.12):

$$\mathbf{e}(\mathbf{r},t)=\sum_{\mathbf{k},\lambda}\mathrm{i}ck\left\{\mathbf{e}^{(\lambda)}(\mathbf{k})\,a^{(\lambda)}(\mathbf{k},t)\,\mathrm{e}^{\mathrm{i}\mathbf{k}\cdot\mathbf{r}}-\overline{\mathbf{e}}^{(\lambda)}(\mathbf{k})\,\overline{a}^{(\lambda)}(\mathbf{k},t)\,\mathrm{e}^{-\mathrm{i}\mathbf{k}\cdot\mathbf{r}}\right\}; \tag{1.8.4}$$

$$\begin{aligned}\mathbf{b}(\mathbf{r},t)&=\sum_{\mathbf{k},\lambda}\mathrm{i}k\left\{\left(\mathbf{k}\times\mathbf{e}^{(\lambda)}(\mathbf{k})\right)a^{(\lambda)}(\mathbf{k},t)\,\mathrm{e}^{\mathrm{i}\mathbf{k}\cdot\mathbf{r}}-\left(\overline{\mathbf{k}}\times\overline{\mathbf{e}}^{(\lambda)}(\mathbf{k})\right)\overline{a}^{(\lambda)}(\mathbf{k},t)\,\mathrm{e}^{-\mathrm{i}\mathbf{k}\cdot\mathbf{r}}\right\}\\&=\sum_{\mathbf{k},\lambda}\mathrm{i}k\left\{\mathbf{b}^{(\lambda)}(\mathbf{k})\;a^{(\lambda)}(\mathbf{k},t)\,\mathrm{e}^{\mathrm{i}\mathbf{k}\cdot\mathbf{r}}-\overline{\mathbf{b}}^{(\lambda)}(\mathbf{k})\;\overline{a}^{(\lambda)}(\mathbf{k},t)\,\mathrm{e}^{-\mathrm{i}\mathbf{k}\cdot\mathbf{r}}\right\},\end{aligned} \tag{1.8.5}$$

where $\mathbf{b}^{(\lambda)}(\mathbf{k})=\mathbf{k}\times\mathbf{e}^{(\lambda)}(\mathbf{k})$ is the magnetic polarisation vector and $\{\mathbf{e},\mathbf{b},\mathbf{k}\}$ are a right-handed orthogonal triad.

To avoid the infinity known as the infrared divergence [62], we carefully quantize the vector potential by considering a region of space and impose a periodic boundary condition, as done for quantum treatments of a particle in a potential well.

Without loss of generality, we choose the volume considered to be a cube of length L, with the allowed values of the Cartesian components of $\boldsymbol{k}$ given by:

$$k_i = n_i\left(\frac{2\pi}{L}\right), \tag{1.8.6}$$

where $n_i \in \mathbb{Z}$ is an integer. Thus the vector potential, and associated fields, gets promoted to operator form through the following relations:

$$(\varepsilon_0 V)^{\frac{1}{2}}\, a(\mathbf{k},t) \to \left(\frac{\hbar}{2ck}\right)^{\frac{1}{2}} a^{(\lambda)}(\mathbf{k}); \tag{1.8.7}$$

$$(\varepsilon_0 V)^{\frac{1}{2}}\, \overline{a}(\mathbf{k},t) \to \left(\frac{\hbar}{2ck}\right)^{\frac{1}{2}} a^{\dagger(\lambda)}(\mathbf{k}), \tag{1.8.8}$$

where $a^{(\lambda)}(\mathbf{k})$ and $a^{\dagger(\lambda)}(\mathbf{k})$ are the Hermitian conjugate annihilation and creation operators, respectively, and the time dependence has been moved to the state vectors, as in the Schrödinger picture. The promotions, Eq. (1.8.7) and (1.8.8), can equally be applied to the case of light fields with polarisation vectors not necessarily orthogonal to the propagation direction (*non-paraxial light*), and is discussed in Chapters 3 and 4. The annihilation and creation operators for a single mode $(\mathbf{k},\lambda)$ act only on that radiation mode, so that their behaviour with respect to number states (Fock states) with population n is given as:

$$\begin{aligned} &a^{(\lambda_m)}(\mathbf{k}_m)\left|n_1(\mathbf{k}_1,\lambda_1),n_2(\mathbf{k}_2,\lambda_2),\ldots,n_m(\mathbf{k}_m,\lambda_m)\right\rangle \\ &\quad=\sqrt{n_m}\left|n_1(\mathbf{k}_1,\lambda_1),n_2(\mathbf{k}_2,\lambda_2),\ldots,(n_m-1)(\mathbf{k}_m,\lambda_m)\right\rangle; \end{aligned} \tag{1.8.9}$$

$$\begin{aligned} &a^{\dagger(\lambda_m)}(\mathbf{k}_m)\left|n_1(\mathbf{k}_1,\lambda_1),n_2(\mathbf{k}_2,\lambda_2),\ldots,n_m(\mathbf{k}_m,\lambda_m)\right\rangle \\ &=\sqrt{n_m+1}\left|n_1(\mathbf{k}_1,\lambda_1),n_2(\mathbf{k}_2,\lambda_2),\ldots,(n_m+1)(\mathbf{k}_m,\lambda_m)\right\rangle, \end{aligned} \tag{1.8.10}$$

where the states with $n_i=0$ are usually omitted. That is, radiation modes in their ground state are ignored unless they are explicitly involved in the interaction. The operators $a^{(\lambda_m)}(\mathbf{k}_m)$ and $a^{\dagger(\lambda_m)}(\mathbf{k}_m)$ alone are not Hermitian, whereas the number operator $a^{\dagger(\lambda_m)}(\mathbf{k}_m)a^{(\lambda_m)}(\mathbf{k}_m)=N^{(\lambda_m)}(\mathbf{k}_m)$ is and acts on a number state as follows:

$$\begin{aligned} &a^{\dagger(\lambda_m)}(\mathbf{k}_m)a^{(\lambda_m)}(\mathbf{k}_m)\left|n_1(\mathbf{k}_1,\lambda_1),n_2(\mathbf{k}_2,\lambda_2),\ldots,n_m(\mathbf{k}_m,\lambda_m)\right\rangle \\ &\qquad=n_m\left|n_1(\mathbf{k}_1,\lambda_1),n_2(\mathbf{k}_2,\lambda_2),\ldots,n_m(\mathbf{k}_m,\lambda_m)\right\rangle, \end{aligned} \tag{1.8.11}$$

which implies a non-zero expectation value for the number operator of that particular mode. Hence, by employing the promotions prescribed in Eq. (1.8.7) and (1.8.8) we obtain the fully quantised expressions for the components of the electromagnetic fields:

$$\begin{aligned} \mathbf{d}^{\perp}(\mathbf{r})&=\varepsilon_0\mathbf{e}(\mathbf{r})=-\boldsymbol{\Pi}(\mathbf{r}) \\ &=\mathrm{i}\sum_{\mathbf{k},\lambda}\left(\frac{\hbar ck\varepsilon_0}{2V}\right)^{\frac{1}{2}}\left\{\mathbf{e}^{(\lambda)}(\mathbf{k})a^{(\lambda)}(\mathbf{k})\mathrm{e}^{\mathrm{i}\mathbf{k}\cdot\mathbf{r}}-\overline{\mathbf{e}}^{(\lambda)}(\mathbf{k})a^{\dagger(\lambda)}(\mathbf{k})\mathrm{e}^{-\mathrm{i}\mathbf{k}\cdot\mathbf{r}}\right\}; \end{aligned} \tag{1.8.12}$$

$$\mathbf{b}(\mathbf{r})=\mathrm{i}\sum_{\mathbf{k},\lambda}\left(\frac{\hbar k}{2\varepsilon_0 cV}\right)^{\frac{1}{2}}\left\{\mathbf{b}^{(\lambda)}(\mathbf{k})a^{(\lambda)}(\mathbf{k})\mathrm{e}^{\mathrm{i}\mathbf{k}\cdot\mathbf{r}}-\overline{\mathbf{b}}^{(\lambda)}(\mathbf{k})a^{\dagger(\lambda)}(\mathbf{k})\mathrm{e}^{-\mathrm{i}\mathbf{k}\cdot\mathbf{r}}\right\}. \tag{1.8.13}$$

Worthy of note is that the above electromagnetic operators are valid in the free-field; and that due consideration of the surrounding molecules in condensed phase systems delivers operators corresponding to *medium-dressed* photons, known as *polaritons* [63]. Application of the operators, Eq. (1.8.12) and (1.8.13), to the radiation Hamiltonian, Eq. (1.6.37), delivers:

$$H_{\text{rad}} = \sum_{\mathbf{k},\lambda} \left(a^{\dagger(\lambda)}(\mathbf{k}) a^{(\lambda)}(\mathbf{k}) \hbar\omega + \frac{1}{2}\hbar\omega \right), \tag{1.8.14}$$

where $\frac{1}{2}\hbar\omega$ is the *zero-point energy* responsible for many differences between quantum electrodynamics and semi-classical theory, and is a perturbing influence on the stationary states of matter systems.

1.9. Perturbation Theory

The aim of perturbation theory is to derive an expression for an analytically unsolvable mathematical problem in terms of a related *solvable* problem. Precisely, the expression is a power series in a small parameter that is a measure of the variation of the desired problem from the known one. Here, the light-matter interaction is used as a perturbation on the separate unperturbed light and matter Hamiltonians. Thus, perturbation theory fails when the interaction energy exceeds the Coulomb binding energy, holding the atoms and molecules together. In quantum electrodynamics time-dependent perturbation theory begins by dividing the total Hamiltonian into two terms [12]:

$$H = H_0 + H_{\text{int}}, \tag{1.9.1}$$

where H_0 is the unperturbed Hamiltonian,

$$H_0 = H_{\text{part}} + H_{\text{rad}}, \tag{1.9.2}$$

and H_{int} provides the perturbation for the system. Here, H_{part} is the Hamiltonian for a system of particles and H_{rad} is the radiation Hamiltonian. To proceed we convert from the Schrödinger picture to the *interaction picture*, in which both the operator and the state vector contains some of the time dependence of the process, by the following prescription:

$$H_{\text{int;I}}(t) = \mathrm{e}^{\mathrm{i}H_0 t/\hbar} H_{\text{int}} \mathrm{e}^{-\mathrm{i}H_0 t/\hbar}; \tag{1.9.3}$$

$$\left|\psi_{\text{I}}(t)\right\rangle = \mathrm{e}^{\mathrm{i}H_0 t/\hbar}\left|\psi\right\rangle, \tag{1.9.4}$$

where the subscript I denotes the fact that we are working with the interaction picture. Note that, by applying the procedure in Eq. (1.9.3) to the unperturbed Hamiltonian, leaves H_0 unchanged, and thus H_0 can be referred to unambiguously. As the time dependence of a quantum system is governed by the Schrödinger wave equation, Eq. (1.8.2), we reformulate in the interaction picture:

$$\frac{d}{dt}\left|\psi_{\text{I}}(t)\right\rangle = \frac{1}{\mathrm{i}\hbar} H_{\text{int;I}}\left|\psi_{\text{I}}(t)\right\rangle. \tag{1.9.5}$$

Performing the time integration on this equation delivers:

$$\left|\psi_{\mathrm{I}}(t)\right\rangle = \left|\psi_{\mathrm{I}}(t_0)\right\rangle + \int_{t_0}^{t} \frac{1}{\mathrm{i}\hbar} H_{\mathrm{int;I}} \left|\psi_{\mathrm{I}}(t_1)\right\rangle dt_1, \tag{1.9.6}$$

where $\left|\psi_{\mathrm{I}}(t_0)\right\rangle$ is the zero$^{\mathrm{th}}$-order approximation of the wavefunction; the integration is over the dummy variable t_1 and is between the start time t_0 and the final time t. To obtain progressively better approximations we start by deriving the first-order solution from the zero$^{\mathrm{th}}$ order solution by the replacement:

$$\left|\psi_{\mathrm{I}}(t_1)\right\rangle \rightarrow \left|\psi_{\mathrm{I}}(t_0)\right\rangle, \tag{1.9.7}$$

which allows Eq. (1.9.6) to be written as:

$$\left|\psi_{\mathrm{I}}^{(1)}(t)\right\rangle = \left\{1 + \int_{t_0}^{t} \frac{1}{\mathrm{i}\hbar} H_{\mathrm{int;I}}\, dt_1\right\} \left|\psi_{\mathrm{I}}(t_0)\right\rangle, \tag{1.9.8}$$

where the superscript (1) denotes the order of the approximation. The second order solution is now obtained by setting $\left|\psi_{\mathrm{I}}^{(1)}(t)\right\rangle \rightarrow \left|\psi_{\mathrm{I}}(t_1)\right\rangle$ so that Eq. (1.9.6) becomes:

$$\left|\psi_{\mathrm{I}}^{(2)}(t)\right\rangle = \left(1 + \int_{t_0}^{t} \frac{1}{\mathrm{i}\hbar} H_{\mathrm{int;I}}(t_1)\, dt_1 - \frac{1}{\hbar^2} \int_{t_1}^{t} \int_{t_0}^{t_1} H_{\mathrm{int;I}}(t_2)\, H_{\mathrm{int;I}}(t_1)\, dt_1 dt_2\right) \left|\psi_{\mathrm{I}}(t_0)\right\rangle, \tag{1.9.9}$$

where a new dummy variable t_2 has been introduced to ensure correct integration. Thus, we can define the zero$^{\mathrm{th}}$-, first- and second-order time evolution operators as:

$$
\begin{aligned}
U_{\mathrm{I}}^{(1)}(t,t_0) &= 1 \\
U_{\mathrm{I}}^{(2)}(t,t_0) &= \left(1+\int_{t_0}^{t}\frac{1}{\mathrm{i}\hbar}H_{\mathrm{int;I}}(t_1)\,dt_1\right) \\
U_{\mathrm{I}}^{(3)}(t,t_0) &= \left(1+\int_{t_0}^{t}\frac{1}{\mathrm{i}\hbar}H_{\mathrm{int;I}}(t_1)\,dt_1-\frac{1}{\hbar^2}\int_{t_1}^{t}\int_{t_0}^{t_1}H_{\mathrm{int;I}}(t_2)\,H_{\mathrm{int;I}}(t_1)\,dt_1dt_2\right)
\end{aligned}
\tag{1.9.10}
$$

and by iteration we obtain the total time evolution operator as:

$$
\begin{aligned}
U_{\mathrm{I}}(t,t_0) &= 1+\int_{t_0}^{t}\frac{1}{\mathrm{i}\hbar}H_{\mathrm{int;I}}(t_1)\,dt_1-\frac{1}{\hbar^2}\int_{t_1}^{t}\int_{t_0}^{t_1}H_{\mathrm{int;I}}(t_2)\,H_{\mathrm{int;I}}(t_1)\,dt_1dt_2 \\
&-\frac{1}{i\hbar^3}\int_{t_2}^{t}\int_{t_1}^{t_2}\int_{t_0}^{t_1}H_{\mathrm{int;I}}(t_3)\,H_{\mathrm{int;I}}(t_2)\,H_{\mathrm{int;I}}(t_1)\,dt_1dt_2dt_3+\ldots,
\end{aligned}
\tag{1.9.11}
$$

where the n^{th} term is given by:

$$
\left(\frac{1}{i\hbar}\right)^n\int_{t_{n-1}}^{t}\int_{t_{n-2}}^{t_{n-1}}\ldots\int_{t_0}^{t_1}H_{\mathrm{int;I}}(t_n)\ldots H_{\mathrm{int;I}}(t_2)\,H_{\mathrm{int;I}}(t_1)\,dt_1dt_2\ldots dt_n. \tag{1.9.12}
$$

Let us now define the initial $|i\rangle$ and final $|f\rangle$ states of the system, as eigenstates of the H_0 operator with eigenvalues E_i and E_f respectively. Let us further suppose that they are not the same state, i.e. they are orthogonal in the sense that:

$$
\langle f|i\rangle=\delta_{fi}. \tag{1.9.13}
$$

If, as before, $|\psi_{\mathrm{I}}(t)\rangle$ is the state of the system at time t, then the probability amplitude to find the system in state f is the projection:

$$\langle f|\psi_{\mathrm{I}}(t)\rangle = \langle f|U_{\mathrm{I}}(t,t_0)|\psi_{\mathrm{I}}(t_0)\rangle = \langle f|U_{\mathrm{I}}(t,t_0)|i\rangle, \tag{1.9.14}$$

where the final step is a re-labelling of $|\psi_{\mathrm{I}}(t_0)\rangle$. The orthogonality of $|i\rangle$ and $|f\rangle$ means that the first term of $U_{\mathrm{I}}(t,t_0)$ vanishes. Thus, the leading order term for the probability amplitude is:

$$\langle f|U_{\mathrm{I}}(t,t_0)|i\rangle = \frac{1}{\mathrm{i}\hbar}\int_{t_0}^{t}\langle f|\mathrm{e}^{\mathrm{i}H_0 t_1/\hbar}H_{\mathrm{int}}\mathrm{e}^{-\mathrm{i}H_0 t_1/\hbar}|i\rangle dt_1, \tag{1.9.15}$$

where we have converted back the Schrödinger picture, via the prescription in Eq. (1.9.3). Thus, the unperturbed Hamiltonian H_0 may now act on the states to reveal their eigenvalues (energies):

$$\begin{aligned}\langle f|U_{\mathrm{I}}(t,t_0)|i\rangle &= \frac{1}{\mathrm{i}\hbar}\int_{t_0}^{t}\langle f|\mathrm{e}^{\mathrm{i}E_f t_1/\hbar}H_{\mathrm{int}}\mathrm{e}^{-\mathrm{i}E_i t_1/\hbar}|i\rangle dt_1 \\ &= \frac{1}{\mathrm{i}\hbar}\int_{t_0}^{t}\mathrm{e}^{\mathrm{i}(E_f-E_i)t_1/\hbar}dt_1\langle f|H_{\mathrm{int}}|i\rangle \\ &= -\frac{1}{(E_f-E_i)}\left(\mathrm{e}^{\mathrm{i}(E_f-E_i)t/\hbar}-\mathrm{e}^{\mathrm{i}(E_f-E_i)t_0/\hbar}\right)\langle f|H_{\mathrm{int}}|i\rangle,\end{aligned} \tag{1.9.16}$$

where the time integration has been performed. By defining $\Delta t = t - t_0$ we obtain:

$$\langle f|U_{\mathrm{I}}(t,t_0)|i\rangle = -\frac{1}{(E_f-E_i)}\left(\mathrm{e}^{\mathrm{i}(E_f-E_i)\Delta t/\hbar}-1\right)\langle f|H_{\mathrm{int}}|i\rangle\mathrm{e}^{\mathrm{i}(E_f-E_i)t_0/\hbar}, \tag{1.9.17}$$

which, by use of the identity $\mathrm{e}^{\mathrm{i}x}-1 = 2\mathrm{i}\cdot\sin(x/2)\mathrm{e}^{\mathrm{i}x/2}$ (from Euler's formula and the trigonometric half-angle identities), delivers:

$$\langle f|U_{\mathrm{I}}(t,t_0)|i\rangle = -2\mathrm{i}\frac{\langle f|H_{\mathrm{int}}|i\rangle}{(E_f - E_i)}\sin\left(\frac{(E_f - E_i)\Delta t}{2\hbar}\right)\mathrm{e}^{\mathrm{i}(E_f - E_i)(t+t_0)/2\hbar}, \tag{1.9.18}$$

The probability of finding our system in state $|f\rangle$ is given by the square modulus of this result; however, we proceed by taking into account *n* closely neighbouring states, as in practice $|f\rangle$ will have a non-zero width:

$$\sum_n \left|\langle f_n|U_{\mathrm{I}}(t,t_0)|i\rangle\right|^2 = \sum_n 4\left|\langle f_n|H_{\mathrm{int}}|i\rangle\right|^2 \frac{1}{(E_{f_n} - E_i)^2}\sin^2\left(\frac{(E_{f_n} - E_i)\Delta t}{2\hbar}\right). \tag{1.9.19}$$

We assume that the states $|f_n\rangle$ are sufficiently close together to justifiably be considered the same, and only differ in their energies. This means that the summation in Eq. (1.9.19) can be converted to an integral over the continuum of energies E_{f_n}:

$$\left|\langle f|U_{\mathrm{I}}(t,t_0)|i\rangle\right|^2 = 4\left|\langle f|H_{\mathrm{int}}|i\rangle\right|^2 \int_{-\infty}^{\infty} \frac{1}{(E_{f_n} - E_i)^2}\sin^2\left(\frac{(E_{f_n} - E_i)\Delta t}{2\hbar}\right)\rho_f\, dE_{f_n}, \tag{1.9.20}$$

where ρ_f is the density of final states, and fortunately the integral is analytically tractable with help from the identity:

$$\int_{-\infty}^{\infty} \frac{\sin^2(ax)}{(ax)^2}dx = a\pi. \tag{1.9.21}$$

Thus,

$$\left|\left\langle f\left|U_{\mathrm{I}}\left(t,t_0\right)\right|i\right\rangle\right|^2=\Delta t\frac{2\pi}{\hbar}\left|\left\langle f\left|H_{\mathrm{int}}\right|i\right\rangle\right|^2\rho_f, \tag{1.9.22}$$

is, to a first-order approximation, the probability that an initial state $|i\rangle$ will transition to the final state $|f\rangle$ in the time interval Δt. Working infinitesimally, $\Delta t\to\delta t$, we can define the rate of transition as:

$$\Gamma=\frac{2\pi}{\hbar}\left|\left\langle f\left|H_{\mathrm{int}}\right|i\right\rangle\right|^2\rho_f, \tag{1.9.23}$$

which is the probability per unit time, and known as the Fermi golden rule [6,11,64] By repeating the above analysis with the full expression for $U_{\mathrm{I}}\left(t,t_0\right)$ we obtain the full transition rate as:

$$\Gamma=\frac{2\pi}{\hbar}\left|M_{fi}\right|^2\rho_f, \tag{1.9.24}$$

where

$$\begin{aligned}M_{fi}=\left\langle f\left|H_{\mathrm{int}}\right|i\right\rangle&+\sum_r\frac{\left\langle f\left|H_{\mathrm{int}}\right|r\right\rangle\left\langle r\left|H_{\mathrm{int}}\right|i\right\rangle}{\left(E_i-E_r\right)}\\&+\sum_{r,s}\frac{\left\langle f\left|H_{\mathrm{int}}\right|s\right\rangle\left\langle s\left|H_{\mathrm{int}}\right|r\right\rangle\left\langle r\left|H_{\mathrm{int}}\right|i\right\rangle}{\left(E_i-E_s\right)\left(E_i-E_r\right)}\\&+\sum_{r,s,t}\frac{\left\langle f\left|H_{\mathrm{int}}\right|t\right\rangle\left\langle t\left|H_{\mathrm{int}}\right|s\right\rangle\left\langle s\left|H_{\mathrm{int}}\right|r\right\rangle\left\langle r\left|H_{\mathrm{int}}\right|i\right\rangle}{\left(E_i-E_t\right)\left(E_i-E_s\right)\left(E_i-E_r\right)}\\&+\ldots,\end{aligned} \tag{1.9.25}$$

is the probability amplitude, or matrix element. Here, *r*, *s*, and *t* correspond to

intermediate states and are called *virtual* in that they are not observed and are summed over, so as not to appear in the final result. As one might imagine, every appearance of H_{int} denotes an interaction between the electromagnetic field and the electron fields in the systems of matter. Thus, the term in Eq. (1.9.25) with n appearances of H_{int} is the leading order contribution to an n-photon process; for example, n-photon absorption.

The formulae derived in this section lay the foundation for the qualitative and quantitative study of the processes presented in this thesis – and much more besides. As far as is known, the QED picture is, in its domain of applicability, exact.

1.10. Appendix A

This appendix follows the procedure outlined in Ref [6]. We are free to choose a vector potential with zero divergence. To begin a proof by contradiction, we assume that the vector potential has nonzero divergence,

$$\nabla \cdot \mathbf{a} \neq 0. \tag{A.1}$$

The fact that we are working within a gauge theory means that we can transform to another vector potential by the addition of the gradient of a scalar field,

$$\mathbf{a} \rightarrow \mathbf{a} + \nabla \chi. \tag{A.2}$$

The divergence of this *new* vector potential is:

$$\nabla \cdot \mathbf{a} = -\nabla^2 \chi; \tag{A.3}$$

and can be made zero by demanding that χ is a solution to the Laplace equation,

$$\nabla^2 \chi = 0. \tag{A.4}$$

1.11. Bibliography

[1] P. Cladé, E. de Mirandes, M. Cadoret, S. Guellati-Khélifa, C. Schwob, F. Nez, L. Julien, and F. Biraben, "Determination of the fine structure constant based on bloch oscillations of ultracold atoms in a vertical optical lattice," *Physical Review Letters* **96**(3) (2006) [doi:10.1103/PhysRevLett.96.033001].

[2] K. Hagiwara, A. D. Martin, D. Nomura, and T. Teubner, "Improved predictions for of the muon and $\alpha_{QED}\left(M_Z^2\right)$," *Physics Letters B* **649**(2-3), 173–179 (2007) [doi:10.1016/j.physletb.2007.04.012].

[3] I. Levine, D. Koltick, B. Howell, E. Shibata, J. Fujimoto, T. Tauchi, K. Abe, T. Abe, I. Adachi, et al., "Measurement of the electromagnetic coupling at large momentum transfer," *Physical Review Letters* **78**(3), 424–427 (1997) [doi:10.1103/PhysRevLett.78.424].

[4] B. Odom, D. Hanneke, B. D'Urso, and G. Gabrielse, "New measurement of the electron magnetic moment using a one-electron quantum cyclotron," *Physical Review Letters* **97**(3) (2006) [doi:10.1103/PhysRevLett.97.030801].

[5] D. Hanneke, S. Fogwell Hoogerheide, and G. Gabrielse, "Cavity control of a single-electron quantum cyclotron: measuring the electron magnetic moment," *arXiv:1009.4831 [physics.atom-ph]*.

[6] D. P. Craig and T. Thirunamachandran, *Molecular Quantum Electrodynamics: An Introduction to Radiation-Molecule Interactions*, Dover Publications, Mineola, N.Y (1998).

[7] W. Lamb and R. Retherford, "Fine structure of the hydrogen atom by a microwave method," *Physical Review* **72**(3), 241–243 (1947) [doi:10.1103/PhysRev.72.241].

[8] R. Jaffe, "Casimir effect and the quantum vacuum," *Physical Review D* **72**(2) (2005) [doi:10.1103/PhysRevD.72.021301].

[9] G. Plunien, "The Casimir effect," *Physics Reports* **134**(2-3), 87–193 (1986) [doi:10.1016/0370-1573(86)90020-7].

[10] S. M. Barnett, A. Aspect, and P. W. Milonni, "On the quantum nature of the Casimir-Polder interaction," *Journal of Physics B: Atomic, Molecular and Optical Physics* **33**(4), L143–L149 (2000) [doi:10.1088/0953-4075/33/4/106].

[11] P. A. M. Dirac, "The quantum theory of the emission and absorption of radiation," *Proceedings of the Royal Society A: Mathematical, Physical and Engineering Sciences* **114**(767), 243–265 (1927) [doi:10.1098/rspa.1927.0039].

[12] P. A. M. Dirac, *The Principles of Quantum Mechanics*, Clarendon Press, Oxford (2011).

[13] E. Fermi, "Quantum theory of radiation," *Reviews of Modern Physics* **4**(1), 87–132 (1932) [doi:10.1103/RevModPhys.4.87].

[14] J. Oppenheimer, "Note on the theory of the interaction of field and matter," *Physical Review* **35**(5), 461–477 (1930) [doi:10.1103/PhysRev.35.461].

[15] F. Bloch and A. Nordsieck, "Note on the radiation field of the electron," *Physical Review* **52**(2), 54–59 (1937) [doi:10.1103/PhysRev.52.54].

[16] V. Weisskopf, "On the self-energy and the electromagnetic field of the electron," *Physical Review* **56**(1), 72–85 (1939) [doi:10.1103/PhysRev.56.72].

[17] H. Bethe, "The electromagnetic shift of energy levels," *Physical Review* **72**(4), 339–341 (1947) [doi:10.1103/PhysRev.72.339].

[18] R. P. Feynman, "Space-time approach to non-relativistic quantum mechanics," *Reviews of Modern Physics* **20**(2), 367 (1948).

[19] R. Feynman, "The theory of positrons," *Physical Review* **76**(6), 749–759 (1949) [doi:10.1103/PhysRev.76.749].

[20] R. Feynman, "Mathematical formulation of the quantum theory of electromagnetic interaction," *Physical Review* **80**(3), 440–457 (1950) [doi:10.1103/PhysRev.80.440].

[21] J. Schwinger, "On quantum-electrodynamics and the magnetic moment of the electron," *Physical Review* **73**(4), 416–417 (1948) [doi:10.1103/PhysRev.73.416].

[22] J. Schwinger, "Quantum electrodynamics. I. A covariant formulation," *Physical Review* **74**(10), 1439–1461 (1948) [doi:10.1103/PhysRev.74.1439].

[23] S. Tomonaga, "On a relativistically invariant formulation of the quantum theory of wave fields," *Progress of Theoretical Physics* **1**(2), 27–42 (1949) [doi:10.1143/PTP.1.27].

[24] F. Dyson, "The radiation theories of Tomonaga, Schwinger, and Feynman," *Physical Review* **75**(3), 486–502 (1949) [doi:10.1103/PhysRev.75.486].

[25] E. A. Power and S. Zienau, "Coulomb gauge in non-relativistic quantum electrodynamics and the shape of spectral lines," *Philosophical Transactions of the Royal Society A: Mathematical, Physical and Engineering Sciences* **251**(999), 427–454 (1959) [doi:10.1098/rsta.1959.0008].

[26] R. G. Woolley, "Molecular quantum electrodynamics," *Proceedings of the Royal Society A: Mathematical, Physical and Engineering Sciences* **321**(1547), 557–572 (1971) [doi:10.1098/rspa.1971.0049].

[27] M. Babiker and R. Loudon, "Derivation of the Power-Zienau-Woolley Hamiltonian in quantum electrodynamics by gauge transformation," *Proceedings of the Royal Society A: Mathematical, Physical and Engineering Sciences* **385**(1789), 439–460 (1983) [doi:10.1098/rspa.1983.0022].

[28] E. Power and T. Thirunamachandran, "Quantum electrodynamics with nonrelativistic sources. I. Transformation to the multipolar formalism for second-quantized electron and Maxwell interacting fields," *Physical Review A* **28**(5), 2649–2662 (1983) [doi:10.1103/PhysRevA.28.2649].

[29] E. Power and T. Thirunamachandran, "Quantum electrodynamics with nonrelativistic sources. II. Maxwell fields in the vicinity of a molecule," *Physical Review A* **28**(5), 2663–2670 (1983) [doi:10.1103/PhysRevA.28.2663].

[30] E. Power and T. Thirunamachandran, "Quantum electrodynamics with nonrelativistic sources. III. Intermolecular interactions," *Physical Review A* **28**(5), 2671–2675 (1983) [doi:10.1103/PhysRevA.28.2671].

[31] E. Power and T. Thirunamachandran, "Quantum electrodynamics with nonrelativistic sources. IV. Poynting vector, energy densities, and other quadratic operators of the electromagnetic field," *Physical Review A* **45**(1), 54–63 (1992) [doi:10.1103/PhysRevA.45.54].

[32] E. Power and T. Thirunamachandran, "Quantum electrodynamics with nonrelativistic sources. V. Electromagnetic field correlations and intermolecular interactions between molecules in either ground or excited states," *Physical Review A* **47**(4), 2539–2551 (1993) [doi:10.1103/PhysRevA.47.2539].

[33] D. L. Andrews, "A unified theory of radiative and radiationless molecular energy transfer," *Chem. Phys.* **135**(2), 195–201 (1989) [doi:10.1016/0301-0104(89)87019-3].

[34] D. L. Andrews and B. S. Sherborne, "Resonant excitation transfer: A quantum electrodynamical study," *J. Chem. Phys.* **86**(7), 4011 (1987) [doi:10.1063/1.451910].

[35] P. Allcock, R. Jenkins, and D. Andrews, "Laser-assisted resonance-energy transfer," *Phys. Rev.* **61**(2) (2000) [doi:10.1103/PhysRevA.61.023812].

[36] D. L. Andrews, "Rayleigh and Raman optical activity: An analysis of the dependence on scattering angle," *J. Chem. Phys.* **72**(7), 4141 (1980) [doi:10.1063/1.439643].

[37] D. L. Andrews, P. Allcock, and A. A. Demidov, "Theory of second harmonic generation in randomly oriented species," *Chem. Phys.* **190**(1), 1–9 (1995) [doi:10.1016/0301-0104(94)00333-6].

[38] Dubetsky and Berman, "Theory of four-wave mixing using an amplitude approach," *Phys. Rev.* **47**(2), 1294–1313 (1993).

[39] D. L. Andrews, "Polarization studies in multiphoton absorption spectroscopy," *J. Chem. Phys.* **75**(2), 530 (1981) [doi:10.1063/1.442102].

[40] J. D. Jackson, *Classical Electrodynamics*, 3rd ed, Wiley, New York (1999).

[41] E. Kreyszig, *Advanced Engineering Mathematics*, Wiley, New York (1999).

[42] G. B. Arfken, *Mathematical Methods for Physicists*, Academic Press, Orlando (1985).

[43] R. P. Cameron, S. M. Barnett, and A. M. Yao, "Optical helicity, optical spin and related quantities in electromagnetic theory," *New Journal of Physics* **14**(5), 053050 (2012) [doi:10.1088/1367-2630/14/5/053050].

[44] M. V. Berry, "Optical currents," *Journal of Optics A: Pure and Applied Optics* **11**(9), 094001 (2009) [doi:10.1088/1464-4258/11/9/094001].

[45] L. Lorenz, "Ueber die Identität der Schwingungen des Lichts mit den elektrischen Strömen," *Annalen der Physik und Chemie* **207**(6), 243–263 (1867) [doi:10.1002/andp.18672070606].

[46] C. Burgess and G. Moore, *The Standard Model*, Cambridge University Press, Cambridge (2006).

[47] S. Lang, *Algebra*, Rev. 3rd ed, Springer, New York (2002).

[48] R. P. Feynman, *Quantum Mechanics and Path Integrals*, Emended ed, Dover Publications, Mineola, N.Y (2010).

[49] F. Hoyle and J. Narlikar, "Cosmology and action-at-a-distance electrodynamics," *Reviews of Modern Physics* **67**(1), 113–155 (1995) [doi:10.1103/RevModPhys.67.113].

[50] H. Minkowski, "Die Grundgleichungen für die elektromagnetischen Vorgänge in bewegten Körpern," *Mathematische Annalen* **68**(4), 472–525 (1910) [doi:10.1007/BF01455871].

[51] K. Hira, "Derivation of the harmonic oscillator propagator using the Feynman path integral and recursive relations," *European Journal of Physics* **34**(3), 777–785 (2013) [doi:10.1088/0143-0807/34/3/777].

[52] S. Ansoldi, A. Aurilia, and E. Spallucci, "Particle propagator in elementary quantum mechanics: a new path integral derivation," *European Journal of Physics* **21**(1), 1–12 (2000) [doi:10.1088/0143-0807/21/1/301].

[53] M. Könenberg, O. Matte, and E. Stockmeye, "Hydrogen-like atoms in relativistic QED," *arXiv:1207.5134 [math-ph]*.

[54] M. E. Peskin, *An Introduction to Quantum Field Theory*, Addison-Wesley Pub. Co, Reading, Mass (1995).

[55] H. J. Groenewold, "On the principles of elementary quantum mechanics," *Physica* **12**(7), 405–460 (1946) [doi:10.1016/S0031-8914(46)80059-4].

[56] V. Chernyak and S. Mukamel, "Gauge invariant formulation of molecular electrodynamics and the multipolar Hamiltonian," *Chemical Physics* **198**(1-2), 133–143 (1995) [doi:10.1016/0301-0104(95)00122-5].

[57] M. Babiker, E. A. Power, and T. Thirunamachandran, "On a generalization of the Power-Zienau-Woolley transformation in quantum electrodynamics and atomic field equations," *Proceedings of the Royal Society A: Mathematical, Physical and Engineering Sciences* **338**(1613), 235–249 (1974) [doi:10.1098/rspa.1974.0084].

[58] W. Heisenberg, "Die selbstenergie des elektrons," *Zeitschrift für Physik* **65**(1-2), 4–13 (1930) [doi:10.1007/BF01397404].

[59] J. Schwinger, "Quantum electrodynamics. II. vacuum polarization and self-energy," *Physical Review* **75**(4), 651–679 (1949) [doi:10.1103/PhysRev.75.651].

[60] W. T. Scott, *The Physics of Electricity and Magnetism*, 2d ed, R. E. Krieger Pub. Co, Huntington, N.Y (1977).

[61] P. W. Atkins, *Atkins' Physical Chemistry*, 8th ed, Oxford University Press, Oxford; New York (2006).

[62] M. Kaku, *Quantum Field Theory: A Modern Introduction*, Oxford University Press, New York (1993).

[63] G. Juzeliūnas, "Molecule-radiation and molecule-molecule processes in condensed media: a microscopic QED theory," *Chemical Physics* **198**(1-2), 145–158 (1995) [doi:10.1016/0301-0104(95)00130-G].

[64] J. Orear, E. Fermi, and Schluter, *Nuclear Physics: A Course Given by Enrico Fermi at the University of Chicago*, University of Chicago Press, Chicago (1974).

Chapter 2

The Two-Level Approximation

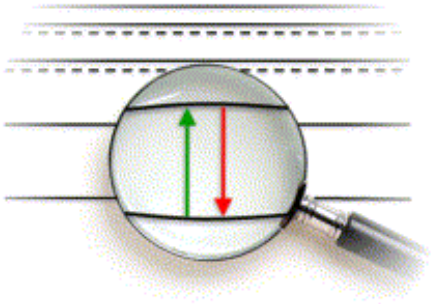

"It is, of course, not really a two-state system… Here we are going to consider… systems which, to some approximation or other, can be considered as two-state systems." – Richard P. Feynman[†]

[†] Feynman, Richard P., *The Feynman Lectures on Physics – Volume III: Quantum Mechanics* (Basic Books, 1965).

2.1 Background

In the development of theory to address quantum mechanical problems, one of the most widely deployed models is the two-level approximation: where the ground state and a single excited state dominate in determining the optical behaviour of an atom or molecule. So ubiquitous is this simplification, that many introductory level quantum mechanics textbooks dedicate entire sections to its application and the study of the physical picture associated with it [1,2]. Of course, some atomic and molecular systems are well represented by a two-energy level approach: for example, ammonia has two inversion states, which, because of a narrow energy barrier between them, exhibit quantum tunnelling [3]. In the context of quantum optics, it is a theoretical basis for a wide range of representations for optical response – from those concerning atoms [4,5] to the more recent studies of quantum dots [6–8]. In the context of quantum information theory, Bialynicki-Birula and Sowiński have formalised the similarity between qubits and two-level atoms [9]. Where a system may legitimately be studied within a two-level representation, the advantages are obvious; calculational simplicity and results cast in formulae that entail a sufficiently small set of parameters to allow correspondence with their experimental realisation. Even though a two-level model has been applied to molecules and chromophores of significantly complex energy level structure [10], even relatively few *atomic* transitions can legitimately studied in terms of to two electronic energy levels [11]. In fact, it has been long-known that the two-level approximation is inadequate to correctly calculate atomic electric dipole absorption frequency shifts near a perfectly conducting interface [12].

In the context of nonlinear optics and atomic photophysics the two-level approximation is applied to the electronic states of systems with discrete energy levels

and is usually enacted by selecting – from the infinite number of states that emerge through the quantum mechanics of any realistic three-dimensional system – the two lowest in energy. The issues in nonlinear optics are different than those in simple system interacting with low intensity radiation, where optical centres will, most likely, interact with photons singly. With the typical intensities of pulsed laser light however (with current experimental limit of 10^{20} Wm^{-2} [13]), there exists a large likelihood of two or more photons interacting simultaneously, within the limits of quantum uncertainty, with an optical centre. Even though the materials most effective for the generation of frequency-converted light have electronic energy level structures much more complicated than atoms (BBO, GaSe, ADP, etc.), the two-level approximation has been widely applied in this context [14–20]; it both delivers results in a mathematically simple form, and relates well to long-established concepts in the theory of chemical structure. In particular, a great deal of studies have developed the connection between molecules with enhanced second harmonic response and *push-pull* chromophore structures (those exhibiting a shifted permanent dipole moment in an electronically excited state, compared with the ground state) [21–25].

Presented in this chapter are analytical and numerical arguments that, in addition to the cautions presented elsewhere [26–28], should be observed when investigating the optical response of atoms and molecules when using the two-level approximation [29–32].

2.2 Perturbation Theory and the Two-Level Approximation

As discussed in the previous chapter, the rate of an electromagnetic interaction can be found from Fermi's golden rule, Eq. (1.9.24), [33]:

$$\Gamma = \frac{2\pi}{\hbar}\left|M_{FI}\right|^2 \rho, \tag{2.2.1}$$

where ρ is the density of final states and M_{FI} is the quantum amplitude that couples the initial and final states. Here, upper-case letters denote system states, comprising both matter and radiation parts. Use of time-dependent perturbation theory is required to fully determine M_{FI} and it secured from the following infinite series (Chapter 1 – Section 9) [34]:

$$\begin{aligned} M_{FI} &= \sum_{p=0}^{\infty} \left\langle F \left| H_{\text{int}} \left(T_0 H_{\text{int}} \right)^p \right| I \right\rangle \\ &= \left\langle F \left| H_{\text{int}} + H_{\text{int}} T_0 H_{\text{int}} + H_{\text{int}} T_0 H_{\text{int}} T_0 H_{\text{int}} + H_{\text{int}} T_0 H_{\text{int}} T_0 H_{\text{int}} T_0 H_{\text{int}} + \ldots \right| I \right\rangle, \end{aligned} \tag{2.2.2}$$

where, $\left|I\right\rangle$ and $\left|F\right\rangle$ represent the initial and final system states, and H_{int} is the interaction operator, Eq. (1.6.36), which, in a quantum electrodynamic framework, acts upon both matter and radiation states. In the above,

$$T_0 \approx \frac{1}{\left(E_I - H_0\right)} \tag{2.2.3}$$

where E_I is the energy of the initial state and H_0 is the unperturbed Hamiltonian, Eq.

(1.9.1). Enacting the completeness relation [35],

$$1 = \sum_R |R\rangle\langle R|, \tag{2.2.4}$$

allows Eq. (2.2.2) to be recast as:

$$\begin{aligned} M_{FI} = \langle F|H_{\text{int}}|I\rangle &+ \sum_R \frac{\langle F|H_{\text{int}}|R\rangle\langle R|H_{\text{int}}|I\rangle}{(E_I - E_R)} \\ &+ \sum_{R,S} \frac{\langle F|H_{\text{int}}|S\rangle\langle S|H_{\text{int}}|R\rangle\langle R|H_{\text{int}}|I\rangle}{(E_I - E_S)(E_I - E_R)} \\ &+ \sum_{R,S,T} \frac{\langle F|H_{\text{int}}|T\rangle\langle T|H_{\text{int}}|S\rangle\langle S|H_{\text{int}}|R\rangle\langle R|H_{\text{int}}|I\rangle}{(E_I - E_T)(E_I - E_S)(E_I - E_R)} \\ &+ \ldots, \end{aligned} \tag{2.2.5}$$

where $|R\rangle$, $|S\rangle$, $|T\rangle$… denote virtual system states, which are operated on by H_0 to deliver E_n: the energy of the state labelled by its subscript.

Commonly the mathematical result for the description of the optical response of an atom or molecule is obtained from the appropriate contributions from the series expansion, Eq. (2.2.5); the leading order contribution for a process involving n photons is, in general, the n^{th} term. The summation over the virtual molecular states is then limited to the set $\{0,1\}$, where 0 and 1 index the ground and excited state respectively. For a given system state, the decomposition into matter and radiation parts can be labelled as:

$$|R\rangle = |\rho_{\text{rad}}\rangle|r_{\text{mat}}\rangle. \tag{2.2.6}$$

Thus, enacting the two-level approximation at a later stage of calculation is exactly equivalent to taking the Hilbert space of system states and allowing the matter subspace to only be composed of, for example, a ground state $|0_{\text{mat}}\rangle$ and a single excited state $|1_{\text{mat}}\rangle$. That is, $|r_{\text{mat}}\rangle \in \{|0_{\text{mat}}\rangle, |1_{\text{mat}}\rangle\}$. This strategy is exactly equivalent to excluding the other state projections from the completeness relation by truncating it to $|0_{\text{mat}}\rangle\langle 0_{\text{mat}}| + |1_{\text{mat}}\rangle\langle 1_{\text{mat}}| = 1_{\text{mat}}$. Therefore, the two-level completeness relation is given as:

$$
\begin{aligned}
1 &\equiv \sum_{R} |R\rangle\langle R| \\
&\equiv \sum_{\rho,r} |\rho_{\text{rad}}\rangle |r_{\text{mat}}\rangle\langle r_{\text{mat}}| \langle \rho_{\text{rad}}| \\
&\equiv \sum_{\rho,r} |\rho_{\text{rad}}\rangle\langle \rho_{\text{rad}}| \, |r_{\text{mat}}\rangle\langle r_{\text{mat}}| \equiv \mathbf{1}_{\text{rad}} \times \mathbf{1}_{\text{mat}} \\
&\equiv \mathbf{1}_{\text{rad}} \times \Bigg(|0_{\text{mat}}\rangle\langle 0_{\text{mat}}| + |1_{\text{mat}}\rangle\langle 1_{\text{mat}}| + \underbrace{\sum_{r \notin \{0,1\}} |r_{\text{mat}}\rangle\langle r_{\text{mat}}|}_{=0} \Bigg) \quad .
\end{aligned}
\tag{2.2.7}
$$

In the rest of the chapter we consider the implications and physical insights that emerge from the development of introductory quantum mechanics and optical theory in the context of such an approximation: limiting the virtual intermediate states to the ground or a single excited state.

2.3 The Two-Level Expectation Value Theorem

First, we show that a physically realistic assumption, used with the two-level approximation, delivers a set of potentially unanticipated consequences and can lead

to patently absurd conclusions. The motivation for this is to demonstrate that the application of the two-level approximation is not valid is when the two basis states have equal expectation values for the position and momentum operators. This is physically justifiable in the specific cases of, for example, atoms or other spherically symmetric systems – the two expectation values being zero in these instances. It will then follow that the two states are have equal energy, so that we have a contradiction. To obtain this contradiction, let us assume that, for an arbitrary Hermitian operator $\hat{A}$, the expectation value of that operator is equal in the two states dictated by the two-level approximation,

$$\langle 0|\hat{A}|0\rangle = \langle 1|\hat{A}|1\rangle. \tag{2.3.1}$$

Then the theorem will show that this implies:

$$\langle 0|f(\hat{A})|0\rangle = \langle 1|f(\hat{A})|1\rangle, \tag{2.3.2}$$

where $f(\hat{A})$ is any analytic function of the Hermitian operator $\hat{A}$. The initial assumption provides us with a base case from which to launch a proof by induction.

The definition of an analytic function is that it can be expanded in terms of a convergent power series about a point, c, in the real plane (as $\hat{A}$, is Hermitian) [36]. Therefore, it can be written in the form:

$$f(\hat{A}) = \sum_{n=0}^{\infty} \frac{f^{(n)}(c)}{n!} (\hat{A} - c)^n, \tag{2.3.3}$$

which converges to $f(\hat{A})$ in a neighbourhood of c. Thus, it suffices to show that:

$$\langle 1 | f(\hat{A}) | 1 \rangle - \langle 0 | f(\hat{A}) | 0 \rangle = 0. \tag{2.3.4}$$

By substituting Eq. (2.3.3) into the left-hand side of Eq. (2.3.4) it emerges that:

$$\begin{aligned} \langle 1 | f(\hat{A}) | 1 \rangle - \langle 0 | f(\hat{A}) | 0 \rangle &= \langle 1 | \sum_{n=0}^{\infty} \frac{f^{(n)}(c)}{n!} (\hat{A} - c)^n | 1 \rangle - \langle 0 | \sum_{n=0}^{\infty} \frac{f^{(n)}(c)}{n!} (\hat{A} - c)^n | 0 \rangle \\ &= \sum_{n=0}^{\infty} \frac{f^{(n)}(c)}{n!} \left[\langle 1 | (\hat{A} - c)^n | 1 \rangle - \langle 0 | (\hat{A} - c)^n | 0 \rangle \right], \end{aligned} \tag{2.3.5}$$

where the pre-factor can be taken outside the bra-ket as it does not carry the operator character of the expression. To reach the desired conclusion, Eq. (2.3.4), it is sufficient to show that:

$$\langle 1 | (\hat{A} - c)^n | 1 \rangle - \langle 0 | (\hat{A} - c)^n | 0 \rangle = 0. \tag{2.3.6}$$

We start by making the division

$$\begin{aligned} &\langle 1 | (\hat{A} - c)^n | 1 \rangle - \langle 0 | (\hat{A} - c)^n | 0 \rangle \\ &= \langle 1 | (\hat{A} - c) \cdot 1 \cdot (\hat{A} - c)^{n-1} | 1 \rangle - \langle 0 | (\hat{A} - c)^{n-1} \cdot 1 \cdot (\hat{A} - c) | 0 \rangle, \end{aligned} \tag{2.3.7}$$

in which we can insert the truncated, two-level form of the completeness relation, Eq. (2.2.7) to obtain:

$$\begin{aligned}&\langle 1|(\hat{A}-c)|0\rangle\langle 0|(\hat{A}-c)^{n-1}|1\rangle-\langle 0|(\hat{A}-c)^{n-1}|1\rangle\langle 1|(\hat{A}-c)|0\rangle\\&+\langle 1|(\hat{A}-c)|1\rangle\langle 1|(\hat{A}-c)^{n-1}|1\rangle-\langle 0|(\hat{A}-c)^{n-1}|0\rangle\langle 0|(\hat{A}-c)|0\rangle\\&\equiv\left((\hat{A}-c)\right)_{11}\left((\hat{A}-c)^{n-1}\right)_{11}-\left((\hat{A}-c)^{n-1}\right)_{00}\left((\hat{A}-c)\right)_{00}\ .\end{aligned}\tag{2.3.8}$$

The final step is obtained by the introduction of subscripts to represent bra-kets and the observation that closed bra-kets commute. Since our assumption, Eq. (2.3.1), is, in this notation, $(\hat{A}-c)_{00}=(\hat{A}-c)_{11}$, we can write our final result as:

$$\left((\hat{A}-c)^{n}\right)_{11}-\left((\hat{A}-c)^{n}\right)_{00}=(\hat{A}-c)_{00}\left[\left((\hat{A}-c)^{n-1}\right)_{11}-\left((\hat{A}-c)^{n-1}\right)_{00}\right].\tag{2.3.9}$$

Thus, if the theorem is true for $n-1$, then Eq. (2.3.9), implies that it is also true for n. As the *n=2* case is true by assumption, Eq. (2.3.1) the remaining infinite set of natural numbers, $n\in\mathbb{N}$, is verified by the cascade of inductive reasoning [37].

2.4 Extensions and Implications of The Theorem

A special case of the above theorem is: if $\langle 0|\hat{A}|0\rangle=\langle 1|\hat{A}|1\rangle$, then:

$$\langle 0|\hat{A}^{n}|0\rangle=\langle 1|\hat{A}^{n}|1\rangle,\tag{2.4.1}$$

which follows from the fact that a polynomial equation is an analytic function. Therefore, extending the theorem to the case of a vector Hermitian operator $\hat{\mathbf{A}}$ (such

as the electric $\hat{\boldsymbol{\mu}}$ and magnetic $\hat{\mathbf{m}}$ dipole moment operators) not only proves the theorem for a power of that operator $\hat{\mathbf{A}}^n$, but also proves it for the cross-terms $\hat{A}_i\hat{A}_j$. Formally, if the vector operator $\hat{\mathbf{A}}$ has identical expectation values in the two basis energy levels, then the expectation values of any string of components $\hat{A}_i\hat{A}_j\ldots\hat{A}_n$ will also have the same expectation values.

An example of when the application of the two-level approximation is not valid is when the two basis states have equal expectation values for the position and momentum operators. This is physically justifiable in the case of, for example, atoms or other spherically symmetric systems – the two expectation values being zero in these instances. It then follows that, from the above theorem, the expectation values of the squares of the operators are also equal. Since we can express the total energy of such a system in terms of these two squared operators, it implies that the two states are degenerate. Explicitly, this is demonstrated in the case of the Hamiltonian for a simple harmonic oscillator; the expectation value for which is given by:

$$\begin{aligned} E_0 &= \langle 0|\hat{H}|0\rangle \\ &= \frac{1}{2m}\langle 0|\hat{p}^2|0\rangle + \frac{1}{2}m\omega^2\langle 0|\hat{x}^2|0\rangle \\ &= \frac{1}{2m}\langle 1|\hat{p}^2|1\rangle + \frac{1}{2}m\omega^2\langle 1|\hat{x}^2|1\rangle \\ &= E_1. \end{aligned} \tag{2.4.2}$$

Thus, taking just two energy levels of a simple harmonic oscillator as a complete basis set leads to the absurd conclusion that both states have equal energies. Whereas the quantum harmonic oscillator is analytically tractable – so this would be an

unlikely choice – we will now address other situations where the same logic would apply less obviously.

That the expectation values of the square of the momenta are equal in the two basis states implies that the kinetic energies T should also be the same. If the potential energy of the system V depends on a power m of the position (as it does in both the harmonic oscillator, and the Lennard-Jones potential [38]), then the Virial Theorem states that [39]:

$$2\langle T\rangle = m\langle V\rangle, \tag{2.4.3}$$

where diagonal brackets denote both the expectation value and the time-average of the quantity between them. By substituting this into the equation for the total energy of a conservative system, we have:

$$\begin{aligned} E &= \langle T\rangle + \langle V\rangle \\ &= \left(1+\frac{2}{m}\right)\langle T\rangle, \end{aligned} \tag{2.4.4}$$

where we infer, once again, that $E_0 = E_1$. It is a commonly satisfied condition that the two basis states have the same expectation value for a particular observable, thus it is unguarded use of the truncated completeness relation that causes this paradox. It is easily verified that removing the restriction on the completeness relation no longer implies the undesirable equal-energy conclusion.

A hidden constraint imposed by the two-level approximation is elucidated by considering the fluctuations in expectation values of quantum operators. For example, if we define the variance of the electric dipole moment by [40]:

$$\Delta\overline{\boldsymbol{\mu}}^2 = \left\langle \boldsymbol{\mu}^2 \right\rangle - \left\langle \boldsymbol{\mu} \right\rangle^2 , \tag{2.4.5}$$

then the theorem on two-level quantum operators, Eq. (2.4.1), implies that, for two energy levels with equal expectation values for dipole moment operators, the fluctuations must be equal. To the extent that electronic distributions in the considered molecules do not obey this criterion, the two-level approximation fails in correctly reproducing the behaviour of the physical system.

It is worthwhile noting that the analytical results presented in this section apply to a wide spectrum of operators. Specifically, the theorem applies to both the momentum operator, $\hat{\mathbf{p}}$, and the electric dipole operator, $\hat{\boldsymbol{\mu}}$; and can therefore provide insight in both the minimal-coupling $\mathbf{p}\cdot\mathbf{a}$ and multipolar $\boldsymbol{\mu}\cdot\mathbf{e}$ formulations of (quantum) electrodynamics. Issues concerning the computational differences between these formalisms were addressed long ago in a series of works by Power and Thirunamachandran [41,42], and Woolley [43,44]. Studying the calculations relating to multiphoton absorption, Meath and Power showed that the two-level approximation is never valid when used in conjunction with a minimal-coupling Hamiltonian [45].

2.5 The Optical Susceptibility Tensors

The aim of this chapter is to discuss the validity of the two-level approximation when applied to the calculations of optical processes. To this end, we first derive the expressions for the polarisability tensor for Rayleigh (elastic) scattering and the hyperpolarisability tensor for second harmonic generation as representative test cases.

For Rayleigh scattering by a single molecule, the quantum amplitude of the process is taken from the second term of the perturbation expansion given in Eq. (2.2.5), where the initial and final states are given by:

$$\begin{aligned} \left|I\right\rangle &= \left|I_{\text{mat}};I_{\text{rad}}\right\rangle \\ &= \left|0_{\text{mat}};1(\mathbf{k},\lambda)\right\rangle \\ \left|F\right\rangle &= \left|0_{\text{mat}};1(\mathbf{k}',\lambda')\right\rangle, \end{aligned} \tag{2.5.1}$$

where $\mathbf{k}$ is the wavevector and λ is the polarisation of the input and emergent radiation. With the virtual intermediate total system states being denoted by $\left|R\right\rangle$, the matrix element, in the electric dipole approximation, is given by

$$\begin{aligned} M_{FI} &= \frac{1}{\varepsilon_0^2}\sum_R \frac{\left\langle 0_{\text{mat}};1(\mathbf{k},\lambda)\right|\boldsymbol{\mu}\cdot\mathbf{d}^{\perp}\left|R\right\rangle\left\langle R\right|\boldsymbol{\mu}\cdot\mathbf{d}^{\perp}\left|0_{\text{mat}};1(\mathbf{k},\lambda)\right\rangle}{\left(E_I - E_R\right)} \\ &= -\left(\frac{\hbar ck}{2\varepsilon_0 V}\right)n^{\frac{1}{2}}\sum_r \left\{\frac{\left(\boldsymbol{\mu}^{0r}\cdot\bar{\mathbf{e}}'\right)\left(\boldsymbol{\mu}^{r0}\cdot\mathbf{e}\right)}{\left(\tilde{E}_{r0}-\hbar ck\right)} + \frac{\left(\boldsymbol{\mu}^{0r}\cdot\mathbf{e}\right)\left(\boldsymbol{\mu}^{0r}\cdot\bar{\mathbf{e}}'\right)}{\left(\tilde{E}_{r0}+\hbar ck\right)}\right\}, \end{aligned} \tag{2.5.2}$$

where $\tilde{E}_{r0} \equiv \tilde{E}_r - \tilde{E}_0$ and the tildes are a reminder that a damping term, $\frac{i}{2}\gamma$, has been included where γ is the full linewidth at half maximum [46,47]. Here, overbars denote complex conjugation. Each term inside the summation corresponds to a different time-ordering of interaction event. By explicitly displaying the index notation of the vector terms, we obtain:

$$\begin{aligned} M_{FI} &= -\left(\frac{\hbar ck}{2\varepsilon_0 V}\right) n^{\frac{1}{2}} \bar{e}_i' e_j \sum_r \left\{ \frac{\mu_i^{0r}\mu_j^{r0}}{\left(\tilde{E}_{r0} - \hbar ck\right)} + \frac{\mu_j^{0r}\mu_i^{r0}}{\left(\tilde{E}_{r0} + \hbar ck\right)} \right\} \\ &= -\left(\frac{\hbar ck}{2\varepsilon_0 V}\right) n^{\frac{1}{2}} \bar{e}_i' e_j \alpha_{ij}(\omega;-\omega), \end{aligned} \tag{2.5.3}$$

where

$$\alpha_{ij}^{00}(\omega;-\omega) = \sum_r \left\{ \frac{\mu_i^{0r}\mu_j^{r0}}{\left(\tilde{E}_{r0} - \hbar ck\right)} + \frac{\mu_j^{0r}\mu_i^{r0}}{\left(\tilde{E}_{r0} + \hbar ck\right)} \right\}, \tag{2.5.4}$$

is the frequency, $\omega = ck$, dependent polarisability. Here, **e** and **e**' are the polarisation vectors of the incident and emergent radiation respectively. It is the value of the components of the polarisability tensor that determine the strength of the scattering events. For example, the response of a polar molecule will be dominated by the $\alpha_{zz}^{00}(\omega;-\omega)$ component, where z is the axial direction.

To derive the optical response tensor of a molecule displaying upconversion – the simultaneous (within the limits of quantum uncertainty) absorption of two identical photons and the emission of a *harmonic* photon with twice the frequency of

the input beam – we begin by characterising the initial and final states:

$$\begin{aligned} |I\rangle &= |0_{\text{mat}}; 2(\mathbf{k},\lambda), 0(2\mathbf{k},\lambda')\rangle \\ |F\rangle &= |0_{\text{mat}}; 0(\mathbf{k},\lambda), 1(2\mathbf{k},\lambda')\rangle, \end{aligned} \tag{2.5.5}$$

where the modulus of the output photon wave-vector is twice that of the input, $k' = 2k$. We substitute the relevant expression for H_{int} into the third term of the perturbative expansion for the matrix element, Eq. (2.2.5):

$$M_{FI} = -\frac{1}{\varepsilon_0^3}\sum_{R,S}\frac{\langle F|\boldsymbol{\mu}\cdot\mathbf{d}^{\perp}|S\rangle\langle S|\boldsymbol{\mu}\cdot\mathbf{d}^{\perp}|R\rangle\langle R|\boldsymbol{\mu}\cdot\mathbf{d}^{\perp}|I\rangle}{(E_I - E_S)(E_I - E_R)}, \tag{2.5.6}$$

which, by explicitly labelling the components of the vectors, becomes:

$$\begin{aligned} M_{FI} = &-i\left(\frac{\hbar c}{2\varepsilon_0 V}\right)^3 k(k')^{\frac{1}{2}}\left(n(n-1)\right)^{\frac{1}{2}}\vec{e}_i' e_j e_k \\ &\times\sum_{r,s}\left\{\frac{\mu_i^{0s}\mu_j^{sr}\mu_k^{r0}}{\left(\tilde{E}_{s0}-2\hbar\omega\right)\left(\tilde{E}_{r0}-\hbar\omega\right)}+\frac{\mu_j^{0s}\mu_i^{sr}\mu_k^{r0}}{\left(\tilde{E}_{s0}+\hbar\omega\right)\left(\tilde{E}_{r0}-\hbar\omega\right)}\right. \\ &\left.+\frac{\mu_j^{0s}\mu_k^{sr}\mu_i^{r0}}{\left(\tilde{E}_{s0}+\hbar\omega\right)\left(\tilde{E}_{r0}+2\hbar\omega\right)}\right\}. \end{aligned} \tag{2.5.7}$$

Upper-case system states, R and S, Eq. (2.2.6), have been converted to lower-case letters to designate the intermediate matter states. We associate the molecular part of the quantum amplitude with the hyperpolarisability tensor and re-express Eq. (2.5.7) as:

$$M_{FI} = -i\left(\frac{\hbar c}{2\varepsilon_0 V}\right)^3 k\left(k'\right)^{\frac{1}{2}}\left(n\left(n-1\right)\right)^{\frac{1}{2}}\vec{e}_i' e_j e_k \beta_{ijk}, \tag{2.5.8}$$

where, evidently,

$$\begin{aligned}\beta_{ijk}^{00}\left(-2\omega;\omega,\omega\right) = \sum_{r,s}\Bigg\{&\frac{\mu_i^{0s}\mu_j^{sr}\mu_k^{r0}}{\left(\tilde{E}_{s0}-2\hbar\omega\right)\left(\tilde{E}_{r0}-\hbar\omega\right)} + \frac{\mu_j^{0s}\mu_i^{sr}\mu_k^{r0}}{\left(\tilde{E}_{s0}+\hbar\omega\right)\left(\tilde{E}_{r0}-\hbar\omega\right)} \\ &+ \frac{\mu_j^{0s}\mu_k^{sr}\mu_i^{r0}}{\left(\tilde{E}_{s0}+\hbar\omega\right)\left(\tilde{E}_{r0}+2\hbar\omega\right)}\Bigg\}.\end{aligned} \tag{2.5.9}$$

It is worth noting that as the *j* and *k* indices correspond to the two identical incident photons, the result must be identical when these indices are exchanged. That is, the 3×3 polarisation tensor, $\vec{e}_i' e_j e_k$, is *j*,*k* symmetric. Therefore, we may construct the *j*,*k* symmetric part of the hyperpolarisability tensor by taking the mean average of β_{ijk}^{00} and β_{ikj}^{00}:

$$\begin{aligned}\beta_{i(jk)}^{00}\left(-2\omega;\omega,\omega\right) &= \frac{1}{2}\left(\beta_{ijk}+\beta_{ikj}\right) \\ &= \frac{1}{2}\sum_{r,s}\Bigg\{\frac{\mu_i^{0s}\mu_j^{sr}\mu_k^{r0}}{\left(\tilde{E}_{s0}-2\hbar\omega\right)\left(\tilde{E}_{r0}-\hbar\omega\right)} + \frac{\mu_i^{0s}\mu_k^{sr}\mu_j^{r0}}{\left(\tilde{E}_{s0}-2\hbar\omega\right)\left(\tilde{E}_{r0}-\hbar\omega\right)} \\ &\quad + \frac{\mu_j^{0s}\mu_i^{sr}\mu_k^{r0}}{\left(\tilde{E}_{s0}+\hbar\omega\right)\left(\tilde{E}_{r0}-\hbar\omega\right)} + \frac{\mu_k^{0s}\mu_i^{sr}\mu_j^{r0}}{\left(\tilde{E}_{s0}+\hbar\omega\right)\left(\tilde{E}_{r0}-\hbar\omega\right)} \\ &\quad + \frac{\mu_j^{0s}\mu_k^{sr}\mu_i^{r0}}{\left(\tilde{E}_{s0}+\hbar\omega\right)\left(\tilde{E}_{r0}+2\hbar\omega\right)} + \frac{\mu_k^{0s}\mu_j^{sr}\mu_i^{r0}}{\left(\tilde{E}_{s0}+\hbar\omega\right)\left(\tilde{E}_{r0}+2\hbar\omega\right)}\Bigg\},\end{aligned} \tag{2.5.10}$$

which is the only part of the response tensor that contributes to the rate.

The higher-order response tensors can be computed in an analogous way and it is by discussion of these quantities that we may investigate the applicability of the two-level approximation in optical problems.

2.6 'Push-Pull' Chromophores

As mentioned above, it is widely considered true that 'push-pull' chromophores – display enhanced second harmonic response [48–56]. 'Push-pull' chromophores are those optical centres that display shifted static dipole moments in their excited states, with respect to their ground state moments, and are thought to display large optical nonlinearity. These often have the form of electron donor and acceptor groups connected with a benzene ring, and are manufactured with the goal of application in electronic andphotonic technologies. Here, we show that this reasoning is derived from a two energy level model is not necessarily accurate. The application of such an approximation is very rarely recognised as potentially misleading in this context [57]. Furthermore, since the publication of the papers that relate to this chapter, it has been experimentally verified that a two-state model gives an incorrect value for hyperpolarisability [58].

We begin our analysis by restricting the set of energy levels, labelled as i, f, r and s in Eq. (2.5.9), to containing only one ground state $|0\rangle$ and a single excited state $|1\rangle$. Under this assumption there are only four possible routes through state space; namely:

$$\begin{aligned}
&|0\rangle \to |0\rangle \to |0\rangle \to |0\rangle \\
&|0\rangle \to |1\rangle \to |0\rangle \to |0\rangle \\
&|0\rangle \to |0\rangle \to |1\rangle \to |0\rangle \\
&|0\rangle \to |1\rangle \to |1\rangle \to |0\rangle ,
\end{aligned} \tag{2.6.1}$$

where the states, from left to right are denoted by i, r, s and f. Each route generates terms in Eq. (2.5.9) depending on the transition dipole moments, $\boldsymbol{\mu}^{01}$ and $\boldsymbol{\mu}^{10}$, and the static dipole moments, $\boldsymbol{\mu}^{00}$ and $\boldsymbol{\mu}^{11}$. It has been shown that nonlinear susceptibilities *only* have a dependence on the static moments in terms of their vector difference– in this case $\mathbf{d} = \boldsymbol{\mu}^{11} - \boldsymbol{\mu}^{00}$. Furthermore, to deliver the correct results it is sufficient to apply the following algorithm [34,59–61]:

$$\begin{aligned}
&\boldsymbol{\mu}^{11} \to \boldsymbol{\mu}^{11} - \boldsymbol{\mu}^{00} = \mathbf{d} \\
&\boldsymbol{\mu}^{00} \to 0 \ .
\end{aligned} \tag{2.6.2}$$

Of the four routes in Eq. (2.6.1) only one does not have a dependence on the ground state dipole moments,

$$|0\rangle \to |1\rangle \to |1\rangle \to |0\rangle , \tag{2.6.3}$$

and Eq. (2.5.9) becomes:

$$\begin{aligned}
&\beta^{00}_{ijk(TLA)}(-2\omega;\omega,\omega) = \\
&\frac{\mu_i^{01} d_j \mu_k^{10}}{\left(\tilde{E}_{10} - 2\hbar\omega\right)\left(\tilde{E}_{10} - \hbar\omega\right)} + \frac{\mu_j^{01} d_i \mu_k^{10}}{\left(\tilde{E}_{10} + \hbar\omega\right)\left(\tilde{E}_{10} - \hbar\omega\right)} + \frac{\mu_j^{01} d_k \mu_i^{10}}{\left(\tilde{E}_{10} + \hbar\omega\right)\left(\tilde{E}_{10} + 2\hbar\omega\right)}.
\end{aligned} \tag{2.6.4}$$

It is this equation that represents the matter in second harmonic generation under the two-level approximation, and is used as justification for the idea that a non-zero **d** is required for a non-zero hyperpolarisability.

Extending this analysis to that of an *n*-photon process allows, via the application of the above mentioned algorithm, each state sequence to be written as:

$$|0\rangle \to |r_1\rangle \to |r_2\rangle \to \ldots \to |r_{n-1}\rangle \to |0\rangle, \tag{2.6.5}$$

where $|r_i\rangle \in \{|0\rangle, |1\rangle\}$. If *n* is odd, then the non-vanishing state sequences must contain at least one $'|1\rangle \to |1\rangle'$, which, by the prescription in Eq. (2.6.2), is replaced by **d**. Therefore, within the two-level approximation, for odd-*n* nonlinear susceptibilities:

$$\mathbf{d} = 0 \;\Rightarrow\; \chi^{(odd)} = 0. \tag{2.6.6}$$

However, for processes that depend on even-order nonlinear susceptibilities, the alternating state sequence $|0\rangle \to |1\rangle \to |0\rangle \to |1\rangle \to |0\rangle \ldots \to |1\rangle \to |0\rangle$, will generate a term that neither vanishes by an appearance of a $|0\rangle \to |0\rangle$ or depends on **d**, by the appearance of a $|1\rangle \to |1\rangle$. Thus:

$$\mathbf{d} = 0 \;\not\Rightarrow\; \chi^{(even)} = 0, \tag{2.6.7}$$

which physically denotes that a non-'push-pull' chromophore does not imply a

vanishing even-order optical susceptibility tensor.

2.7 Two-level Model for Elastic Scattering

By examining the calculations corresponding to Rayleigh (elastic scattering) we can come to a conclusion as to whether this process is well represented by two energy levels. Slight rearrangement of Eq. (2.5.4) leads to:

$$\begin{aligned}\alpha_{ij}^{00}(\omega;-\omega) &= \alpha_{ij}^{TLA} + \alpha_{ij}^{BG} \\ &= \left(\frac{\mu_i^{0u}\mu_j^{u0}}{\left(\tilde{E}_{u0} - \hbar ck\right)} + \frac{\mu_j^{0u}\mu_i^{u0}}{\left(\tilde{E}_{u0} + \hbar ck\right)} \right) + \frac{\mu_i^{0u'}\mu_j^{u'0}}{\left(\tilde{E}_{u'0} - \hbar ck\right)} + \frac{\mu_j^{0u'}\mu_i^{u'0}}{\left(\tilde{E}_{u'0} + \hbar ck\right)} + \cdots \end{aligned} \tag{2.7.1}$$

where the superscripts *TLA* and *BG* denote two-level and background terms. Here, $|u'\rangle$ is a third energy level. It is worth noting that terms solely dependant on μ_i^{00} and μ_j^{00} vanish, and it is this aspect of the calculations that forms a basis for the algorithmic method outlined in Ref. [34,59–61]. In the following, we compare the magnitude of these terms in two representative merocyanine dyes that are known to have large nonlinear susceptibilities. Furthermore, the considered molecules are electrically neutral, polar molecules so that their optical response is dominated by the axial components of their respective tensors. Compound (1) is 1-methyl-4-[(oxocyclohexadienylidene)ethylidene]-1,4-dihydropyridine and dye (2) is 1-methyl-4-[(dicyanomethylidene)hexadienylidene]-1,4-dihydropyridine; A diagram of their chemical structure is displayed in Fig. 2.1.

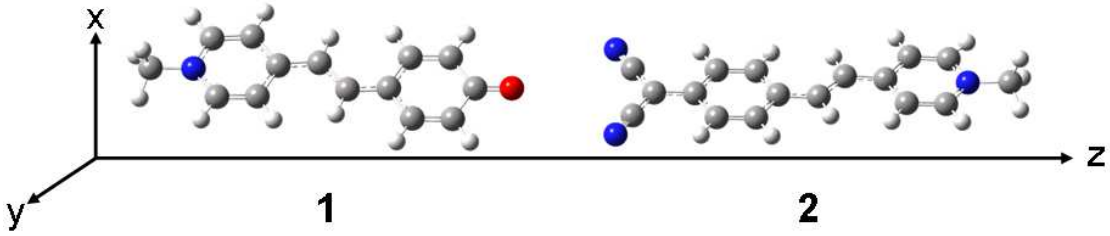

Fig. 2.1. Structure of the two merocyanine laser dyes discussed here.

We begin by comparing the dispersion curves for the α_{zz} component of the molecules with just one excited state included (dashed line) in the sum-over-states, to that with twenty excited states included (solid line). The *ab intio* computations were performed by Peck and Oganesyan [30] for a range of frequency values in the visible and near-UV range. In Fig. 2.2., it will be observed that the deviation of the two-level curve from that of the twenty-one level is minimal at this scale; a small structural

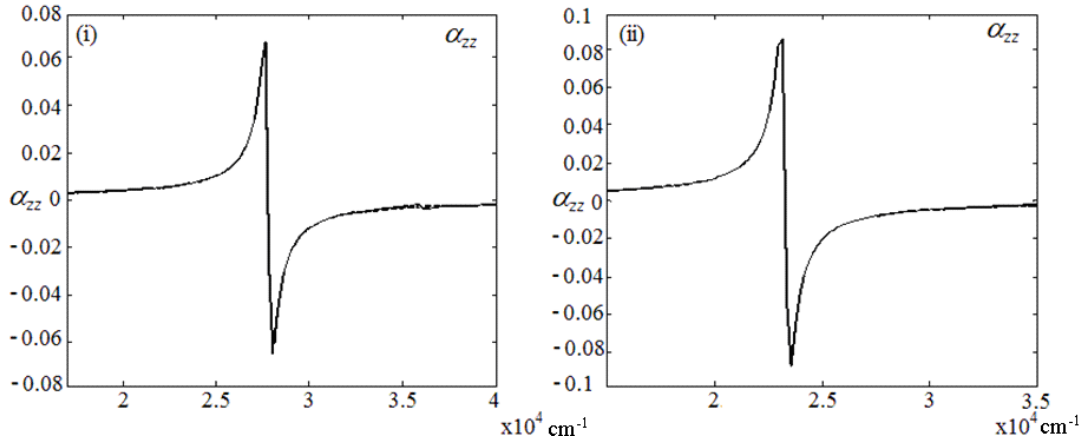

Fig. 2.2. The most intense features in the spectra of compounds 1 – (i), and 2 – (ii) arising from the zz component of the polarisability. The horizontal scale is in wavenumbers (cm^{-1}). The difference between the two-level and 21-level result has its maximum of 2.5% in Fig (i) and 2% in Fig (ii). In both images it is near to the 3.5 x10^{4}cm^{-1} position.

difference is seen at approximately 3.5×10^4 cm^{-1}. To further validate the claim that, for these molecules, two energy levels are adequate to describe the polarisability

tensor, we plot the following measure:

$$\breve{\alpha}_{ij}(N) = 100 \cdot \frac{\overline{|\alpha_{ij}(N)|}}{|\alpha_{ij}(2)|}, \tag{2.7.2}$$

where the argument N, indicates the number of excited states used in the computation, and the overbar represents averaging over the frequency interval. The measure, $\breve{\alpha}_{ij}(N)$, is then an indication of the percentage departure from the two-level model; a value close to 100(%) indicates good agreement.

The two plots in Fig. 2.3. fully support the claim that the two-level approximation is a satisfactory description of optical processes that depend on the polarisability of the active optical centre.

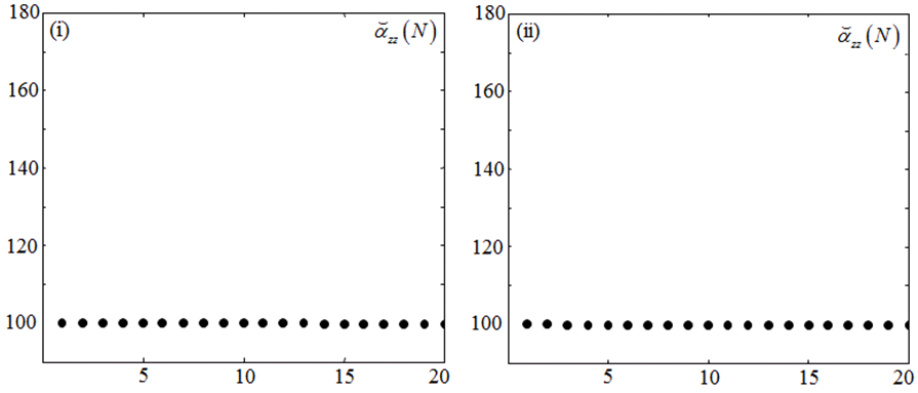

Fig. 2.3 Plot of $\breve{\alpha}_{ij}(N)$ against number of excited states in compound 1 (i) and 2 (ii). The value of $\breve{\alpha}_{ij}(N)$ varies by a maximum of 2.5% over the whole range of excited states.

2.8 Two-level Model for Second Harmonic Generation

In the previous section it was verified, by example, that the two-level approximation

is valid in the application of nonlinear optical techniques to elastic scattering. However, it will now be shown that the same cannot be said for a process one order of optical nonlinearity higher; namely, second harmonic generation. As in Eq. (2.7.1), we partition the hyperpolarisability tensor into two-level and background terms:

$$\begin{aligned}\beta_{ijk}^{00}(-2\omega;\omega,\omega) &= \beta_{ijk}^{\mathrm{TLA}} + \beta_{ijk}^{\mathrm{BG}} \\ &= \left(\frac{\mu_i^{0u} d_j \mu_k^{0u}}{\left(\tilde{E}_{u0} - 2\hbar\omega\right)\left(\tilde{E}_{u0} - \hbar\omega\right)} + \frac{\mu_j^{0u} d_i \mu_k^{0u}}{\left(\tilde{E}_{u0} + \hbar\omega\right)\left(\tilde{E}_{u0} - \hbar\omega\right)} \right. \\ &\quad \left. + \frac{\mu_j^{0u} d_k \mu_i^{0u}}{\left(\tilde{E}_{u0} + \hbar\omega\right)\left(\tilde{E}_{u0} + 2\hbar\omega\right)} \right) + \frac{\mu_i^{0u'} d'_j \mu_k^{0u'}}{\left(\tilde{E}_{u'0} - 2\hbar\omega\right)\left(\tilde{E}_{u'0} - \hbar\omega\right)} \\ &\quad + \frac{\mu_j^{0u'} d'_i \mu_k^{0u'}}{\left(\tilde{E}_{u'0} + \hbar\omega\right)\left(\tilde{E}_{u'0} - \hbar\omega\right)} + \frac{\mu_j^{0u'} d'_k \mu_i^{0u'}}{\left(\tilde{E}_{u'0} + \hbar\omega\right)\left(\tilde{E}_{u'0} + 2\hbar\omega\right)} \\ &\quad + \frac{\mu_i^{0u} \mu_j^{uu'} \mu_k^{0u'}}{\left(\tilde{E}_{u0} - 2\hbar\omega\right)\left(\tilde{E}_{u'0} - \hbar\omega\right)} + \frac{\mu_j^{0u} \mu_i^{uu'} \mu_k^{0u'}}{\left(\tilde{E}_{u0} + \hbar\omega\right)\left(\tilde{E}_{u'0} - \hbar\omega\right)} \\ &\quad + \frac{\mu_j^{0u} \mu_k^{uu'} \mu_i^{0u'}}{\left(\tilde{E}_{u0} + \hbar\omega\right)\left(\tilde{E}_{u'0} + 2\hbar\omega\right)} + \frac{\mu_i^{0u'} \mu_j^{u'u} \mu_k^{0u}}{\left(\tilde{E}_{u'0} - 2\hbar\omega\right)\left(\tilde{E}_{u0} - \hbar\omega\right)} \\ &\quad + \frac{\mu_j^{0u'} \mu_i^{u'u} \mu_k^{0u}}{\left(\tilde{E}_{u'0} + \hbar\omega\right)\left(\tilde{E}_{u0} - \hbar\omega\right)} + \frac{\mu_j^{0u'} \mu_k^{u'u} \mu_i^{0u}}{\left(\tilde{E}_{u'0} + \hbar\omega\right)\left(\tilde{E}_{u0} + 2\hbar\omega\right)} + \ldots, \end{aligned} \tag{2.8.1}$$

where $|u'\rangle$ is a third excited state and $\mathbf{d}' = \boldsymbol{\mu}^{u'u'} - \boldsymbol{\mu}^{00}$. From this partition it is clear that we can justify the two-level approximation if the bracketed terms in Eq. (2.8.1) dominate.

To study the effect of a third energy level on the denominators in Eq. (2.8.1) we proceed by assuming similar values for the numerators. While this may not be a realistic assumption, it provides an insight into the complexity of systems frequently

assumed to comprise just one excited energy level. We begin by constructing a set of new variables from Fig. 2.4. – $\Delta\tilde{E}_1 = \tilde{E}_{u0} - \hbar\omega$, $\Delta\tilde{E}'_1 = \tilde{E}_{u'0} - \hbar\omega$, $-\Delta\tilde{E}_2 = 2\hbar\omega - \tilde{E}_{u0}$, and $\Delta\tilde{E}'_2 = \tilde{E}_{u'0} - 2\hbar\omega$. For convenience, we choose the pair $\left\{\Delta\tilde{E}_1, \Delta\tilde{E}'_1\right\}$ as a basis set; the other two new variables can be constructed from these via $\Delta\tilde{E}_2 = \Delta\tilde{E}_1 - \hbar\omega$ and $\Delta\tilde{E}'_2 = \Delta\tilde{E}'_1 - \hbar\omega$. With this replacement, Eq. (2.8.1) becomes:

$$
\begin{aligned}
\beta_{ijk}^{00}\left(-2\omega;\omega,\omega\right) &= \beta_{ijk}^{\mathrm{TLA}} + \beta_{ijk}^{\mathrm{BG}} \\
&= \left(-\frac{\mu_i^{0u} d_j \mu_k^{0u}}{\Delta\tilde{E}_1\left(\Delta\tilde{E}_1 - \hbar\omega\right)} + \frac{\mu_j^{0u} d_i \mu_k^{0u}}{\Delta\tilde{E}_1\left(\Delta\tilde{E}_1 + 2\hbar\omega\right)} \right. \\
&\quad \left. + \frac{\mu_j^{0u} d_k \mu_i^{0u}}{\left(\Delta\tilde{E}_1 + 3\hbar\omega\right)\left(\Delta\tilde{E}_1 + 2\hbar\omega\right)} \right) - \frac{\mu_i^{0u'} d'_j \mu_k^{0u'}}{\Delta\tilde{E}'_1\left(\Delta\tilde{E}'_1 - \hbar\omega\right)} \\
&\quad + \frac{\mu_j^{0u'} d'_i \mu_k^{0u'}}{\Delta\tilde{E}'_1\left(\Delta\tilde{E}'_1 + 2\hbar\omega\right)} + \frac{\mu_j^{0u'} d'_k \mu_i^{0u'}}{\left(\Delta\tilde{E}'_1 + 2\hbar\omega\right)\left(\Delta\tilde{E}'_1 + 2\hbar\omega\right)} \\
&\quad - \frac{\mu_i^{0u} \mu_j^{uu'} \mu_k^{0u'}}{\Delta\tilde{E}'_1\left(\Delta\tilde{E}_1 - \hbar\omega\right)} + \frac{\mu_j^{0u} \mu_i^{uu'} \mu_k^{0u'}}{\Delta\tilde{E}'_1\left(\Delta\tilde{E}_1 + 2\hbar\omega\right)} \\
&\quad + \frac{\mu_j^{0u} \mu_k^{uu'} \mu_i^{0u'}}{\Delta\tilde{E}'_1\left(\Delta\tilde{E}_1 + 3\hbar\omega\right)} - \frac{\mu_i^{0u'} \mu_j^{u'u} \mu_k^{0u}}{\Delta\tilde{E}_1\left(\Delta\tilde{E}'_1 - \hbar\omega\right)} \\
&\quad + \frac{\mu_j^{0u'} \mu_i^{u'u} \mu_k^{0u}}{\Delta\tilde{E}'_1\left(\Delta\tilde{E}'_1 + 2\hbar\omega\right)} + \frac{\mu_j^{0u'} \mu_k^{u'u} \mu_i^{0u}}{\left(\Delta\tilde{E}'_1 + 3\hbar\omega\right)\left(\Delta\tilde{E}_1 + 2\hbar\omega\right)} + \ldots.
\end{aligned}
\tag{2.8.2}
$$

When the input light has energy markedly less than that of the first excited state, analysis of Eq. (2.8.2) shows that terms 1, 4, 7 and 10 will all have large values due to their denominators. As we have two linearly independent variables upon which the hyperpolarisability depends, we may plot a contour landscape of the denominator terms, as shown in Fig. 2.5. By introducing β' (as defined in Fig. 2.5.) we may visualise the added contributions to the hyperpolarisability tensor from the denominators corresponding to an additional energy level. To remove the

singularities associated with exact resonance conditions the energy differences include a representative damping factor of value $\gamma \sim 0.1\hbar\omega$. The white regions in the map

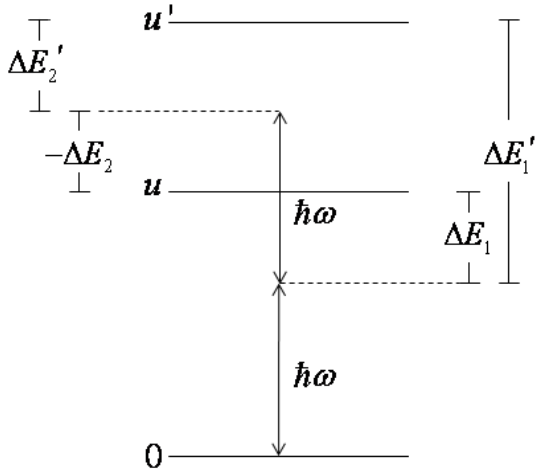

Fig. 2.4. Diagram of three energy levels. Here, $\hbar\omega$ is the energy of the input photons and u, u' label the first and second excited levels; $\Delta\tilde{E}_1$, $\Delta\tilde{E}_2$, $\Delta\tilde{E}_1'$, $\Delta\tilde{E}_2'$ are defined in Section 5.

correspond to values of $\Delta\tilde{E}_1$ and $\Delta\tilde{E}'$ where the background contributions to the hyperpolarisability are at least as great as the two-level contributions; it must be supposed that further energy levels add more corrections. However, the darkest regions of the landscape indicate pairs of energy offset values that give rise to values of β_{ijk}^{00} that are less than 20% different in value than the same tensor calculated with just two energy levels; the use of such an approximation is then defensible.

Instead of imposing the approximate equality of the numerators in Eq. (2.8.1)we now analyse the dispersion curves for the hyperpolarisability for second harmonic generation. Displayed in Fig. 2.6. are the dispersion curves – computed by Peck and Oganesyan [30] – for the axial component of the hyperpolarisabilty calculated with a single excited state (dashed line) and twenty excited states (solid line). Except for

regions far from resonance, both compounds display large deviations from the two-

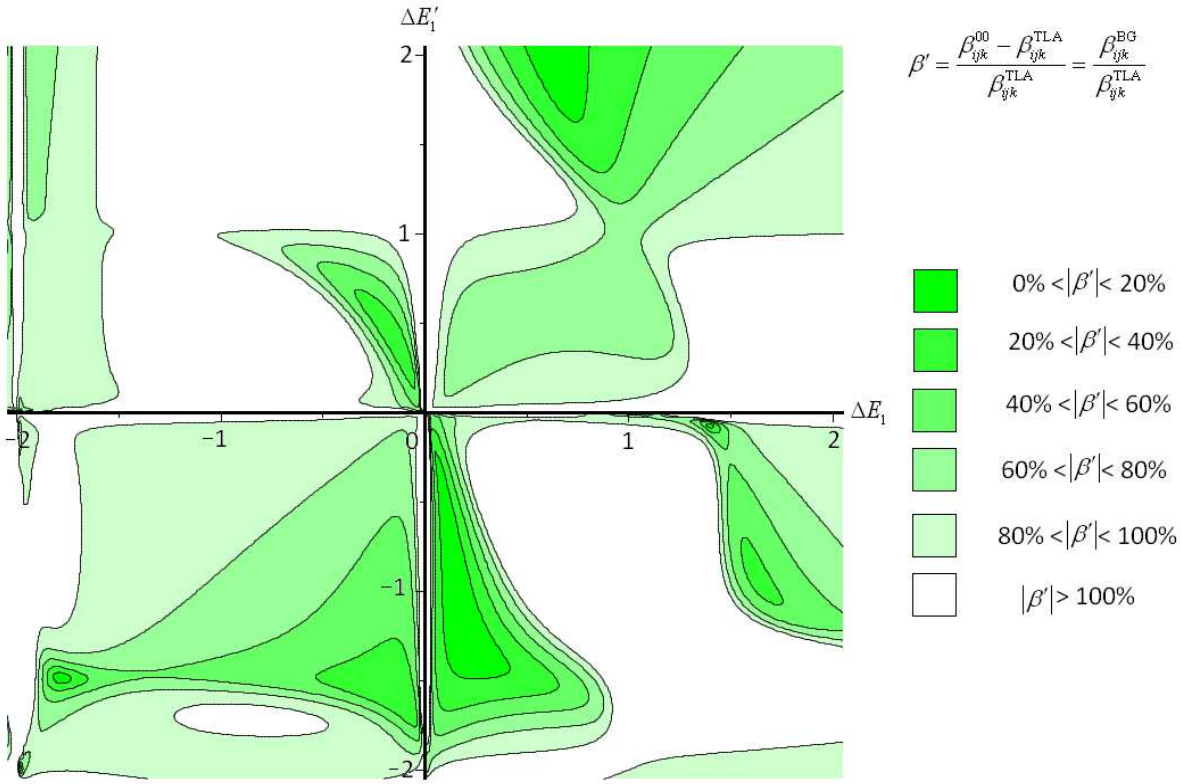

Fig. 2.5. A landscape illustrating the magnitude of β' for the hyperpolarisability corresponding to second harmonic generation, β_{ijk}^{00}. The horizontal and vertical scales are in units of $\hbar\omega$.

level results, suggesting that the two-level approximation fails for optical processes of this order. To address the issue of convergence, we introduce the analogue of Eq. (2.7.2) for the hyperpolarisability tensor:

$$\tilde{\beta}_{ijk}(N) = 100 \cdot \frac{\overline{|\beta_{ijk}(N)|}}{\beta_{ijk}(2)}, \tag{2.8.3}$$

where, once again, a value close to 100(%) indicates good agreement. Presented in Fig. 2.7. displays the value of this measure for increasing *N*. The plot for compound 1

(i) displays increasing divergence from the two-level result as the number of excited states increases above 15, whereas the equivalent plot for compound 2 (ii) exhibits an

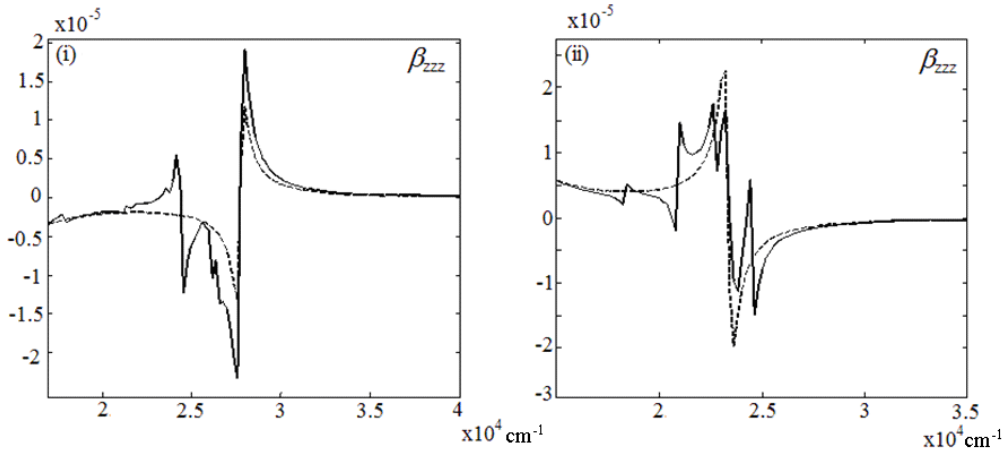

Fig. 2.6. The most intense features in the spectra of compounds 1 – (i), and 2 – (ii) arising from the zzz component of the hyperpolarisability for second harmonic generation. The horizontal scale is in wavenumbers (cm-1).

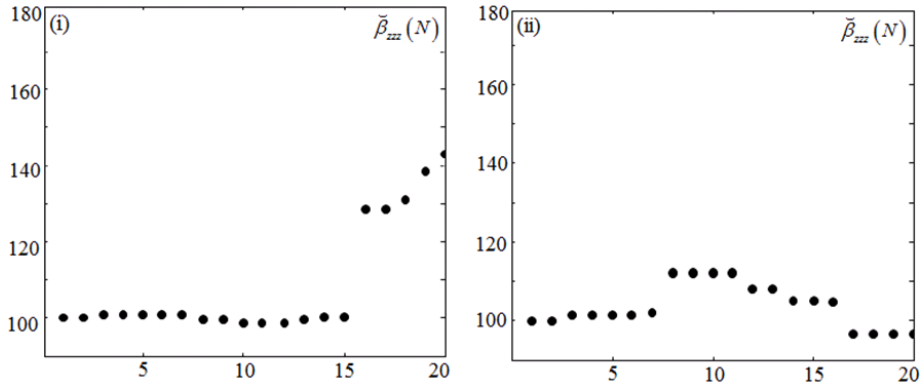

Fig. 2.7. Plot $\breve{\beta}_{ijk}(N)$ against of number of excited states in compound 1 (i) and 2 (ii).

approximately 16% divergence from the two-level result when 8-11 excited states are included. With the inclusion of 12-20 excited states the value of $\breve{\beta}_{ijk}(N)$ reduces to closer to the two-level result. Therefore, in both cases it is not guaranteed that the

two-level approximation gives a similar value to an *N*-level approximation when $N \to \infty$.

2.9 Other Hyperpolarisability Components

To ensure that the above divergence is not just associated with the zzz component of the hyperpolarisability, the dispersion curves for the other components are presented in Fig. 2.8. Clearly, for both molecules and for both components, the two-level approximation completely fails to discern *any* dispersion characteristics on this scale. In Fig. 2.8.(b) a 21-level sum over states calculation reveals a resonance with magnitude ~1% of that corresponding to the zzz component. Despite this small value, it is still surprising to see that the result based on the two-level approximation does not even hint that there might be a resonance in this frequency range. These small absolute magnitudes, in practise, will make a negligible difference to the rate due to the zzz components being 10^3-10^6 times larger than the off-diagonal components. By extension of the error-gauging parameter, displayed in Fig. 2.5., to the other diagonal components of $\beta_{ijk}^{00}(-2\omega;\omega,\omega)$ we may quantify the extent of the two-level failure for these molecules at varying wavenumbers, Fig. 2.9.

It is observed in Fig. 2.8. that for all diagonal components of the hyperpolarisability the two-level model differs from the 21-level model by varying amounts in the near-UV and visible parts of the spectrum. In both compounds the β'_{xxx} value is ~10^6 – indicating that two- and 21- level calculations differ by a factor of a million.

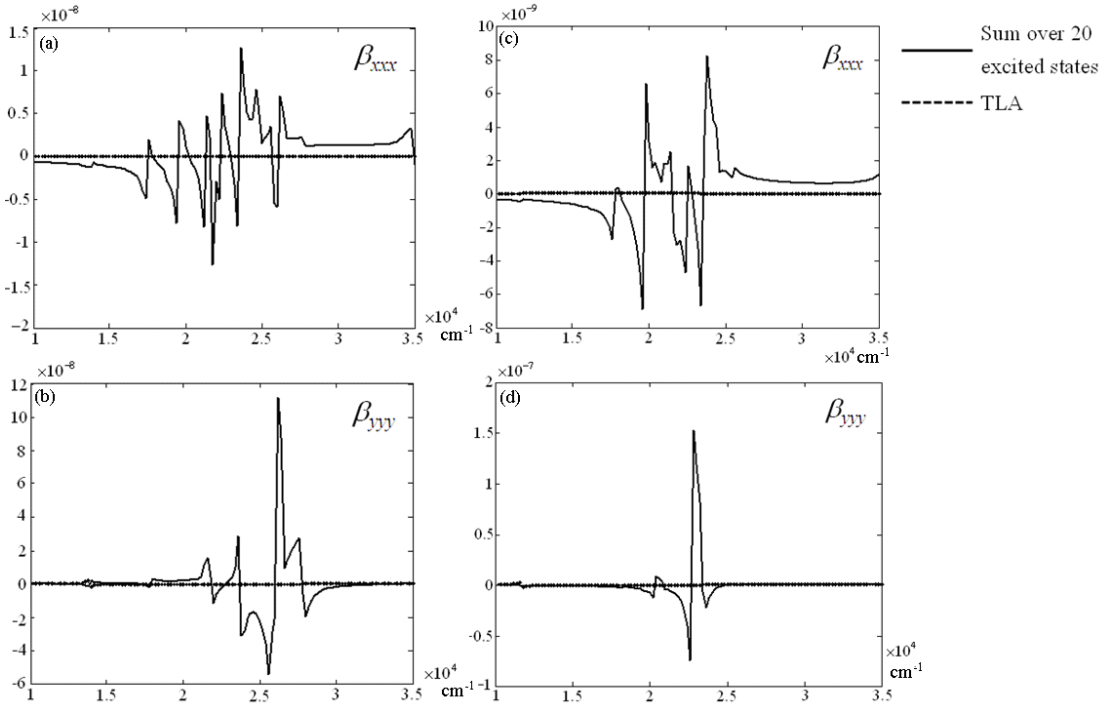

Fig. 2.8. Dispersion curves for the (a) *xxx* and (b) *yyy* components of compound 1, and (c) *xxx* and (d) *yyy* components of compound 2.

To conclude, it is worthwhile to display the variation of the error-gauging parameter for off-diagonal hyperpolarisability elements, Fig. 2.9. Interestingly, by observation of the dispersion curves, it is apparent that the value of the error-gauging parameter tends to be higher in the range corresponding to resonance. Thus, the two-level approximation applied to second harmonic generation is invalid over almost the entire range of frequencies considered here, especially close to resonance features.

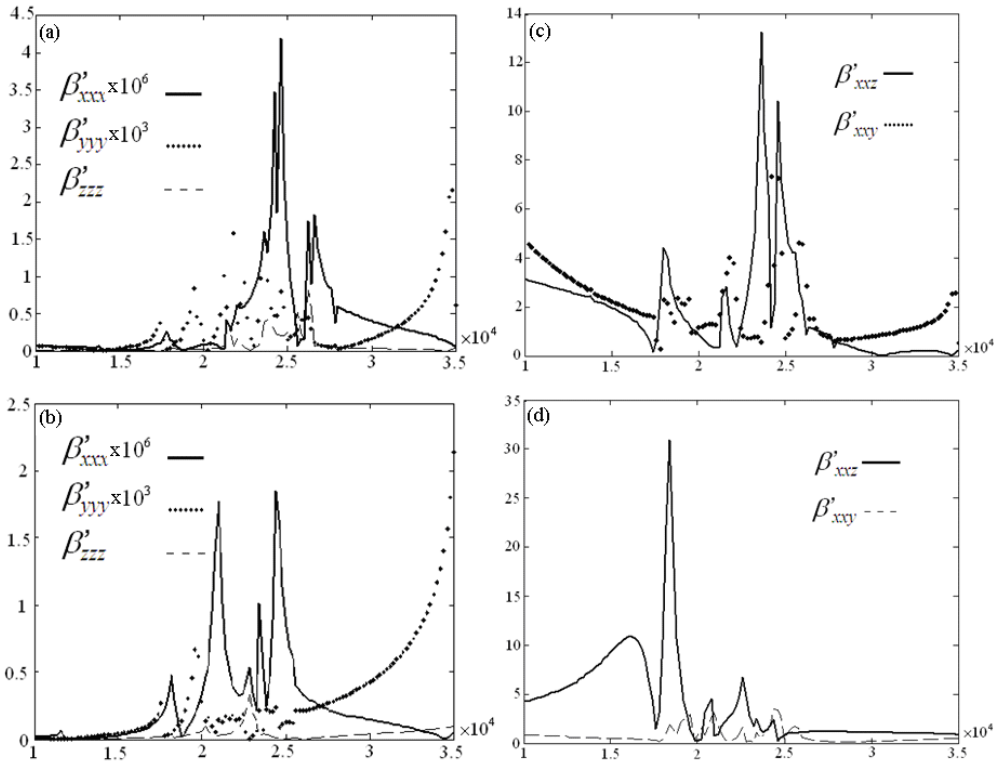

Fig. 2.9. Values of the diagonal components of the error-gauging parameter $\beta' = \beta_{\mathrm{BG}} / \beta_{\mathrm{TLA}}$ for (a) compound 1 and (b) compound 2, and values of a representative set of off-diagonal components of the error-gauging parameter $\beta' = \beta_{\mathrm{BG}} / \beta_{\mathrm{TLA}}$ for (c) compound 1 and (d) compound 2.

2.10 Counting Terms in Optical Susceptibility Tensors

Even for the hydrogen atom, which has known atomic wavefunctions, analytical calculation of the transition dipoles proves difficult. Beyond hydrogen-like atoms these vectors become only numerically tractable, usually requiring time consuming computational techniques [29,30,62–65]. Here we demonstrate that the number of terms in each optical susceptibility tensor puts constraints on their calculational ease.

Generally the polarisability tensor takes the following form:

$$\alpha_{ij}^{mo(n)}\left(\pm\omega_a,\pm\omega_b\right)=\sum_{r=0}^{n}\left(\frac{\mu_i^{mr}\mu_j^{ro}}{E_{ro}\mp\hbar\omega_a}+\frac{\mu_j^{mr}\mu_i^{ro}}{E_{ro}\mp\hbar\omega_a}\right), \tag{2.10.1}$$

where the superscript (n) denotes the number of energy levels included in the sum-over-states. Each term inside the brackets corresponds to a time-ordering of the Feynman diagrams and is summed over the possible values of the intermediate state label, r. It is readily observed that the number of terms in Eq. (2.10.1), when including n energy levels is $2n+1$. Turning our attention to the first hyperpolarisability tensor allows us to directly compute:

$$N\left(3\right)=6n^2 \tag{2.10.2}$$

as the number of terms in the second-order optical susceptibility tensor. In general, the p^{th} order susceptibility has a product of p transition dipoles with fixed initial and final states, and a $(p-1)$-fold sum over the n possible intermediate states. From combinatorial mathematics we observe that choosing $(p-1)$ repeatable elements from a set of n delivers $n^{(p-1)}$ possible arrangements. It is then seen that the p^{th} order optical susceptibility has $N(p)$ terms, with

$$N\left(p\right)=p!n^{(p-1)}, \tag{2.10.3}$$

where the factor $p!$ is included to account for the number of time-orderings. In some cases the number of time-orderings can be reduced; for example, a reduction to $(p-2)!$ in harmonic generation occurs by virtue of the symmetrical input photon labels. It can be seen that in the case of the polarisability tensor the inclusion of an

addition energy level increases the number of terms, linearly, by two. For the first hyperpolarisability, however, increasing the set of n energy levels to $n + 1$ demands an $12n + 6$ extra terms. In the general case, for a p^{th}-order optical susceptibility, increasing the set of n energy levels by one delivers an increase in number of terms by:

$$\begin{aligned} N(p,n+1)-N(p,n) &= p!(n+1)^{(p-1)} - p!n^{(p-1)} \\ &= p!\sum_{k=0}^{p-1}\binom{p-1}{k} n^{(p-k-1)} - p!n^{(p-1)} \\ &= p!\sum_{k=1}^{p-1}\binom{p-1}{k} n^{(p-k-1)}, \end{aligned} \tag{2.10.4}$$

where $\binom{n}{k}$ is a binomial coefficient. For example, in calculating the first hyperpolarisability tensor, $p = 3$, increasing the set of energy levels from ten to eleven requires computation of an additional 126 terms. The precise number of terms in the first four optical susceptibility tensors (ignoring any index symmetry) are displayed in Fig. 2.12. For example, a four-wave mixing process calculated with 40 possible intermediate energy levels requires calculation of 310 million terms.

However, in the language of complexity theory, these computations are at least solvable in polynomial time with respect to n as there are, approximately $O(n^{(p-1)})$ terms to calculate [66].

p \ n	2	5	10	20	30	40
$2-\alpha_{ij}$	2	10	20	40	60	80
$3-\beta_{ijk}$	24	150	600	2400	5400	9600
$4-\chi^{(3)}_{ijkl}$	190	3000	2.4×10^4	1.9×10^5	6.4×10^5	1.5×10^6
$5-\chi^{(4)}_{ijklm}$	1900	7.5×10^4	1.2×10^6	1.9×10^7	9.7×10^7	3.1×10^8

Fig. 2.12. The values of $N(p,n)$, the number of terms in the p^{th}-order nonlinear susceptibility tensor taking into account n energy levels, to two significant figures.

2.11 Conclusion

The purpose of the above has been to study the criteria for the validity of the two-level approximation, generally and in the context of nonlinear optics. It has been determined that the use of a two-state model undermines realism in return for calculational ease [29–32].

First, we presented an analytical theorem on the expectation values of quantum operators that showed the invalidity of the two-level approximation in even simple systems. As an example, we proved that applying a two-level model to a quantum harmonic oscillator led to the absurd conclusion that the different energy levels must have the same energy. Furthermore, by application of the Virial theorem it was shown that this *reductio ad absurdum* argument applies to a wider class of problems.

Such analysis forces not only that the expectation value of quantum operators in the two basis states be equal, but also the equality of fluctuations in those two states. To the extent that these criteria are not satisfied the two-level approximation fails.

Secondly, we discussed the validity of the two-level approximation when applied to the optical susceptibility tensors of nonlinear optical processes. After deriving the molecular response tensors for Rayleigh scattering and second harmonic generation, we challenged the commonly held idea that 'push-pull' chromophores are associated with enhanced second harmonic response; this idea is justifiable only within the two-level approximation. It was then shown that *ab initio* calculations combined with introduction of an error-gauging parameter indicated that for two specified molecules the two-level approximation was indeed valid. However, it has been shown that the sum over all molecular states of any optical susceptibility is zero, which demands that, when considering just two energy levels, the excited state tensor is precisely the negative of the ground state tensor, $\chi^{00} = \chi^{uu}$ [67].

The extension of these arguments to second harmonic generation began by plotting a visually representative landscape, which, under the strict assumption of similarly valued numerators, indicated regions where a two-level model gave similar (and vastly different) results to that obtained by introducing a third energy level. The dispersion curves of two organic chromophores – again calculated by Peck and Oganesyan [31] – were exhibited and, in contrast to those for Rayleigh scattering, indicated that a twenty excited state calculation differed vastly from the two-level result. An error gauging parameter was introduced, which indicated that the

hyperpolarisability for the second harmonic response of these molecules does not converge as the number of included energy levels increases.

Finally, it was proved that the number of terms in the p^{th}-order optical susceptibility is polynomial of order $n^{(p-1)}$, where n is the number of energy levels included in the sum-over-states computation. The physical implications of deploying the two-level approximation are not obvious and mostly unrealistic, thus the implications of such a model deserve wider recognition.

2.12 Bibliography

[1] R. P. Feynman, *The Feynman Lectures on Physics*, New millennium ed, Basic Books, New York (2011).

[2] D. J. Griffiths, *Introduction to Quantum Mechanics*, 2nd ed, Pearson Prentice Hall, Upper Saddle River, NJ (2005).

[3] P. W. Atkins, *Atkins' Physical Chemistry*, 8th ed, Oxford University Press, Oxford; New York (2006).

[4] B. W. Shore, *The Theory of Coherent Atomic Excitation*, Wiley, New York (1990).

[5] L. Allen, *Optical Resonance and Two-Level Atoms*, Dover, New York (1987).

[6] M. S. Skolnick and D. J. Mowbray, "Self-Assembled semiconductor quantum dots: Fundamental Physics and Device Applications," *Annual Review of Materials Research* **34**(1), 181–218 (2004) [doi:10.1146/annurev.matsci.34.082103.133534].

[7] W. G. van der Wiel, T. Fujisawa, S. Tarucha, and L. P. Kouwenhoven, "A double quantum dot as an artificial two-level system," *Japanese Journal of Applied Physics* **40**(Part 1, No. 3B), 2100–2104 (2001) [doi:10.1143/JJAP.40.2100].

[8] A. Zrenner, E. Beham, S. Stufler, F. Findeis, M. Bichler, and G. Abstreiter, "Coherent properties of a two-level system based on a quantum-dot photodiode," *Nature* **418**(6898), 612–614 (2002) [doi:10.1038/nature00912].

[9] I. Bialynicki-Birula and T. Sowiński, "Quantum electrodynamics of qubits," *Physical Review A* **76**(6) (2007) [doi:10.1103/PhysRevA.76.062106].

[10] S. Mukamel, *Principles of Nonlinear Optical Spectroscopy*, Oxford University Press, New York; Oxford (1999).

[11] S. C. Rand, *Lectures on Light: Nonlinear and Quantum Optics Using the Density Matrix*, Oxford University Press, Oxford, England; New York (2010).

[12] G. Barton, "Frequency shifts near an interface: inadequacy of two-level atomic models," *Journal of Physics B: Atomic and Molecular Physics* **7**(16), 2134–2142 (1974) [doi:10.1088/0022-3700/7/16/012].

[13] C. N. Danson, P. A. Brummitt, R. J. Clarke, J. L. Collier, B. Fell, A. J. Frackiewicz, S. Hawkes, C. Hernandez-Gomez, P. Holligan, et al., "Vulcan petawatt: Design, operation and interactions at 5 × 1020 Wcm–2," *Laser and Particle Beams* **23**(01) (2005) [doi:10.1017/S0263034605050159].

[14] J. L. Oudar and D. S. Chemla, "Hyperpolarizabilities of the nitroanilines and their relations to the excited state dipole moment," *The Journal of Chemical Physics* **66**(6), 2664 (1977) [doi:10.1063/1.434213].

[15] B. Dick, "Importance of initial and final states as intermediate states in two-photon spectroscopy of polar molecules," *The Journal of Chemical Physics* **76**(12), 5755 (1982) [doi:10.1063/1.442971].

[16] R. Wortmann, P. Krämer, C. Glania, S. Lebus, and N. Detzer, "Deviations from Kleinman symmetry of the second-order polarizability tensor in molecules with low-lying perpendicular electronic bands," *Chemical Physics* **173**(1), 99–108 (1993) [doi:10.1016/0301-0104(93)80221-T].

[17] D. L. Andrews and W. J. Meath, "On the role of permanent dipoles in second harmonic generation," *Journal of Physics B: Atomic, Molecular and Optical Physics* **26**(23), 4633–4641 (1993) [doi:10.1088/0953-4075/26/23/030].

[18] B. N. Jagatap and W. J. Meath, "On the competition between permanent dipole and virtual state two-photon excitation mechanisms, and two-photon optical excitation pathways, in molecular excitation," *Chemical Physics Letters* **258**(1-2), 293–300 (1996) [doi:10.1016/0009-2614(96)00620-3].

[19] M. Drobizhev, F. Meng, A. Rebane, Y. Stepanenko, E. Nickel, and C. W. Spangler, "Strong two-photon absorption in new asymmetrically substituted porphyrins: interference between charge-transfer and intermediate-resonance pathways," *J Phys Chem B* **110**(20), 9802–9814 (2006) [doi:10.1021/jp0551770].

[20] R. W. Boyd, *Nonlinear Optics*, Academic Press, San Diego, California (2008).

[21] P. Kaur, M. Kaur, G. Depotter, S. Van Cleuvenbergen, I. Asselberghs, K. Clays, and K. Singh, "Thermally stable ferrocenyl 'push–pull' chromophores with tailorable and switchable second-order non-linear optical response: synthesis and structure–property relationship," *Journal of Materials Chemistry* **22**(21), 10597 (2012) [doi:10.1039/c2jm31387a].

[22] F. Terenziani, S. Ghosh, A.-C. Robin, P. K. Das, and M. Blanchard-Desce, "Environmental and excitonic effects on the First hyperpolarizability of polar molecules and related dimers," *The Journal of Physical Chemistry B* **112**(37), 11498–11505 (2008) [doi:10.1021/jp800191p].

[23] A. Corozzi, B. Mennucci, R. Cammi, and J. Tomasi, "Structure versus solvent effects on nonlinear optical properties of push–pull systems: a quantum-mechanical study based on a polarizable continuum model," *The Journal of Physical Chemistry A* **113**(52), 14774–14784 (2009) [doi:10.1021/jp904906n].

[24] F. Quist, C. Vandevelde, D. Didier, A. Teshome, I. Asselberghs, K. Clays, and S. Sergeyev, "Push–pull chromophores comprising benzothiazolium acceptor and thiophene auxiliary donor moieties: Synthesis, structure, linear and quadratic

non-linear optical properties," *Dyes and Pigments* **81**(3), 203–210 (2009) [doi:10.1016/j.dyepig.2008.10.004].

[25] J. Rotzler, D. Vonlanthen, A. Barsella, A. Boeglin, A. Fort, and M. Mayor, "Variation of the backbone conjugation in NLO model compounds: torsion-angle-restricted, biphenyl-based push-pull-systems," *European Journal of Organic Chemistry* **2010**(6), 1096–1110 (2010) [doi:10.1002/ejoc.200901358].

[26] D. R. Reichman and R. J. Silbey, "On the relaxation of a two-level system: Beyond the weak-coupling approximation," *The Journal of Chemical Physics* **104**(4), 1506 (1996) [doi:10.1063/1.470916].

[27] M. Frasca, "A modern review of the two-level approximation," *Annals of Physics* **306**(2), 193–208 (2003) [doi:10.1016/S0003-4916(03)00078-2].

[28] J. Cheng and J. Zhou, "Validity of the two-level approximation in the interaction of few-cycle light pulses with atoms," *Physical Review A* **67**(4) (2003) [doi:10.1103/PhysRevA.67.041404].

[29] D. L. Andrews, D. S. Bradshaw, and M. M. Coles, "Limitations and improvements upon the two-level approximation for molecular nonlinear optics," 10 February 2011, 79171K–79171K–12 [doi:10.1117/12.873749].

[30] M. M. Coles, J. N. Peck, V. S. Oganesyan, and D. L. Andrews, "Failure of the two-level and sum over states methods in nonlinear optics, demonstrated by ab initio methods," 1 June 2012, 84340K–84340K–11 [doi:10.1117/12.920547].

[31] M. M. Coles, J. N. Peck, V. S. Oganesyan, and D. L. Andrews, "Assessing limitations to the two-level approximation in nonlinear optics for organic chromophores by ab initio methods," 8 September 2011, 81130K–81130K–11 [doi:10.1117/12.894006].

[32] D. L. Andrews, D. S. Bradshaw, and M. M. Coles, "Perturbation theory and the two-level approximation: A corollary and critique," *Chemical Physics Letters* **503**(1-3), 153–156 (2011) [doi:10.1016/j.cplett.2010.12.055].

[33] L. Mandel, *Optical Coherence and Quantum Optics*, Cambridge University Press, Cambridge; New York (1995).

[34] L. C. D. Romero and D. L. Andrews, "Effects of permanent dipole moments in high-order optical nonlinearity," *Journal of Physics B: Atomic, Molecular and Optical Physics* **32**(9), 2277–2293 (1999) [doi:10.1088/0953-4075/32/9/317].

[35] W. H. Louisell, *Quantum Statistical Properties of Radiation*, Wiley, New York (1973).

[36] S. G. Krantz, *A Primer of Real Analytic Functions*, 2nd ed, Birkhäuser, Boston (2002).

[37] G. Smith, *Introductory Mathematics, Algebra, and Analysis*, Springer, Berlin; New York (1998).

[38] D. A. McQuarrie, *Physical Chemistry: A Molecular Approach*, University Science Books, Sausalito, California (1997).

[39] H. Goldstein and J. L. Safko, *Classical Mechanics*, Addison Wesley, San Francisco (2002).

[40] D. P. Craig and T. Thirunamachandran, *Molecular Quantum Electrodynamics: An Introduction to Radiation-Molecule Interactions*, Dover Publications, Mineola, N.Y (1998).

[41] E. Power and T. Thirunamachandran, "Quantum electrodynamics with nonrelativistic sources. I. Transformation to the multipolar formalism for second-quantized electron and Maxwell interacting fields," *Physical Review A* **28**(5), 2649–2662 (1983) [doi:10.1103/PhysRevA.28.2649].

[42] E. A. Power, "On the nature of the Hamiltonian for the interaction of radiation with atoms and molecules: (e/mc)p·A, –μ·E, and all that," *American Journal of Physics* **46**(4), 370 (1978) [doi:10.1119/1.11313].

[43] R. G. Woolley, "Charged particles, gauge invariance, and molecular electrodynamics," *International Journal of Quantum Chemistry* **74**(5), 531–545 (1999) [doi:10.1002/(SICI)1097-461X].

[44] R. G. Woolley, "Gauge invariance in non-relativistic electrodynamics," *Proceedings of the Royal Society A: Mathematical, Physical and Engineering Sciences* **456**(2000), 1803–1819 (2000) [doi:10.1098/rspa.2000.0587].

[45] W. J. Meath and E. A. Power, "On the importance of permanent moments in multiphoton absorption using perturbation theory," *Journal of Physics B: Atomic and Molecular Physics* **17**(5), 763–781 (1984) [doi:10.1088/0022-3700/17/5/017].

[46] D. Andrews, S. Naguleswaran, and G. Stedman, "Phenomenological damping of nonlinear-optical response tensors," *Physical Review A* **57**(6), 4925–4929 (1998) [doi:10.1103/PhysRevA.57.4925].

[47] A. Buckingham and P. Fischer, "Phenomenological damping in optical response tensors," *Physical Review A* **61**(3) (2000) [doi:10.1103/PhysRevA.61.035801].

[48] I. López-Duarte, J. E. Reeve, J. Pérez-Moreno, I. Boczarow, G. Depotter, J. Fleischhauer, K. Clays, and H. L. Anderson, "'Push-no-pull' porphyrins for second harmonic generation imaging," *Chemical Science* **4**(5), 2024 (2013) [doi:10.1039/c3sc22306j].

[49] K. S. Suslick, C. T. Chen, G. R. Meredith, and L. T. Cheng, "Push-pull porphyrins as nonlinear optical materials," *Journal of the American Chemical Society* **114**(17), 6928–6930 (1992) [doi:10.1021/ja00043a055].

[50] M. Yeung, A. C. H. Ng, M. G. B. Drew, E. Vorpagel, E. M. Breitung, R. J. McMahon, and D. K. P. Ng, "Facile synthesis and nonlinear optical properties of push–pull 5,15-diphenylporphyrins," *The Journal of Organic Chemistry* **63**(21), 7143–7150 (1998) [doi:10.1021/jo971597c].

[51] I. D. L. Albert, T. J. Marks, and M. A. Ratner, "Large molecular hyperpolarizabilities in 'push–pull' porphyrins. Molecular planarity and auxiliary donor–acceptor effects," *Chemistry of Materials* **10**(3), 753–762 (1998) [doi:10.1021/cm970478a].

[52] S. M. LeCours, H.-W. Guan, S. G. DiMagno, C. H. Wang, and M. J. Therien, "Push–pull arylethynyl porphyrins: new chromophores that exhibit large molecular first-order hyperpolarizabilities," *Journal of the American Chemical Society* **118**(6), 1497–1503 (1996) [doi:10.1021/ja953610l].

[53] T.-G. Zhang, Y. Zhao, I. Asselberghs, A. Persoons, K. Clays, and M. J. Therien, "Design, synthesis, linear, and nonlinear optical properties of conjugated (porphinato)zinc(II)-based donor–acceptor chromophores featuring nitrothiophenyl and nitrooligothiophenyl electron-accepting moieties," *Journal of the American Chemical Society* **127**(27), 9710–9720 (2005) [doi:10.1021/ja0402553].

[54] T. Ishizuka, L. E. Sinks, K. Song, S.-T. Hung, A. Nayak, K. Clays, and M. J. Therien, "The roles of molecular structure and effective optical symmetry in evolving dipolar chromophoric building blocks to potent octopolar nonlinear optical chromophores," *Journal of the American Chemical Society* **133**(9), 2884–2896 (2011) [doi:10.1021/ja105004k].

[55] N. Jiang, G. Zuber, S. Keinan, A. Nayak, W. Yang, M. J. Therien, and D. N. Beratan, "Design of coupled porphyrin chromophores with unusually large hyperpolarizabilities," *The Journal of Physical Chemistry C* **116**(17), 9724–9733 (2012) [doi:10.1021/jp2115065].

[56] T. Verbiest, *Second-Order Nonlinear Optical Characterization Techniques: An Introduction*, CRC Press, Boca Raton (2009).

[57] S. Brasselet and J. Zyss, "Relation between quantum and geometric dimensionalities in molecular nonlinear optics: beyond the two-level model for anisotropic systems," *Journal of Nonlinear Optical Physics & Materials* **05**(04), 671–693 (1996) [doi:10.1142/S0218863596000490].

[58] A. Capobianco, R. Centore, C. Noce, and A. Peluso, "Molecular hyperpolarizabilities of push–pull chromophores: A comparison between theoretical and experimental results," *Chemical Physics* **411**, 11–16 (2013) [doi:10.1016/j.chemphys.2012.11.019].

[59] D. L. Andrews, L. C. D. Romero, and W. J. Meath, "An algorithm for the nonlinear optical susceptibilities of dipolar molecules, and an application to third harmonic generation," *Journal of Physics B: Atomic, Molecular and Optical Physics* **32**(1), 1–17 (1999) [doi:10.1088/0953-4075/32/1/003].

[60] D. L. Andrews and L. D. Romero, "Local coherence and the temporal development of second harmonic emission," *Journal of Physics B: Atomic, Molecular and Optical Physics* **34**(11), 2177–2187 (2001) [doi:10.1088/0953-4075/34/11/310].

[61] G. Juzeliūnas, L. Dávila Romero, and D. Andrews, "Eliminating ground-state dipole moments in quantum optics via canonical transformation," *Physical Review A* **68**(4) (2003) [doi:10.1103/PhysRevA.68.043811].

[62] T. Ansbacher, H. K. Srivastava, T. Stein, R. Baer, M. Merkx, and A. Shurki, "Calculation of transition dipole moment in fluorescent proteins—towards efficient energy transfer," *Physical Chemistry Chemical Physics* **14**(12), 4109 (2012) [doi:10.1039/c2cp23351g].

[63] J. E. Bloor, "Finite field ab initio calculations of the dipole polarizabilities and first and second hyperpolarizabilities using multiple sets of polarization funct," *Journal of Molecular Structure: Theochem* **234**, 173–183 (1991) [doi:10.1016/0166-1280(91)89011-O].

[64] A. W. Kanzler, H. Sun, and K. F. Freed, "Dipole moments, transition moments, oscillator strengths, radiative lifetimes, and overtone intensities for CH and CH+ as computed by quasi-degenerate many-body perturbation theory," *International Journal of Quantum Chemistry* **39**(3), 269–286 (1991) [doi:10.1002/qua.560390306].

[65] B. F. Minaev and L. G. Telyatnik, "Ab initio calculation of transition dipole moments for transitions between valence states in oxygen molecules," *Optics and Spectroscopy* **91**(6), 883–890 (2001) [doi:10.1134/1.1429701].

[66] M. Sipser, *Introduction to the Theory of Computation*, Thomson Course Technology, Boston (2006).

[67] L. C. D. Romero and D. L. Andrews, "A sum rule for nonlinear optical susceptibilities," *Journal of Optics B: Quantum and Semiclassical Optics* **6**(1), 59–62 (2004) [doi:10.1088/1464-4266/6/1/010].

Chapter 3

Measures of Optical Angular Momentum

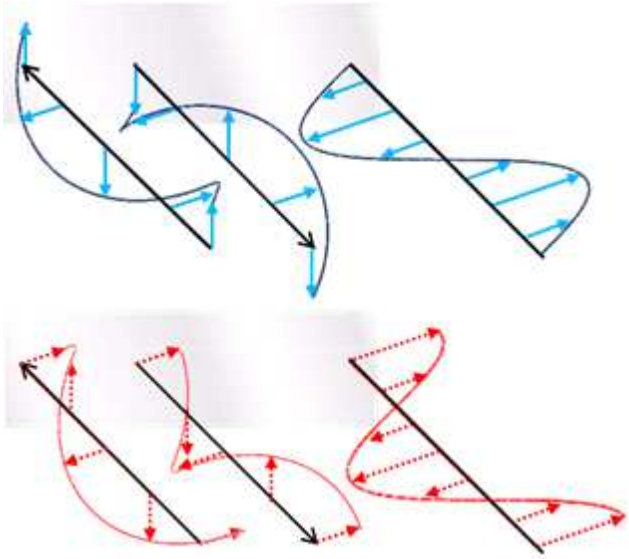

"This unexpected discovery … is a source of mathematical 'embarras de richesses' because of the lack of any ready physical interpretation for the quantities that are found to be conserved."

– Daniel M. Lipkin[†]

[†] Lipkin, Daniel M., Existence of a New Conservation Law in Electromagnetic Theory – *Journal of Mathematical Physics Vol 5 No. 1 – p696* (1964).

3.1 Background

Conservation laws are important in electromagnetic theory because they put constraints on how a system may evolve with time. For example, if a photon travels in free space, we would be very surprised if, upon looking after a time-interval, its direction of motion had reversed. Here, of course, we have not considered the conservation of linear momentum, which arises from the spatially integrated Lagrangian (density) being invariant under a continuous translation. By 1918, Emmy Noether had shown that for both particles and fields, *every* differentiable symmetry of a system's action corresponds to a conservation law [1], connecting a *Noether charge* and the flow of a *Noether current* [2]. The quantum version of Noether's theorem necessarily involves taking the expectation values of the four-currents, and is called the Ward-Takahashi identity [3]. It emerges that the infinitesimal spatial rotation symmetries of the action correspond to the conservation of angular momentum. In fact, this is a special case of the hyperbolic space-time rotations, known as Lorentz transformations, which generate a whole host of conservation laws [4].

In 1909, John Poynting suggested that electromagnetic radiation has, in the case of circular polarisations, an associated angular momentum [5]. Robert Beth's famous experiment in 1936 showed that, by measuring the torque on the thread suspending a half-wave plate through which circularly polarised light was passed, light does indeed posses intrinsic angular momentum of $\pm\hbar$ per photon [6]. A modern version of this experiment, performed with optical tweezers, rotates micrometre-sized birefringent calcite spheres by transferring angular momentum from the optical trap [7]. Moreover, it has been shown that the spin angular momentum (associated with the

polarisation) and the orbital angular momentum (associated with an optical field with a twisted phase) can produce mechanically equivalent effects [8].

In this chapter we show that the optical angular momentum can be divided into parts that satisfy duplex symmetry (electric-magnetic democracy). The spin and orbital parts of the angular momentum are analysed in a quantum optical framework and are shown to depend on number operators in characteristic ways. Furthermore, the spin part is shown to obey a continuity equation with the electromagnetic helicity. Both measures are evaluated using plane wave and Laguerre-Gaussian modes, and, as expected, the spin and helicity measures are not affected by the introduction of orbital angular momentum. We then investigate the recently rediscovered optical chirality density and corresponding flux to show that, in the paraxial approximation, they are proportional only to the spin part of the optical angular momentum. Beams with nonzero values of these measures do not have any orbital angular momentum characteristics. Finally, it is shown that the infinite hierarchy of helicity- and spin-type measures, introduced by Cameron, Barnett and Yao, all emerge with similar quantum operator form, and a general expression is provided. Thus, the motivation for this chapter is to develop a fully quantised description of the various optical angular momentum measures. Such an analysis has results that match exactly to the classical light description, developed by Bliokh and Nori. Furthermore, the orbital and spin parts of the electromagnetic field emerge as dependant upon number operators, which can easily be recast in terms of intensities to relate to experimental work. A description of this kind also leads to a similar description of the recently rediscovered optical chirality density (Lipkin zilch) and an intuitive proof that 'superchiral light' does not exist.

3.2 Symmetry

By demanding that an infinitesimal space-time translation, $q^\mu \to q^\mu + t^\mu$, where t is a constant translation and Greek superscripts denote the four space-time coordinates, leaves the spatially integrated field Lagrangian unchanged, it emerges that a set of quantities are conserved. In this case, it is the electromagnetic stress-energy tensor [3,4]:

$$T_\nu^\mu = \begin{bmatrix} \frac{1}{2}\left(\varepsilon_0 \mathbf{E}^2 + \frac{1}{\mu_0}\mathbf{B}^2\right) & S_x/c & S_y/c & S_z/c \\ S_x/c & \sigma_{xx} & \sigma_{xy} & \sigma_{xz} \\ S_y/c & \sigma_{yx} & \sigma_{yy} & \sigma_{yx} \\ S_z/c & \sigma_{zx} & \sigma_{zy} & \sigma_{zz} \end{bmatrix}, \tag{3.2.1}$$

where the S_i are the components of the Poynting vector, $\mathbf{S} = 1/\mu_0 (\mathbf{E} \times \mathbf{B})$, and $\sigma_{ij} = -\varepsilon_0 E_i E_j - 1/\mu_0 2 B_i B_j + 1/2\left(\varepsilon_0 E^2 + 1/\mu_0 B^2\right)\delta_{ij}$. Here, $u = 1/2\left(\varepsilon_0 \mathbf{E}^2 + 1/\mu_0 \mathbf{B}^2\right)$ is the energy density. In a system of charges we obtain the continuity equation:

$$\frac{\partial u}{\partial t} + \nabla \cdot \mathbf{S} = -\mathbf{j} \cdot \mathbf{e}, \tag{3.2.2}$$

where $\mathbf{j}$ is the current density. Of course, in a free field, this becomes a conservation equation, and it is revealed that the flow of the Poynting vector out of (or in to) any volume is the rate of change energy density in that volume.

If we instead demand that the action is invariant under the set of Lorentz transformations, which contains the subset of three-dimensional spatial rotations, we obtain another conserved current; namely:

$$M_{\nu}^{\mu o} = T_{\nu}^{o} x^{\mu} - T_{\nu}^{\mu} x^{o}, \tag{3.2.3}$$

where $\partial^{\nu} M_{\nu}^{\mu o} = 0$. If we only consider the three-dimensional spatial rotations and use the electromagnetic Lagrangian, we obtain the conservation of the cross-product of the position vector, **r**, with the Poynting vector, which is interpreted at the angular momentum of the electromagnetic field.

Thus, the conservation of energy-momentum is a consequence of the invariance of the action under a space-time transformation and the conservation of angular momentum is a consequence of the invariance of the action under a spatial rotation. Furthermore, it can be shown that the electromagnetic field Lagrangian is invariant under a shift in the velocity of the observer (a Lorentz transformation), which gives rise to a proof that the electric and magnetic fields are different manifestations of the same force [9].

3.3 Optical Angular Momentum

From Noether's theorem it is determined that the angular momentum for the electromagnetic field is given by:

$$\mathbf{J} = \varepsilon_0 \int \partial^3 \mathbf{r} \left\{ \mathbf{r} \times (\mathbf{e} \times \mathbf{b}) \right\}, \tag{3.3.1}$$

where (**e**×**b**) is the Poynting vector [10]. We first make a trivial division,

$$\mathbf{J} = \frac{\varepsilon_0}{2} \int \partial^3 \mathbf{r} \left\{ \mathbf{r} \times (\mathbf{e} \times \mathbf{b}) \right\} - \frac{\varepsilon_0}{2} \int \partial^3 \mathbf{r} \left\{ \mathbf{r} \times (\mathbf{b} \times \mathbf{e}) \right\}, \tag{3.3.2}$$

and substitute the vector potential of the **b** field in the left term and of the **e** field in the right term, to obtain:

$$\mathbf{J} = \frac{\varepsilon_0}{2} \int \partial^3 \mathbf{r} \left\{ \mathbf{r} \times (\mathbf{e} \times \nabla \times \mathbf{a}) + \mathbf{r} \times (\mathbf{b} \times \nabla \times \mathbf{c}) \right\}. \tag{3.3.3}$$

We proceed by making explicit the indices of the vectors in our expression:

$$J_i = \frac{\varepsilon_0}{2} \int \partial^3 \mathbf{r} \left\{ r_j \varepsilon_{ijk} \left(\mathbf{e} \times \nabla \times \mathbf{a} \right)_k + r_j \varepsilon_{ijk} \left(\mathbf{b} \times \nabla \times \mathbf{c} \right)_k \right\}, \tag{3.3.4}$$

where ε_{ijk} is the antisymmetric Levi-Civita symbol [11]. Further decomposition into index notation delivers:

$$\begin{aligned} J_i &= \frac{\varepsilon_0}{2} \int \partial^3 \mathbf{r} \left\{ r_j \varepsilon_{ijk} \varepsilon_{klm} e_l \left(\nabla \times \mathbf{a} \right)_m + r_j \varepsilon_{ijk} \varepsilon_{klm} b_l \left(\nabla \times \mathbf{c} \right)_m \right\}, \\ &= \frac{\varepsilon_0}{2} \int \partial^3 \mathbf{r} \left\{ r_j \varepsilon_{ijk} \varepsilon_{klm} e_l \varepsilon_{mnp} \partial_n a_p + r_j \varepsilon_{ijk} \varepsilon_{klm} b_l \varepsilon_{mnp} \partial_n c_p \right\}. \end{aligned} \tag{3.3.5}$$

The Levi-Civita has the following properties [11]:

$$\begin{aligned}&\varepsilon_{klm}=\varepsilon_{mkl}=\varepsilon_{lmk}\\&\varepsilon_{mkl}\varepsilon_{mnp}=\delta_{kn}\delta_{lp}-\delta_{kp}\delta_{ln}.\end{aligned}\tag{3.3.6}$$

Therefore, the expression can be rearranged to:

$$\begin{aligned}J_i&=\frac{\varepsilon_0}{2}\int\partial^3\mathbf{r}\left\{r_j\varepsilon_{ijk}\left(\delta_{kn}\delta_{lp}-\delta_{kp}\delta_{ln}\right)e_l\partial_n a_p+r_j\varepsilon_{ijk}\left(\delta_{kn}\delta_{lp}-\delta_{kp}\delta_{ln}\right)b_l\partial_n c_p\right\}\\&=\frac{\varepsilon_0}{2}\int\partial^3\mathbf{r}\left\{r_j\varepsilon_{ijk}\left(e_l\partial_k a_l-e_l\partial_l a_k\right)+r_j\varepsilon_{ijk}\left(b_l\partial_k c_l-b_l\partial_l c_k\right)\right\}.\end{aligned}\tag{3.3.7}$$

The $r_j\varepsilon_{ijk}e_l\partial_l a_k$ and the $r_j\varepsilon_{ijk}b_l\partial_l c_k$ terms can be integrated by parts to deliver

$$\begin{aligned}\int\partial^3\mathbf{r}\,r_j\varepsilon_{ijk}e_l\partial_l a_k&=\left[r_j\varepsilon_{ijk}e_l a_k\right]_{\mathbf{r}=-\infty}^{\mathbf{r}=\infty}-\varepsilon_{ijk}\int\partial^3\mathbf{r}\left(\left(\partial_l r\right)_j e_l a_k+r_j\left(\partial_l e_l\right)a_k\right)\\\int\partial^3\mathbf{r}\,r_j\varepsilon_{ijk}b_l\partial_l c_k&=\left[r_j\varepsilon_{ijk}b_l c_k\right]_{\mathbf{r}=-\infty}^{\mathbf{r}=\infty}-\varepsilon_{ijk}\int\partial^3\mathbf{r}\left(\left(\partial_l r_j\right)b_l c_k+r_j\left(\partial_l b_l\right)c_k\right),\end{aligned}\tag{3.3.8}$$

where the square brackets are zero if the fields vanish at infinity and

$$\begin{aligned}&\partial_l e_l=\nabla\cdot\mathbf{e}=0\\&\partial_l b_l=\nabla\cdot\mathbf{b}=0,\end{aligned}\tag{3.3.9}$$

in the absence of charges. We are then left with

$$J_i=\frac{\varepsilon_0}{2}\int\partial^3\mathbf{r}\left\{r_j\varepsilon_{ijk}\left(e_l\left(\partial_k a_l\right)+\left(\partial_l r_j\right)e_l a_k\right)+r_j\varepsilon_{ijk}\left(b_l\left(\partial_k c_l\right)+\left(\partial_l r_j\right)b_l c_k\right)\right\}.\tag{3.3.10}$$

Noting that $\partial_l r_j=\delta_{lj}$ enables us to write

$$J_i = \frac{\varepsilon_0}{2}\int \partial^3\mathbf{r}\left\{\varepsilon_{ijk}\left(e_j a_k + b_j c_k\right) + r_j\varepsilon_{ijk}\left(e_l\partial_k a_l + b_l\partial_k c_l\right)\right\}, \tag{3.3.11}$$

which, returning to vector notation, is expressed as

$$\mathbf{J} = \frac{\varepsilon_0}{2}\int \partial^3\mathbf{r}\left\{\left(\mathbf{e}\times\mathbf{a} + \mathbf{b}\times\mathbf{c}\right) + \left(e_l\left(\mathbf{r}\times\nabla\right)a_l + b_l\left(\mathbf{r}\times\nabla\right)c_l\right)\right\}. \tag{3.3.12}$$

We can identify the spin part as

$$\mathbf{S} = \frac{\varepsilon_0}{2}\int \partial^3\mathbf{r}\left(\mathbf{e}\times\mathbf{a} + \mathbf{b}\times\mathbf{c}\right), \tag{3.3.13}$$

and the orbital part as

$$\mathbf{L} = \frac{\varepsilon_0}{2}\int \partial^3\mathbf{r}\left\{e_l\left(\mathbf{r}\times\nabla\right)a_l + b_l\left(\mathbf{r}\times\nabla\right)c_l\right\}. \tag{3.3.14}$$

If the trivial division in Eq. (3.3.2) is not made, the resultant division is:

$$\begin{aligned}&\mathbf{J} = \mathbf{S} + \mathbf{L};\\ &\mathbf{S} = \varepsilon_0\int \partial^3\mathbf{r}\left(\mathbf{e}\times\mathbf{a}\right);\\ &\mathbf{L} = \varepsilon_0\int \partial^3\mathbf{r}\left\{e_l\left(\mathbf{r}\times\nabla\right)a_l\right\},\end{aligned} \tag{3.3.15}$$

which are not invariant under the Heaviside-Lamor (or duplex) transformation and therefore do not abide by electric-magnetic democracy [12–15]:

$$\begin{aligned}\mathbf{E} &\to \mathbf{E}\cos\theta + c\mathbf{B}\sin\theta \\ \mathbf{B} &\to \mathbf{B}\cos\theta - c^{-1}\mathbf{E}\sin\theta.\end{aligned} \tag{3.3.16}$$

It is worth noting that the expressions. Eq. (3.3.13) and (3.3.14) are not gauge invariant due to the appearance of the vector potentials; however, use of the paraxial approximation allows this separation [16]. The gauge invariant separation was proposed long ago by Darwin [17], and in the context of this thesis delivers identical results, as the vector potentials are purely transverse.

In the free field, it can be shown that the spin and orbital parts are independently conserved [18], but are not separately angular momenta, in that their quantum operators do not satisfy the same commutation relations with the other elements of the Poincaré group, as the total angular momentum. However, the components of these quantities are separately measureable and play different roles in the interaction of light and matter [19].

3.4 The Spin Part of Optical Angular Momentum

In this chapter we will compute the exact form of the spin and orbital parts of the optical angular momentum within a quantum electrodynamic framework. Precisely, a mode analysis on these operators reveals expressions in terms of photon annihilation and creation operators [20].

For clarity, we calculate the quantum electrodynamic expressions for the parts of the electromagnetic angular momentum given in Eq. (3.3.15); in the free-field the results emerge identical to those using the duplex-symmetric forms given in Eq. (3.3.13) and (3.3.14). The operator for the electromagnetic vector potential of a plane wave mode is given by:

$$\mathbf{a}(\mathbf{r}) = \sum_{\mathbf{k},\eta} \left(\frac{\hbar}{2\varepsilon_0 ckV} \right)^{\frac{1}{2}} \left\{ \mathbf{e}^{(\eta)}(\mathbf{k})\, a^{(\eta)}(\mathbf{k})\, \mathrm{e}^{\mathrm{i}\mathbf{k}\cdot\mathbf{r}} + \overline{\mathbf{e}}^{(\eta)}(\mathbf{k})\, a^{\dagger(\eta)}(\mathbf{k})\, \mathrm{e}^{-\mathrm{i}\mathbf{k}\cdot\mathbf{r}} \right\}, \tag{3.4.1}$$

where $a^{(\eta)}(\mathbf{k})$ is the annihilation operator for a mode with polarisation label η and wavevector $\mathbf{k}$, respectively. The polarisation vector for the mode with the same labels is given by $\mathbf{e}^{(\eta)}(\mathbf{k})$. The electric and magnetic field operators are obtained from:

$$\mathbf{e} = -\frac{\partial \mathbf{a}}{\partial t} \tag{3.4.2}$$

$$\mathbf{b} = \nabla \times \mathbf{a}. \tag{3.4.3}$$

First we substitute the mode expansions for the electromagnetic fields into the expression for the spin operator:

$$
\begin{aligned}
\mathbf{S} &= \varepsilon_0 \int \partial^3\mathbf{r}\,(\mathbf{e}\times\mathbf{a}) \\
&= \varepsilon_0 \int \partial^3\mathbf{r} \sum_{\substack{\mathbf{k},\eta \\ \mathbf{k}',\eta'}} i\left(\frac{\hbar ck}{2\varepsilon_0 V}\right)^{\frac{1}{2}}\left(\frac{\hbar}{2\varepsilon_0 Vck'}\right)^{\frac{1}{2}}\cdot \\
&\quad \Big\{\left(\mathbf{e}^{(\eta)}(\mathbf{k})\times\mathbf{e}^{(\eta')}(\mathbf{k}')\right)a^{(\eta)}(\mathbf{k})\,a^{(\eta')}(\mathbf{k}')\,\mathrm{e}^{\mathrm{i}(\mathbf{k}+\mathbf{k}')\cdot\mathbf{r}} + \\
&\quad \left(\mathbf{e}^{(\eta)}(\mathbf{k})\times\overline{\mathbf{e}}^{(\eta')}(\mathbf{k}')\right)a^{(\eta)}(\mathbf{k})\,a^{\dagger(\eta')}(\mathbf{k}')\,\mathrm{e}^{\mathrm{i}(\mathbf{k}-\mathbf{k}')\cdot\mathbf{r}} - \\
&\quad \left(\overline{\mathbf{e}}^{(\eta)}(\mathbf{k})\times\mathbf{e}^{(\eta')}(\mathbf{k}')\right)a^{\dagger(\eta)}(\mathbf{k})\,a^{(\eta')}(\mathbf{k}')\,\mathrm{e}^{\mathrm{i}(\mathbf{k}'-\mathbf{k})\cdot\mathbf{r}} - \\
&\quad \left(\overline{\mathbf{e}}^{(\eta)}(\mathbf{k})\times\overline{\mathbf{e}}^{(\eta')}(\mathbf{k}')\right)a^{\dagger(\eta)}(\mathbf{k})\,a^{\dagger(\eta')}(\mathbf{k}')\,\mathrm{e}^{-\mathrm{i}(\mathbf{k}+\mathbf{k}')\cdot\mathbf{r}}\Big\},
\end{aligned}
\tag{3.4.4}
$$

where the **r**-dependence of the modes is contained in the exponential. Therefore, we may enact the normalisation conditions:

$$
\begin{aligned}
\int_V \partial^3\mathbf{r}\, e^{\pm i(\mathbf{k}+\mathbf{k}')\cdot\mathbf{r}} &= \begin{cases} V \text{ for } \mathbf{k} = -\mathbf{k}' \\ 0 \text{ otherwise} \end{cases} \\
\int_V \partial^3\mathbf{r}\, e^{\pm i(\mathbf{k}-\mathbf{k}')\cdot\mathbf{r}} &= \begin{cases} V \text{ for } \mathbf{k} = \mathbf{k}' \\ 0 \text{ otherwise} \end{cases}.
\end{aligned}
\tag{3.4.5}
$$

After simplification of the pre-factor, our expression becomes:

$$
\begin{aligned}
\mathbf{S} &= \sum_{\mathbf{k},\eta,\eta'} \frac{\hbar}{2}\cdot \\
&\quad \Big\{-\left(\mathbf{e}^{(\eta)}(\mathbf{k})\times\mathbf{e}^{(\eta')}(\mathbf{-k})\right)a^{(\eta)}(\mathbf{k})\,a^{(\eta')}(\mathbf{-k}) + \\
&\quad i\left(\mathbf{e}^{(\eta)}(\mathbf{k})\times\overline{\mathbf{e}}^{(\eta')}(\mathbf{k})\right)a^{(\eta)}(\mathbf{k})\,a^{\dagger(\eta')}(\mathbf{k}) - \\
&\quad i\left(\overline{\mathbf{e}}^{(\eta)}(\mathbf{k})\times\mathbf{e}^{(\eta')}(\mathbf{k})\right)a^{\dagger(\eta)}(\mathbf{k})\,a^{(\eta')}(\mathbf{k}) + \\
&\quad \left(\overline{\mathbf{e}}^{(\eta)}(\mathbf{k})\times\overline{\mathbf{e}}^{(\eta')}(\mathbf{-k})\right)a^{\dagger(\eta)}(\mathbf{k})\,a^{\dagger(\eta')}(\mathbf{-k})\Big\}.
\end{aligned}
\tag{3.4.6}
$$

Any measurement of the spin operator will be delivered as an expectation value, thus the first and last terms vanish. In fact, even if we leave these terms in at this stage, they will vanish when we introduce an orthogonal polarisation basis. We therefore obtain:

$$\begin{aligned}\mathbf{S} &= \sum_{\mathbf{k},\eta,\eta'} \frac{i\hbar}{2} \cdot \\ &\left(\mathbf{e}^{(\eta)}(\mathbf{k}) \times \overline{\mathbf{e}}^{(\eta')}(\mathbf{k})\right) a^{(\eta)}(\mathbf{k}) a^{\dagger(\eta')}(\mathbf{k}) - \left(\overline{\mathbf{e}}^{(\eta)}(\mathbf{k}) \times \mathbf{e}^{(\eta')}(\mathbf{k})\right) a^{\dagger(\eta)}(\mathbf{k}) a^{(\eta')}(\mathbf{k}) \\ &= \sum_{\mathbf{k},\eta,\eta'} 2i\hbar \cdot \left(\mathbf{e}^{(\eta)}(\mathbf{k}) \times \overline{\mathbf{e}}^{(\eta')}(\mathbf{k})\right) \left\{a^{(\eta)}(\mathbf{k}) a^{\dagger(\eta')}(\mathbf{k}) + a^{\dagger(\eta')}(\mathbf{k}) a^{(\eta)}(\mathbf{k})\right\},\end{aligned} \tag{3.4.7}$$

where in the last step we have used the anti-commutative property of the cross-product and exchanged the dummy polarisation labels in the right-hand term. Now we may sum over a suitable basis set of polarisation vectors. First we address the case of linearly polarised light,

$$\begin{aligned}\mathbf{e}^{(H)}(\mathbf{k}) &= \hat{\mathbf{i}} \\ \mathbf{e}^{(V)}(\mathbf{k}) &= \hat{\mathbf{j}},\end{aligned} \tag{3.4.8}$$

where *H* and *V* correspond to horizontal and vertical polarisations respectively, and $\hat{\mathbf{i}}$ and $\hat{\mathbf{j}}$ are the Cartesian unit vectors, with $\left(\hat{\mathbf{i}},\hat{\mathbf{j}},\hat{\mathbf{k}}\right)$ forming an orthogonal right-handed triad. We trivially obtain:

$$\mathbf{S} = 0. \tag{3.4.9}$$

However, if we instead consider a circularly polarised basis:

$$\begin{aligned}\mathbf{e}^{(L)}(\mathbf{k}) &= \bar{\mathbf{e}}^{(R)}(\mathbf{k}) = \frac{1}{\sqrt{2}}\left(\hat{\mathbf{i}} + i\hat{\mathbf{j}}\right) \\ \mathbf{e}^{(R)}(\mathbf{k}) &= \bar{\mathbf{e}}^{(L)}(\mathbf{k}) = \frac{1}{\sqrt{2}}\left(\hat{\mathbf{i}} - i\hat{\mathbf{j}}\right),\end{aligned} \tag{3.4.10}$$

we obtain the following prescription:

$$\begin{aligned}\mathbf{e}^{(L/R)}(\mathbf{k}) \times \bar{\mathbf{e}}^{(L/R)}(\mathbf{k}) &= \mp i\hat{\mathbf{k}} \\ \mathbf{e}^{(L/R)}(\mathbf{k}) \times \bar{\mathbf{e}}^{(R/L)}(\mathbf{k}) &= 0.\end{aligned} \tag{3.4.11}$$

The calculation of the operator form of the spin part of the angular momentum then proceeds as:

$$\begin{aligned}\mathbf{S} &= \sum_{\mathbf{k}} \left\{ a^{\dagger(L)}(\mathbf{k}) a^{(L)}(\mathbf{k}) - a^{\dagger(R)}(\mathbf{k}) a^{(R)}(\mathbf{k}) \right\} \hbar\hat{\mathbf{k}} \\ &= \sum_{\mathbf{k}} \left(\hat{N}^{(L)}(\mathbf{k}) - \hat{N}^{(R)}(\mathbf{k}) \right) \hbar\hat{\mathbf{k}},\end{aligned} \tag{3.4.12}$$

where $\hat{N}^{(L/R)}(\mathbf{k})$ is the number operator for the mode with wavevector $\mathbf{k}$. Thus, calculating the expectation value of the spin operator for an optical state delivers the difference between the expected number of left- and right- handed photons in each mode, multiplied by Planck's constant and the unit vector in the direction perpendicular to the plane of polarisation. Thus, a single photon state vector is an eigenstate of the spin operator, with eigenvalue $\pm\hbar\hat{\mathbf{k}}$.

3.5 Poincaré Sphere Representation of Polarisation

To generalise this result we may include a degree of freedom in the analysis – corresponding to an arbitrarily chosen pair of polarisation vectors. We can represent the superposition state of a two-level quantum mechanical system geometrically as a point on the Bloch sphere. In (quantum) optics this is also known as the Poincaré sphere, where any pair of basis polarisation vectors can be depicted as two separate points on the surface of the sphere [21]. Furthermore, a suitable basis set should satisfy the orthogonality condition, $\mathbf{e}^{(n)} \cdot \overline{\mathbf{e}}^{(m)} = \delta_{nm}$, and correspond to diametrically opposing points on the Poincaré sphere. To satisfy these conditions, we introduce a polarisation vector $\mathbf{e}^{(1)}(\mathbf{k})$, characterised by angular coordinates θ and ϕ, Fig. 3.1. with its counterpart basis vector given by:

$$\begin{aligned} \mathbf{e}^{(1)}(\mathbf{k}) &= \sin\theta\hat{\mathbf{i}} + e^{i\phi}\cos\theta\hat{\mathbf{j}} \\ \mathbf{e}^{(2)}(\mathbf{k}) &= \cos\theta\hat{\mathbf{i}} - e^{i\phi}\sin\theta\hat{\mathbf{j}}. \end{aligned} \tag{3.5.1}$$

Thus, to calculate the value of the spin part of the angular momentum in a more general form, we may replace Eq. (3.4.10) and (3.4.11) with our new prescription:

$$\begin{aligned} \mathbf{e}_1 \times \overline{\mathbf{e}}_1 &= \begin{vmatrix} \hat{\mathbf{i}} & \hat{\mathbf{j}} & \hat{\mathbf{k}} \\ \sin\theta & e^{i\phi}\cos\theta & 0 \\ \sin\theta & e^{-i\phi}\cos\theta & 0 \end{vmatrix} = -i\sin(2\theta)\sin(\phi)\hat{\mathbf{k}} \\ \mathbf{e}_2 \times \overline{\mathbf{e}}_2 &= \begin{vmatrix} \hat{\mathbf{i}} & \hat{\mathbf{j}} & \hat{\mathbf{k}} \\ \cos\theta & -e^{i\phi}\sin\theta & 0 \\ \cos\theta & -e^{-i\phi}\sin\theta & 0 \end{vmatrix} = i\sin(2\theta)\sin(\phi)\hat{\mathbf{k}} \end{aligned} \tag{3.5.2}$$

Thus, the spin part emerges as:

$$\mathbf{S} = \sin(2\theta)\sin(\phi)\sum_{\mathbf{k}}\left(\hat{N}^{(1)}(\mathbf{k}) - \hat{N}^{(2)}(\mathbf{k})\right)\hbar\hat{\mathbf{k}}, \tag{3.5.3}$$

where we recover the linear polarisation case, Eq. (3.4.9), by setting $\theta = 0$, $\phi = 0$ for horizontal polarisation and $\theta = \pi/2$, $\phi = 0$ for vertical polarisation. We also recover the circularly polarised case, Eq. (3.4.12), by setting $\theta = \pi/4$, $\phi = \pm\pi/2$ for left- and right- handed polarisations respectively, and note that such an expression unambiguously reveals pure left- (right-) handed light as generator of the maximum (minimum) value for the spin operator.

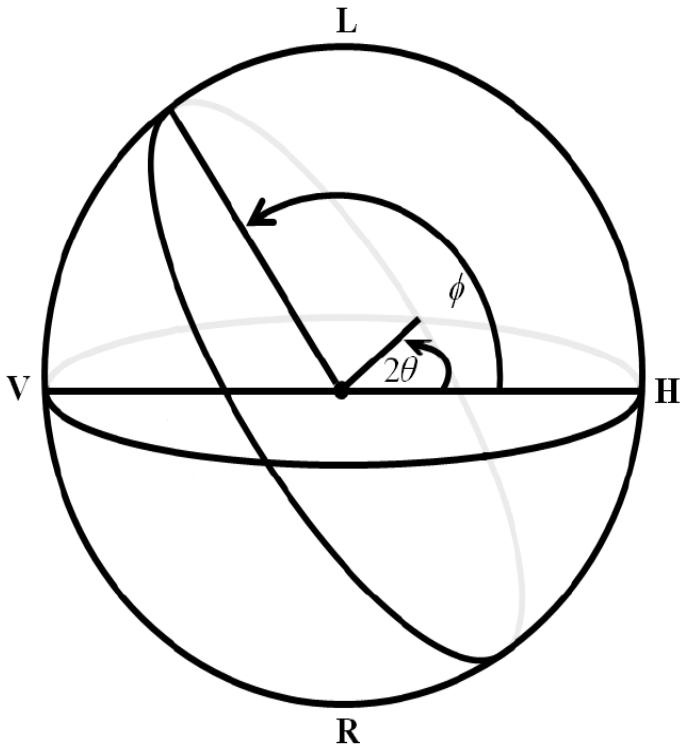

Fig. 3.1. The Poincaré sphere representation of optical polarisation basis vectors determined by angular coordinates θ and ϕ.

3.6 Electromagnetic Helicity

Here we will show that the spin part of the optical angular momentum satisfies a conservation equation with the electromagnetic helicity, and that a quantum optical analysis of these measures relates perfectly to known results in particle physics. Precisely, the helicity of a fundamental particle is defined as the projection of the spin angular momentum on to the direction of propagation. For particles travelling at less than the speed of light, this means that the helicity is not invariant (as a Lorentz boost changes the relative propagation direction, but not the direction of the spin). However, for particles travel at the speed of light, like the photon, the helicity is an invariant property, and is known to be directly related to the chirality. We now derive the helicity from the assumption that there is a scalar that satisfies a continuity equation with the spin angular momentum. To determine the scalar operator that has spin as the corresponding flux, we begin by computing the divergence of the spin:

$$\begin{aligned}\nabla\cdot\mathbf{S} &= \frac{\varepsilon_0}{2}\int\partial^3\mathbf{r}\,\nabla\cdot\left(\mathbf{e}\times\mathbf{a}+\mathbf{b}\times\mathbf{c}\right)\\ &= \frac{\varepsilon_0}{2}\int\partial^3\mathbf{r}\left\{\mathbf{a}\cdot\left(\nabla\times\mathbf{e}\right)-\mathbf{e}\cdot\left(\nabla\times\mathbf{a}\right)+\mathbf{c}\cdot\left(\nabla\times\mathbf{b}\right)-\mathbf{b}\cdot\left(\nabla\times\mathbf{c}\right)\right\}\\ &= \frac{\varepsilon_0}{2}\int\partial^3\mathbf{r}\left\{\mathbf{a}\cdot\left(-\frac{\partial\mathbf{b}}{\partial t}\right)+\varepsilon_0\mu_0\mathbf{e}\cdot\left(\frac{\partial\mathbf{c}}{\partial t}\right)+\varepsilon_0\mu_0\mathbf{c}\cdot\left(\frac{\partial\mathbf{e}}{\partial t}\right)-\mathbf{b}\cdot\left(\frac{\partial\mathbf{a}}{\partial t}\right)\right\},\end{aligned} \tag{3.6.1}$$

which is observed to be a time derivative:

$$\begin{aligned}\nabla\cdot\mathbf{S} &= -\frac{\varepsilon_0}{2}\frac{\partial}{\partial t}\int\partial^3\mathbf{r}\left\{\mathbf{a}\cdot\mathbf{b}-\varepsilon_0\mu_0\mathbf{c}\cdot\mathbf{e}\right\}\\ &= -c^2\frac{\partial}{\partial t}\int\partial^3\mathbf{r}\left\{\frac{1}{2\mu_0}\mathbf{a}\cdot\mathbf{b}-\frac{\varepsilon_0}{2}\mathbf{c}\cdot\mathbf{e}\right\}.\end{aligned} \tag{3.6.2}$$

Thus, we have derived the helicity, h,

$$h = \int \partial^3 \mathbf{r} \left\{ \frac{1}{2\mu_0} \mathbf{a} \cdot \mathbf{b} - \frac{\varepsilon_0}{2} \mathbf{c} \cdot \mathbf{e} \right\}, \tag{3.6.3}$$

and spin, which are related by:

$$c^2 \frac{\partial h}{\partial t} + \nabla \cdot \mathbf{S} = 0, \tag{3.6.4}$$

or equivalently they form a four-vector in Minkowski space [22]. Using the same quantum optical mode expansion as in analysis of the spin angular momentum operator, we obtain:

$$\begin{aligned} h &= \int \partial^3 \mathbf{r} \left\{ \frac{1}{2\mu_0} \mathbf{a} \cdot \mathbf{b} - \frac{\varepsilon_0}{2} \mathbf{c} \cdot \mathbf{e} \right\} \\ &= \hbar \sin 2\theta \sin \phi \sum_{\mathbf{k}} \left\{ a^{\dagger(1)}(\mathbf{k}) a^{(1)}(\mathbf{k}) - a^{\dagger(2)}(\mathbf{k}) a^{(2)}(\mathbf{k}) \right\} \\ &= \hbar \sin 2\theta \sin \phi \sum_{\mathbf{k}} \left\{ \hat{N}^{(1)}(\mathbf{k}) - \hat{N}^{(2)}(\mathbf{k}) \right\}. \end{aligned} \tag{3.6.5}$$

This relates with the particle physics definition of helicity as the projection of the spin onto the direction of propagation [23].

3.7 Light with Orbital Angular Momentum

To address situations in which the radiation might carry *orbital* angular momentum,

we first return to a classical wave, free to propagate only in the z-direction:

$$\mathbf{a}(\mathbf{r},t) = \mathbf{e}u(\mathbf{r})e^{i(kz-\omega t)}, \tag{3.7.1}$$

where $u(\mathbf{r})$ is the amplitude function and $\mathbf{e}$ is a polarisation vector, both in the plane transverse to z. Through introduction of the Lorenz gauge we obtain the Maxwellian wave equation in paraxial form, also known as the Helmholtz equation [24]:

$$\left(\nabla_{x,y}^2 + 2ik\frac{\partial}{\partial z}\right)u(\mathbf{r}) = 0, \tag{3.7.2}$$

where the subscript on the gradient operator denote which variables one differentiates with respect to and k is the longitudinal wavenumber. In Cartesian coordinates the amplitude function can be expressed as the product of $u_n(x,z)$ and $u_m(y,z)$, two functions that individually obey paraxial wave equations in their respective transverse direction. Normalised solutions to such wave equations are expressible as the product of a Gaussian function with a Hermite polynomial; they are commonly known as Hermite-Gaussian beams [25].

Expressing the paraxial wave-equation, Eq. (3.7.2), in cylindrical polar coordinates delivers:

$$\left(\frac{1}{r}\frac{\partial}{\partial r} + \frac{\partial^2}{\partial^2 r} + \frac{1}{r}\frac{\partial^2}{\partial^2 \varphi} + 2ik\frac{\partial}{\partial z}\right)u_{lp}(r,\varphi,z) = 0, \tag{3.7.3}$$

where r is the radial coordinate and φ is the azimuthal angle. The form of this equation lends itself to cylindrically symmetric solutions expressible as the product of a Gaussian function with a generalised Laguerre polynomial; they are commonly known as Laguerre-Gaussian beams. It will be shown that Laguerre-Gaussian beams are eigenfunctions of the orbital angular momentum operator, and therefore carry $\pm l\hbar$ units of orbital angular momentum along the direction of propagation. In a classical framework, the Laguerre-Gaussian modes are given by:

$$u_{lp}(r,\varphi,z)=\frac{C_{lp}}{w(z)}\left(\frac{r\sqrt{2}}{w(z)}\right)^{|l|}e^{-\frac{r^2}{w^2(z)}}L_p^{|l|}\left(\frac{2r^2}{w^2(z)}\right)e^{\frac{ikr^2z}{2\left(z_R^2+z^2\right)}}e^{il\varphi}e^{-i(2p+|l|+1)\chi(z)}, \tag{3.7.4}$$

where $L_p^{|l|}$ are the generalised Laguerre polynomials, $w(z)$ is the beam waist and $2z_R$ is the Rayleigh range. The normalisation constant is given by C_{lp} and $\chi(z)$ is the Gouy phase of the beam, which indicates that when a Gaussian beam passes through a focus it acquires a π phase shift. The intensity distribution of a Laguerre-Gaussian mode is that of progressively (outward from $r = 0$) fainter concentric rings with the number of rings determined by the radial index, $p + 1$.

Experiments can be constructed that have a Rayleigh range of several metres [26], so that it is reasonable to assume beam collimation is maintained for $z_R \gg z$. Under this assumption, we have:

$$\begin{aligned} &w(z)\to w_0;\\ &e^{\frac{ikr^2z}{2\left(z_R^2+z^2\right)}}e^{-i(2p+|l|+1)\chi(z)}\to 1. \end{aligned} \tag{3.7.5}$$

Thus, our amplitude function can be expressed as:

$$u_{lp}(r,\varphi,z) = f_{l,p}(r)e^{-il\varphi}, \tag{3.7.6}$$

where the exponential phase factor corresponds to an orbital angular momentum eigenvalue of $l\hbar$ [27] , and the radial distribution function for the mode with azimuthal index l and radial index p is given by:

$$f_{lp}(r) = \frac{C_{lp}}{w_0}\left(\frac{r\sqrt{2}}{w_0}\right)^{|l|} e^{-\frac{r^2}{w_0^2}} L_p^{|l|}\left(\frac{2r^2}{w_0^2}\right). \tag{3.7.7}$$

Such functions are orthogonal, in the sense that:

$$\int_0^\infty \partial r\, f_{l,p}(r)\,\overline{f}_{l,q}(r)\,r = A_{lp}^2 w_0^2 \delta_{pq}, \tag{3.7.8}$$

where, regardless of indices, A_{lp} = 1/2 due to the properties of the generalised Laguerre polynomials [28].

The electric and magnetic field vectors are derivable from the electromagnetic vector potential, which, most generally, is written as a linear combination of all possible solutions to Eq. (3.7.3):

$$\mathbf{a}(\mathbf{r},t) = \sum_{\mathbf{k},\eta,l,p} \left\{ \mathbf{e}_{l,p}{}^{(\eta)}(\mathbf{k}) a_{\mathbf{k},\eta,l,p} u_{l,p}(r,\varphi) e^{ikz-i\omega t} + \overline{\mathbf{e}}_{l,p}{}^{(\eta)}(\mathbf{k}) \overline{a}_{\mathbf{k},\eta,l,p} \overline{u}_{l,p}(r,\varphi) e^{-ikz+i\omega t} \right\}, \tag{3.7.9}$$

where $a_{\mathbf{k},\eta,l,p}$ are the complex coefficients. The wavevector $\mathbf{k}$ is constrained to the propagation direction, so is given by $k\hat{\mathbf{z}}$. By promoting the complex coefficients to operators,

$$\begin{aligned} a_{\mathbf{k},\eta,l,p} &\to \left(\frac{\hbar}{2ck\varepsilon_0 V}\right)^{\frac{1}{2}} a_{lp}^{(\eta)}(\mathbf{k}); \\ \overline{a}_{\mathbf{k},\eta,l,p} &\to \left(\frac{\hbar}{2ck\varepsilon_0 V}\right)^{\frac{1}{2}} a_{lp}^{(\eta)\dagger}(\mathbf{k}), \end{aligned} \tag{3.7.10}$$

and using the properties of the amplitude function, we obtain the quantum optical mode expansion for a Laguerre-Gaussian mode:

$$\mathbf{a} = \sum_{k,\eta,l,p} \left(\frac{\hbar}{2\varepsilon_0 ckV}\right)^{\frac{1}{2}} \left\{ \mathbf{e}_{l,p}{}^{(\eta)}(\mathbf{k}) a^{(\eta)}(\mathbf{k}) f_{l,p}(r) e^{ikz-il\varphi} + \overline{\mathbf{e}}_{l,p}{}^{(\eta)}(\mathbf{k}) a^{\dagger(\eta)}(\mathbf{k}) \overline{f}_{l,p}(r) e^{-ikz+il\varphi} \right\}. \tag{3.7.11}$$

Here we work within the Heisenberg picture, so that the annihilation and creation operators implicitly contain the time-dependence of the vector potential. The annihilation and creation operators introduced here raise and lower the photon occupancy number in the usual way and satisfy the expected commutation relations [29].

Both set of solutions to the paraxial wave-equation form a complete basis and can therefore describe any state of a paraxial light field and can be represented as a superposition of the other. Furthermore, there are many other solutions to Maxwellian wave equations; for example, in elliptical coordinates one can obtain an

orthogonal set of Ince-Gaussian modes, which have Hermite-Gaussian and Laguerre-Gaussian modes as special cases. It is worth noting that Hypergeometric-Gaussian modes, with a singular phase profile, are also eigenfunctions of the orbital angular momentum operator [30], and warrant further study in context of quantum formulations of optical angular momentum.

Having derived the quantum optical vector potential for Laguerre-Gaussian modes we can now begin analysis of the orbital angular momentum operator. For clarity, presented here is calculation of the non duplex-symmetric form of the orbital angular momentum operator, as presented in Eq. (3.3.15), where, analysis of the fully symmetric form of this expression, Eq. (3.3.14), delivers the same result in free-space. With this vector potential, the related electric field is given by:

$$\mathbf{e} = i\sum_{k,\eta,l,p}\left(\frac{\hbar ck}{2\varepsilon_0 V}\right)^{\frac{1}{2}}\left\{\mathbf{e}_{l,p}{}^{(\eta)}(\mathbf{k})a^{(\eta)}(\mathbf{k})f_{l,p}(r)e^{ikz-il\varphi} - \overline{\mathbf{e}}_{l,p}{}^{(\eta)}(\mathbf{k})a^{\dagger(\eta)}(\mathbf{k})\overline{f}_{l,p}(r)e^{-ikz+il\varphi}\right\}. \tag{3.7.12}$$

We note that in an axially symmetric beam the only nonzero component of the orbital part of the angular momentum is the part directed along the z-axis. This component is given by:

$$L_z = \varepsilon_0\int\partial^3\mathbf{r}\left\{e_m\left(\mathbf{r}\times\nabla\right)_z a_m\right\}, \tag{3.7.13}$$

where, in cylindrical polar coordinates,

$$\begin{aligned}(\mathbf{r}\times\nabla)_z &= \left|\begin{array}{ccc}\hat{\mathbf{r}} & \hat{\boldsymbol{\varphi}} & \hat{\mathbf{z}} \\ r & \varphi & z \\ \dfrac{\partial}{\partial r} & \dfrac{1}{r}\dfrac{\partial}{\partial\varphi} & \dfrac{\partial}{\partial z}\end{array}\right|_z \\ &= \frac{\partial}{\partial\varphi} - \varphi\frac{\partial}{\partial r}.\end{aligned} \tag{3.7.14}$$

The system is rotationally symmetric (and, within the Rayleigh range, effectively invariant with respect to z), thus:

$$(\mathbf{r}\times\nabla)_z = \frac{\partial}{\partial\varphi}. \tag{3.7.15}$$

We may then calculate the z component of the orbital part of the angular momentum:

$$\begin{aligned}L_z &= \varepsilon_0\int\partial^3\mathbf{r}\left\{e_m\frac{\partial}{\partial\varphi}a_m\right\}, \\ &= \int\partial^3\mathbf{r}\sum_{\substack{k,\eta,l,p \\ k',\eta',l',p'}}\left(\frac{\hbar}{2V}\right)\left(\frac{k}{k'}\right)^{\frac{1}{2}}\times \\ &\left\{e_{l,p(m)}{}^{(\eta)}(\mathbf{k})a^{(\eta)}(\mathbf{k})f_{l,p}(r)e^{ikz-il\varphi} - \overline{e}_{l,p(m)}{}^{(\eta)}(\mathbf{k})a^{\dagger(\eta)}(\mathbf{k})\overline{f}_{l,p}(r)e^{-ikz+il\varphi}\right\}\cdot \\ &\left\{l'e_{l',p'(m)}{}^{(\eta')}(\mathbf{k}')a^{(\eta')}(\mathbf{k}')f_{l',p'}(r)e^{ik'z-il'\varphi} - l'\overline{e}_{l',p'(m)}{}^{(\eta')}(\mathbf{k}')a^{\dagger(\eta')}(\mathbf{k}')\overline{f}_{l',p'}(r)e^{-ik'z+il'\varphi}\right\},\end{aligned} \tag{3.7.16}$$

where × represents scalar multiplication and the subscript (m) labels components of the polarisation vector. By enacting the multiplication and returning to vector notation, we obtain:

$$
\begin{aligned}
L_z = \int \partial^3 \mathbf{r} \sum_{\substack{k,\eta,l,p \\ k',\eta',l',p'}} \left(\frac{\hbar}{2V}\right)\left(\frac{k}{k'}\right)^{\frac{1}{2}} \times \\
l' \left[\mathbf{e}_{l,p}{}^{(\eta)}(\mathbf{k}) \cdot \mathbf{e}_{l',p'}{}^{(\eta')}(\mathbf{k}') \right] a^{(\eta)}(\mathbf{k}) a^{(\eta')}(\mathbf{k}') f_{l,p}(r) f_{l',p'}(r) e^{i(k+k')z - i(l+l')\varphi} \\
-l' \left[\mathbf{e}_{l,p}{}^{(\eta)}(\mathbf{k}) \cdot \overline{\mathbf{e}}_{l',p'}{}^{(\eta')}(\mathbf{k}') \right] a^{(\eta)}(\mathbf{k}) a^{\dagger(\eta')}(\mathbf{k}') f_{l,p}(r) \overline{f}_{l',p'}(r) e^{i(k-k')z - i(l-l')\varphi} \\
-l' \left[\overline{\mathbf{e}}_{l,p}{}^{(\eta)}(\mathbf{k}) \cdot \mathbf{e}_{l',p'}{}^{(\eta')}(\mathbf{k}') \right] a^{\dagger(\eta)}(\mathbf{k}) a^{(\eta')}(\mathbf{k}') f_{l',p'}(r) \overline{f}_{l,p}(r) e^{-i(k-k')z + i(l-l')\varphi} \\
+l' \left[\overline{\mathbf{e}}_{l,p}{}^{(\eta)}(\mathbf{k}) \cdot \overline{\mathbf{e}}_{l',p'}{}^{(\eta')}(\mathbf{k}') \right] a^{\dagger(\eta)}(\mathbf{k}) a^{\dagger(\eta')}(\mathbf{k}') \overline{f}_{l,p}(r) \overline{f}_{l',p'}(r) e^{-i(k+k')z + i(l+l')\varphi}.
\end{aligned}
\tag{3.7.17}
$$

We note that in cylindrical polar coordinates the volume element is given by:

$$
r\,\partial r\,\partial\varphi\,\partial z. \tag{3.7.18}
$$

We may then integrate the r, φ and z dependent sections of Eq. (3.7.17) separately:

$$
\begin{aligned}
L_z = \int \partial r \sum_{\substack{k,\eta,l,p \\ k',\eta',l',p'}} \left(\frac{\hbar}{2V}\right)\left(\frac{k}{k'}\right)^{\frac{1}{2}} \times \\
l' \left[\mathbf{e}_{l,p}{}^{(\eta)}(\mathbf{k}) \cdot \mathbf{e}_{l',p'}{}^{(\eta')}(\mathbf{k}') \right] a^{(\eta)}(\mathbf{k}) a^{(\eta')}(\mathbf{k}') f_{l,p}(r) f_{l',p'}(r) r \int_0^{\infty} e^{i(k+k')z} \partial z \int_0^{2\pi} e^{-i(l+l')\varphi} \partial\varphi \\
-l' \left[\mathbf{e}_{l,p}{}^{(\eta)}(\mathbf{k}) \cdot \overline{\mathbf{e}}_{l',p'}{}^{(\eta')}(\mathbf{k}') \right] a^{(\eta)}(\mathbf{k}) a^{\dagger(\eta')}(\mathbf{k}') f_{l,p}(r) \overline{f}_{l',p'}(r) r \int_0^{\infty} e^{i(k-k')z} \partial z \int_0^{2\pi} e^{-i(l-l')\varphi} \partial\varphi \\
-l' \left[\overline{\mathbf{e}}_{l,p}{}^{(\eta)}(\mathbf{k}) \cdot \mathbf{e}_{l',p'}{}^{(\eta')}(\mathbf{k}') \right] a^{\dagger(\eta)}(\mathbf{k}) a^{(\eta')}(\mathbf{k}') f_{l',p'}(r) \overline{f}_{l,p}(r) r \int_0^{\infty} e^{-i(k-k')z} \partial z \int_0^{2\pi} e^{i(l-l')\varphi} \partial\varphi \\
+l' \left[\overline{\mathbf{e}}_{l,p}{}^{(\eta)}(\mathbf{k}) \cdot \overline{\mathbf{e}}_{l',p'}{}^{(\eta')}(\mathbf{k}') \right] a^{\dagger(\eta)}(\mathbf{k}) a^{\dagger(\eta')}(\mathbf{k}') \overline{f}_{l,p}(r) \overline{f}_{l',p'}(r) r \int_0^{\infty} e^{-i(k+k')z} \partial z \int_0^{2\pi} e^{i(l+l')\varphi} \partial\varphi.
\end{aligned}
\tag{3.7.19}
$$

Here, the z-dependent sections satisfy the same normalisation conditions as Eq. (3.4.5) and the φ-dependent sections satisfy:

$$\int_0^{2\pi} \partial\varphi\, e^{\pm i(l+l')\varphi} = \begin{cases} 1 \text{ for } l = -l' \\ 0 \text{ otherwise} \end{cases}$$
$$\int_0^{2\pi} \partial\varphi\, e^{\pm i(l-l')\varphi} = \begin{cases} 1 \text{ for } l = l' \\ 0 \text{ otherwise} \end{cases}. \tag{3.7.20}$$

After enacting these normalisation conditions, we are left with:

$$\begin{aligned} L_z = & \sum_{\substack{k,\eta,l,p \\ \eta',p'}} \frac{\hbar}{2} \times \\ & l\left[\mathbf{e}_{l,p}^{(\eta)}(\mathbf{k}) \cdot \mathbf{e}_{l,p'}^{(\eta')}(-\mathbf{k})\right] a^{(\eta)}(\mathbf{k}) a^{(\eta')}(-\mathbf{k}) \int_0^\infty f_{l,p}(r) f_{-l,p'}(r) r \partial r \\ & -l\left[\mathbf{e}_{l,p}^{(\eta)}(\mathbf{k}) \cdot \overline{\mathbf{e}}_{l,p'}^{(\eta')}(\mathbf{k})\right] a^{(\eta)}(\mathbf{k}) a^{\dagger(\eta')}(\mathbf{k}) \int_0^\infty f_{l,p}(r) \overline{f}_{l,p'}(r) r \partial r \\ & -l\left[\overline{\mathbf{e}}_{l,p}^{(\eta)}(\mathbf{k}) \cdot \mathbf{e}_{l,p'}^{(\eta')}(\mathbf{k})\right] a^{\dagger(\eta)}(\mathbf{k}) a^{(\eta')}(\mathbf{k}) \int_0^\infty f_{l,p'}(r) \overline{f}_{l,p}(r) r \partial r \\ & +l\left[\overline{\mathbf{e}}_{l,p}^{(\eta)}(\mathbf{k}) \cdot \overline{\mathbf{e}}_{l,p'}^{(\eta')}(-\mathbf{k})\right] a^{\dagger(\eta)}(\mathbf{k}) a^{\dagger(\eta')}(-\mathbf{k}) \int_0^\infty \overline{f}_{l,p}(r) \overline{f}_{-l,p'}(r) r \partial r. \end{aligned} \tag{3.7.21}$$

As before, any meaningful result will be delivered as the expectation value of an optical state, thus the first and last terms vanish as they do not leave the state unchanged. Furthermore, enacting the radial normalisation condition delivers:

$$\begin{aligned} L_z = & \sum_{\substack{k,\eta,l,p \\ \eta'}} \frac{\hbar}{2} \times \\ & -l\left[\mathbf{e}_{l,p}^{(\eta)}(\mathbf{k}) \cdot \overline{\mathbf{e}}_{l,p}^{(\eta')}(\mathbf{k})\right] a^{(\eta)}(\mathbf{k}) a^{\dagger(\eta')}(\mathbf{k}) \\ & -l\left[\overline{\mathbf{e}}_{l,p}^{(\eta)}(\mathbf{k}) \cdot \mathbf{e}_{l,p}^{(\eta')}(\mathbf{k})\right] a^{\dagger(\eta)}(\mathbf{k}) a^{(\eta')}(\mathbf{k}). \end{aligned} \tag{3.7.22}$$

To proceed, we sum over the pairs of general polarisation vectors given in Eq. (3.5.1), with scalar product given by:

$$\mathbf{e}^{(s)}(\mathbf{k})\cdot\overline{\mathbf{e}}^{(t)}(\mathbf{k})=\delta_{st}. \tag{3.7.23}$$

Thus, our expression becomes:

$$\begin{aligned} L_z &= \sum_{k,l,p} -l\hbar\left(a^{\dagger(1)}(\mathbf{k})a^{(1)}(\mathbf{k})+a^{\dagger(2)}(\mathbf{k})a^{(2)}(\mathbf{k})\right) \\ &\Rightarrow \\ \mathbf{L} &= -\sum_{k,l,p} l\hbar\left(N^{(1)}_{l,p}(\mathbf{k})+N^{(2)}_{l,p}(\mathbf{k})\right)\hat{\mathbf{k}}. \end{aligned} \tag{3.7.24}$$

Crucially, the results of Sections 3.5 and 3.5, when enacted with mode expansions explicitly containing orbital angular momentum, still deliver the exact same expressions for spin and helicity, Eq. (3.5.3) and (3.6.3). It is then evident that in the paraxial regime the total angular momentum can be expressed as the sum of Eq. (3.5.3) and (3.7.24) delivering:

$$\begin{aligned} \mathbf{J} &= \sum_{k,l,p}\left\{\sin(2\theta)\sin(\phi)\left(\hat{N}^{(1)}_{l,p}(\mathbf{k})-\hat{N}^{(2)}_{l,p}(\mathbf{k})\right)-l\left(\hat{N}^{(1)}_{l,p}(\mathbf{k})+\hat{N}^{(2)}_{l,p}(\mathbf{k})\right)\right\}\hbar\hat{\mathbf{k}} \\ &= \sum_{k,l,p}\left\{\left(\sin(2\theta)\sin(\phi)-l\right)\hat{N}^{(1)}_{l,p}(\mathbf{k})-\left(\sin(2\theta)\sin(\phi)+l\right)\hat{N}^{(2)}_{l,p}(\mathbf{k})\right\}\hbar\hat{\mathbf{k}}. \end{aligned} \tag{3.7.25}$$

This represents a new compartmentalisation of the orbital and spin parts of the optical angular momentum into terms that depend on the sum and difference of number operators for modes of opposing polarisation helicity [31]. Such an expression also explains the mechanical equivalence of the spin and orbital parts in angular momentum exchange with matter [8]. Furthermore, such analysis gives a basis, through Eq. (3.7.15), for the use of heuristic orbital angular momentum operator

$-i\hbar\frac{\partial}{\partial\varphi}$. Intuitively, the form of these equations represents the fact that the spin and orbital degrees of freedom are distinct and separable in the paraxial approximation, and in the free-field. Both angular momenta are quantised and an arbitrary electromagnetic field has total spin/orbital angular momentum given by the sum of the number of photons in each spin/orbital state. For spin angular momentum, this has two values: +1 and -1; however, for orbital angular momentum, this ± l, where l is any natural number.

3.8 Optical Chirality/The Lipkin Zilch

In 1964, Daniel M Lipkin observed that in an arbitrary electromagnetic free field, Maxwell's equations guarantee the conservation of the quantity [32]:

$$\chi=\frac{\varepsilon_0}{2}\mathbf{e}\cdot\left(\nabla\times\mathbf{e}\right)+\frac{1}{2\mu_0}\mathbf{b}\cdot\left(\nabla\times\mathbf{b}\right), \tag{3.8.1}$$

with respect to a corresponding flux:

$$\boldsymbol{\phi}=\frac{\boldsymbol{\varepsilon}_0 c^2}{2}\left[\mathbf{e}\times\left(\nabla\times\mathbf{b}\right)+\mathbf{b}\times\left(\nabla\times\mathbf{e}\right)\right]. \tag{3.8.2}$$

That is, these two quantities are related by the following conservation equation:

$$\frac{\partial\chi}{\partial t}+\nabla\cdot\boldsymbol{\phi}=0. \tag{3.8.3}$$

In a modern context [33], these quantities are known as the *optical chirality density*, Eq. (3.8.1), and the *optical chirality flux*, Eq. (3.8.2), and have recently been the subject of considerable debate regarding physical interpretation and relation to other measures of helicity and optical angular momentum. Lipkin originally dismissed these quantities as having no ready physical interpretation, except that an observation of the units of the 'zilch' (ergs per second) suggests that it "might provide a measure of optical activity in the field". Importantly, the units are not the same as those of angular momentum. It was later discovered that the optical chirality measures are associated with conservation of electromagnetic polarisation [34]. The rest of this chapter aims to develop, in precise quantum electrodynamic terms, a description of these measures in a photonic context. Furthermore, it has been shown by Cameron, Barnett and Yao [15] that the optical chirality and the helicity, Eq. (3.6.3) form the basis of an infinite family of *helicity-type* measures. In Section 3.9 it is demonstrated that the infinite hierarchy of helicity-type and the related *spin-type* measures all have a strikingly similar form in a quantum electrodynamic formalism.

In the quantum field picture, Eq. (3.8.1) and (3.8.2) are promoted to operator status. As with the computation of the spin and helicity measures, both terms are easily shown to deliver equal contributions in a free field. Thus, for calculational clarity we need only look at a single term (multiplied by two). Our *ansatz* is that we should integrate the optical chirality density over a spatial volume to bring results in coincidence with the form of the electromagnetic helicity:

$$\int_V \partial^3\mathbf{r}\chi = \varepsilon_0 \int_V \partial^3\mathbf{r}\, \mathbf{e}\cdot\left(\nabla\times\mathbf{e}\right). \tag{3.8.4}$$

Introducing the mode expansion for the electric field of a plane wave and using vector subscript notation delivers:

$$\begin{aligned}
&\varepsilon_0 \int_V \partial^3\mathbf{r}\, \mathbf{e}\cdot\left(\nabla\times\mathbf{e}\right) = \varepsilon_0 \int_V \partial^3\mathbf{r}\, e_k \varepsilon_{klm} \partial_l e_m \\
&= -i\int_V \partial^3\mathbf{r}\varepsilon_0\varepsilon_{klm}\sum_{\mathbf{k},\eta}\left(\frac{\hbar ck}{2\varepsilon_0 V}\right)^{\frac{1}{2}}\left\{e_k{}^{(\eta)}(\mathbf{k})a^{(\eta)}(\mathbf{k})e^{i(\mathbf{k}\cdot\mathbf{r})} - \overline{e}_k{}^{(\eta)}(\mathbf{k})a^{\dagger(\eta)}(\mathbf{k})e^{-i(\mathbf{k}\cdot\mathbf{r})}\right\}\times \\
&\sum_{\mathbf{k}',\eta'}\left(\frac{\hbar ck'}{2\varepsilon_0 V}\right)^{\frac{1}{2}} k_l'\left\{e_m{}^{(\eta')}(\mathbf{k}')a^{(\eta')}(\mathbf{k}')e^{i(\mathbf{k}'\cdot\mathbf{r})} + \overline{e}_m{}^{(\eta')}(\mathbf{k}')a^{\dagger(\eta')}(\mathbf{k}')e^{-i(\mathbf{k}'\cdot\mathbf{r})}\right\},
\end{aligned} \tag{3.8.5}$$

where × represents scalar multiplication. Enacting the multiplication delivers:

$$\begin{aligned}
&\varepsilon_0 \int_V \partial^3\mathbf{r}\,\chi = \\
&= -\int_V \partial^3\mathbf{r}\frac{\hbar ci}{2V}\varepsilon_{klm}\sum_{\substack{\mathbf{k},\eta\\ \mathbf{k}',\eta'}}\left(kk'\right)^{\frac{1}{2}}k_l'\times \\
&\left\{e_k{}^{(\eta)}(\mathbf{k})e_m{}^{(\eta')}(\mathbf{k}')a^{(\eta)}(\mathbf{k})a^{(\eta')}(\mathbf{k}')e^{i(\mathbf{k}+\mathbf{k}')\cdot\mathbf{r}} + e_k{}^{(\eta)}(\mathbf{k})\overline{e}_m{}^{(\eta')}(\mathbf{k}')a^{(\eta)}(\mathbf{k})a^{\dagger(\eta')}(\mathbf{k}')e^{i(\mathbf{k}-\mathbf{k}')\cdot\mathbf{r}}\right\} \\
&\left\{-\overline{e}_k{}^{(\eta)}(\mathbf{k})e_m{}^{(\eta')}(\mathbf{k}')a^{\dagger(\eta)}(\mathbf{k})a^{(\eta')}(\mathbf{k}')e^{i(\mathbf{k}'-\mathbf{k})\cdot\mathbf{r}} - \overline{e}_k{}^{(\eta)}(\mathbf{k})\overline{e}_m{}^{(\eta')}(\mathbf{k}')a^{\dagger(\eta)}(\mathbf{k})a^{\dagger(\eta')}(\mathbf{k}')e^{-i(\mathbf{k}+\mathbf{k}')\cdot\mathbf{r}}\right\}.
\end{aligned} \tag{3.8.6}$$

As an expedient, we may drop the first and last terms, as taking expectation values of precisely defined photon number states will cause these terms to vanish. Thus, we obtain:

$$\begin{aligned}
&\varepsilon_0 \int_V \partial^3\mathbf{r}\,\chi = \\
&= -\frac{\hbar ci}{2}\varepsilon_{klm}\sum_{\mathbf{k},\eta,\eta'} kk_l\times \\
&\left\{e_k{}^{(\eta)}(\mathbf{k})\overline{e}_m{}^{(\eta')}(\mathbf{k})a^{(\eta)}(\mathbf{k})a^{\dagger(\eta')}(\mathbf{k}) - \overline{e}_k{}^{(\eta)}(\mathbf{k})e_m{}^{(\eta')}(\mathbf{k})a^{\dagger(\eta)}(\mathbf{k})a^{(\eta')}(\mathbf{k})\right\},
\end{aligned} \tag{3.8.7}$$

where the normalisation condition, Eq. (3.4.5), has been used. By reinstating the vector character of the polarisation vectors we obtain:

$$\begin{aligned}\varepsilon_{klm}k_l e_k^{(\eta)}(\mathbf{k})\overline{e}_m^{(\eta')}(\mathbf{k}) &= \mathbf{e}^{(\eta)}(\mathbf{k})\cdot\left(\mathbf{k}\times\overline{\mathbf{e}}^{(\eta')}(\mathbf{k})\right);\\ \varepsilon_{klm}k_l \overline{e}_k^{(\eta)}(\mathbf{k})e_m^{(\eta')}(\mathbf{k}) &= \overline{\mathbf{e}}^{(\eta)}(\mathbf{k})\cdot\left(\mathbf{k}\times\mathbf{e}^{(\eta')}(\mathbf{k})\right).\end{aligned} \tag{3.8.8}$$

From the general polarisation basis, given in Eq. (3.5.1), we determine that the only contributions to Eq. (3.8.7) are when the polarisations η and η' in Eq. (3.8.8) are identical. This is shown explicitly in Appendix B. Thus, our expression becomes:

$$\begin{aligned}&\varepsilon_0\int_V \partial^3\mathbf{r}\,\chi =\\ &=-\frac{\hbar c i}{2}\sum_{\mathbf{k},\eta,\eta'} k\left\{ik\sin 2\theta\sin\phi a^{(1)}(\mathbf{k})a^{\dagger(1)}(\mathbf{k})+ik\sin 2\theta\sin\phi a^{\dagger(1)}(\mathbf{k})a^{(1)}(\mathbf{k})\right.\\ &\left.-ik\sin(2\theta)\sin\phi a^{(2)}(\mathbf{k})a^{\dagger(2)}(\mathbf{k})-ik\sin(2\theta)\sin\phi a^{\dagger(2)}(\mathbf{k})a^{(2)}(\mathbf{k})\right\},\end{aligned} \tag{3.8.9}$$

which, after simplification and use of the annihilation and creation operator commutation relations, becomes:

$$\begin{aligned}&\varepsilon_0\int_V \partial^3\mathbf{r}\,\chi =\\ &\qquad=\hbar c\sin 2\theta\sin\phi\sum_{\mathbf{k}} k^2\left\{a^{\dagger(1)}(\mathbf{k})a^{(1)}(\mathbf{k})-a^{\dagger(2)}(\mathbf{k})a^{(2)}(\mathbf{k})\right\}\\ &\qquad=\hbar c\sin 2\theta\sin\phi\sum_{\mathbf{k}} k^2\left\{\hat{N}^{(1)}(\mathbf{k})-\hat{N}^{(2)}(\mathbf{k})\right\},\end{aligned} \tag{3.8.10}$$

where the last step delivers our expression in terms of number operators. This result remains identical when using a non-plane wave basis for derivation of this expression,

such as the Laguerre-Gaussian vector potential given in Eq. (3.7.11). From this expression we readily obtain Lipkin's observation that the optical chirality has dimensions of energy per time. Furthermore, by starting with the optical chirality density, Eq. (3.8.1), and replacing some of the electric and magnetic field vectors with their curls, we obtain:

$$\chi = -\frac{\varepsilon_0}{2}\mathbf{e}\cdot\left(\nabla\times\nabla\times\mathbf{c}\right)+\frac{1}{2\mu_0}\mathbf{b}\cdot\left(\nabla\times\nabla\times\mathbf{a}\right), \tag{3.8.11}$$

which, after using the vector identity $\nabla\times\nabla\times\mathbf{v} = \nabla\left(\nabla\cdot\mathbf{v}\right)-\nabla^2\mathbf{v}$, for any vector field v, becomes:

$$\begin{aligned}\chi &= \frac{\varepsilon_0}{2}\mathbf{e}\cdot\left(\nabla^2\mathbf{c}\right)-\frac{1}{2\mu_0}\mathbf{b}\cdot\left(\nabla^2\mathbf{a}\right)\\ &= k^2\left(\frac{1}{2\mu_0}\mathbf{a}\cdot\mathbf{b}-\frac{\varepsilon_0}{2}\mathbf{c}\cdot\mathbf{e}\right).\end{aligned} \tag{3.8.12}$$

Thus, in a monochromatic (not necessarily parallel) beam we have the relation:

$$k^2\int_V \partial^3\mathbf{r}\,\chi = h \tag{3.8.13}$$

where h is the helicity, as given in Eq. (3.6.5). By mode analysis or vector manipulation it is similarly found that the spatially integrated optical chirality flux is given by:

$$\int_V \partial^3\mathbf{r}\,\boldsymbol{\phi} = \sin(2\theta)\sin(\phi)\sum_{\mathbf{k}}\left(\hat{N}^{(1)}(\mathbf{k}) - \hat{N}^{(2)}(\mathbf{k})\right)\hbar k^2\hat{\mathbf{k}}. \tag{3.8.14}$$

Thus, for a monochromatic field:

$$k^2\int_V \partial^3\mathbf{r}\,\boldsymbol{\phi} = \mathbf{S}. \tag{3.8.15}$$

These monochromatic correspondences have been observed in a classical momentum representation [35] and using a Riemann-Silberstein vector formalism [36]. In the next chapter we will determine what physical effects become manifest when matter interacts with light possessing non-zero values of these measures with matter.

3.9 Family of Helicity-type and Spin-type Measures

It was shown by Cameron, Barnett and Yao [15] that the starting with free-space Maxwell-like equations, involving the vector potentials:

$$\begin{aligned}
&\nabla\cdot\mathbf{c} = 0;\\
&\nabla\cdot\mathbf{a} = 0;\\
&\nabla\times\mathbf{c} = -\frac{\partial\mathbf{a}}{\partial t};\\
&\nabla\times\mathbf{a} = \frac{1}{c^2}\frac{\partial\mathbf{c}}{\partial t},
\end{aligned} \tag{3.9.1}$$

and replacing every **a** and **c**, the magnetic and electric vector potentials, with their curls delivers, first, Maxwell's equations. Continuing to replace any appearance of a field with its curl reveals an infinite list of Maxwell-like equations. Moreover, for any

conserved electromagnetic quantity one can replace each appearance of the fields with their curls, or curls of curls, etc., generating an infinite list of related conserved quantities. It is easy to check that optical chirality density and its associated flux can be derived from the helicity and spin operators by repeating such a replacement. More generally, it is now shown that starting with the electromagnetic helicity, Eq. (3.6.5), and spin, Eq. (3.3.15), operators, and repeatedly taking curls, creates an infinite set of pairs of helicity-type and spin-type measures. It will be shown that *all* measures are proportional to the difference in populations of optical modes with opposing helicity. Furthermore, it is observed that the helicity and spin satisfy a continuity relation, Eq. (3.6.4); this is mirrored by a corresponding continuity in the optical chirality density and associated flux, and in any higher order counterparts. In contrast, it has been shown that other orbital angular momentum measures are not conserved; precisely, the total number of optical vortices on a cross-section of a paraxial beam [37].

To prove that all measures in the Cameron-Barnett-Yao infinite hierarchy are proportional to the difference in populations of optical modes with opposing helicity, we observe that taking each successive curl of the field operators in the expressions for the spin and helicity has three effects: through the exponential factor in the quantum optical mode expansion, each operator is multiplied by ik, which, by the bilinearity of each term, results in an overall multiplication of k^2; the comparative signs of the positive and negative frequency terms alternate; and the polarisation vectors are exchanged in a two-cycle,

$$\mathbf{e}^{(1/2)}(\mathbf{k}) \to \hat{\mathbf{k}} \times \mathbf{e}^{(1/2)}(\mathbf{k}) \to \mathbf{e}^{(1/2)}(\mathbf{k}) . \to \dots \ . \tag{3.9.2}$$

Therefore, each of the helicity-type measures will always involve the dot product of the electric polarisation vector with the complex conjugate of the corresponding *magnetic polarisation vector* [38], $\hat{\mathbf{k}}\times\mathbf{e}^{(1/2)}(\mathbf{k})$. With the generalised polarisation vector basis, Eq. (3.5.1), these products emerge as:

$$\begin{aligned}
\mathbf{e}^{(1)}(\mathbf{k})\cdot\overline{\left[\hat{\mathbf{k}}\times\mathbf{e}^{(1)}(\mathbf{k})\right]} &= \left(\sin\theta\hat{\mathbf{i}}+e^{i\phi}\cos\theta\hat{\mathbf{j}}\right)\cdot\left(-e^{-i\phi}\cos\theta\hat{\mathbf{i}}+\sin\theta\hat{\mathbf{j}}\right)\\
&= e^{i\phi}\sin\theta\cos\theta-e^{-i\phi}\sin\theta\cos\theta\\
&= i\sin(2\theta)\sin(\phi);\\
\mathbf{e}^{(2)}(\mathbf{k})\cdot\overline{\left[\hat{\mathbf{k}}\times\mathbf{e}^{(2)}(\mathbf{k})\right]} &= \left(\cos\theta\hat{\mathbf{i}}-e^{i\phi}\sin\theta\hat{\mathbf{j}}\right)\cdot\left(e^{-i\theta}\sin\theta\hat{\mathbf{i}}+\cos\theta\hat{\mathbf{j}}\right)\\
&= -e^{i\phi}\sin\theta\cos\theta+e^{-i\phi}\sin\theta\cos\theta\\
&= -i\sin(2\theta)\sin(\phi).
\end{aligned} \tag{3.9.3}$$

Similarly, the spin-type measures involve either the vector cross product of the electric or magnetic polarisation vectors with itself, which emerge as:

$$\begin{aligned}
\left[\hat{\mathbf{k}}\times\mathbf{e}^{(1)}(\mathbf{k})\right]\times\overline{\left[\hat{\mathbf{k}}\times\mathbf{e}^{(1)}(\mathbf{k})\right]} &= \begin{vmatrix}\hat{\mathbf{i}} & \hat{\mathbf{j}} & \hat{\mathbf{k}}\\ -e_y & e_x & 0\\ -\overline{e}_y & \overline{e}_x & 0\end{vmatrix} = \left[e^{-i\phi}\cos\theta\sin\theta-e^{i\phi}\cos\theta\sin\theta\right]\hat{\mathbf{k}}\\
&= -i\sin(2\theta)\sin(\phi)\hat{\mathbf{k}};\\
\left[\hat{\mathbf{k}}\times\mathbf{e}^{(2)}(\mathbf{k})\right]\times\overline{\left[\hat{\mathbf{k}}\times\mathbf{e}^{(2)}(\mathbf{k})\right]} &= \begin{vmatrix}\hat{\mathbf{i}} & \hat{\mathbf{j}} & \hat{\mathbf{k}}\\ -e_y & e_x & 0\\ -\overline{e}_y & \overline{e}_x & 0\end{vmatrix} = \left[e^{i\phi}\sin\theta\cos\theta-e^{-i\phi}\sin\theta\cos\theta\right]\hat{\mathbf{k}}\\
&= i\sin(2\theta)\sin(\phi)\hat{\mathbf{k}},
\end{aligned} \tag{3.9.4}$$

and

$$\begin{aligned}\mathbf{e}^{(1)}(\mathbf{k})\times\overline{\mathbf{e}}^{(1)}(\mathbf{k}) &= \begin{vmatrix}\hat{\mathbf{i}} & \hat{\mathbf{j}} & \hat{\mathbf{k}}\\ \sin\theta & e^{i\phi}\cos\theta & 0\\ \sin\theta & e^{-i\phi}\cos\theta & 0\end{vmatrix} = -i\sin(2\theta)\sin(\phi)\hat{\mathbf{k}};\\ \mathbf{e}^{(2)}(\mathbf{k})\times\overline{\mathbf{e}}^{(2)}(\mathbf{k}) &= \begin{vmatrix}\hat{\mathbf{i}} & \hat{\mathbf{j}} & \hat{\mathbf{k}}\\ \cos\theta & -e^{i\phi}\sin\theta & 0\\ \cos\theta & -e^{-i\phi}\sin\theta & 0\end{vmatrix} = i\sin(2\theta)\sin(\phi)\hat{\mathbf{k}},\end{aligned} \tag{3.9.5}$$

With these prescriptions it is clear that the only nonzero terms are those containing the number operator $\hat{N}^{(1/2)}(\mathbf{k}) \equiv a^{\dagger(1/2)}(\mathbf{k})a^{(1/2)}(\mathbf{k})$ with the polarization state matching that of the polarization vector. Thus, *all* helicity- type and spin-type operators obtained via repeated curls of the field operators have resulting formulae all containing the distinctive dependence on the difference between number operators for optical modes of opposing helicity. More generally, these quantum operators are delivered as:

$$\int_V \partial^3\mathbf{r}\, h^{(j)} = \hbar c\sin(2\theta)\sin(\phi)\sum_{\mathbf{k}} k^{2j}\left\{\hat{N}^{(1)}(\mathbf{k}) - \hat{N}^{(2)}(\mathbf{k})\right\}; \tag{3.9.6}$$

$$\int_V \partial^3\mathbf{r}\,\mathbf{S}^{(j)} = \hbar\sin(2\theta)\sin(\phi)\sum_{\mathbf{k}} k^{2j}\left\{\hat{N}^{(1)}(\mathbf{k}) - \hat{N}^{(2)}(\mathbf{k})\right\}\hat{\mathbf{k}}, \tag{3.9.7}$$

where the superscript labels the different generations of helicity- and spin- type measures, with (j = 0) and (j = 1) representing the helicity/spin densities and optical chirality/chirality flux generations respectively [31]. We can immediately conclude that the maximum (minimum) value that any of the above operators may attain is when acting on a state containing purely left- (right-) handed photons.

3.10 Conclusion

It has been shown that careful analysis of the optical angular momentum allows division into parts that satisfy duplex symmetry (electric-magnetic democracy). Introduction of a general Poincaré sphere representation of polarisation allows the analysis a greater degree of generality. In a quantum optical framework, the orbital and spin parts of the angular momentum have been shown to depend on the sum and difference of number operators for modes of opposing helicity, respectively. The Noether charge that corresponds to the spin was delivered as the electromagnetic helicity. In a plane wave analysis, both measures depend on the difference between numbers of optical modes with polarisation vectors diametrically opposed to the Poincaré sphere. This result extends to the case of beams with orbital angular momentum. The involvement of orbital angular momentum has been tackled by investigation of Laguerre-Gaussian modes, which form a complete basis set for rotationally symmetric beams.

A similar analysis of the recently rediscovered optical chirality density and corresponding flux showed that they are proportional only to difference of number operators for modes of opposing helicity. Introduction of a Laguerre-Gaussian basis reveals that beams with nonzero values of the optical chirality do not necessarily have any orbital angular momentum characteristics. Finally, it is shown that the infinite hierarchy of helicity- and spin- type measures, introduced by Cameron, Barnett and Yao, all emerge with similar quantum operator form: identical to the helicity and spin operators, except with an additional k^2 inside the mode summation for each successive operator pair.

Recently, it has been claimed that light with nonzero values of optical chirality can differentiate between left- and right- handed molecules many times better than pure circularly polarised light [39–41]. The analysis in this chapter unambiguously shows that the maximum value any helicity- or spin- type measure can take is that of pure left- or right- handed light. In the next chapter we provide a quantum electrodynamic analysis of the experiments that claim to show such effects.

3.11 Appendix B – Polarisation Vectors dot product

This appendix explicitly calculates the various combinations of polarisation vector dot and cross products, used in Section 3.8 to compute the spatially integrated optical chirality density and flux in terms of quantum number operators.

$$\begin{aligned}
\overline{\mathbf{e}}^{(1)}(\mathbf{k})\cdot\left[\mathbf{k}\times\mathbf{e}^{(1)}(\mathbf{k})\right] &= \overline{\mathbf{e}}^{(1)}(\mathbf{k})\cdot\begin{vmatrix} \hat{\mathbf{i}} & \hat{\mathbf{j}} & \hat{\mathbf{k}} \\ 0 & 0 & k \\ \sin\theta & e^{i\phi}\cos\theta & 0 \end{vmatrix} \\
&= \left(\sin\theta\hat{\mathbf{i}} + e^{-i\phi}\cos\theta\hat{\mathbf{j}}\right)\cdot\left(-ke^{i\phi}\cos\theta\hat{\mathbf{i}} + k\sin\theta\hat{\mathbf{j}}\right) \\
&= -\frac{k}{2}\sin 2\theta\left(e^{-i\phi} - e^{i\phi}\right) \\
&= -k\sin 2\theta\sinh i\phi \\
&= -ik\sin 2\theta\sin\phi \\
&= -\mathbf{e}^{(1)}(\mathbf{k})\cdot\left[\mathbf{k}\times\overline{\mathbf{e}}^{(1)}(\mathbf{k})\right];
\end{aligned} \tag{A.1}$$

$$\begin{aligned}
\mathbf{e}^{(2)}(\mathbf{k})\cdot\left[\mathbf{k}\times\overline{\mathbf{e}}^{(2)}(\mathbf{k})\right] &= \mathbf{e}^{(2)}(\mathbf{k})\cdot\begin{vmatrix} \hat{\mathbf{i}} & \hat{\mathbf{j}} & \hat{\mathbf{k}} \\ 0 & 0 & k \\ \cos\theta & -e^{-i\phi}\sin\theta & 0 \end{vmatrix} \\
&= \left(\cos\theta\hat{\mathbf{i}} - e^{i\phi}\sin\theta\hat{\mathbf{j}}\right)\cdot\left(ke^{-i\phi}\sin\theta\hat{\mathbf{i}} + k\cos\theta\hat{\mathbf{j}}\right) \\
&= ke^{-i\phi}\sin\theta\cos\theta - ke^{i\phi}\sin\theta\cos\theta \\
&= \frac{k}{2}\sin(2\theta)\left(e^{i\phi} - e^{-i\phi}\right) \\
&= -ik\sin(2\theta)\sin\phi \\
&= -\overline{\mathbf{e}}^{(2)}(\mathbf{k})\cdot\left[\mathbf{k}\times\mathbf{e}^{(2)}(\mathbf{k})\right];
\end{aligned} \tag{A.2}$$

$$\begin{aligned}
\overline{\mathbf{e}}^{(2)}(\mathbf{k})\cdot\left[\mathbf{k}\times\mathbf{e}^{(1)}(\mathbf{k})\right] &= \mathbf{e}^{(2)}(\mathbf{k})\cdot\begin{vmatrix} \hat{\mathbf{i}} & \hat{\mathbf{j}} & \hat{\mathbf{k}} \\ 0 & 0 & k \\ \sin\theta & e^{i\phi}\cos\theta & 0 \end{vmatrix} \\
&= \left(\cos\theta\hat{\mathbf{i}} - e^{-i\phi}\sin\theta\hat{\mathbf{j}}\right)\cdot\left(-ke^{i\phi}\cos\theta\hat{\mathbf{i}} + k\sin\theta\hat{\mathbf{j}}\right) \\
&= -k\left(e^{i\phi}\cos^2\theta - e^{-i\phi}\sin^2\theta\right) \\
&= -\mathbf{e}^{(2)}(\mathbf{k})\cdot\left[\mathbf{k}\times\overline{\mathbf{e}}^{(1)}(\mathbf{k})\right];
\end{aligned} \tag{A.3}$$

$$\begin{aligned}\overline{\mathbf{e}}^{(1)}(\mathbf{k})\cdot\left[\mathbf{k}\times\mathbf{e}^{(2)}(\mathbf{k})\right] &= \overline{\mathbf{e}}^{(1)}(\mathbf{k})\cdot\begin{vmatrix}\hat{\mathbf{i}} & \hat{\mathbf{j}} & \hat{\mathbf{k}}\\ 0 & 0 & k\\ \cos\theta & -e^{i\phi}\sin\theta & 0\end{vmatrix}\\ &= \left(\sin\theta\hat{\mathbf{i}}+e^{-i\phi}\cos\theta\hat{\mathbf{j}}\right)\cdot\left(ke^{i\phi}\sin\theta\hat{\mathbf{i}}+k\cos\theta\hat{\mathbf{j}}\right)\\ &= k\left(e^{i\phi}\sin^2\theta+e^{-i\phi}\cos^2\theta\right)\\ &= -\mathbf{e}^{(1)}(\mathbf{k})\cdot\left[\mathbf{k}\times\overline{\mathbf{e}}^{(2)}(\mathbf{k})\right].\end{aligned} \tag{A.4}$$

3.12 Bibliography

[1] E. Noether, "Invariant variation problems," *Transport theory and statistical physics* **1**(3), 186–207 (1918) [doi:10.1080/00411457108231446].

[2] Latin American School of Physics, *Group theory and its applications in physics, 1980: Latin American School of Physics, Mexico City*, American Institute of Physics, New York (1981).

[3] M. E. Peskin, *An Introduction to Quantum Field Theory*, Addison-Wesley Pub. Co, Reading, Mass (1995).

[4] M. Kaku, *Quantum Field Theory: A Modern Introduction*, Oxford University Press, New York (1993).

[5] J. H. Poynting, "The wave motion of a revolving shaft, and a suggestion as to the angular momentum in a beam of circularly polarised light," *Proceedings of the Royal Society A: Mathematical, Physical and Engineering Sciences* **82**(557), 560–567 (1909) [doi:10.1098/rspa.1909.0060].

[6] R. Beth, "Mechanical detection and measurement of the angular momentum of light," *Physical Review* **50**(2), 115–125 (1936) [doi:10.1103/PhysRev.50.115].

[7] D. N. Moothoo, J. Arlt, R. S. Conroy, F. Akerboom, A. Voit, and K. Dholakia, "Beth's experiment using optical tweezers," *American Journal of Physics* **69**(3), 271 (2001) [doi:10.1119/1.1309520].

[8] N. B. Simpson, K. Dholakia, L. Allen, and M. J. Padgett, "Mechanical equivalence of spin and orbital angular momentum of light: an optical spanner," *Optics Letters* **22**(1), 52 (1997) [doi:10.1364/OL.22.000052].

[9] R. P. Feynman, *The Feynman Lectures on Physics*, New millennium ed, Basic Books, New York (2011).

[10] C. Cohen-Tannoudji, J. Dupont-Roc, and G. Grynberg, *Photons and Atoms: Introduction to Quantum Electrodynamics*, Wiley, New York, NY (1997).

[11] G. B. Arfken, *Mathematical Methods for Physicists*, Academic Press, Orlando (1985).

[12] J. D. Jackson, *Classical Electrodynamics*, 3rd ed, Wiley, New York (1999).

[13] J. Larmor, "A dynamical theory of the electric and luminiferous medium.," *Proceedings of the Royal Society of London* **54**(326-330), 438–461 (1893) [doi:10.1098/rspl.1893.0092].

[14] O. Heaviside, "On the forces, stresses, and fluxes of energy in the electromagnetic field," *Philosophical Transactions of the Royal Society A:*

Mathematical, Physical and Engineering Sciences **183**(0), 423–480 (1892) [doi:10.1098/rsta.1892.0011].

[15] R. P. Cameron, S. M. Barnett, and A. M. Yao, "Optical helicity, optical spin and related quantities in electromagnetic theory," *New Journal of Physics* **14**(5), 053050 (2012) [doi:10.1088/1367-2630/14/5/053050].

[16] I. Bialynicki-Birula and Z. Bialynicka-Birula, "Canonical separation of angular momentum of light into its orbital and spin parts," *Journal of Optics* **13**(6), 064014 (2011) [doi:10.1088/2040-8978/13/6/064014].

[17] C. G. Darwin, "Notes on the theory of radiation," *Proceedings of the Royal Society A: Mathematical, Physical and Engineering Sciences* **136**(829), 36–52 (1932) [doi:10.1098/rspa.1932.0065].

[18] S. J. Van Enk and G. Nienhuis, "Commutation rules and eigenvalues of spin and orbital angular momentum of radiation fields," *Journal of Modern Optics* **41**(5), 963–977 (1994) [doi:10.1080/09500349414550911].

[19] S. J. van Enk and G. Nienhuis, "Spin and orbital angular momentum of photons," *Europhysics Letters (EPL)* **25**(7), 497–501 (1994) [doi:10.1209/0295-5075/25/7/004].

[20] M. M. Coles and D. L. Andrews, "Chirality and angular momentum in optical radiation," *Physical Review A* **85**(6) (2012) [doi:10.1103/PhysRevA.85.063810].

[21] G. Auletta, *Quantum Mechanics*, Cambridge University Press, Cambridge, UK□; New York (2009).

[22] G. L. Naber, *The Geometry of Minkowski Spacetime: An Introduction to the Mathematics of the Special Theory of Relativity*, Springer-Verlag, New York (1992).

[23] I. J. R. Aitchison and A. J. G. Hey, *Gauge Theories in Particle Physics: A Practical Introduction*, CRC, Boca Raton, Fla (2013).

[24] A. Sommerfeld, *Partial Differential Equations in Physics Lectures on Theoretical Physics. vol. 6 vol. 6*, Academic Press, New York (1967).

[25] A. E. Siegman, *Lasers*, University Science Books, Mill Valley, Calif. (1986).

[26] Feng-Lei Hong, J. Ishikawa, J. Yoda, J. Ye, Long-Sheng Ma, and J. L. Hall, "Frequency comparison of $^{127}I_2$-stabilized Nd:YAG lasers," *IEEE Transactions on Instrumentation and Measurement* **48**(2), 532–536 (1999) [doi:10.1109/19.769651].

[27] L. Allen, M. J. Padgett, and M. Babiker, "IV The Orbital Angular Momentum of Light," in *Progress in Optics* **39**, pp. 291–372, Elsevier (1999).

[28] M. Abramowitz and I. A. Stegun, *Handbook of Mathematical Functions: With Formulas, Graphs and Mathematical tables*, Dover, New York (1972).

[29] L. C. D. Romero, D. L. Andrews, and M. Babiker, "A quantum electrodynamics framework for the nonlinear optics of twisted beams," *Journal of Optics B: Quantum and Semiclassical Optics* **4**(2), S66–S72 (2002) [doi:10.1088/1464-4266/4/2/370].

[30] E. Karimi, G. Zito, B. Piccirillo, L. Marrucci, and E. Santamato, "Hypergeometric-Gaussian modes," *Optics Letters* **32**(21), 3053 (2007) [doi:10.1364/OL.32.003053].

[31] M. M. Coles and D. L. Andrews, "Photonic measures of helicity: optical vortices and circularly polarized reflection," *Optics Letters* **38**(6), 869 (2013) [doi:10.1364/OL.38.000869].

[32] D. M. Lipkin, "Existence of a new conservation law in electromagnetic theory," *Journal of Mathematical Physics* **5**(5), 696 (1964) [doi:10.1063/1.1704165].

[33] Y. Tang and A. E. Cohen, "Optical chirality and its interaction with matter," *Physical Review Letters* **104**(16) (2010) [doi:10.1103/PhysRevLett.104.163901].

[34] W. I. Fushchich and A. G. Nikitin, "The complete sets of conservation laws for the electromagnetic field," *Journal of Physics A: Mathematical and General* **25**(5), L231–L233 (1992) [doi:10.1088/0305-4470/25/5/004].

[35] K. Y. Bliokh and F. Nori, "Characterizing optical chirality," *Physical Review A* **83**(2) (2011) [doi:10.1103/PhysRevA.83.021803].

[36] J. E. S. Bergman, S. M. Mohammadi, T. D. Carozzi, L. K. S. Daldorff, B. Thidé, R. Karlsson, and M. Eriksson, "Conservation Laws in generalized Riemann-Silberstein electrodynamics," *Eriksson*.

[37] F. S. Roux, "Fluid dynamical enstrophy and the number of optical vortices in a paraxial beam," *Optics Communications* **268**(1), 15–22 (2006) [doi:10.1016/j.optcom.2006.07.008].

[38] D. P. Craig and T. Thirunamachandran, *Molecular Quantum Electrodynamics: An Introduction to Radiation-Molecule Interactions*, Dover Publications, Mineola, N.Y (1998).

[39] Y. Tang and A. E. Cohen, "Enhanced enantioselectivity in excitation of chiral molecules by superchiral light," *Science* **332**(6027), 333–336 (2011) [doi:10.1126/science.1202817].

[40] E. Hendry, T. Carpy, J. Johnston, M. Popland, R. V. Mikhaylovskiy, A. J. Lapthorn, S. M. Kelly, L. D. Barron, N. Gadegaard, et al., "Ultrasensitive detection and characterization of biomolecules using superchiral fields," *Nature Nanotechnology* **5**(11), 783–787 (2010) [doi:10.1038/nnano.2010.209].

[41] E. Hendry, R. V. Mikhaylovskiy, L. D. Barron, M. Kadodwala, and T. J. Davis, "Chiral electromagnetic fields generated by arrays of nanoslits," *Nano Letters* **12**(7), 3640–3644 (2012) [doi:10.1021/nl3012787].

Chapter 4

The Interaction of Twisted Light with Matter

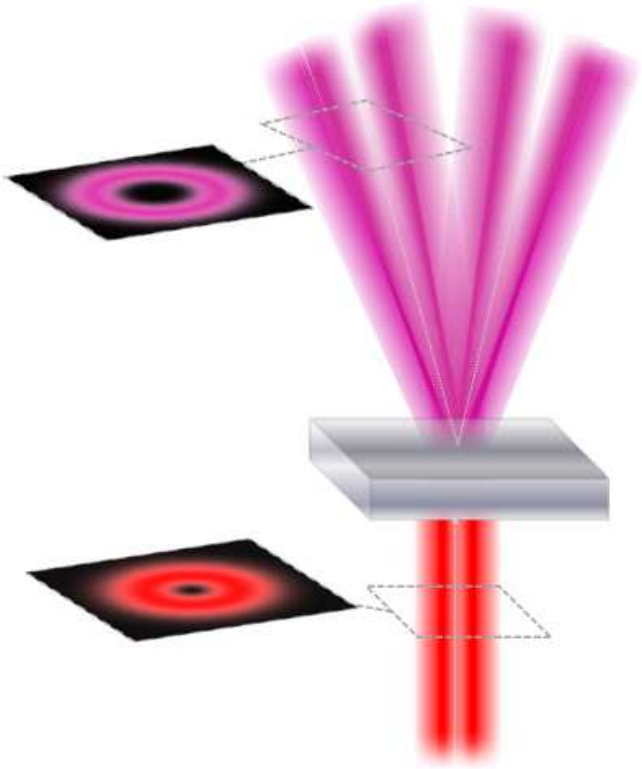

"Spin. n. a quantum characteristic of an elementary particle that is visualized as the rotation of the particle on its axis and that is responsible for measurable angular momentum."

"Spin. n. a special point of view, emphasis, or interpretation presented for the purpose of influencing opinion."

– Merriam-Webster Dictionary[†]

[†] Merriam Webster Dictionary, Merriam Webster, U.S.; Revised edition (2004)

4.1 Background

In 1974, Nye and Berry showed theoretically that whenever three or more waves interfere there will be lines of phase indeterminacy that imply zero amplitude at these locations [1]. In the context of optics, the details of these phase dislocations were not recognised until the 1990s; namely, that beams with these properties convey orbital angular momentum [2–6]. These one-dimensional vortex lines have been shown to spontaneously form knots [7], even in simple nonlinear optical systems [8,9]. Moreover, the well-known speckle pattern present in laser beam profiles is associated with optical vortices in these regions [10,11]. In contrast, it has been long known that the spin part of the optical angular momentum, associated with polarisation, determines circular differential response for chiral molecules [12]. However, it is now known that orbital angular momentum does not play a role in the electronic dipole transitions, only in centre of mass motion [13,14]; this was later verified experimentally [15,16]. On the beam axis the spin and orbital parts of the angular momentum have mechanically equivalent effects: they cause the rotation of a weakly absorbing dielectric microsphere [17].

Beams with orbital angular momentum are commonly created by the conversion of a conventional optical beam, with spiral phase plates [18], spatial light modulators [19,20] and q-plates [21,22]. In fact, it is now possible to convert transverse electromagnetic mode (TEM) beams into tailored complex beams, in which both the phase and the polarisation of the output is predetermined [23,24]. These beams often have complex polarisation structures, varying over the beam profile and may also display polarisation singularities [25]. Demanding material inhomogeneity and

anisotropy, q-plates allow the entanglement of the spin and orbital degrees of freedom of photons [26], which, in the context of quantum computing, provides a means for spin-orbit information transfer [21,27]. Thus, possibilities for encoding, processing and transmitting information of higher dimensionality than in pure spin states [28] have been met with renewed optimism [29–36].

The potential applications associated with optical vortex beams are numerous: for example, in optical manipulation [37–39], in optical sensing [40], and in contrast enhanced ghost imaging [41]. In fact, it has recently been shown that light with orbital angular momentum has several astrophysical applications [42], such as adaptive optics [43], high contrast imaging of exoplanets [44] and speculation that rotating black holes produce light with orbital angular momentum [45]. Furthermore, there have been recent reports that the orbital angular momentum of light can enhance higher-order multipole effects [46] and new selection rules for atomic transitions [47].

Since the previous chapter disproved the possibility that the optical chirality density can allow 'superchiral' electromagnetic fields, the motivation for the work in this chapter is to develop a theoretical understanding of the experiments of Tang and Cohen. Molecular QED is used in the description of circular dichroism near to a reflecting surface, and gives results that tie in perfectly with the experimental reports of Tang and Cohen. Furthermore, a six-wave mixing process is described that can display many of the interesting entanglement features of spontaneous parametric down-conversion, except with the added benefit of being possible in an isotropic medium.

4.2 Bilinear Measures

To begin, it is worthwhile considering the mathematical form of optical measures of freely propagating radiation. All observations, therefore, emerge as expectation values that do not demolish the radiation state. In the previous chapter we displayed the components of the electromagnetic stress-energy tensor, each containing the product of precisely two field operators. Furthermore, the division into spin and orbital parts, the helicity and the infinite hierarchy of chiral measures are all *bilinear* terms in the electric and magnetic (or related) fields. Evaluating these quantities with a plane-wave or Laguerre-Gaussian mode expansion reveals resultant formulae with terms containing precisely one annihilation and one creation operator. It is this feature that allows many optical measures of interest to be constructed as dependant on number operators.

To address the case of non-paraxial beams we introduce, as a representative test case, an exact classical solution for the electric field vector of a beam bearing orbital angular momentum [48]:

$$\begin{aligned}\mathbf{E}(x) = e^{il\phi}\int_0^k d\kappa E(\kappa) e^{ik_z z}\times\Big\{&\left(\alpha_u e_x + \alpha_v e_y\right) J_l(\kappa\rho) \\ &+ e_z \frac{\kappa}{2k_z}\left[\left(i\alpha_u - \alpha_v\right) e^{-i\phi} J_{l-1}(\kappa\rho) - \left(i\alpha_u + \alpha_v\right) e^{i\phi} J_{l+1}(\kappa\rho)\right]\Big\},\end{aligned} \tag{4.2.1}$$

where $J_l(\kappa\rho)$ are Bessel functions, with l topological charge, l, the z component of the wavevector $k_z = \left(k^2 - \kappa^2\right)^{1/2}$ and the complex constants α_u, α_v satisfy $|\alpha_u|^2 + |\alpha_v|^2 = 1$. To promote Eq. (4.2.1) to a quantum operator, we recognise that α_u

and α_v correspond to orthogonal plane polarisations, such as horizontal and vertical, and demand that they are promoted to operator status through:

$$\begin{aligned}\alpha_v &\to \frac{i}{\sqrt{2}}\left\{a^{(\mathrm{L})}(\mathbf{k}) \pm a^{(\mathrm{R})}(\mathbf{k})\right\};\\ \alpha_u &\to \frac{1}{\sqrt{2}}\left\{a^{(\mathrm{L})}(\mathbf{k}) \pm a^{(\mathrm{R})}(\mathbf{k})\right\},\end{aligned} \tag{4.2.2}$$

where the superscript L/R denote left- and right- handed circular polarisations, respectively. Thus, the quantum optical form of Eq. (4.2.1) is an expression that is linear in the annihilation and creation operators. To summarise: for both paraxial and non-paraxial light, the stress-energy tensor components and all angular momentum observables are bilinear in $a^{(\eta)}(\mathbf{k})$ and $a^{\dagger(\eta)}(\mathbf{k})$.

To generalise this analysis, we postulate a quantum operator $\hat{\mathbf{Q}}$ given by an analytical function of fields containing strings of annihilation and creation operators. Such functions permit power series expansions and are therefore amenable to the following analysis. For two operators $\hat{\mathbf{A}}$ and $\hat{\mathbf{B}}$, their normal order is denoted here as $\overleftarrow{\hat{\mathbf{A}}\hat{\mathbf{B}}}$. In quantum field theory, a product of quantum fields and, equivalently, a product of the annihilation and creation operators of those fields, is said to be *normally ordered* when all annihilation operators are to the right of all creation operators. Normal ordering can be defined in many other ways, but for the present purposes the usual definition works perfectly. For the same two operators $\hat{\mathbf{A}}$ and $\hat{\mathbf{B}}$, their contraction is denoted $\hat{\mathbf{A}} \circ \hat{\mathbf{B}}$, and is defined to be:

$$\hat{\mathbf{A}} \circ \hat{\mathbf{B}} = \hat{\mathbf{A}}\hat{\mathbf{B}} - \overleftrightarrow{\hat{\mathbf{A}}\hat{\mathbf{B}}}. \tag{4.2.3}$$

For the product of an annihilation and creation operator the contraction is given by:

$$a^{(\lambda)}(\mathbf{k}) \circ a^{\dagger(\eta)}(\mathbf{p}) = a^{(\lambda)}(\mathbf{k}) a^{\dagger(\eta)}(\mathbf{p}) - \overleftrightarrow{a^{(\lambda)}(\mathbf{k}) a^{\dagger(\eta)}(\mathbf{p})} = \delta_{\lambda,\eta}\delta_{\mathbf{p},\mathbf{k}}, \tag{4.2.4}$$

which is effectively a restatement of the annihilation and creation operator commutation relation. Wick's Theorem [49] states that a product of annihilation and creation operators can be written as the normal ordering of that product, plus the normal order of the product after all single contractions, plus the normal ordering after all double contractions, etc [50]. It is worth noting that this contraction is a real number – precisely, either 1 or 0. Thus, the above contraction will reduce the number of operators in any given string by 2. Simply, from Wick's Theorem, any string of annihilation and creation operators can be decomposed into a set of terms that are all in normal order. Significantly, the difference between the number of annihilation and creation operators is a constant for all terms in the decomposition.

We have determined that, by Wick's Theorem, the operator $\hat{\mathbf{Q}}$ transforms into a series of terms, each with the form:

$$\underbrace{a^{\dagger(\eta)} \ldots a^{\dagger(\eta)}}_{r} \underbrace{a^{(\eta)} \ldots a^{(\eta)}}_{s}, \tag{4.2.5}$$

where the mode label, $\mathbf{k}$, has been dropped for convenience. If r and s are the number of times each operator appears, then $(r - s)$ is a constant dictated by $\hat{\mathbf{Q}}$ and inherited

by all terms. Taking the expectation value of the terms of such an operator over a number (Fock) state delivers:

$$\left\langle n\left|\underbrace{a^{\dagger}\ldots a^{\dagger}}_{r}\underbrace{a\ldots a}_{s}\right|n\right\rangle=\frac{n!^{2}}{(n-r)!(n-s)!}\left\langle n-r\,|\,n-s\right\rangle, \tag{4.2.6}$$

which, due to the orthogonality of the state vectors, only gives a non-vanishing result when $r = s$. Thus, when investigating the properties of number states, Hermitian operators must contain terms with equal numbers of annihilation and creation operators.

For greater generality, we extend this argument to coherent states [51], which, unlike Fock states, are not necessarily orthogonal. Taking the expectation of the terms in $\hat{\mathbf{Q}}$ gives:

$$\left\langle \alpha\left|\underbrace{a^{\dagger}\ldots a^{\dagger}}_{r}\underbrace{a\ldots a}_{s}\right|\alpha\right\rangle=\bar{\alpha}^{r}\alpha^{s}, \tag{4.2.7}$$

where the coherent state, $|\alpha\rangle$, is an eigenstate of the annihilation operator, with eigenvalue α, a complex number. Thus, unequal numbers of annihilation and creation operators are not prohibited for coherent states by the same reasoning as for precisely defined number states. However, explicitly displaying the time dependence of the raising and lowering operators gives:

$$\begin{aligned} a^{(\eta)}(\mathbf{k},t) &= a^{(\eta)}(\mathbf{k},0)e^{-i\omega t}; \\ a^{\dagger(\eta)}(\mathbf{k},t) &= a^{\dagger(\eta)}(\mathbf{k},0)e^{i\omega t}, \end{aligned} \tag{4.2.8}$$

where $\omega = ck$ is the photon frequency. Substitution of these expressions into Eq. (4.2.7) reveals that a normally ordered string of annihilation and creation operators will contain a residual oscillating phase factor if the numbers of each operator are imbalanced. Precisely, the phase factor will be $e^{(r-s)i\omega t}$, which, is inherited by all terms in the normally ordered decomposition prescribed by Wick's theorem. Thus, unless $r = s$, the real part of this factor, involved in any measurement, acquires a zero expectation value. Finally, a general optical state – representable as a linear combination of either number or coherent states – will similarly deliver only nonzero values when electromagnetic measures have terms with equal numbers of annihilation and creation operators.

4.3 Connecting Molecular and Optical Chirality

We now introduce a framework for discussing the symmetry principles involved in the interaction of optical handedness with molecular chirality. Using a multipolar representation of the interaction Hamiltonian, we can model each photonic interaction as:

$$H_{\text{int}} = -\int \partial^3 \mathbf{r} \{\mathbf{p}(\mathbf{r}) \cdot \mathbf{e}(\mathbf{r}) + \mathbf{m}(\mathbf{r}) \cdot \mathbf{b}(\mathbf{r})\}, \tag{4.3.1}$$

where $\mathbf{p}(\mathbf{r})$ is the molecular polarisation field (comprising all electric multipoles), $\mathbf{e}(\mathbf{r})$ and $\mathbf{b}(\mathbf{r})$ are the transverse electric and magnetic fields respectively, and $\mathbf{m}(\mathbf{r})$ is the molecular magnetisation field (comprising all magnetic multipoles) [52]. Here, we have ignored the diamagnetisation term, whose contribution is of the order α^2, the fine structure constant – the same order as magnetic quadrupole and electric octupole contributions [53]. A Taylor series expansion of the polarisation and magnetisation fields makes explicit the multipole orders, denoted *En* and *Mn* respectively. The leading order contributions are denoted $E1$, $E2$ and $M1$, and correspond to the electric dipole, $\boldsymbol{\mu}$, electric quadrupole, Q_{ij}, and magnetic dipole, $\mathbf{m}$, quantum operators, where the latter two are smaller than the electric dipole interaction by the order of the fine structure constant [51]. For the work considered in this thesis we only consider the electric and magnetic dipole interactions, whose effects, it will be shown, provide the leading order chiral response terms. The electric dipole operators change sign under space inversion (space-odd) but retain their sign under time reversal (time-even), whereas the magnetic dipole operator is space-even and time-odd [13].

In a quantum electrodynamic framework, the rate of an optical process is determined from Fermi's rule, which, in turn, is determined by the probability amplitude. The probability amplitude is a complex scalar and is obtained through application of time-dependent perturbation theory. For a general *n*-order optical process, the quantum amplitude is delivered as a series of scalar terms, each the inner product of two rank *r* tensors [54]:

$$M_{FI} \sim \sum_{e=0}^{n} \sum_{m=n-e}^{n} \mathbf{S}^{(r)}_{e;m;n-e-m} \otimes \mathbf{T}^{(r)}_{e;m;n-e-m} , \tag{4.3.2}$$

where $\otimes$ denotes the tensor inner product and e, m correspond to the number of electric and magnetic interaction. If we only consider the $E1$, $E2$ and $M1$ interactions, labelled by e_1, m_1, q, then $r = e_1 + m_1 + 2q$. The tilde, in Eq. (4.3.2), is introduced as, for clarity, we have ignored the space-time-inversion invariant constants (also labelled by e, m, n), which therefore do not contribute to discussions of the dynamical symmetries, which are all contained in the **S** and **T** tensors. Here, the **S** tensor is an outer product of electric and magnetic field vector components, and **T** is an outer product of molecular transition integrals (in the dipole approximation these are electric and magnetic transition dipole components). As the probability amplitude is scalar with the dimensions of energy, the total product $\mathbf{S}^{(r)}_{e;m;n-e-m} \otimes \mathbf{T}^{(r)}_{e;m;n-e-m}$ must not change sign under space or time inversion. Therefore, the parity signatures of each pair of **S** and **T** tensors must be identical to satisfy this condition.

Evaluating the probability (or rate) from the square modulus of the probability amplitude delivers a series of *diagonal* terms with no discriminatory chiral behaviour, as quadratic dependence on either radiation or molecular tensor is space- and time-even and it is space inversion that physically corresponds to changing molecular or optical handedness. Thus, it is the *interference* terms that may have odd spatial parity and will contribute to differential response. Furthermore, this analysis makes it clear that the total probability is a sum over all diagonal and off-diagonal terms. Thus, a non-zero result only arises from the chiral radiation modes being disproportionately populated, or by unequal populations of left- and right- handed molecules.

4.4 Differential Absorption from a Single Beam

It has recently been suggested that the optical chirality density determines the rate of differential absorption of circularly polarised light by chiral molecules. Moreover, it has been suggested that "superchiral light", with values of optical chirality density greater than pure circularly polarised light [55,56], can exist in suitably constructed experiments, and correspond to regions of enhanced chiroptical prominence [57–60]. Although, there may exist mechanisms by which the chiral response of optical centres can be enhanced, it was shown in the previous chapter that the optical chirality has maximum values for circularly polarised light [61,62]. This has also been shown in a classical setting by Bliokh and Nori [63], and in terms of Riemann-Silberstein vectors by Bergman [64].

To relate these measures to experiment, we calculate the difference between the Fermi rates for absorption by left- and right- handed molecules in a single beam,

$$\Gamma_{CD}^{(+)} - \Gamma_{CD}^{(-)}, \tag{4.4.1}$$

where (+) and (–) represent the left- and right- handed enantiomer respectively. Each term is directly proportional to the square modulus of the probability amplitude corresponding to the transition between the initial and final states:

$$\Gamma = \frac{2\pi}{\hbar}\left|M_{fi}\right|^2 \rho. \tag{4.4.2}$$

In accordance with the prescription set out in Section 4.3, the resultant formula will emerge as the inner product of a molecular tensor with a radiation tensor; the latter will prove to be proportional to both the optical chirality and the electromagnetic helicity measures derived in the previous chapter. We begin by characterising the initial state of the system,

$$\left|\text{mol}\right\rangle\left|\text{rad}\right\rangle = \left|\psi_0\right\rangle\left|n^{(L)}(\mathbf{k}), n^{(R)}(\mathbf{k})\right\rangle \tag{4.4.3}$$

where the molecular state is characterised by the ground-state wave-equation of the molecule, and the radiation state is assumed to be two modes with the same wave-vector $\boldsymbol{k}$, only differing in their circular handedness. With this notation, the final state of the system is given by:

$$\left|\text{mol}\right\rangle\left|\text{rad}\right\rangle = \left|\psi_\alpha\right\rangle\left|n^{(L)}(\mathbf{k}), n^{(R)}(\mathbf{k})-1\right\rangle, \tag{4.4.4}$$

for the absorption of a right-handed photon, and

$$\left|\text{mol}\right\rangle\left|\text{rad}\right\rangle = \left|\psi_\alpha\right\rangle\left|n^{(L)}(\mathbf{k})-1, n^{(R)}(\mathbf{k})\right\rangle, \tag{4.4.5}$$

for the absorption of a left-handed photon. Here α represents the excited state of the molecule. By use of Eq. (4.3.1) within the electric and magnetic dipole approximation, the amplitude for the transition between the prescribed initial and final state is given by:

$$\begin{aligned} M_{FI} &= \left\langle n^{(L)}-1, n^{(R)} \right| \left\langle n^{(L)}, n^{(R)}-1 \right| \left\langle \psi_\alpha \right| -\boldsymbol{\mu}\cdot\mathbf{e}^{\perp} - \mathbf{m}\cdot\mathbf{b} \left| \psi_0 \right\rangle \left| n^{(L)}, n^{(R)} \right\rangle \\ &= -\left\langle \psi_\alpha \right| \boldsymbol{\mu} \left| \psi_0 \right\rangle \cdot \left\langle n^{(L)}-1 \right| \mathbf{e}^{\perp} \left| n^{(L)} \right\rangle - \left\langle \psi_\alpha \right| \mathbf{m} \left| \psi_0 \right\rangle \cdot \left\langle n^{(L)}-1 \right| \mathbf{b} \left| n^{(L)} \right\rangle \\ &\quad -\left\langle \psi_\alpha \right| \boldsymbol{\mu} \left| \psi_0 \right\rangle \cdot \left\langle n^{(R)}-1 \right| \mathbf{e}^{\perp} \left| n^{(R)} \right\rangle - \left\langle \psi_\alpha \right| \mathbf{m} \left| \psi_0 \right\rangle \cdot \left\langle n^{(R)}-1 \right| \mathbf{b} \left| n^{(R)} \right\rangle \\ &= M_{fi}(E1) + M_{fi}(M1), \end{aligned} \tag{4.4.6}$$

where the label **k** has been suppressed for convenience. We want to calculate the square modulus of this amplitude as, in accordance with the Fermi rule (and Max Born's interpretation of normalised wavefunctions), it corresponds to the rate (or, in the case of time independent results, probability) of transition. This delivers:

$$\begin{aligned} \left| M_{FI}^{(+/-)} \right|^2 &= \left| M_{FI}^{(+/-)}(E1) + M_{FI}^{(+/-)}(M1) \right|^2 \\ &= \left| M_{FI}^{(+/-)}(E1) \right|^2_{(1)} + \left| M_{FI}^{(+/-)}(M1) \right|^2_{(2)} \\ &\quad +2\Re e\left\{ M_{FI}^{(+/-)}(E1)\, \overline{M_{FI}^{(+/-)}(M1)} \right\}_{(3)}, \end{aligned} \tag{4.4.7}$$

where subscripts are used for numbering purposes so that the terms can be tackled individually. The matrix element, Eq. (4.4.6), and the final result, will depend on the electric and magnetic transition dipole moments, $\boldsymbol{\mu}^{\alpha 0}$ and $\boldsymbol{m}^{\alpha 0}$ respectively, which, in cases where the wavefunctions are not analytically tractable, must be calculated by numerical means. Considering that the electric and magnetic dipoles can be calculated by computational methods it remains to evaluate the following four Dirac bra-kets:

$$\begin{array}{ll} \left\langle n^{(L)}(\mathbf{k})-1 \right| \mathbf{e}^{\perp} \left| n^{(L)}(\mathbf{k}) \right\rangle & \left\langle n^{(L)}(\mathbf{k})-1 \right| \mathbf{b} \left| n^{(L)}(\mathbf{k}) \right\rangle \\ \left\langle n^{(R)}(\mathbf{k})-1 \right| \mathbf{e}^{\perp} \left| n^{(R)}(\mathbf{k}) \right\rangle & \left\langle n^{(R)}(\mathbf{k})-1 \right| \mathbf{b} \left| n^{(R)}(\mathbf{k}) \right\rangle \end{array} \tag{4.4.8}$$

By using either a plane wave or a Laguerre-Gaussian description of the electric and magnetic fields, we observe that in each case only the annihilation term in the quantum mode expansion delivers a non-zero result. Thus, we obtain, for the left-handed electric term:

$$\begin{aligned}\left\langle n^{(L)}-1\left|\mathbf{e}^{\perp}\right|n^{(L)}\right\rangle &= \left\langle n^{(L)}-1\left|i\left(\frac{\hbar ck}{2\varepsilon_0 V}\right)^{1/2}\mathbf{e}^{(L)}e^{ikz-il\phi}a^{(L)}\right|n^{(L)}\right\rangle \\ &= \left\langle n^{(L)}-1\left|n^{(L)}-1\right\rangle i\,n^{(L)}\left(\frac{\hbar ck}{2\varepsilon_0 V}\right)^{1/2}\mathbf{e}^{(L)}e^{ikz-il\phi} \\ &= i\,n^{(L)}\left(\frac{\hbar ck}{2\varepsilon_0 V}\right)^{1/2}\mathbf{e}^{(L)}e^{ikz-il\phi}.\end{aligned} \tag{4.4.9}$$

Similarly we have that:

$$\begin{aligned}\left\langle n^{(R)}-1\left|\mathbf{e}^{\perp}\right|n^{(R)}\right\rangle &= in^{(R)}\left(\frac{\hbar ck}{2\varepsilon_0 V}\right)^{1/2}\mathbf{e}^{(R)}e^{ikz-il\phi}; \\ \left\langle n^{(L)}-1\left|\mathbf{b}\right|n^{(L)}\right\rangle &= in^{(L)}\left(\frac{\hbar k}{2\varepsilon_0 cV}\right)^{1/2}\mathbf{b}^{(L)}e^{ikz-il\phi}; \\ \left\langle n^{(R)}-1\left|\mathbf{b}\right|n^{(R)}\right\rangle &= in^{(R)}\left(\frac{\hbar k}{2\varepsilon_0 cV}\right)^{1/2}\mathbf{b}^{(R)}e^{ikz-il\phi},.\end{aligned} \tag{4.10}$$

where $\mathbf{e}^{(L/R)}$ and $\mathbf{b}^{(L/R)}$ are the electric and magnetic polarisation vectors for the mode with wave-vector $\mathbf{k}$. With this information we can evaluate Eq. (4.4.7). The terms labelled by (1) and (2) will be identical for either enantiomer, so will vanish in an expression for the difference in the rate of absorption for enantiomers of differing handedness. This corroborates with the result in Section 3, which demands that chiral phenomena emerge from quantum interference between terms of different symmetry character. Therefore, the difference in Fermi rates is given by:

$$\begin{aligned}\Gamma^{(+)}-\Gamma^{(-)} &\sim \left|M^{(+)}(E1)+M^{(+)}(M1)\right|^2-\left|M^{(-)}(E1)+M^{(-)}(M1)\right|^2 \\ &=\underbrace{\left|M^{(+)}(E1)\right|^2-\left|M^{(-)}(E1)\right|^2}_{=0} \\ &+\underbrace{\left|M^{(+)}(M1)\right|^2-\left|M^{(-)}(M1)\right|^2}_{=0} \\ &+2\Re e\left\{\left|M^{(+)}(E1)\overline{M^{(+)}(M1)}\right|-\left|M^{(-)}(E1)\overline{M^{(-)}(M1)}\right|\right\}\end{aligned} \tag{4.4.11}$$

Making the indices of the molecular and radiation tensors explicit, delivers the difference in transition probabilities as:

$$\begin{aligned}&2\Re e\left\{\left|M^{(+)}(E1)\overline{M^{(+)}(M1)}\right|-\left|M^{(-)}(E1)\overline{M^{(-)}(M1)}\right|\right\} \\ &=2\Re e\left(\mu_i^{\alpha 0(+)}m_j^{\alpha 0(+)}\cdot\left\langle n^{(L)}-1\middle|\mathbf{e}^{\perp}\middle|n^{(L)}\right\rangle\cdot\overline{\left\langle n^{(L)}-1\middle|\mathbf{b}\middle|n^{(L)}\right\rangle}\right) \\ &-\left(\mu_i^{\alpha 0(+)}m_j^{\alpha 0(+)}\left\langle n^{(R)}-1\middle|\mathbf{e}^{\perp}\middle|n^{(R)}\right\rangle\overline{\left\langle n^{(R)}-1\middle|\mathbf{b}\middle|n^{(R)}\right\rangle}\right) \\ &=\left(\frac{\hbar k}{\varepsilon_0}\right)\Re e\left\{e_i^{(L)}\overline{b}_j^{(L)}\mu_i^{\alpha 0(+)}m_j^{\alpha 0(+)}n^{(L)}-e_i^{(R)}\overline{b}_j^{(R)}\mu_i^{\alpha 0(-)}m_j^{\alpha 0(-)}n^{(R)}\right\}.\end{aligned} \tag{4.4.12}$$

To proceed, we note that the quantum mechanical magnetic dipole operator is given as [49]:

$$\mathbf{m}=-\frac{i\hbar\rho}{2}\int\partial^3\mathbf{r}\left(\mathbf{r}\times\nabla\right), \tag{4.4.13}$$

where ρ is the charge density. Choosing the molecular wavefunction to be real, demands an associated real electric dipole moment, and accordingly requires the magnetic dipole to be purely imaginary. We then obtain the prescription:

$$\begin{aligned}\boldsymbol{\mu}^{\beta 0(+)} &= \boldsymbol{\mu}^{\beta 0(-)} \\ \mathbf{m}^{\beta 0(+)} &= -\mathbf{m}^{\beta 0(-)},\end{aligned} \tag{4.4.14}$$

so that we may present the result in terms of just one enantiomeric form:

$$\left|M_{FI}^{(+)}\right|^2 - \left|M_{FI}^{(-)}\right|^2 = \left(\frac{\hbar k}{\varepsilon_0}\right)\Re e\left\{\mu_i^{\alpha 0(+)} m_j^{\alpha 0(+)}\left(e_i^{(L)}\overline{b}_j^{(L)} n^{(L)} + e_i^{(R)}\overline{b}_j^{(R)} n^{(R)}\right)\right\}. \tag{4.4.15}$$

Shown in Appendix C, is the relationship between the electric and magnetic polarisation vectors; enacting these relations and performing a three-dimensional isotropic rotational average delivers:

$$\left\langle \Gamma^{(+)}\right\rangle - \left\langle \Gamma^{(-)}\right\rangle = \left(\frac{2\pi\rho k}{3\varepsilon_0}\right)\Im \mathrm{m}\left(\boldsymbol{\mu}^{\alpha 0(+)}\cdot\mathbf{m}^{\alpha 0(+)}\right)\left(n^{(L)}(\mathbf{k}) - n^{(R)}(\mathbf{k})\right), \tag{4.4.16}$$

where ρ is the density of final states. In terms of number operators, this is given by:

$$\begin{aligned}&\left\langle \Gamma^{(+)}\right\rangle - \left\langle \Gamma^{(-)}\right\rangle \sim \Im \mathrm{m}\left(\boldsymbol{\mu}^{\alpha 0(+)}\cdot\mathbf{m}^{\alpha 0(+)}\right)\times \\ &\left\langle n^{(L)}(\mathbf{k}), n^{(R)}(\mathbf{k})\middle| k\left(\hat{N}^{(L)}(\mathbf{k}) - \hat{N}^{(R)}(\mathbf{k})\right)\middle| n^{(L)}(\mathbf{k}), n^{(R)}(\mathbf{k})\right\rangle,\end{aligned} \tag{4.4.17}$$

where × represents scalar multiplication. In a monochromatic beam or, equivalently, for each optical mode this result is proportional to the both the helicity and the spatially integrated optical chirality density:

$$\begin{aligned}\left\langle \Gamma^{(+)} \right\rangle - \left\langle \Gamma^{(-)} \right\rangle &\sim \Im \mathrm{m}\left(\boldsymbol{\mu}^{\alpha 0(+)} \cdot \mathbf{m}^{\alpha 0(+)} \right) k \int \partial^3 \mathbf{r}\, \chi \\ &\sim \Im \mathrm{m}\left(\boldsymbol{\mu}^{\alpha 0(+)} \cdot \mathbf{m}^{\alpha 0(+)} \right) kh,\end{aligned} \tag{4.4.18}$$

where h is the helicity operator.

It has been explicitly shown above that the differential rate of absorbing left- and right- handed light by chiral molecules in a single beam is given by a product of $\Im \mathrm{m}\left(\boldsymbol{\mu}^{\alpha 0(+)} \cdot \mathbf{m}^{\alpha 0(+)} \right)$ representing the inherent chirality of the matter, and any of the helicity-type measures displayed in the previous chapter. Therefore, for single beams there is no mechanism by which chiral molecules can differentially absorb light at a rate above (or below) that of pure circularly polarised light.

4.5 Mirrors and Standing Waves

The experimental set-up of Tang and Cohen [57,65], is a normally incident circularly polarised beam reflected by a mirror with the sample of chiral molecules positioned at varying distances from the mirror. They report nodal enhancements to the dissymmetry in left- and right- handed molecule absorption rates. Theoretically this is modelled by counterpropagating beams, one each for the incident and reflected radiation. It is noted that the sign of the **k** vector changes by definition, and the sign of the **j** vector must change to preserve (**E**, **B**, **k**) as a right-handed triad. Therefore, it is readily apparent that $\hat{\mathbf{i}} = \hat{\mathbf{i}}, \hat{\mathbf{j}} = -\hat{\mathbf{j}}, \hat{\mathbf{k}} = -\hat{\mathbf{k}}$. The reflection conserves spin, but the wavevector is reversed; thus the helicity, signifying the projection of the spin onto the direction of propagation, is reversed. The electric field is space-odd, so reverses sign

on reflection, whereas the magnetic field is space-even, so retains its sign. Classically, it is easily shown that the superposition of an incident and reflected beam is a standing wave:

$$\begin{aligned}\mathbf{E}_I(\mathbf{k})+\mathbf{E}_R(-\mathbf{k}) &= \\ &= \frac{1}{\sqrt{2}}\left[\left(\hat{\mathbf{i}}+i\hat{\mathbf{j}}\right)e^{ikz}+\left(\hat{\mathbf{i}}'-i\hat{\mathbf{j}}'\right)e^{-ikz}\right] \\ &= \frac{1}{\sqrt{2}}\left[\left(\hat{\mathbf{i}}+i\hat{\mathbf{j}}\right)e^{ikz}+\left(\hat{\mathbf{i}}+i\hat{\mathbf{j}}\right)e^{-ikz}\right] \\ &= \sqrt{2}\left(\hat{\mathbf{i}}+i\hat{\mathbf{j}}\right)\cos(kz).\end{aligned} \tag{4.5.1}$$

Analysis of Eq. (4.5.1) and the symmetry properties of the optical fields delivers a superposition of the incident and reflected electric fields that has minima and maxima in different locations to the magnetic counterpart, Fig. 4.1. Due to quantum uncertainty, neither the electric nor magnetic field vanishes entirely. The circular differential response of a chiral molecule at this location might exhibit an electronic transition that is both $E1$ and $M1$ (electric dipole and magnetic dipole) allowed with large $E1$-$M1$ interference contributions – the leading-order chiral correction. Moreover, engaging the optical centre with this radiation field can suppress the achiral $E1^2$ absorption rate contribution.

4.6 Circular Dichroism in Counterpropagating Beams

To describe the absorption of a chiral molecule in the vicinity of a partially reflecting surface, we choose to model the radiation as a coherent state, an eigenstate of the annihilation operator:

$$a^{(\eta)}(\mathbf{k})\left|\alpha(\mathbf{k},\eta)\right\rangle = \alpha(\mathbf{k},\eta)\left|\alpha(\mathbf{k},\eta)\right\rangle, \tag{4.6.1}$$

where $\left|\alpha(\mathbf{k},\eta)\right\rangle$ denotes the coherent state with wavevector $\mathbf{k}$ and polarisation η.

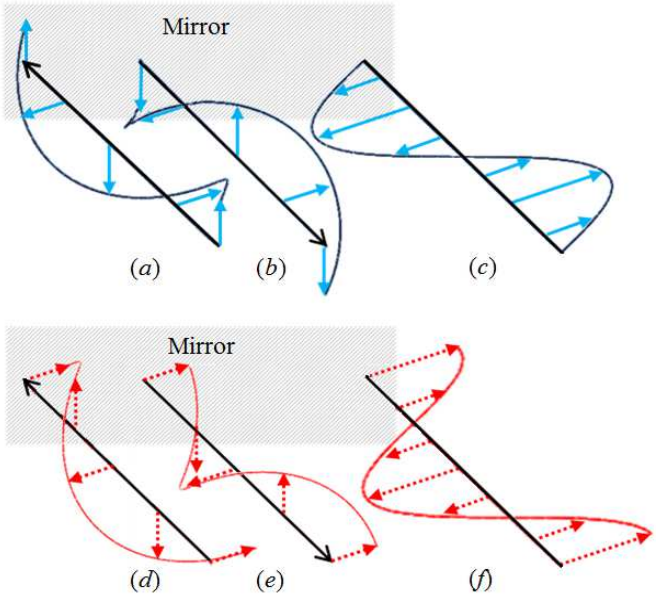

Fig. 4.1. The electric (top) and magnetic (bottom) field vectors of reflected circularly polarized light. The superposition (*c*,*f*) of the input (*a*,*d*) and reflected (*b*,*e*) beams results in states with minima and maxima in different locations for the electric and magnetic fields.

Coherent states model the electromagnetic field when the average population of a mode is large and only describable as a probability distribution (specifically, a Poisson distribution) over a range of occupation numbers. In the limit of large occupation numbers the quantum description of the electromagnetic field is identical to the classical description, in which one can make exact simultaneous measurements of, for example, the phase and amplitude. Coherent states, then, are most like classical states, in which there is minimum uncertainty in the phase and photon

number. In contrast, phase states and number states individually have precisely determined optical phase and photon number, respectively, with the other variable completely unknown [66]. Notably, the expectation value of a coherent state mode with respect to the number operator is the square modulus of the complex number indexing that mode:

$$\left\langle \alpha(\mathbf{k},\eta)\right| \hat{N}(\mathbf{k},\eta)\left|\alpha(\mathbf{k},\eta)\right\rangle = \left|\alpha\right|^2, \tag{4.6.2}$$

and the probability of measuring any given number of photons, n, follows a Poisson distribution with variance of $\left|\alpha\right|^2$ [51]:

$$\left|\left\langle n|\alpha\right\rangle\right|^2 = \frac{\left|\alpha\right|^{2n}}{n!}e^{-|\alpha|^2} = P\left(n;\left|\alpha\right|^2\right). \tag{4.6.3}$$

With this notation, we can characterise the initial state of the total – molecular and radiation parts of – the system:

$$\left|\text{mol}\right\rangle\left|\text{rad}\right\rangle = \left|\psi_0\right\rangle\left|\alpha\left(\mathbf{k},e^{(L)}(\mathbf{k})\right),\alpha'\left(\mathbf{k}',e'^{(R)}(\mathbf{k}')\right)\right\rangle, \tag{4.6.4}$$

where the molecular state is characterised by the wavefunction of the optical centre, the radiation state consists of the incident and reflected radiation, and the reflected wavevectors is given by $\mathbf{k}' = -\mathbf{k}$. Without loss of generality, this model assumes a left-handed input beam, which demands a right-handed reflected beam. Similarly, the final state of the system is given by:

$$|\text{mol}\rangle|\text{rad}\rangle = |\psi_\beta\rangle\left|\alpha\left(\mathbf{k}, e^{(L)}(\mathbf{k})\right), \alpha'\left(\mathbf{k}', e'^{(R)}(\mathbf{k}')\right)\right\rangle, \tag{4.6.5}$$

where represents the molecular excited state, and the radiation state is unchanged by the absorption from either mode. The probability amplitude for the absorption by a molecule in this region is then given by:

$$\begin{aligned} M_{FI} &= \langle\alpha'|\langle\alpha|\langle\psi_\beta|-\boldsymbol{\mu}\cdot\mathbf{e}^{\perp}-\mathbf{m}\cdot\mathbf{b}|\psi_0\rangle|\alpha\rangle|\alpha'\rangle \\ &= -\langle\psi_\beta|\boldsymbol{\mu}|\psi_0\rangle\cdot\langle\alpha|\mathbf{e}^{\perp}|\alpha\rangle\langle\alpha'|\alpha'\rangle - \langle\psi_\beta|\mathbf{m}|\psi_0\rangle\cdot\langle\alpha|\mathbf{b}|\alpha\rangle\langle\alpha'|\alpha'\rangle \\ &\quad -\langle\psi_\beta|\boldsymbol{\mu}|\psi_0\rangle\cdot\langle\alpha'|\mathbf{e}^{\perp}|\alpha'\rangle\langle\alpha|\alpha\rangle - \langle\psi_\beta|\mathbf{m}|\psi_0\rangle\cdot\langle\alpha'|\mathbf{b}|\alpha'\rangle\langle\alpha|\alpha\rangle \\ &\quad -\langle\psi_\beta|\boldsymbol{\mu}|\psi_0\rangle\cdot\langle\alpha|\mathbf{e}^{\perp}|\alpha'\rangle\langle\alpha|\alpha'\rangle - \langle\psi_\beta|\mathbf{m}|\psi_0\rangle\cdot\langle\alpha|\mathbf{b}|\alpha'\rangle\langle\alpha|\alpha'\rangle \\ &\quad -\langle\psi_\beta|\boldsymbol{\mu}|\psi_0\rangle\cdot\langle\alpha'|\mathbf{e}^{\perp}|\alpha\rangle\langle\alpha'|\alpha\rangle - \langle\psi_\beta|\mathbf{m}|\psi_0\rangle\cdot\langle\alpha'|\mathbf{b}|\alpha\rangle\langle\alpha'|\alpha\rangle. \end{aligned} \tag{4.6.6}$$

However, to model the partial reflection of the mirror the expectation value of incident coherent state $|\alpha|^2$ is assumed to be much larger than that of the reflected state $|\alpha'|^2$ so that the overlap,

$$\langle\alpha'|\alpha\rangle = e^{-1/2\left(|\alpha|^2+|\alpha'|^2-2\alpha\alpha'\right)} \approx 0, \tag{4.6.7}$$

is approximately zero. Then the probability amplitude can be simplified to:

$$\begin{aligned} M_{FI} &= -\boldsymbol{\mu}^{\beta 0}\cdot\langle\alpha|\mathbf{e}^{\perp}|\alpha\rangle - \mathbf{m}^{\beta 0}\cdot\langle\alpha|\mathbf{b}|\alpha\rangle \\ &\quad -\boldsymbol{\mu}^{\beta 0}\cdot\langle\alpha'|\mathbf{e}^{\perp}|\alpha'\rangle - \mathbf{m}^{\beta 0}\cdot\langle\alpha'|\mathbf{b}|\alpha'\rangle \\ &= M_{FI}(\alpha) + M_{FI}(\alpha'). \end{aligned} \tag{4.6.8}$$

To identify the differential rate of absorption, we calculate the square modulus of this expression with both left- and right- handed molecules. Again, using subscripts so that terms can be tackled individually, the probability is given by:

$$\begin{aligned}\left|M_{FI}^{(+/-)}\right|^2 &= \left|M_{FI}(\alpha)+M_{FI}(\alpha')\right|^2 \\ &= \left|M_{FI}(\alpha)\right|^2_{(1)} + \left|M_{FI}(\alpha')\right|^2_{(2)} \\ &\quad +2\Re e\left\{M_{FI}(\alpha)\overline{M_{FI}(\alpha')}\right\}_{(3)},\end{aligned} \tag{4.6.9}$$

As with the single beam case, the electric and magnetic transition dipole moments can be calculated computationally, so it remains to calculate the following four terms:

$$\begin{matrix}\langle\alpha|\mathbf{e}^{\perp}|\alpha\rangle & \langle\alpha|\mathbf{b}|\alpha\rangle \\ \langle\alpha'|\mathbf{e}^{\perp}|\alpha'\rangle & \langle\alpha'|\mathbf{b}|\alpha'\rangle\end{matrix}. \tag{4.6.10}$$

Since we are calculating the rate of absorption, we enact the expectation values of the fields, where only the annihilation term contributes:

$$\begin{aligned}\langle\alpha|\mathbf{e}^{\perp}|\alpha\rangle &= \langle\alpha|i\left(\frac{\hbar ck}{2\varepsilon_0 V}\right)^{1/2}\mathbf{e}^{(L)}(\mathbf{k})e^{i\mathbf{k}\cdot\mathbf{r}}a^{(L)}(\mathbf{k})|\alpha\rangle \\ &= \langle\alpha|\alpha\rangle\int_V \partial^3\mathbf{r}\, i\alpha\left(\frac{\hbar ck}{2\varepsilon_0 V}\right)^{1/2}\mathbf{e}^{(L)}(\mathbf{k})e^{i\mathbf{k}\cdot\mathbf{r}} \\ &= \int_V \partial^3\mathbf{r}\, i\alpha\left(\frac{\hbar ck}{2\varepsilon_0 V}\right)^{1/2}\mathbf{e}^{(L)}(\mathbf{k})e^{i\mathbf{k}\cdot\mathbf{r}}.\end{aligned} \tag{4.6.11}$$

Here, only a plane wave representation of the fields has been used, as using a Laguerre-Gaussian description does not change the final result: no orbital angular momentum is transferred to the mirror. This is true for normally reflecting mirrors,

however a phase conjugate mirror can be constructed, where incident light with orbital angular momentum is converted to light with opposite handedness. This means that $2l$ units of orbital angular momentum is transferred to the mirror, and a phonon is created that propagates into the mirror. For the present purposes, we assume no orbital angular momentum is transferred to the mirror. Similarly, for the other terms of Eq. (4.6.10), we have that:

$$\begin{aligned}
\langle \alpha' | \mathbf{e}^{\perp} | \alpha' \rangle &= \int_V \partial^3 \mathbf{r}\, i\alpha' \left(\frac{\hbar c k}{2\varepsilon_0 V} \right)^{1/2} \mathbf{e}'^{(R)}(\mathbf{k}') e^{i\mathbf{k}'\cdot\mathbf{r}} \\
\langle \alpha | \mathbf{b} | \alpha \rangle &= \int_V \partial^3 \mathbf{r}\, i\alpha \left(\frac{\hbar k}{2\varepsilon_0 c V} \right)^{1/2} \mathbf{b}^{(L)}(\mathbf{k}) e^{i\mathbf{k}\cdot\mathbf{r}} \\
\langle \alpha' | \mathbf{b} | \alpha' \rangle &= \int_V \partial^3 \mathbf{r}\, i\alpha' \left(\frac{\hbar k}{2\varepsilon_0 c V} \right)^{1/2} \mathbf{b}'^{(R)}(\mathbf{k}') e^{i\mathbf{k}'\cdot\mathbf{r}}.
\end{aligned} \tag{4.6.12}$$

First, we take term (1) from Eq. (4.6.9):

$$\begin{aligned}
\left| M_{FI}^{(+/-)}(\alpha) \right|^2 &= \left(-\mu_i^{\beta 0} \cdot \langle \alpha | e_i^{\perp} | \alpha \rangle - m_i^{\beta 0} \cdot \langle \alpha | b_i | \alpha \rangle \right) \\
&\quad \cdot \left(-\overline{\mu}_j^{\beta 0} \cdot \overline{\langle \alpha | e_j^{\perp} | \alpha \rangle} - \overline{m}_j^{\beta 0} \cdot \overline{\langle \alpha | b_j | \alpha \rangle} \right) \\
&= \left(\mu_i^{\beta 0} \overline{\mu}_j^{\beta 0} \langle \alpha | e_i^{\perp} | \alpha \rangle \overline{\langle \alpha | e_j^{\perp} | \alpha \rangle} + \mu_i^{\beta 0} \overline{m}_j^{\beta 0} \langle \alpha | e_i^{\perp} | \alpha \rangle \overline{\langle \alpha | b_j | \alpha \rangle} \right) \\
&\quad + \left(m_i^{\beta 0} \overline{\mu}_j^{\beta 0} \langle \alpha | b_i | \alpha \rangle \overline{\langle \alpha | e_j^{\perp} | \alpha \rangle} + m_i^{\beta 0} \overline{m}_j^{\beta 0} \langle \alpha | b_i | \alpha \rangle \overline{\langle \alpha | b_j | \alpha \rangle} \right),
\end{aligned} \tag{4.6.13}$$

where the overbar represents complex conjugation. Then, using the calculations of the Dirac bra-kets from Eq. (4.6.11) and (4.6.12), we obtain:

$$\begin{aligned}\left|M_{FI}^{(+/-)}(\alpha)\right|^2 &= \mu_i^{\beta 0(+/-)}\mu_j^{\beta 0(+/-)}|\alpha|^2\left(\frac{\hbar ck}{2\varepsilon_0}\right)e_i^{(L)}(\mathbf{k})\bar{e}_j^{(L)}(\mathbf{k}) \\ &+m_i^{\beta 0(+/-)}\bar{m}_j^{\beta 0(+/-)}|\alpha|^2\left(\frac{\hbar k}{2\varepsilon_0 c}\right)b_i^{(L)}(\mathbf{k})\bar{b}_j^{(L)}(\mathbf{k}) \\ &+\mu_i^{\beta 0(+/-)}\bar{m}_j^{\beta 0(+/-)}|\alpha|^2\left(\frac{\hbar k}{2\varepsilon_0}\right)e_i^{(L)}(\mathbf{k})\bar{b}_j^{(L)}(\mathbf{k}) \\ &+m_i^{\beta 0(+/-)}\bar{\mu}_j^{\beta 0(+/-)}|\alpha|^2\left(\frac{\hbar k}{2\varepsilon_0}\right)b_i^{(L)}(\mathbf{k})\bar{e}_j^{(L)}(\mathbf{k}),\end{aligned} \tag{4.6.14}$$

where the electric and magnetic polarisation vectors possess all of the vector character of the electromagnetic fields, and thus display the index notation. The quantisation volume has been removed by box normalisation. Furthermore, by Appendix C and our arguments in section 4.5., we have that:

$$\begin{aligned}b^{(L)} &= -ie^{(L)} \quad b^{(R)} = ie^{(R)} \\ e^{(L)} &= -e'^{(R)} \quad e^{(R)} = -e'^{(L)}\end{aligned}, \tag{4.6.15}$$

where the reflected polarisation vectors are denoted by primed characters. With this notation Eq. (4.6.14) becomes:

$$\begin{aligned}\left|M_{FI}^{(+/-)}(\alpha)\right|^2 &= \mu_i^{\beta 0(+/-)}\mu_j^{\beta 0(+/-)}|\alpha|^2\left(\frac{\hbar ck}{2\varepsilon_0}\right)e_i^{(L)}e_j^{(R)} \\ &+m_i^{\beta 0(+/-)}\bar{m}_j^{\beta 0(+/-)}|\alpha|^2\left(\frac{\hbar k}{2\varepsilon_0 c}\right)e_i^{(L)}e_j^{(R)} \\ &-i\mu_i^{\beta 0(+/-)}m_j^{\beta 0(+/-)}|\alpha|^2\left(\frac{\hbar k}{2\varepsilon_0}\right)e_i^{(L)}e_j^{(R)} \\ &-im_i^{\beta 0(+/-)}\mu_j^{\beta 0(+/-)}|\alpha|^2\left(\frac{\hbar k}{2\varepsilon_0}\right)e_i^{(L)}e_j^{(R)},\end{aligned} \tag{4.6.16}$$

which, by Eq. (4.6.2), is:

$$\left|M_{FI}^{(+/-)}(\alpha)\right|^2 = \left(\frac{\hbar k}{2\varepsilon_0}\right) e_i^{(L)} e_j^{(R)} \overline{n}_L \times \left\{ c\mu_i^{\beta 0(+/-)} \mu_j^{\beta 0(+/-)} + \frac{1}{c} m_i^{\beta 0(+/-)} \overline{m}_j^{\beta 0(+/-)} - i\mu_i^{\beta 0(+/-)} m_j^{\beta 0(+/-)} - i m_i^{\beta 0(+/-)} \mu_j^{\beta 0(+/-)} \right\}, \tag{4.6.17}$$

where $\overline{n}_L$ denotes the expected number of left-handed photons and × represents scalar multiplication. By identical analysis term (2) of Eq. (4.6.9) is delivered as:

$$\left|M_{FI}^{(+/-)}(\alpha')\right|^2 = \left(\frac{\hbar k}{2\varepsilon_0}\right) e_i^{(L)} e_j^{(R)} \overline{n}_R' \times \left\{ c\mu_i^{\beta 0(+/-)} \mu_j^{\beta 0(+/-)} + \frac{1}{c} m_i^{\beta 0(+/-)} \overline{m}_j^{\beta 0(+/-)} + i\mu_i^{\beta 0(+/-)} m_j^{\beta 0(+/-)} + i m_i^{\beta 0(+/-)} \mu_j^{\beta 0(+/-)} \right\}. \tag{4.6.18}$$

The change in sign of the *E*1-*M*1 interference terms comes as a result of the changed handedness of the radiation. The interference term between the input and emergent radiation – term (3) of Eq. (4.6.9) – is similarly calculated as:

$$\begin{aligned} & 2\Re e\left\{ M_{FI}(\alpha) \overline{M_{FI}(\alpha')} \right\} \\ & = 2\Re e\left\{ \left(-\mu_i^{\beta 0} \cdot \langle \alpha | e_i^{\perp} | \alpha \rangle - m_i^{\beta 0} \cdot \langle \alpha | b_i | \alpha \rangle \right) \right. \\ & \quad \left. \cdot \left(-\overline{\mu}_j^{\beta 0} \cdot \overline{\langle \alpha' | e_j^{\perp} | \alpha' \rangle} - \overline{m}_j^{\beta 0} \cdot \overline{\langle \alpha' | b_j | \alpha' \rangle} \right) \right\} \\ & = 2\Re e \int_V \partial^3 \mathbf{r} \left\{ \mu_i^{\beta 0} \mu_j^{\beta 0} \langle \alpha | e_i^{\perp} | \alpha \rangle \overline{\langle \alpha' | e_j^{\perp} | \alpha' \rangle} + 2\mu_i^{\beta 0} \overline{m}_j^{\beta 0} \langle \alpha | e_i^{\perp} | \alpha \rangle \overline{\langle \alpha' | b_j | \alpha' \rangle} \right. \\ & \quad \left. + 2 m_i^{\beta 0} \mu_j^{\beta 0} \langle \alpha | b_i | \alpha \rangle \overline{\langle \alpha' | e_j^{\perp} | \alpha' \rangle} + 2 m_i^{\beta 0} \overline{m}_j^{\beta 0} \langle \alpha | b_i | \alpha \rangle \overline{\langle \alpha' | b_j | \alpha' \rangle} \right\}. \end{aligned} \tag{4.6.19}$$

Once again, we substitute the quantum electrodynamic mode expansions from Eq. (4.6.11) and (4.6.12), to obtain:

$$
\begin{aligned}
2\Re e\left\{M_{FI}(\alpha)\overline{M_{FI}(\alpha')}\right\} = 2\Re e\int_V \partial^3\mathbf{r}\,\Bigg\{ & \mu_i^{\beta 0}\mu_j^{\beta 0}\alpha\alpha'\left(\frac{\hbar ck}{2\varepsilon_0 V}\right)e_i^{(L)}\overline{e}_j'^{(R)}e^{i(\mathbf{k}-\mathbf{k}')\cdot\mathbf{r}} \\
& + 2\mu_i^{\beta 0}\overline{m}_j^{\beta 0}\alpha\alpha'\left(\frac{\hbar k}{2\varepsilon_0 V}\right)e_i^{(L)}\overline{b}_j'^{(R)}e^{i(\mathbf{k}-\mathbf{k}')\cdot\mathbf{r}} \\
& + 2m_i^{\beta 0}\mu_j^{\beta 0}\alpha\alpha'\left(\frac{\hbar k}{2\varepsilon_0 V}\right)b_i^{(L)}\overline{e}_j'^{(R)}e^{i(\mathbf{k}-\mathbf{k}')\cdot\mathbf{r}} \\
& + 2m_i^{\beta 0}\overline{m}_j^{\beta 0}\alpha\alpha'\left(\frac{\hbar k}{2\varepsilon_0 cV}\right)b_i^{(L)}\overline{b}_j'^{(R)}e^{i(\mathbf{k}-\mathbf{k}')\cdot\mathbf{r}}\Bigg\}.
\end{aligned}
\tag{4.6.20}
$$

To remove the quantisation volume, we set the z-axis as the direction normal to the mirror so that:

$$
\begin{aligned}
\int_V \partial^3\mathbf{r}\,e^{i(\mathbf{k}-\mathbf{k}')\cdot\mathbf{r}} &= \int_V \partial^3\mathbf{r}\,e^{i(k_x-k_x')x+i(k_y-k_y')y+i(k_z-k_z')z} \\
&= e^{2ik_z z}\int_V \partial^3\mathbf{r}\,e^{i(k_x-k_x')x+i(k_y-k_y')y} \\
&= \begin{cases} Ve^{2ik_z z} \text{ for } k_x = k_x';\ k_y = k_y' \\ 0 \qquad \text{Otherwise.} \end{cases}
\end{aligned}
\tag{4.6.21}
$$

As mentioned above, the probability of a given number state occurring in a coherent state follows a Poisson distribution, thus:

$$
\begin{aligned}
\left\langle\alpha\left|\hat{N}^2\right|\alpha\right\rangle &= \left\langle\alpha\left|a^\dagger aa^\dagger a\right|\alpha\right\rangle = |\alpha|^2\left\langle\alpha\left|aa^\dagger\right|\alpha\right\rangle \\
&= |\alpha|^2\left\langle\alpha\left|a^\dagger a+1\right|\alpha\right\rangle = |\alpha|^4 + |\alpha|^2 .
\end{aligned}
\tag{4.6.22}
$$

Furthermore, the uncertainty in the precise occupation number is given by:

$$\begin{aligned}\Delta n &= \left\{\left\langle\alpha\right|\hat{N}^2\left|\alpha\right\rangle - \left\langle\alpha\right|\hat{N}\left|\alpha\right\rangle^2\right\}^{\frac{1}{2}} \\ &= \left\{|\alpha|^4 + |\alpha|^2 - |\alpha|^4\right\}^{\frac{1}{2}} \\ &= |\alpha|.\end{aligned} \tag{4.6.23}$$

Then we may rewrite Eq. (4.6.19) as:

$$\begin{aligned}&2\Re e\left\{M_{fi}(\alpha)\overline{M_{fi}(\alpha')}\right\} = \\ &= 2\Re e\left\{-\mu_i^{\beta 0}\mu_j^{\beta 0}\alpha\alpha'\left(\frac{\hbar ck}{2\varepsilon_0}\right)e_i^{(L)}e_j^{(R)}e^{2ik_z z} + 2i\mu_i^{\beta 0}\overline{m}_j^{\beta 0}\alpha\alpha'\left(\frac{\hbar k}{2\varepsilon_0}\right)e_i^{(L)}e_j^{(R)}e^{2ik_z z}\right. \\ &\left. +2im_i^{\beta 0}\mu_j^{\beta 0}\alpha\alpha'\left(\frac{\hbar k}{2\varepsilon_0}\right)e_i^{(L)}e_j^{(R)}e^{2ik_z z} + 2m_i^{\beta 0}\overline{m}_j^{\beta 0}\alpha\alpha'\left(\frac{\hbar k}{2\varepsilon_0 c}\right)e_i^{(L)}e_j^{(R)}e^{2ik_z z}\right\} \\ &= -\Re e\left\{\Delta n_L\Delta n_R'\left(\frac{\hbar k}{\varepsilon_0}\right)e_i^{(L)}e_j^{(R)}e^{2ik_z z}\times\right. \\ &\left.\left(c\mu_i^{\beta 0}\mu_j^{\beta 0} - \frac{1}{c}m_i^{\beta 0}\overline{m}_j^{\beta 0} - i\mu_i^{\beta 0}\overline{m}_j^{\beta 0} - im_i^{\beta 0}\mu_j^{\beta 0}\right)\right\}\end{aligned} \tag{4.6.24}$$

Thus, combining all terms of Eq. (4.6.9), delivers:

$$\begin{aligned}&\left|M_{FI}^{(+/-)}\right|^2 = \left(\frac{\hbar k}{2\varepsilon_0}\right)e_i^{(L)}e_j^{(R)}\times \\ &\left\{\overline{n}_L\left(c\mu_i^{\beta 0(+/-)}\mu_j^{\beta 0(+/-)} + \frac{1}{c}m_i^{\beta 0(+/-)}\overline{m}_j^{\beta 0(+/-)} - i\mu_i^{\beta 0(+/-)}m_j^{\beta 0(+/-)} - im_i^{\beta 0(+/-)}\mu_j^{\beta 0(+/-)}\right)\right. \\ &\left.+\overline{n}_R'\left(c\mu_i^{\beta 0(+/-)}\mu_j^{\beta 0(+/-)} + \frac{1}{c}m_i^{\beta 0(+/-)}\overline{m}_j^{\beta 0(+/-)} + i\mu_i^{\beta 0(+/-)}m_j^{\beta 0(+/-)} + im_i^{\beta 0(+/-)}\mu_j^{\beta 0(+/-)}\right)\right. \\ &\left.-2\Delta n_L\Delta n_R' e^{2ik_z z}\times\right. \\ &\left.\left(c\mu_i^{\beta 0(+/-)}\mu_j^{\beta 0(+/-)} - \frac{1}{c}m_i^{\beta 0(+/-)}\overline{m}_j^{\beta 0(+/-)} - i\mu_i^{\beta 0(+/-)}\overline{m}_j^{\beta 0(+/-)} - im_i^{\beta 0(+/-)}\mu_j^{\beta 0(+/-)}\right)\right\}\end{aligned} \tag{4.6.25}$$

As with the single beam case, it is known that the electric and magnetic transition dipole moments can be chosen to be purely real and purely imaginary, respectively, so that they satisfy Eq. (4.4.14). We can now obtain the difference in probability amplitudes for left- and right- handed molecules in the region close to a partially reflecting mirror:

$$\left|M_{fi}^{(+)}\right|^2-\left|M_{fi}^{(-)}\right|^2= \Re e\left\{\left(\frac{\hbar k}{2\varepsilon_0}\right)e_i^{(L)}(\mathbf{k})e_j^{(R)}(\mathbf{k})\left(i\mu_i^{\beta 0(+)}m_j^{\beta 0(+)}+im_i^{\beta 0(+)}\mu_j^{\beta 0(+)}\right)\left(\overline{n}_R{}'-\overline{n}_L\right)\right. \\ \left.+\left(i\mu_i^{\beta 0(+)}m_j^{\beta 0(+)}-im_i^{\beta 0(+)}\mu_j^{\beta 0(+)}\right)\left(2\Delta n_L\Delta n_R' e^{2ik_z z}\right)\right\}. \tag{4.6.26}$$

Adhering to basic symmetry constraints equation Eq. (4.6.26) changes sign under parity inversion, equivalent to swapping the handedness of the input radiation, $L\leftrightarrow R$. Acknowledging the imaginary character of the magnetic dipole moment, we set:

$$m=iM;\qquad M\in\Re \tag{4.6.27}$$

which gives us the prescription that $im\rightarrow -M$. Applying this condition and contracting the vector indices delivers:

$$\left|M_{FI}^{(+)}\right|^2-\left|M_{FI}^{(-)}\right|^2=\left(\frac{\hbar k}{\varepsilon_0}\right)\left\{\left[\mu_x^{\beta 0(+)}M_x^{\beta 0(+)}+\mu_y^{\beta 0(+)}M_y^{\beta 0(+)}\right]\left(\overline{n}_L-\overline{n}_R'\right)\right. \\ \left.+2\Re e\left[\mu_x^{\beta 0(+)}M_y^{\beta 0(+)}-\mu_y^{\beta 0(+)}M_x^{\beta 0(+)}\right]\Delta n_L\Delta n_R' e^{2ik_z z}\right\}. \tag{4.6.28}$$

Finally, converting the exponential to trigonometric form allows us to explicitly obtain the real part of the expression:

$$\left|M_{FI}^{(+)}\right|^2-\left|M_{FI}^{(-)}\right|^2=\left(\frac{\hbar k}{\varepsilon_0}\right)\left\{\left[\mu_x^{\beta 0(+)}M_x^{\beta 0(+)}+\mu_y^{\beta 0(+)}M_y^{\beta 0(+)}\right]\left(\bar{n}_L-\bar{n}_R'\right)\right.$$
$$\left.+2\left[\mu_x^{\beta 0(+)}M_y^{\beta 0(+)}-\mu_y^{\beta 0(+)}M_x^{\beta 0(+)}\right]\Delta n_L\Delta n_R'\cos\left(2k_z z\right)\right\}. \tag{4.6.29}$$

Thus, it can be seen that if the distance between the mirror and the absorber is $z=(2n+1)\pi/4k_z$, then the interference term will become zero and the resulting expression is identical to the single beam case:

$$\left|M_{FI}^{(+)}\right|^2-\left|M_{FI}^{(-)}\right|^2=\left(\frac{\hbar k}{\varepsilon_0}\right)\left[\mu_x^{\beta 0(+)}M_x^{\beta 0(+)}+\mu_y^{\beta 0(+)}M_y^{\beta 0(+)}\right]\left(\bar{n}_L-\bar{n}_R'\right), \tag{4.6.30}$$

where the link with the helicity and chirality measures from the previous is apparent through the appearance of the difference in occupation numbers for modes of opposing helicity. Precisely, there are three features of the system that will cause this interference term to vanish. Firstly, if the cosine function returns a zero result, then the interference term vanishes. This signifies regions where the electric field of one beam is parallel or antiparallel to the magnetic field of the other, Fig. 4.2. In this case, the interference of the two beams will have mirror symmetry in the plane containing the direction of propagation and the two, now parallel, field vectors; thus there is no three-dimensional basis for engaging molecular chirality, except by the helicity of the individual beams. Secondly, if the molecule has transverse components of the electric and magnetic dipoles related by:

$$\frac{\mu_x^{\beta 0(+)}}{\mu_y^{\beta 0(+)}} = \frac{M_y^{\beta 0(+)}}{M_x^{\beta 0(+)}}, \tag{4.6.31}$$

then the interference term vanishes. Finally, taking an isotropic rotational average of Eq. (4.6.29) delivers a zero results for the interference term, corresponding to the conditions of a freely rotating sample in a fluid. Of course, if the uncertainty in photon number, in either beam, is zero, then the rate of circular dichroism is identical to that for precisely determined number states.

4.7 Analysis of Recent Experiments

In the experiment by Tang and Cohen, they observe nodal enhancements in the dissymmetry of circularly polarised absorption, which corresponds precisely to the sinusoidal distance dependence term in Eq. (4.6.29) [57]. Furthermore, they note that "The energy density in the dim regions is so small that shot noise begins to drown out the signal. The more we enhance the dissymmetry, the noisier the signal". By setting the electric and magnetic transition dipoles to unity in Eq. (4.6.29), the ratio of the two terms becomes:

$$\begin{aligned} \frac{M_{FI}^{CD}}{M_{FI}^{INTER}} &\sim \frac{\left(\bar{n}_L - \bar{n}'_R\right)}{\Delta n_L \Delta n'_R} \\ &= \frac{\sqrt{|\alpha|^2}}{\Delta n'_R} + \frac{\sqrt{|\alpha'|^2}}{\Delta n_L}, \end{aligned} \tag{4.7.1}$$

which is the sum of the signal-to-noise ratios for the incident and reflected beams, weighted by the uncertainty in photon population for the opposing beam [67]. Thus, the enhancements in circular differential response, for this experimental set-up,

display a connection with the phase-photon number uncertainty relation, and seem only explicable in terms of a quantised electromagnetic field.

Using a quantised field representation, we have shown that circular dichroism responds only to the polarisation state of the radiation and does not engage the optical orbital angular momentum. It was shown that Eq. (4.6.29), corresponding to Tang and Cohen's recent experiment, has two terms: one with characteristic dependence on photon occupation numbers for modes of opposing helicity, and one with a sinusoidal dependence on distance from the mirror. Importantly, the nodal positions for the $E1$-$M1$ interference term do not coincide with the positions at which the electric field vanishes (within the limits quantum uncertainty). Thus, there are distances from the mirror where the normally dominant achiral $E1^2$ contribution to the absorption rate is suppressed and the chiral $E1$-$M1$ contribution is large, Fig. 4.2. Due to the manifestly discrete nature of the electromagnetic field at low intensities, this displays a relation with the uncertainties in the Poisson-distributed photon occupation number, and, moreover, the signal-to-noise ratio, Eq. (4.7.1). To summarise, it is proven that although there are certainly nodal enhancements (or reductions) in the differential absorption rate, the effect is a result of beam superposition, and does not support the existence of "superchiral light".

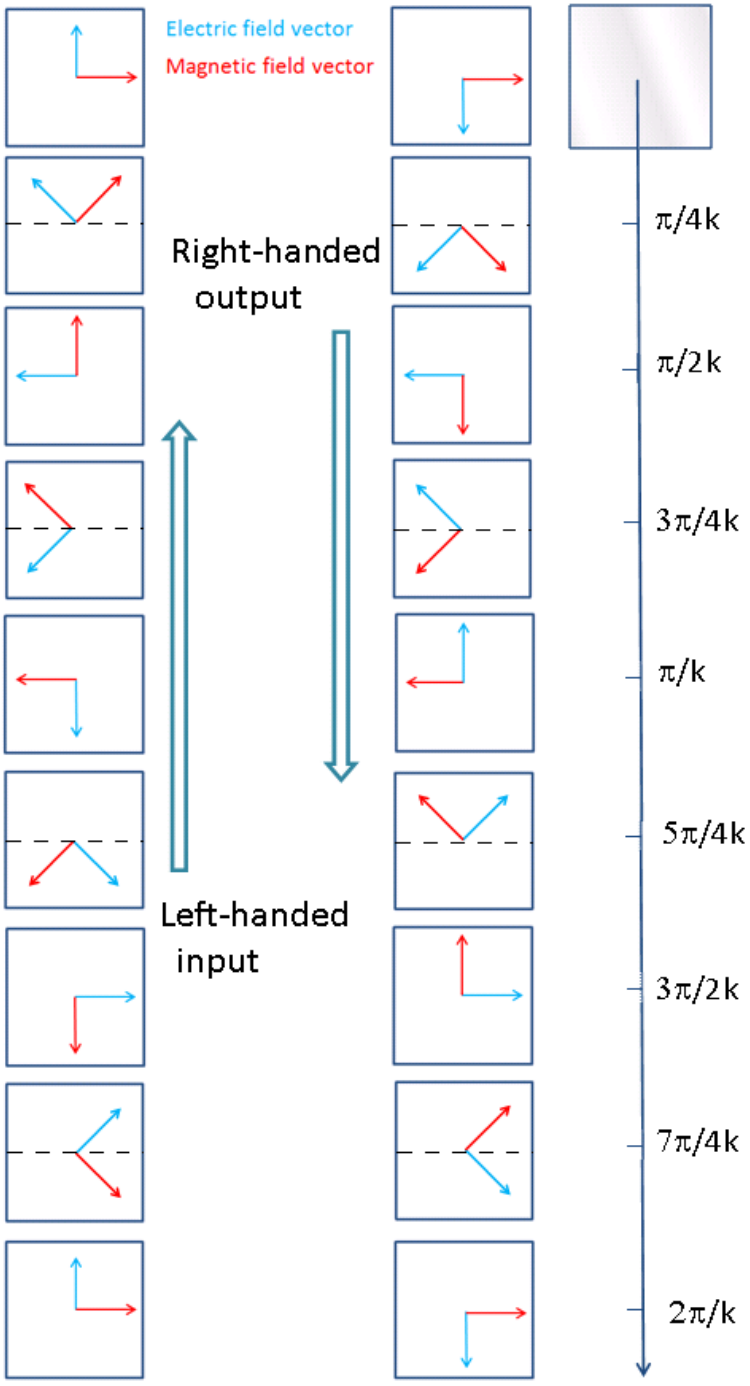

Fig. 4.2. The electric and magnetic field vectors of reflected circularly polarized light. Noted are the positions where the alignment of the electric and magnetic field vectors of different beams forbids the interaction of the chiral molecules with the interference of the circularly polarised beams. The dotted lines show the lines of mirror symmetry responsible for the forbidden chiral interactions.

Kadodwala et al. recently provided experimental results that were interpreted as verifying the capability of the optical chirality density to identify regions of enhanced

chiral dissymmetry. They used left- and right- handed gold gammadions (swastikas) of length 400 nm and thickness 100 nm, with a 5-nm chromium adhesion layer, deposited on a glass substrate with a periodicity of 800 nm. Using UV-visible circular dichroism spectroscopy the optical properties of these planar chiral metamaterials were probed under various liquids, and resonances in the CD spectra, associated with the excitation of localized surface plasmon resonances, were observed. It is well known that surface plasmons amplify local electric fields in systems fabricated with a metal substrate [68]. In these situations, both conventional optical and chiroptical response will exhibit much larger than usual effects [69–72]. In support of their conclusions, Kadodwala et al. exhibited the results of calculating both the electric field strengths and the corresponding value of the optical chirality around the PCM [58].

It is possible to generate optical states of more chiral character, through the involvement of orbital angular momentum. However, these additional contributions have no effect on internal dipole transitions and cannot be measured by spectroscopic means [13,16]. Instead, the orbital angular momentum is observable through mechanical rather than chiroptical effects. The possibility of engaging the orbital angular momentum of light through spin-orbit coupling in nanostructures has not been considered here [73].

4.8 Six-Wave Mixing of Optical Vortices

Second harmonic generation is normally forbidden in isotropic media [74,75]. This is due to the process being dependant on an even-order optical susceptibility, which gives vanishing values for the Fermi rate after performing an isotropic rotational average. Theoretical predictions by Allcock and Andrews have shown that engaging odd-order susceptibilities, corresponding to an even number of light-matter interactions, allows a six-wave mixing process, in which four pump photons are converted into two second harmonic output photons [76]. It emerges that the harmonic photons are generated on opposite sides of an output cone, where wave-vector matching is achieved. This principle has been displayed experimentally with third-harmonic generation in a sapphire crystal, with conical output angle ~10° [77].

In this section it is shown that by considering a pump with a predetermined amount of orbital angular momentum per photon, the conservation of both linear and angular momentum allows for more than one output possibility. Precisely, there are four input photons, each with $l = 1$ units of orbital angular momentum; upon interaction with nonlinear optical matter, two output photons are created with double the frequency of the input photons. There are now three possible configurations of orbital angular momentum, assuming conservation: (2,2), (3,1) and (4,0). The allowed pairs of output photons indicates quantum entanglement of the orbital angular momentum degree of freedom, as has been observed in recent experimental studies [78,79]. It is the topic of on-going investigation, whether similar effects can be anticipated from input photons of varying l and p numbers.

To begin, the leading order term in the probability amplitude for the process is obtain from sixth order perturbation theory, Eq. (1.9.25):

$$M_{FI} \sim \sum_{R,S,T,U,V} \frac{\langle F|H_{\text{int}}|V\rangle\langle V|H_{\text{int}}|U\rangle\langle U|H_{\text{int}}|T\rangle\langle T|H_{\text{int}}|S\rangle\langle S|H_{\text{int}}|R\rangle\langle R|H_{\text{int}}|I\rangle}{(E_I-E_R)(E_I-E_S)(E_I-E_T)(E_I-E_U)(E_I-E_V)}, \quad (4.8.1)$$

where I, F denote the initial and final system states, and R, S, T, U, V denote virtual intermediate states to be summed over. In the following model, parameters are chosen to simulate an 800 nm wavelength laser focussed onto the conversion material. The output angle of the emergent radiation is determined by the wave vector matching condition, Fig 4.C. Simply, the sum of the wavevectors of the emergent radiation

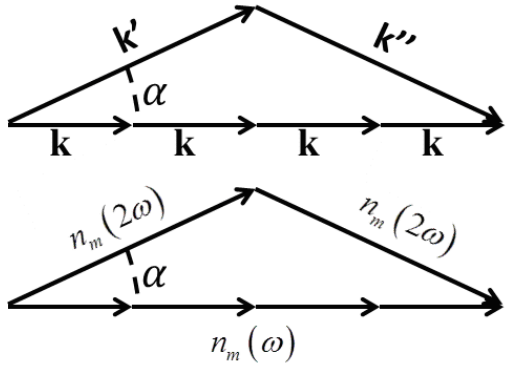

Fig. 4.3. Visual representation of the wavevector matching condition and its relation to the refractive index of the conversion material for a photon of frequency ω and a harmonic photon of frequency 2ω.

should match the sum of the input wavevectors:

$$4\mathbf{k} = \mathbf{k}' + \mathbf{k}''. \quad (4.8.2)$$

The speed of light in a medium, m, is reduced by a factor of the refractive index in

that medium, thus:

$$\begin{aligned} 4n_m(\omega)\frac{\omega}{c}\hat{\mathbf{k}} &= n_m(2\omega)\frac{2\omega}{c}\hat{\mathbf{k}}' + n_m(2\omega)\frac{2\omega}{c}\hat{\mathbf{k}}'' \\ 2n_m(\omega)\hat{\mathbf{k}} &= n_m(2\omega)\hat{\mathbf{k}}' + n_m(2\omega)\hat{\mathbf{k}}''. \end{aligned} \tag{4.8.3}$$

Furthermore, we can now obtain the conical angle α as:

$$\cos\alpha = \frac{n_m(\omega)}{n_m(2\omega)}, \tag{4.8.4}$$

which, from Fig. 4.3. implies that:

$$k' = k'' = \frac{2n_m(2\omega)}{n_m(\omega)}k. \tag{4.8.5}$$

In the experiments performed by Boyd *et al*. the conical angle was angle ~10°, which is consistent with the paraxial approximation to within 1%. This implies that the ratio of refractive indices, Eq. (4.8.4), is ~0.98. Thus, it is now possible to use, within the electric dipole approximation, the paraxial quantum electrodynamic interaction Hamiltonian with Eq. (4.8.1), to obtain:

$$M_{FI} \sim \underbrace{-\left(\frac{\hbar c}{2\varepsilon_0 V}\right)^3 (k)^2 (k'k'')^{\frac{1}{2}} (n)^{\frac{1}{2}} (n-1)^{\frac{1}{2}} (n-2)^{\frac{1}{2}} (n-3)^{\frac{1}{2}} \times}_{(1)}$$
$$\underbrace{\left[\mathbf{e}_{l_i,p_i}^{(\eta_i)}(\mathbf{k})\right]^{\hat{4}} \overline{\mathbf{e}}_{l_{f1},p_{f1}}^{(\eta_{f1})}(\mathbf{k}') \overline{\mathbf{e}}_{l_{f2},p_{f2}}^{(\eta_{f2})}(\mathbf{k}'') \chi^{(5)}_{(ij)(klmn)}}_{(2)} \times \tag{4.8.6}$$
$$\underbrace{\left[f_{l_i,p_i}(r)\right]^4 \overline{f}_{l_{f1},p_{f1}}(r') \overline{f}_{l_{f2},p_{f2}}(r'')}_{(3)} \underbrace{e^{i\left(4\mathbf{k}-\mathbf{k}'-\mathbf{k}''\right)\cdot\mathbf{r}-i\left(4l_i\varphi-l_{f1}\varphi'-l_{f2}\varphi''\right)}}_{(4)},$$

where × represents scalar multiplication and the numbering has been introduced so that terms can be tackled individually. The subscript *i* refers to the input photons and the subscripts f_1, f_2 denote the emergent harmonic photons. Term (1) can be simplified to:

$$-\left(\frac{\hbar c}{2\varepsilon_0}\right)^3 \frac{1}{V} (k)^3 \frac{2n_m(2\omega)}{n_m(\omega)} \frac{\sqrt{n}\sqrt{n-1}\sqrt{n-2}\sqrt{n-3}}{V^2}$$
$$\sim -\frac{1}{4}\left(\frac{1}{\varepsilon_0}\right)^3 \hbar c k \frac{1}{V} \frac{n_m(2\omega)}{n_m(\omega)} \sqrt{g^{(4)}}\, \overline{I}^2, \tag{4.8.7}$$

where, to relate to experiment, *I* is the irradiance and $g^{(4)}$ is the degree of fourth-order coherence. Analysis of term (2) of the probability amplitude has been performed by Williams and shows the non-zero value of an isotropic rotational average. This is due to this process being a coherent parametric process, where the observable emerges from the square modulus of the rotationally averaged quantum amplitude. Furthermore, the analysis indicates that plane polarised input delivers the most efficient conversion rate, and that the emergent radiation will be primarily polarised parallel to the input polarisation [80]. The exponential term (4) delivers the normalisation condition for linear momentum and orbital angular momentum

conservation, and cancels with the V^{-1} in Eq. (4.8.7). Importantly, term (3) contains the entire radial variation of the matrix element and, therefore, the intensity distribution. Thus, we may plot this factor to obtain the variation of the output beams with respect to the pairs of allowed topological charge. We ignore the Laguerre-Gaussian modes with radial index $p > 0$, as the beam width, w, increases outwards with a monotonic dependence on p. Thus, the Fermi rate inherits the w^{-2p} dependence of the radial distribution functions and delivers successively smaller contributions for non-zero p modes, compared to the $p = 0$ counterpart. Importantly, the radial variation of the output for the three possible pairs of orbital angular momentum modes differs only in intensity and not in structure, Fig. 4.4. Moreover, the relative magnitude of each output pair has a Pascal's triangle form, displayed in Fig. 4.4.

Such observations are particularly interesting in light of recent observations of unexpectedly weighted topological charges in a four-wave mixing process [81]. This study inherently involves the entanglement of orbital angular momentum states of photons, in which there has been recent interest [82,83]. Furthermore, in regions close to the conversion material the ring structure of each output photon will significantly overlap, analysis of which will certainly display features of increasing angle-angular momentum uncertainty [33,84].

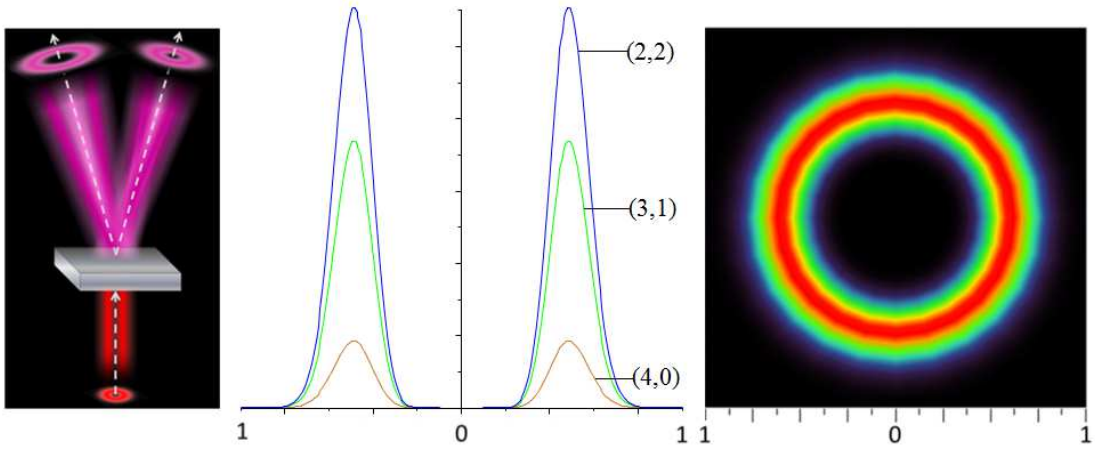

l =	(4,0)	(3,1)	(2,2)
Mag.	1	4	6

Fig. 4.4. (Left) Visual representation of the proposed experimental set-up. (Middle) Normalised intensity plots of the emission cone for varying combinations of orbital angular momentum in the output photons, (l_1, l_2), at a distance 100 wavelengths from the conversion material. (Right) Cross-sectional intensity distribution of the (2, 2) output (centred around the input beam axis) with radial distance scale matching the middle diagram. (Table) The relative magnitudes of output from the three pairs of orbital angular momentum.

4.9 Conclusion

Presented above are the details of a series of recent papers delivering a quantum electrodynamic treatment of recent experiments, delivering the rates of circular differential processes and their relation to measures of helicity, spin and recently rediscovered measures of chirality [61,62,85–87]. It emerges that an increase in circular dichroism at regular intervals from the mirror is associated only with the known behaviour of the electromagnetic field vectors and corresponds to Tang and Cohen's claim of nodal enhancements [57]. Furthermore, any increase or decrease in differential response at these locations is limited by the phase-photon number uncertainty principle and displays features associated with the reported shot-noise

[65], deriving from the quantum nature of light.

It was also shown that, for both paraxial and non-paraxial light, known electromagnetic quantities are all bilinear in the electric and magnetic fields, and, correspondingly, have exactly one annihilation and creation operator. In general, it was shown that, when taking expectation values, measureable electromagnetic measures must contain equal numbers of annihilation and creation operators. This avoids the introduction of a rapidly oscillating phase factor, the real part of which averages to zero in any realistic measurement [85].

The section on six-wave mixing of optical vortices demonstrates the quantum entanglement of pairs of optical vortex modes, and was presented recently in a journal article [80]. In particular, measurement of one photon heralds the detection of the other. It was shown that the probability for each output displays a neat combinatorial weighting, associated with Pascal's triangle. Furthermore, strict analysis shows that such a process is allowed in isotropic media with plane polarised input.

4.10 Appendix C

The electric and magnetic polarisation vectors are related by [51]:

$$\begin{aligned} e^{(L)} &= \frac{1}{\sqrt{2}}\left(\hat{\mathbf{i}} + i\hat{\mathbf{j}}\right) \quad e^{(R)} = \frac{1}{\sqrt{2}}\left(\hat{\mathbf{i}} - i\hat{\mathbf{j}}\right) \\ b^{(L)} &= -ie^{(L)} \qquad\qquad b^{(R)} = ie^{(R)} \end{aligned}. \tag{C.1}$$

Since the incident and reflected coordinates are related by:

$$\hat{\mathbf{i}} = \hat{\mathbf{i}}, \hat{\mathbf{j}} = -\hat{\mathbf{j}}, \hat{\mathbf{k}} = -\hat{\mathbf{k}}, \tag{C.2}$$

we have that:

$$\begin{aligned} e^{(L)} &= -e'^{(R)} \quad e^{(R)} = -e'^{(L)} \\ b^{(L)} &= -b'^{(R)} \quad e^{(R)} = -b'^{(L)} \end{aligned}. \tag{C.3}$$

4.11 Bibliography

[1] J. F. Nye and M. V. Berry, "Dislocations in wave trains," *Proceedings of the Royal Society A: Mathematical, Physical and Engineering Sciences* **336**(1605), 165–190 (1974) [doi:10.1098/rspa.1974.0012].

[2] N. R. Heckenberg, R. McDuff, C. P. Smith, H. Rubinsztein-Dunlop, and M. J. Wegener, "Laser beams with phase singularities," *Optical and quantum electronics* **24**(9), S951–S962 (1992) [doi:10.1007/BF01588597].

[3] G. Indebetouw, "Optical vortices and their propagation," *Journal of Modern Optics* **40**(1), 73–87 (1993) [doi:10.1080/09500349314550101].

[4] M. Soskin, V. Gorshkov, M. Vasnetsov, J. Malos, and N. Heckenberg, "Topological charge and angular momentum of light beams carrying optical vortices," *Physical Review A* **56**(5), 4064–4075 (1997) [doi:10.1103/PhysRevA.56.4064].

[5] G. F. Brand, "Phase singularities in beams," *American Journal of Physics* **67**(1), 55 (1999) [doi:10.1119/1.19191].

[6] S. J. van Enk and G. Nienhuis, "Spin and orbital angular momentum of photons," *Europhysics Letters (EPL)* **25**(7), 497–501 (1994) [doi:10.1209/0295-5075/25/7/004].

[7] A. S. Desyatnikov, D. Buccoliero, M. R. Dennis, and Y. S. Kivshar, "Spontaneous knotting of self-trapped waves," *Scientific Reports* **2** (2012) [doi:10.1038/srep00771].

[8] W. T. M. Irvine and D. Bouwmeester, "Linked and knotted beams of light," *Nature Physics* **4**(9), 716–720 (2008) [doi:10.1038/nphys1056].

[9] M. Arrayás and J. L. Trueba, "Exchange of helicity in a knotted electromagnetic field," *Annalen der Physik* **524**(2), 71–75 (2012) [doi:10.1002/andp.201100119].

[10] A. Y. Okulov, "Angular momentum of photons and phase conjugation," *Journal of Physics B: Atomic, Molecular and Optical Physics* **41**(10), 101001 (2008) [doi:10.1088/0953-4075/41/10/101001].

[11] I. Freund, "Optical vortices in Gaussian random wave fields: statistical probability densities," *Journal of the Optical Society of America A* **11**(5), 1644 (1994) [doi:10.1364/JOSAA.11.001644].

[12] D. L. Andrews and T. Thirunamachandran, "A quantum electrodynamical theory of differential scattering based on a model with two chromophores. I. differential Rayleigh scattering of circularly polarized light," *Proceedings of the Royal Society A: Mathematical, Physical and Engineering Sciences* **358**(1694), 297–310 (1978) [doi:10.1098/rspa.1978.0012].

[13] D. L. Andrews, L. C. D. Romero, and M. Babiker, "On optical vortex interactions with chiral matter," *Optics Communications* **237**(1-3), 133–139 (2004) [doi:10.1016/j.optcom.2004.03.093].

[14] M. Babiker, C. R. Bennett, D. L. Andrews, and L. C. Dávila Romero, "Orbital angular momentum exchange in the interaction of twisted light with molecules," *Phys. Rev. Lett.* **89**(14), 143601 (2002).

[15] W. Löffler, D. J. Broer, and J. P. Woerdman, "Circular dichroism of cholesteric polymers and the orbital angular momentum of light," *Physical Review A* **83**(6) (2011) [doi:10.1103/PhysRevA.83.065801].

[16] F. Araoka, T. Verbiest, K. Clays, and A. Persoons, "Interactions of twisted light with chiral molecules: An experimental investigation," *Physical Review A* **71**(5) (2005) [doi:10.1103/PhysRevA.71.055401].

[17] N. B. Simpson, K. Dholakia, L. Allen, and M. J. Padgett, "Mechanical equivalence of spin and orbital angular momentum of light: an optical spanner," *Optics Letters* **22**(1), 52 (1997) [doi:10.1364/OL.22.000052].

[18] M. W. Beijersbergen, R. P. C. Coerwinkel, M. Kristensen, and J. P. Woerdman, "Helical-wavefront laser beams produced with a spiral phaseplate," *Optics Communications* **112**(5-6), 321–327 (1994) [doi:10.1016/0030-4018(94)90638-6].

[19] N. R. Heckenberg, R. McDuff, C. P. Smith, and A. G. White, "Generation of optical phase singularities by computer-generated holograms," *Optics Letters* **17**(3), 221 (1992) [doi:10.1364/OL.17.000221].

[20] A. S. Ostrovsky, C. Rickenstorff-Parrao, and V. Arrizón, "Generation of the 'perfect' optical vortex using a liquid-crystal spatial light modulator," *Optics Letters* **38**(4), 534 (2013) [doi:10.1364/OL.38.000534].

[21] L. Marrucci, C. Manzo, and D. Paparo, "Optical spin-to-orbital angular momentum conversion in inhomogeneous anisotropic media," *Physical Review Letters* **96**(16) (2006) [doi:10.1103/PhysRevLett.96.163905].

[22] B. Piccirillo, V. D'Ambrosio, S. Slussarenko, L. Marrucci, and E. Santamato, "Photon spin-to-orbital angular momentum conversion via an electrically tunable q-plate," *Applied Physics Letters* **97**(24), 241104 (2010) [doi:10.1063/1.3527083].

[23] U. Ruiz, P. Pagliusi, C. Provenzano, K. Volke-Sepúlveda, and G. Cipparrone, "Polarization holograms allow highly efficient generation of complex light beams," *Optics Express* **21**(6), 7505 (2013) [doi:10.1364/OE.21.007505].

[24] L. Marrucci, "The q-plate and its future," *Journal of Nanophotonics* **7**(1), 078598 (2013) [doi:10.1117/1.JNP.7.078598].

[25] F. Cardano, E. Karimi, L. Marrucci, C. de Lisio, and E. Santamato, "Generation and dynamics of optical beams with polarization singularities," *Optics Express* **21**(7), 8815 (2013) [doi:10.1364/OE.21.008815].

[26] E. Karimi, J. Leach, S. Slussarenko, B. Piccirillo, L. Marrucci, L. Chen, W. She, S. Franke-Arnold, M. J. Padgett, et al., "Spin-orbit hybrid entanglement of photons and quantum contextuality," *Physical Review A* **82**(2) (2010) [doi:10.1103/PhysRevA.82.022115].

[27] E. Nagali, F. Sciarrino, F. De Martini, L. Marrucci, B. Piccirillo, E. Karimi, and E. Santamato, "Quantum information transfer from spin to orbital angular momentum of photons," *Physical Review Letters* **103**(1) (2009) [doi:10.1103/PhysRevLett.103.013601].

[28] S. Bandyopadhyay, *Introduction to Spintronics*, CRC Press, Boca Raton (2008).

[29] D. T. Pegg, J. A. Vaccaro, and S. M. Barnett, "Quantum-optical phase and canonical conjugation," *Journal of Modern Optics* **37**(11), 1703–1710 (1990) [doi:10.1080/09500349014551931].

[30] J. Leach, B. Jack, J. Romero, A. K. Jha, A. M. Yao, S. Franke-Arnold, D. G. Ireland, R. W. Boyd, S. M. Barnett, et al., "Quantum correlations in optical angle-orbital angular momentum variables," *Science* **329**(5992), 662–665 (2010) [doi:10.1126/science.1190523].

[31] A. Hasegawa, "Theory of information transfer in optical fibers: A tutorial review," *Optical Fiber Technology* **10**(2), 150–170 (2004) [doi:10.1016/j.yofte.2003.11.002].

[32] C. Liu, Z. Dutton, C. H. Behroozi, and L. V. Hau, "Observation of coherent optical information storage in an atomic medium using halted light pulses," *Nature* **409**(6819), 490–493 (2001) [doi:10.1038/35054017].

[33] G. Gibson, J. Courtial, M. J. Padgett, M. Vasnetsov, V. Pas'ko, S. M. Barnett, and S. Franke-Arnold, "Free-space information transfer using light beams carrying orbital angular momentum," *Optics Express* **12**(22), 5448 (2004) [doi:10.1364/OPEX.12.005448].

[34] P. Jia, Y. Yang, C. J. Min, H. Fang, and X.-C. Yuan, "Sidelobe-modulated optical vortices for free-space communication," *Optics Letters* **38**(4), 588 (2013) [doi:10.1364/OL.38.000588].

[35] L. Veissier, A. Nicolas, L. Giner, D. Maxein, A. S. Sheremet, E. Giacobino, and J. Laurat, "Reversible optical memory for twisted photons," *Optics Letters* **38**(5), 712 (2013) [doi:10.1364/OL.38.000712].

[36] J. Wang, J.-Y. Yang, I. M. Fazal, N. Ahmed, Y. Yan, H. Huang, Y. Ren, Y. Yue, S. Dolinar, et al., "Terabit free-space data transmission employing orbital angular momentum multiplexing," *Nature Photonics* **6**(7), 488–496 (2012) [doi:10.1038/nphoton.2012.138].

[37] D. S. Bradshaw and D. L. Andrews, "Optically induced forces and torques: Interactions between nanoparticles in a laser beam," *Physical Review A* **72**(3) (2005) [doi:10.1103/PhysRevA.72.033816].

[38] D. S. Bradshaw and D. L. Andrews, "Interactions between spherical nanoparticles optically trapped in Laguerre-Gaussian modes," *Optics Letters* **30**(22), 3039 (2005) [doi:10.1364/OL.30.003039].

[39] S. Franke-Arnold, J. Leach, M. J. Padgett, V. E. Lembessis, D. Ellinas, A. J. Wright, J. M. Girkin, P. Ohberg, and A. S. Arnold, "Optical ferris wheel for ultracold atoms," *Opt Express* **15**(14), 8619–8625 (2007). [10.1364/OE.15.008619]

[40] A. Fraine, N. Uribe-Patarroyo, D. Simon, O. Minaeva, and A. Sergienko, "Object Identification Using Correlated Orbital Angular Momentum States," 2013, JTh2A.93, OSA [doi:10.1364/CLEO_QELS.2013.JTh2A.93].

[41] B. Jack, J. Leach, J. Romero, S. Franke-Arnold, M. Ritsch-Marte, S. M. Barnett, and M. J. Padgett, "Holographic ghost imaging and the violation of a Bell inequality," *Phys. Rev. Lett.* **103**(8), 083602 (2009). [10.1103/PhysRevLett.103.083602]

[42] M. Harwit, "Photon Orbital Angular Momentum in Astrophysics," *The Astrophysical Journal* **597**(2), 1266–1270 (2003) [doi:10.1086/378623].

[43] G. Anzolin, F. Tamburini, A. Bianchini, G. Umbriaco, and C. Barbieri, "Optical vortices with starlight," *Astronomy and Astrophysics* **488**(3), 1159–1165 (2008) [doi:10.1051/0004-6361:200810469].

[44] E. Serabyn, D. Mawet, and R. Burruss, "An image of an exoplanet separated by two diffraction beamwidths from a star," *Nature* **464**(7291), 1018–1020 (2010) [doi:10.1038/nature09007].

[45] F. Tamburini, B. Thidé, G. Molina-Terriza, and G. Anzolin, "Twisting of light around rotating black holes," *Nature Physics* **7**(3), 195–197 (2011) [doi:10.1038/nphys1907].

[46] V. E. Lembessis and M. Babiker, "Enhanced Quadrupole Effects for Atoms in Optical Vortices," *Phys. Rev. Lett.* **110**(8) (2013) [doi:10.1103/PhysRevLett.110.083002].

[47] A. Picón, A. Benseny, J. Mompart, J. R. Vázquez de Aldana, L. Plaja, G. F. Calvo, and L. Roso, "Transferring orbital and spin angular momenta of light to atoms," *New J. Phys.* **12**(8), 083053 (2010) [doi:10.1088/1367-2630/12/8/083053].

[48] S. M. Barnett and L. Allen, "Orbital angular momentum and nonparaxial light beams," *Optics Communications* **110**(5-6), 670–678 (1994) [doi:10.1016/0030-4018(94)90269-0].

[49] G. Wick, "The evaluation of the collision matrix," *Physical Review* **80**(2), 268–272 (1950) [doi:10.1103/PhysRev.80.268].

[50] L. E. Ballentine, *Quantum Mechanics: A Modern Development*, World Scientific, Singapore (1998).

[51] D. P. Craig and T. Thirunamachandran, *Molecular Quantum Electrodynamics: An Introduction to Radiation-Molecule Interactions*, Dover Publications, Mineola, N.Y (1998).

[52] D. L. Andrews, *Optical Harmonics in Molecular Systems*, Wiley-VCH, Weinheim (2002).

[53] D. L. Andrews and P. Allcock, "A quantum electrodynamical foundation for molecular photonics," in *Advances in Chemical Physics* **119**, M. W. Evans, Ed., pp. 603–675, John Wiley & Sons, Inc., New York, USA.

[54] S. Naguleswaran and G. E. Stedman, "Time reversal selection rules and gauge invariance in nonlinear optics," *Journal of Physics B: Atomic, Molecular and Optical Physics* **29**(17), 4027–4040 (1996) [doi:10.1088/0953-4075/29/17/023].

[55] N. Yang and A. E. Cohen, "Local geometry of electromagnetic fields and its role in molecular multipole transitions," *The Journal of Physical Chemistry B* **115**(18), 5304–5311 (2011) [doi:10.1021/jp1092898].

[56] Y. Tang and A. E. Cohen, "Optical chirality and its interaction with matter," *Physical Review Letters* **104**(16) (2010) [doi:10.1103/PhysRevLett.104.163901].

[57] Y. Tang and A. E. Cohen, "Enhanced enantioselectivity in excitation of chiral molecules by superchiral light," *Science* **332**(6027), 333–336 (2011) [doi:10.1126/science.1202817].

[58] E. Hendry, T. Carpy, J. Johnston, M. Popland, R. V. Mikhaylovskiy, A. J. Lapthorn, S. M. Kelly, L. D. Barron, N. Gadegaard, et al., "Ultrasensitive detection and characterization of biomolecules using superchiral fields," *Nature Nanotechnology* **5**(11), 783–787 (2010) [doi:10.1038/nnano.2010.209].

[59] E. Hendry, R. V. Mikhaylovskiy, L. D. Barron, M. Kadodwala, and T. J. Davis, "Chiral electromagnetic fields generated by arrays of nanoslits," *Nano Letters* **12**(7), 3640–3644 (2012) [doi:10.1021/nl3012787].

[60] C. Rosales-Guzmán, K. Volke-Sepulveda, and J. P. Torres, "Light with enhanced optical chirality," *Optics Letters* **37**(17), 3486 (2012) [doi:10.1364/OL.37.003486].

[61] M. M. Coles and D. L. Andrews, "Chirality and angular momentum in optical radiation," *Physical Review A* **85**(6) (2012) [doi:10.1103/PhysRevA.85.063810].

[62] D. L. Andrews and M. M. Coles, "Measures of chirality and angular momentum in the electromagnetic field," *Optics Letters* **37**(15), 3009 (2012) [doi:10.1364/OL.37.003009].

[63] K. Y. Bliokh and F. Nori, "Characterizing optical chirality," *Physical Review A* **83**(2) (2011) [doi:10.1103/PhysRevA.83.021803].

[64] J. E. S. Bergman, S. M. Mohammadi, T. D. Carozzi, L. K. S. Daldorff, B. Thidé, R. Karlsson, and M. Eriksson, "Conservation laws in generalized Riemann-Silberstein electrodynamics," [arXiv:0803.2383 (physics.optics)].

[65] A. G. Smart, "A mirror gives light an extra twist," *Physics Today* **64**(6), 16 (2011) [doi:10.1063/1.3603909].

[66] W. H. Louisell, *Quantum Statistical Properties of Radiation*, Wiley, New York (1973).

[67] L. Cohen, H. V. Poor, and M. O. Scully, *Classical, Semi-Classical and Quantum Noise*, Springer, New York (2012).

[68] P. Bharadwaj, B. Deutsch, and L. Novotny, "Optical Antennas," *Advances in Optics and Photonics* **1**(3), 438 (2009) [doi:10.1364/AOP.1.000438].

[69] D. A. Genov, M. Ambati, and X. Zhang, "Surface plasmon amplification in planar metal films," *IEEE Journal of Quantum Electronics* **43**(11), 1104–1108 (2007) [doi:10.1109/JQE.2007.905904].

[70] D. Bergman and M. Stockmann, "Surface plasmon amplification by stimulated emission of radiation: Quantum generation of coherent surface plasmons in nanosystems," *Physical Review Letters* **90**(2) (2003) [doi:10.1103/PhysRevLett.90.027402].

[71] N. M. Lawandy, "Localized surface plasmon singularities in amplifying media," *Applied Physics Letters* **85**(21), 5040 (2004) [doi:10.1063/1.1825058].

[72] L. He, M. D. Musick, S. R. Nicewarner, F. G. Salinas, S. J. Benkovic, M. J. Natan, and C. D. Keating, "Colloidal Au-enhanced surface plasmon resonance for ultrasensitive detection of DNA hybridization," *Journal of the American Chemical Society* **122**(38), 9071–9077 (2000) [doi:10.1021/ja001215b].

[73] Y. Gorodetski, N. Shitrit, I. Bretner, V. Kleiner, and E. Hasman, "Observation of optical spin symmetry breaking in nanoapertures," *Nano Letters* **9**(8), 3016–3019 (2009) [doi:10.1021/nl901437d].

[74] D. Andrews and N. Blake, "Forbidden nature of multipolar contributions to second-harmonic generation in isotropic fluids," *Physical Review A* **38**(6), 3113–3115 (1988) [doi:10.1103/PhysRevA.38.3113].

[75] D. L. Andrews, "Harmonic generation in free molecules," *Journal of Physics B: Atomic and Molecular Physics* **13**(20), 4091–4099 (1980) [doi:10.1088/0022-3700/13/20/021].

[76] P. Allcock and D. L. Andrews, "Six-wave mixing: secular resonances in a higher-order mechanism for second-harmonic generation," *Journal of Physics B: Atomic, Molecular and Optical Physics* **30**(16), 3731–3742 (1997) [doi:10.1088/0953-4075/30/16/011].

[77] K. Moll, D. Homoelle, A. Gaeta, and R. Boyd, "Conical harmonic generation in isotropic materials," *Physical Review Letters* **88**(15) (2002) [doi:10.1103/PhysRevLett.88.153901].

[78] S. Franke-Arnold, S. Barnett, M. Padgett, and L. Allen, "Two-photon entanglement of orbital angular momentum states," *Physical Review A* **65**(3) (2002) [doi:10.1103/PhysRevA.65.033823].

[79] J. Romero, D. Giovannini, S. Franke-Arnold, S. M. Barnett, and M. J. Padgett, "Increasing the dimension in high-dimensional two-photon orbital angular momentum entanglement," *Physical Review A* **86**(1) (2012) [doi:10.1103/PhysRevA.86.012334].

[80] M. M. Coles, M. D. Williams, and D. L. Andrews, "Second harmonic generation in isotropic media: six-wave mixing of optical vortices," *Optics Express* **21**(10), 12783 (2013) [doi:10.1364/OE.21.012783].

[81] S. Franke-Arnold, "Orbital angular momentum of photons, atoms, and electrons," 5 March 2013, 86370P–86370P–10 [doi:10.1117/12.2002984].

[82] H. Arnaut and G. Barbosa, "Orbital and intrinsic angular momentum of single photons and entangled pairs of photons generated by parametric down-conversion," *Physical Review Letters* **85**(2), 286–289 (2000) [doi:10.1103/PhysRevLett.85.286].

[83] A. Hamadou Ibrahim, F. S. Roux, M. McLaren, T. Konrad, and A. Forbes, "Orbital-angular-momentum entanglement in turbulence," *Physical Review A* **88**(1) (2013) [doi:10.1103/PhysRevA.88.012312].

[84] S. Franke-Arnold, S. M. Barnett, E. Yao, J. Leach, J. Courtial, and M. Padgett, "Uncertainty principle for angular position and angular momentum," *New Journal of Physics* **6**, 103–103 (2004) [doi:10.1088/1367-2630/6/1/103].

[85] M. M. Coles and D. L. Andrews, "Photonic measures of helicity: optical vortices and circularly polarized reflection," *Optics Letters* **38**(6), 869 (2013) [doi:10.1364/OL.38.000869].

[86] M. M. Coles and D. L. Andrews, "Directions in optical angular momentum," SPIE 863707–863707–9 (2013) [doi:10.1117/12.2004430].

[87] D. L. Andrews and M. M. Coles, "Optical superchirality and electromagnetic angular momentum," SPIE 827405–827405–7 (2012) [doi:10.1117/12.906360].

Chapter 5

Medium Modified Absorption

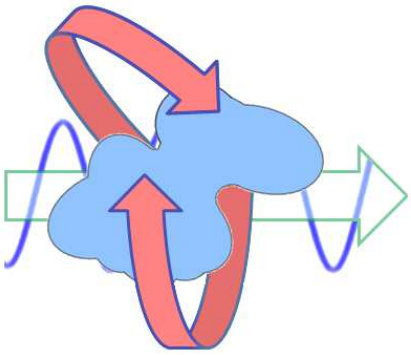

"A voyage to Europe in the summer of 1921 gave me the first opportunity of observing the wonderful blue opalescence of the Mediterranean Sea. It seemed not unlikely that the phenomenon owed its origin to the scattering of sunlight by the molecules of the water. To test this explanation, it appeared desirable to ascertain the laws governing the diffusion of light in liquids."

– Chandrasekhar Raman[†]

[†] Raman, Chandrasekhar V., - Nobel Lecture: The Molecular Scattering of Light". (1930).

5.1 Background

It is well known that the local electronic environment of atoms and molecules can influence optical processes, such as resonance energy transfer [1]. Many biological systems, for example, contain complex systems of molecules with shifted absorption bands due to nearby optical centres. For example, in widely studied light-harvesting complexes, the photosynthetic system bacteriochlorophyll B800 will absorb radiation and then only pass excitation on when its energy bands have been shifted by the presence of a neighbouring B850 [2,3]. Up to this date, quantum electrodynamic calculations on the influence, of a neighbouring, off-resonant molecule on photon absorption [4–6], have centred on the experimentally verified phenomenon of induced circular dichroism, where a chiral mediator confers circular differential absorption on an achiral acceptor [7–9].

Here, we investigate the influence of a neighbour, M, on the absorption by an acceptor molecule, A. The mediator is assumed to have an electronic level slightly above the input photon energy, so that it is not a competing acceptor. The key issues are analysed in a quantum electrodynamic framework, by studying the effect of a second body on optical absorption. It emerges that the second body result can be extended by integrating over all possible positions and orientations of the mediators and thereby modelling a continuous medium in which the acceptor is embedded. Developing such a theory is shown to provide links with both the molecular and bulk properties of materials. Moreover, it proves possible to determine which properties need to be optimised in order to tailor the medium modified effect.

5.2 Medium Modified Absorption

Here, we develop in precise quantum electrodynamic terms, the mathematical modelling of photon absorption, and then extend this analysis to a medium modified case. The initial and final system states are given by:

$$\left|\text{Initial}\right\rangle = \left|\psi_0^{(A)};\psi_0^{(M)}\right\rangle\left|n(\mathbf{k},\eta)\right\rangle; \tag{5.2.1}$$

$$\left|\text{Final}\right\rangle = \left|\psi_\beta^{(A)};\psi_0^{(M)}\right\rangle\left|(n-1)(\mathbf{k},\eta)\right\rangle; \tag{5.2.2}$$

where ψ designates the wavefunction of either the acceptor, A, or inert mediator, M. Moreover, the subscript of ψ corresponds to either: the ground state, 0, or the excited state β. The radiation is modelled as a precisely defined number state of wavevector $\mathbf{k}$ and polarisation label η. The energy of the absorbed photon must adhere to the conservation of energy; that is:

$$E_\beta - E_0 \approx \hbar ck. \tag{5.2.3}$$

According to the Feynman prescription, the contributions to the matrix element are terms corresponding to all topologically distinct Feynman diagrams [10], and are displayed in Fig 5.1. The probability amplitude for the process is then given by the sum of three terms:

$$M_{FI} = M_{FI}^{(A)} + M_{FI}^{(MA)} + M_{FI}^{(AM)}, \tag{5.2.4}$$

where $M_{FI}^{(A)}$ is the amplitude for absorption by the acceptor molecule, A; the second term, $M_{FI}^{(MA)}$, corresponds to the mediator molecule, M, absorbing a photon and then transferring the energy to the acceptor molecule, and $M_{FI}^{(AM)}$ denotes the absorption of a photon by A, which then interacts with M. We intend to determine the rate from the Fermi Golden Rule, Eq. (1.23), which depends on the square modulus of Eq. (5.2.4):

$$\begin{aligned} \left|M_{FI}\right|^2 = & \underbrace{\left|M_{FI}^{(A)}\right|^2}_{(1)} + \underbrace{\left|M_{FI}^{(MA)}\right|^2}_{(2)} + \underbrace{\left|M_{FI}^{(AM)}\right|^2}_{(3)} + \\ & 2\Re e\Big\{ \underbrace{M_{FI}^{(A)}\overline{M_{FI}^{(MA)}}}_{(4)} + \underbrace{M_{FI}^{(A)}\overline{M_{FI}^{(AM)}}}_{(5)} + \underbrace{M_{FI}^{(MA)}\overline{M_{FI}^{(AM)}}}_{(6)} \Big\}, \end{aligned} \tag{5.2.5}$$

where numbering has been introduced so that terms can be tackled individually. The leading order term is term (1), which corresponds to absorption when the mediator is absent. The terms (2) and (3) are small in comparison to term (1), as they derive from a higher order of perturbation theory. This, in turn, implies that term (6) is also small. Thus, the first correction terms to absorption are terms (4) and (5).

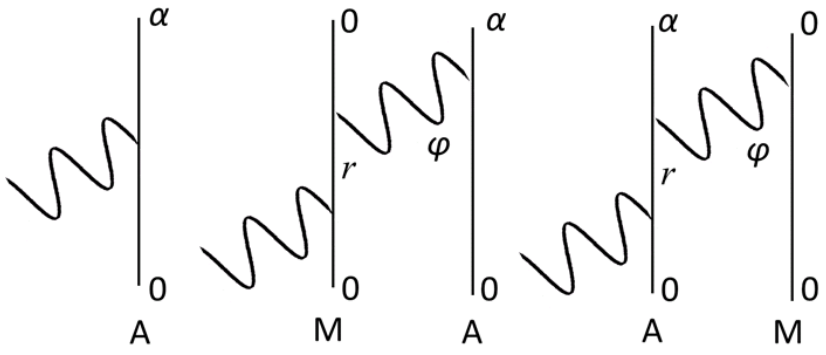

Fig. 5.1. Feynman diagrams for absorption (a), and the dynamic (b) and static (c) modification considered here, which are described by first and third order perturbation theory. The molecular virtual intermediate state is labelled by r, and the virtual photon is designated φ.

5.3. Free-Space Absorption

To begin, we calculate the leading order term, when the medium is not involved. In the electric dipole approximation, we have:

$$\begin{aligned} M_{FI}^{(A)} &= \langle F | H_{\text{int}} | I \rangle \\ &= -\langle n-1(\mathbf{k},\eta) | \langle \psi_\beta^{(A)}; \psi_0^{(M)} | \boldsymbol{\mu} \cdot \mathbf{e} | \psi_0^{(A)}; \psi_0^{(M)} \rangle | n(\mathbf{k},\eta) \rangle \\ &= -\langle \psi_\beta^{(A)}; \psi_0^{(M)} | \boldsymbol{\mu} | \psi_0^{(A)}; \psi_0^{(M)} \rangle \cdot \langle n-1(\mathbf{k},\eta) | \mathbf{e} | n(\mathbf{k},\eta) \rangle \\ &= -\mathrm{i}\boldsymbol{\mu}^{(A)\beta 0} \cdot \mathbf{e}^{(\eta)}(\mathbf{k}) \left(\frac{n\hbar ck}{2V\varepsilon_0} \right)^{\frac{1}{2}} \mathrm{e}^{\mathrm{i}\mathbf{k}\cdot\mathbf{r}_A}, \end{aligned} \tag{5.2.6}$$

where we have assumed that the wavefunctions are real and $\mathbf{r}_A$ is the position vector of the acceptor. The square modulus of this, or term (1) from Eq. (5.2.5), is:

$$\left| M_{FI}^{(A)} \right|^2 = \left(\frac{n\hbar ck}{2V\varepsilon_0} \right) \left| \boldsymbol{\mu}^{(A)\beta 0} \cdot \mathbf{e}^{(\eta)}(\mathbf{k}) \right|^2, \tag{5.2.7}$$

which, by substituting into the Fermi Golden Rule and performing an isotropic rotational average [11], becomes:

$$\left\langle \Gamma^{(A)} \right\rangle = \left(\frac{\pi nck\rho}{3V\varepsilon_0} \right) \left| \boldsymbol{\mu}^{(A)\beta 0} \right|^2. \tag{5.2.8}$$

This result is now well-known [5], and is presented as a means for comparing the magnitude of the modification by the mediator.

5.4. Static Correction Term

To begin calculation of the correction terms, we compute $M_{FI}^{(AM)}$ from third-order perturbation theory:

$$M_{FI}^{(MA)} = \sum_{R,S} \frac{\langle F|H_{\text{int}}|S\rangle\langle S|H_{\text{int}}|R\rangle\langle R|H_{\text{int}}|I\rangle}{(E_I - E_S)(E_I - E_R)}. \tag{5.2.9}$$

In the electric dipole approximation, the interaction Hamiltonian is given by $H_{\text{int}} = -\boldsymbol{\mu}\cdot\mathbf{e}^{\perp}$ so that the result emerges as dependent on a sum over wavevectors and polarisation labels. Converting the wavevector sum to an integral, by the following prescription [5]:

$$\frac{1}{V}\sum_{\mathbf{k}} \to \int \frac{\partial^3\mathbf{k}}{(2\pi)^3}, \tag{5.2.10}$$

and using a program of contour integration, delivers this term of the quantum amplitude, Eq. (5.2.4), as:

$$M_{FI}^{(AM)} \sim \sum_{\eta} e_j^{(\eta)} \alpha_{jk}^{A(0\beta)} V_{kl}(\omega, R_{MA})\mu_l^{M(00)}, \tag{5.2.11}$$

where $\alpha_{ij}^{A(0\beta)}$ is the polarisability tensor for the acceptor molecule and where $V_{ij}(k, R_{MA})$ is the fully-retarded dipole dipole interaction tensor (discussed in the next subsection). Here, the tilde denotes that we have ignored the pre-factors for

calculational simplicity. This delivers the static interference term of the probability – term (5) of Eq. (5.2.5) – as:

$$2\Re e\left\{M_{FI}^{(A)}\overline{M_{FI}^{(AM)}}\right\} \sim 2\Re e\left\{\sum_{\eta,\eta'} e_i^{(\eta)}\overline{e}_j^{(\eta')}\mu_i^{A(\beta 0)}\overline{\mu}_l^{M(00)}\overline{\alpha}_{jk}^{M(\beta 0)}\overline{V}_{kl}\left(k,R_{MA}\right)\right\}. \tag{5.2.12}$$

As this term explicitly depends on $\overline{\mu}_l^{M(00)}$, we can assume that this contribution to the rate vanishes if the molecules comprising the medium have no static dipole moment.

5.5. Dynamic Correction Term

To begin calculation of the remaining correction term, we compute $M_{FI}^{(MA)}$, as before, from third-order perturbation theory, which delivers this term of the quantum amplitude as:

$$M_{FI}^{(MA)} \sim \sum_{\eta} e_j^{(\eta)}\alpha_{jk}^{M(00)}V_{kl}\left(\omega,R_{MA}\right)\mu_l^{A(\beta 0)}, \tag{5.2.13}$$

where $\alpha_{ij}^{M(00)}$ is the polarisability tensor for the molecule *M*. Term (4) from Eq. (5.2.5), then becomes:

$$2\Re e\left\{M_{FI}^{(A)}\overline{M_{FI}^{(MA)}}\right\} \sim 2\Re e\left\{\sum_{\eta,\eta'} e_i^{(\eta)}\overline{e}_j^{(\eta')}\mu_i^{A(\beta 0)}\overline{\mu}_l^{A(\beta 0)}\overline{\alpha}_{jk}^{M(00)}\overline{V}_{kl}\left(k,R_{MA}\right)\right\}, \tag{5.2.14}$$

where $V_{ij}\left(k,R_{MA}\right)$ is the fully retarded dipole-dipole interaction tensor and is given by [12]:

$$V_{ij}\left(k,R_{MA}\right)=\frac{e^{ikR_{MA}}}{4\pi\varepsilon_0 R_{MA}^3}\Big[\left(\delta_{ij}-3\hat{R}_{MAi}\hat{R}_{MAj}\right)-ikR_{MA}\left(\delta_{ij}-3\hat{R}_{MAi}\hat{R}_{MAj}\right) -k^2R_{MA}^2\left(\delta_{ij}-\hat{R}_{MAi}\hat{R}_{MAj}\right)\Big]. \tag{5.2.15}$$

It is worth noting that in the multipolar formalism of quantum electrodynamics the interaction tensor can be generalised to couplings between electric and magnetic multipoles of any order [13–15]. Therefore, the form of Eq. (5.2.14) can be modified to permit calculation of modifications to absorption in a medium with strong magnetic dipole or electric quadrupole transition moments. In fact, it is through involvement of the magnetic transition dipole moments that an achiral molecule may display induced circular dichroism in the presence of a neighbouring chiral molecule [4]. The transfer tensor given here, Eq. (5.2.15), is the form appropriate for species interacting in a vacuum. We now introduce a modified form, developed specifically to accommodate the effects of a surrounding medium [16]:

$$V_{ij}^{bath}\left(k,\mathbf{R}_{MA}\right)=\frac{1}{n^2}\left(\frac{n^2+2}{3}\right)^2 V_{ij}\left(nk,\mathbf{R}_{MA}\right), \tag{5.2.16}$$

where n is the complex refractive index of the surroundings at the wavelength corresponding to the transfer energy. At this juncture, the surrounding medium, characterised by n, is not assumed to be composed of M. Substituting Eq. (5.2.15) and (5.2.16) into Eq. (5.2.14) delivers:

$$\Re e\left\{2\sum_{\eta,\eta'} e_i^{(\eta)}\overline{e}_j^{(\eta')}\mu_i^{A(\beta 0)}\overline{\mu}_l^{A(\beta 0)}\overline{\alpha}_{jk}^{M(00)}\overline{V}_{kl}^{bath}\left(k,R_{MA}\right)\right\}$$

$$=\Re e\left\{\sum_{\eta,\eta'} e_i^{(\eta)}\overline{e}_j^{(\eta')}\frac{e^{-i\overline{n}kR_{MA}}}{2\pi\varepsilon_0 R_{MA}^3}\frac{1}{\overline{n}^2}\left(\frac{\overline{n}^2+2}{3}\right)^2\mu_i^{A(\beta 0)}\overline{\mu}_l^{A(\beta 0)}\overline{\alpha}_{jk}^{M(00)}\times\left[\left(\delta_{kl}-3\hat{R}_{MAk}\hat{R}_{MAl}\right)\right.\right. \quad (5.2.17)$$

$$\left.\left.+i\overline{n}kR_{MA}\left(\delta_{kl}-3\hat{R}_{MAk}\hat{R}_{MAl}\right)-\overline{n}^2k^2R_{MA}^2\left(\delta_{kl}-\hat{R}_{MAk}\hat{R}_{MAl}\right)\right]\right\}.$$

As the initial and final states of *M* are identical, *M* is not observed. Therefore, each possible mediator must be taken into account (precisely, summed over), so that term (4) of Eq. (5.2.5) becomes:

$$\Re e\left\{\sum_{M,\eta,\eta'}\frac{e^{-i\overline{n}kR_{MA}}}{2\pi\varepsilon_0 R_{MA}^3}\frac{1}{\overline{n}^2}\left(\frac{\overline{n}^2+2}{3}\right)^2 e_i^{(\eta)}\overline{e}_j^{(\eta')}\mu_i^{A(\beta 0)}\overline{\mu}_l^{A(\beta 0)}\overline{\alpha}_{jk}^{M(00)}\times\left[\left(\delta_{kl}-3\hat{R}_{MAk}\hat{R}_{MAl}\right)\right.\right. \quad (5.2.18)$$

$$\left.\left.+i\overline{n}kR_{MA}\left(\delta_{kl}-3\hat{R}_{MAk}\hat{R}_{MAl}\right)-\overline{n}^2k^2R_{MA}^2\left(\delta_{kl}-\hat{R}_{MAk}\hat{R}_{MAl}\right)\right]\right.$$

We now assume that species *M* will have a physically random orientation to justify performing an isotropic rotational average with respect to the orientation of *M*. This expedient allows analytical calculation and avoids computational work involving predetermined orientations. Enacting the rotational average and contracting the vector indices enables the expression to be written as:

$$\Re e\left\{\sum_{M}\frac{e^{-i\overline{n}kR_{MA}}}{6\pi\varepsilon_0 R_{MA}^3}\frac{1}{\overline{n}^2}\left(\frac{\overline{n}^2+2}{3}\right)^2\overline{\alpha}_{\lambda\lambda}^{M(00)}\times\right.$$

$$\mathbf{e}\cdot\boldsymbol{\mu}^{A(\beta 0)}\left[\left\{\overline{\mathbf{e}}\cdot\overline{\boldsymbol{\mu}}^{A(\beta 0)}-3\left(\overline{\mathbf{e}}\cdot\hat{\mathbf{R}}_{MA}\right)\left(\overline{\boldsymbol{\mu}}^{A(\beta 0)}\cdot\hat{\mathbf{R}}_{MA}\right)\right\}\right. \quad (5.2.19)$$

$$+i\overline{n}kR_{MA}\left\{\overline{\mathbf{e}}\cdot\overline{\boldsymbol{\mu}}^{A(\beta 0)}-3\left(\overline{\mathbf{e}}\cdot\hat{\mathbf{R}}_{MA}\right)\left(\overline{\boldsymbol{\mu}}^{A(\beta 0)}\cdot\hat{\mathbf{R}}_{MA}\right)\right\}$$

$$\left.\left.-\overline{n}^2k^2R_{MA}^2\left\{\overline{\mathbf{e}}\cdot\overline{\boldsymbol{\mu}}^{A(\beta 0)}-\left(\overline{\mathbf{e}}\cdot\hat{\mathbf{R}}_{MA}\right)\left(\overline{\boldsymbol{\mu}}^{A(\beta 0)}\cdot\hat{\mathbf{R}}_{MA}\right)\right\}\right]\right.,$$

where × represents scalar multiplication and we have used the orthogonality of the electric polarisation vectors. To aid interpretation of the mathematical result, let us assume that the input radiation propagates at an angle γ to the dipole moment of the acceptor molecule. In such a case, the scalar products become cosines:

$$\begin{aligned}&\Re e\left\{\sum_M \frac{e^{-i\bar{n}kR_{MA}}}{6\pi\varepsilon_0 R_{MA}^3}\frac{1}{\bar{n}^2}\left(\frac{\bar{n}^2+2}{3}\right)^2 \bar{\alpha}_{\lambda\lambda}^{M(00)}\left|\boldsymbol{\mu}^{A(\beta 0)}\right|^2 \cos(\gamma)\times\right.\\&\left[\left\{\cos(\gamma)-3\cos(\theta-\gamma)\cos(\theta)\right\}+i\bar{n}kR_{MA}\left\{\cos(\gamma)-3\cos(\theta-\gamma)\cos(\theta)\right\}\right.\\&\left.\left.-\bar{n}^2k^2R_{MA}^2\left\{\cos(\gamma)-3\cos(\theta-\gamma)\cos(\theta)\right\}\right]\right\},\end{aligned} \tag{5.2.20}$$

where we are working in spherical coordinates and θ is the polar coordinate. To correctly model a continuous medium, the sum over all mediators is promoted to an integral over all positions of *M*,

$$\begin{aligned}&\Re e\left\{\iiint_{R_{MA}} \frac{e^{-i\bar{n}kR_{MA}}}{6\pi\varepsilon_0 R_{MA}^3}\frac{1}{\bar{n}^2}\left(\frac{\bar{n}^2+2}{3}\right)^2 \bar{\alpha}_{\lambda\lambda}^{M(00)}\left|\boldsymbol{\mu}^{A(\beta 0)}\right|^2 \cos(\gamma)\times\right.\\&\left[\left\{\cos(\gamma)-3\cos(\theta-\gamma)\cos(\theta)\right\}+i\bar{n}kR_{MA}\left\{\cos(\gamma)-3\cos(\theta-\gamma)\cos(\theta)\right\}\right.\\&\left.\left.-\bar{n}^2k^2R_{MA}^2\left\{\cos(\gamma)-\cos(\theta-\gamma)\cos(\theta)\right\}\right]R_{MA}^2\sin(\theta)\,d\theta d\phi dR_{MA}\right\},\end{aligned} \tag{5.2.21}$$

where $R_{MA}^2\sin(\theta)\,d\theta d\phi dR_{MA}$ is the volume element and a function $f\left(R_{MA},\theta,\phi\right)$ is integrated over every point in $\mathbb{R}^3$ by the triple integral [17]:

$$\int_{\phi=0}^{2\pi}\int_{\theta=0}^{\pi}\int_{R_{MA}=0}^{\infty} f\left(R_{MA}^2,\theta,\phi\right)R_{MA}^2\sin(\theta)\,d\theta d\phi dR_{MA}. \tag{5.2.22}$$

First enacting the θ integral, allows us to make use of the following results:

$$\int_0^{\pi} \cos(\gamma)\sin(\theta)\left[\cos(\gamma)-3\cos(\theta-\gamma)\cos(\theta)\right]d\theta = 0; \tag{5.2.23}$$

$$\int_0^{\pi} \cos(\gamma)\sin(\theta)\left[\cos(\gamma)-\cos(\theta-\gamma)\cos(\theta)\right]d\theta = \frac{4\cos^2(\gamma)}{3}. \tag{5.2.24}$$

Thus, we observe the vanishing of terms that are both R independent and dependent on R^{-1}. Then our expression becomes:

$$-\Re e\left\{\iint_{R_{MA}} \frac{e^{-i\bar{n}kR_{MA}}}{6\pi\varepsilon_0} R_{MA}\left(\frac{\bar{n}^2+2}{3}\right)^2 \bar{\alpha}_{\lambda\lambda}^{M(00)}\left|\boldsymbol{\mu}^{A(\beta 0)}\right|^2 k^2 \frac{4\cos^2(\gamma)}{3} d\phi dR_{MA}\right\}. \tag{5.2.25}$$

Integrating over the azimuthal angular coordinate merely introduces a factor of 2π. By imposing a minimum distance between the acceptor molecule and the molecules in the medium, $R_{\min}$, we can use the following identity:

$$\int_{R_{\min}}^{\infty} e^{-i\bar{n}kR_{MA}} R_{MA}\,\partial R_{MA} = -\frac{e^{-ik\bar{n}R_{\min}}\left(1+ik\bar{n}R_{\min}\right)}{k^2\bar{n}^2} \text{ for } \Im\mathrm{m}\left(\bar{n}k\right) < 0. \tag{5.2.26}$$

The wavenumber is purely real and overbar denotes complex conjugation, thus this identity is valid for $\Im\mathrm{m}(n) > 0$, when the medium is absorptive. We then obtain the first medium induced correction to the matrix element for absorption:

$$\Re e\left\{\frac{4}{9\varepsilon_0}\cos^2(\gamma)\left(\frac{\bar{n}^2+2}{3}\right)^2\frac{e^{-ik\bar{n}R_{\min}}\left(1+ik\bar{n}R_{\min}\right)}{\bar{n}^2}\bar{\alpha}_{\lambda\lambda}^{M(00)}\left|\boldsymbol{\mu}^{A(\beta 0)}\right|^2\right\}, \tag{5.2.27}$$

where $\Im m(n)>0$. The zeros of Eq. (5.2.27) can be readily identified as $\gamma = n\pi - \pi/2$, and when $R_{\min}$ tends to infinity. By letting $R_{\min}$ tend to zero we obtain:

$$\Re e\left\{\frac{4}{9\varepsilon_0}\cos^2(\gamma)\left(\frac{\bar{n}^2+2}{3\bar{n}}\right)^2\bar{\alpha}_{\lambda\lambda}^{M(00)}\left|\boldsymbol{\mu}^{A(\beta 0)}\right|^2\right\}. \tag{5.2.28}$$

Furthermore, by rotational averaging with respect to the input radiation or, equivalently, the orientation of the acceptor molecule *A* - eliminating the dependence on γ, we obtain:

$$\Re e\left\{\frac{4}{9\varepsilon_0}\left(\frac{\bar{n}^2+2}{3\bar{n}}\right)^2\bar{\alpha}_{\lambda\lambda}^{M(00)}\left|\boldsymbol{\mu}^{A(\beta 0)}\right|^2\right\}. \tag{5.2.29}$$

It is now possible to compare the free-field term and the dynamic correction. It is clear that for the modification of absorption to become significant the medium requires large diagonal elements of the associated polarisability tensor. The transition dipole of the acceptor molecule does not affect the modification in rate since it appears in both Eq. (5.2.7) and (5.2.29).

5.5. Conclusion

To fully determine the optimum criteria for modifying optical absorption by a molecule it is necessary to take into account more than one acceptor molecule. It is anticipated that the emerging result would depend on the ratio of acceptors to mediators. Furthermore, for a complete description it would be necessary to model the situation in which all mediators have some alignment preference, in low temperature samples or in the presence of a static field, for example. Such a situation would require use of weighted rotational averaging [18], and would require explicit calculation of the static correction terms. It is interesting to note that while this result is analytically tractable; it has recently been shown that calculations corresponding to modification of resonance energy transfer by a third body is not, and requires use of numerical methods [19]. The inclusion of the magnetic dipole interaction in the above calculations would reveal medium induced chiral effects. It is anticipated that, although this would introduce another tier of complexity, the analysis would stem from the same order of perturbation theory and therefore be solvable by analytical means.

5.3 Bibliography

[1] G. J. Daniels and D. L. Andrews, "The electronic influence of a third body on resonance energy transfer," *The Journal of Chemical Physics* **116**(15), 6701 (2002) [doi:10.1063/1.1461819].

[2] J. L. Herek, N. J. Fraser, T. Pullerits, P. Martinsson, T. Polívka, H. Scheer, R. J. Cogdell, and V. Sundström, "B800→B850 energy transfer mechanism in bacterial LH2 complexes investigated by B800 pigment exchange," *Biophysical Journal* **78**(5), 2590–2596 (2000) [doi:10.1016/S0006-3495(00)76803-2].

[3] G. D. Scholes and G. R. Fleming, "On the mechanism of light harvesting in photosynthetic purple bacteria: B800 to B850 energy transfer," *The Journal of Physical Chemistry B* **104**(8), 1854–1868 (2000) [doi:10.1021/jp993435l].

[4] D. P. Craig, E. A. Power, and T. Thirunamachandran, "The dynamic terms in induced circular dichroism," *Proceedings of the Royal Society A: Mathematical, Physical and Engineering Sciences* **348**(1652), 19–38 (1976) [doi:10.1098/rspa.1976.0021].

[5] D. P. Craig and T. Thirunamachandran, *Molecular Quantum Electrodynamics: An Introduction to Radiation-Molecule Interactions*, Dover Publications, Mineola, N.Y (1998).

[6] D. P. Craig, E. A. Power, and T. Thirunamachandran, "Induced circular dichroism: A theoretical description," *Chemical Physics Letters* **27**(2), 149–153 (1974) [doi:10.1016/0009-2614(74)90191-2].

[7] S. F. Mason, "Induced circular dichroism," *Chemical Physics Letters* **32**(2), 201–203 (1975) [doi:10.1016/0009-2614(75)85103-7].

[8] F. D. Saeva and J. J. Wysocki, "Induced circular dichroism in cholesteric liquid crystals," *Journal of the American Chemical Society* **93**(22), 5928–5929 (1971) [doi:10.1021/ja00751a075].

[9] D. Krois and U. H. Brinker, "Induced circular dichroism and UV−Vis absorption spectroscopy of cyclodextrin inclusion complexes: structural elucidation of supramolecular azi-adamantane (spiro[adamantane-2,3'-diazirine])," *Journal of the American Chemical Society* **120**(45), 11627–11632 (1998) [doi:10.1021/ja982299f].

[10] R. D. Mattuck, *A Guide to Feynman Diagrams in the Many-Body Problem*, 2nd ed, Dover Publications, New York (1992).

[11] D. L. Andrews and T. Thirunamachandran, "On three-dimensional rotational averages," *The Journal of Chemical Physics* **67**(11), 5026 (1977) [doi:10.1063/1.434725].

[12] D. L. Andrews, *Structured Light and its Applications: An Introduction to Phase-Structured Beams and Nanoscale Optical Forces*, Academic, Amsterdam; Boston (2008).

[13] A. Salam, "A general formula for the rate of resonant transfer of energy between two electric multipole moments of arbitrary order using molecular quantum electrodynamics," *The Journal of Chemical Physics* **122**(4), 044112 (2005) [doi:10.1063/1.1830430].

[14] G. D. Scholes and D. L. Andrews, "Damping and higher multipole effects in the quantum electrodynamical model for electronic energy transfer in the condensed phase," *The Journal of Chemical Physics* **107**(14), 5374 (1997) [doi:10.1063/1.475145].

[15] D. L. Andrews, "Optical angular momentum: Multipole transitions and photonics," *Physical Review A* **81**(3) (2010) [doi:10.1103/PhysRevA.81.033825].

[16] G. Juzeliūnas, "Molecule-radiation and molecule-molecule processes in condensed media: a microscopic QED theory," *Chemical Physics* **198**(1-2), 145–158 (1995) [doi:10.1016/0301-0104(95)00130-G].

[17] G. B. Arfken, *Mathematical Methods for Physicists*, Academic Press, Orlando (1985).

[18] D. Andrews and M. Harlow, "Phased and Boltzmann-weighted rotational averages," *Physical Review A* **29**(5), 2796–2806 (1984) [doi:10.1103/PhysRevA.29.2796].

[19] D. L. Andrews and J. S. Ford, "Resonance energy transfer: Influence of neighboring matter absorbing in the wavelength region of the acceptor," *The Journal of Chemical Physics* **139**(1), 014107 (2013) [doi:10.1063/1.4811793].

Chapter 6

Future Work

"You see, wire telegraph is a kind of a very, very long cat. You pull his tail in New York and his head is meowing in Los Angeles. And radio operates exactly the same way: you send signals here, they receive them there. The only difference is that there is no cat."

[†]Einstein, Albert.

6.1 Introduction

In these final sections, the results from all chapters are discussed, identifying further avenues of investigation. We discuss the possibilities for future work by relaxing the approximations that have been made, and note further questions that these studies have revealed.

6.2 The Two-Level Approximation

With the emergence of progressively advanced computer software and hardware, it becomes harder to justify use of the two-level approximation in the computation of nonlinear optical susceptibilities. However, the use of the two-level approximation is still important in a pedagogical context, where problems with more than two energy levels are often not analytically tractable. It could be envisaged that introduction of empirical wavefunctions for the different classes of molecules (arranged according to their symmetry groups) could allow calculation of the important optical susceptibility tensors, giving indications of whether or not the two-level approximation is valid.

Analytically, knowledge of the energy level spacing may provide access to information on the convergence of the optical susceptibility tensors. However, at present it still remains unknown in advance which number of energy levels (if any) is required to ensure convergence of each term of perturbation theory.

6.3 Measures of Helicity

It is well-known that the electromagnetic Lagrangian is rotationally symmetric, which leads, via Noether's Theorem, to the conservation of electromagnetic angular momentum. It has recently been shown that the electromagnetic helicity is approximately generated by the mixing of electric and magnetic fields, the so-called duplex or Heaviside-Larmor symmetry [1]. By replacing the appearances of the electric and magnetic fields in the Lagrangian by their curls, the same calculations lead to the conclusion that optical chirality is generated by the 'rotation' of these new fields into a mixture of the two. That is, the duplex-like symmetry for the curl of the electric and magnetic fields delivers the conservation of optical chirality. However, a fully-satisfactory description of what symmetries generate the spin- and helicity- type measures has not been found.

Furthermore, whether or not the infinite hierarchy of spin- and helicity- type measures correspond to different physical phenomena, remains to be seen. From the quantum optical description, it can easily be shown that the combination of a left-handed red photon and a right-handed blue photon has zero helicity; yet a non-zero optical chirality. Furthermore, the appearance of k^2 in the expression for the optical chirality indicates that the optical chirality may play a role in chiral discrimination in a medium. To support this observation, it has been shown that the optical chirality is conserved in a homogeneous, dispersive medium [2]. However, since all helicity- and spin- type measures have the same basis states, it is apparent that manipulation of the optical chirality provides no way to encode more information in a photon than is accessible by manipulation of the optical helicity.

6.4 The Interaction of Twisted Light with Matter

To extend the analysis in Chapter 4, it is worthwhile to consider not just absorption near to a mirror, but higher-order chiral processes, such as differential scattering. It is anticipated that nodal enhancements will similarly arise. Of course, the analysis of the electric and magnetic field superposition states for radiation near to a mirror is equally valid in these cases; there will still be regions in which chiral phenomena is forbidden by symmetry arguments.

It will be interesting to investigate various nonlinear optical processes near to a phase conjugate mirror, where the topological charge is reversed. Such a situation may engineer standing wave-like behaviour in the phase of the beam, as opposed to the electric and magnetic field vectors. Of course, it is now known that orbital angular momentum does not play a role in internal electric dipole transitions [3], however it is conceivable that in carefully constructed situations the vector potential ceases to be approximately invariant over the volume of the optical centre. As such, the electric dipole approximation may no longer be valid and the higher-order multipoles will have to be engaged.

6.5 Optical Vortex Generation by Nanoantenna Arrays

A series of recent work has centred on the generation of optical vortex light from molecular chromophore arrays [4,5]. The arrangement of three nanoantennas in a structure satisfying C_3 or C_{3h} symmetry allows the formation of a delocalised

excitation. By analysis of the molecular point group, it emerges that there are two degenerate delocalised excitations with a phase factor corresponding to optical emission with topological charge of either -1 or 1. On relaxation, such wavefunctions necessarily produces radiation imprinted with an identical phase structure. By breaking the *x*-*y* symmetry of the set-up the energy levels will be split, allowing predetermined selection of emission of the sought handedness.

Furthermore, it transpires that by increasing the number of nanoantennas, the topological charge of the emission can be tailored to any integral value. Precisely, arrangements of nanoemitters with C_n or C_{nh} symmetry have pairs of delocalised excitations with topological charges of every integral value between $-\lfloor (n-1)/2 \rfloor$ (signifying the largest integer greater than or equal to $(n-1)/2$) and $+\lfloor (n-1)/2 \rfloor$. Experimental verification of these theoretical principles is the centre of ongoing research at the University of Ottawa.

6.6 Summary

In **Chapter One**, we laid the foundations of a fully quantised framework for the interaction of light and matter, when the optical fields are weaker than the Coulomb interaction between the electron field and the molecular nuclei. These fields are weak enough so that the interaction can be considered a perturbation on the matter and radiation states. Thus, atomic and molecular problems in quantum electrodynamics are treated within the confines of perturbation theory, so that

encountering fields strong enough to compete with the Coulomb interactions requires different methods altogether.

In **Chapter Two**, we studied the validity of the two-level approximation, generally and in the context of nonlinear optics. We presented an analytical theorem on the expectation values of quantum operators, showing the invalidity of the two-level approximation in even simple systems. Furthermore, the two-level approximation when applied to the optical susceptibility tensors of nonlinear optical processes was discussed, and the commonly held idea that 'push-pull' chromophores are associated with enhanced second harmonic response was challenged. It was then shown that *ab initio* calculations (performed by Peck and Oganesyan) combined with introduction of an error-gauging parameter indicated that for two specified molecules the two-level approximation was valid in the case of Rayleigh scattering and invalid in the case of second harmonic generation. Finally, it was proved that the number of terms in the p^{th}-order optical susceptibility is a polynomial of order $n^{(p-1)}$, where n is the number of energy levels included in the sum-over-states computation, which puts these calculations in the class of problems quickly solvable by a computer. In summary, for both analytical and computational problems it was determined that the use of a two-state model undermines realism in return for calculational ease [6–9].

In **Chapter Three**, it was shown that careful analysis of the optical angular momentum allows division into parts that satisfy duplex symmetry. Introduction of a general Poincaré sphere representation of polarisation determined the orbital and spin parts of the angular momentum as dependant on the sum and difference of number operators for modes of opposing helicity, respectively. These results were extended

to the case of beams with orbital angular momentum. A similar analysis of the optical chirality density and corresponding flux showed that they are proportional only to the difference of number operators for modes of opposing helicity. Introduction of a Laguerre-Gaussian basis revealed that beams with nonzero values of the optical chirality also do not possess orbital angular momentum characteristics. The infinite hierarchy of helicity- and spin- type measures, introduced by Cameron, Barnett and Yao, all emerge with similar quantum operator form: identical to the helicity and spin operators, except with an additional k^2 inside the mode summation for each successive pair of operators. Such analysis dispels the recent claim that light with nonzero values of optical chirality can differentiate between left- and right- handed molecules many times better than pure circularly polarised light. A quantum optical analysis proved that the maximum (or minimum) value any helicity- or spin- type measure can take is that of pure left- or right- handed light.

In **Chapter Four**, it was shown that, when taking expectation values, measureable electromagnetic measures must contain equal numbers of annihilation and creation operators. This avoids the introduction of a rapidly oscillating phase factor, the real part of which averages to zero in any realistic measurement [9]. The subsequent sections detailed a quantum electrodynamic treatment of recent experiments, delivering the rates of circular differential processes and their relation to measures of helicity, spin and recently rediscovered measures of chirality [10–14]. The increase in circular dichroism at regular intervals from the mirror corresponds to Tang and Cohen's claim of nodal enhancements [15] and is associated only with the known behaviour of the electromagnetic field vectors. Furthermore, any increase or decrease in differential response at these locations was shown to be limited by the phase-

photon number uncertainty principle and displays features associated with the reported shot-noise [16], deriving from the quantum nature of light. The section on six-wave mixing of optical vortices demonstrated the quantum entanglement of pairs of optical vortex modes, where the probability for each output displays a neat combinatorial weighting, associated with Pascal's triangle [17].

In **Chapter Five**, it was shown that a quantum electrodynamic framework for the effect of a third body on absorption could be extended by integrating over all possible positions of the mediators. Developing such a theory provided links with both the molecular and bulk properties of materials. Moreover, it was determined which properties need to be optimised in order to tailor the medium modified effect.

In this final chapter, possible avenues of further investigation were identified, along with speculation of what results might emerge.

"Need we add that mathematicians themselves are not infallible?"
-Henri Poincaré

6.7 Bibliography

[1] S. M. Barnett, R. P. Cameron, and A. M. Yao, "Duplex symmetry and its relation to the conservation of optical helicity," *Physical Review A* **86**(1) (2012) [doi:10.1103/PhysRevA.86.013845].

[2] T. G. Philbin, "Lipkin's conservation law, Noether's theorem, and the relation to optical helicity," *Physical Review A* **87**(4) (2013) [doi:10.1103/PhysRevA.87.043843].

[3] M. Babiker, C. Bennett, D. Andrews, and L. Dávila Romero, "Orbital angular momentum exchange in the interaction of twisted light with molecules," *Physical Review Letters* **89**(14) (2002) [doi:10.1103/PhysRevLett.89.143601].

[4] M. D. Williams, M. M. Coles, K. Saadi, D. S. Bradshaw and D. L. Andrews, Optical vortex generation from molecular chromophore arrays, *Physical Review Letters* (Accepted – In press).

[5] M. M. Coles, M. D. Williams, K. Saadi, D. S. Bradshaw and D. L. Andrews, Chiral nanoemitter array: a launchpad for optical vortices, *Laser & Photonics Reviews*, (Accepted – In press).

[6] D. L. Andrews, D. S. Bradshaw, and M. M. Coles, "Perturbation theory and the two-level approximation: A corollary and critique," *Chemical Physics Letters* **503**(1-3), 153–156 (2011) [doi:10.1016/j.cplett.2010.12.055].

[7] M. M. Coles, J. N. Peck, V. S. Oganesyan, and D. L. Andrews, "Failure of the two-level and sum over states methods in nonlinear optics, demonstrated by ab initio methods," 1 June 2012, 84340K–84340K–11 [doi:10.1117/12.920547].

[8] D. L. Andrews, D. S. Bradshaw, and M. M. Coles, "Limitations and improvements upon the two-level approximation for molecular nonlinear optics," *SPIE 79171K* (2011) [doi:10.1117/12.873749].

[9] M. M. Coles, J. N. Peck, V. S. Oganesyan, and D. L. Andrews, "Assessing limitations to the two-level approximation in nonlinear optics for organic chromophores by ab initio methods," *SPIE 81130K* (2011) [doi:10.1117/12.894006].

[10] M. M. Coles and D. L. Andrews, "Photonic measures of helicity: optical vortices and circularly polarized reflection," *Optics Letters* **38**(6), 869 (2013) [doi:10.1364/OL.38.000869].

[11] M. M. Coles and D. L. Andrews, "Chirality and angular momentum in optical radiation," *Physical Review A* **85**(6) (2012) [doi:10.1103/PhysRevA.85.063810].

[12] D. L. Andrews and M. M. Coles, "Measures of chirality and angular momentum in the electromagnetic field," *Optics Letters* **37**(15), 3009 (2012) [doi:10.1364/OL.37.003009].

[13] M. M. Coles and D. L. Andrews, "Directions in optical angular momentum," *SPIE 863707* (2013) [doi:10.1117/12.2004430].

[14] D. L. Andrews and M. M. Coles, "Optical superchirality and electromagnetic angular momentum," 9 February 2012, 827405–827405–7 [doi:10.1117/12.906360].

[15] Y. Tang and A. E. Cohen, "Enhanced enantioselectivity in excitation of chiral molecules by superchiral light," *Science* **332**(6027), 333–336 (2011) [doi:10.1126/science.1202817].

[16] A. G. Smart, "A mirror gives light an extra twist," *Physics Today* **64**(6), 16 (2011) [doi:10.1063/1.3603909].

[17] M. M. Coles, M. D. Williams, and D. L. Andrews, "Second harmonic generation in isotropic media: six-wave mixing of optical vortices," *Optics Express* **21**(10), 12783 (2013) [doi:10.1364/OE.21.012783].